REGENERATING THE NUCLEUS PULPOSUS WITHIN THE INTERVERTEBRAL DISC WITH INJECTABLE CELL-SEEDED BIOMATERIALS

R. J. Williams

A thesis submitted in partial fulfilment of the requirements of University of Sheffield for the degree if Doctor of Philosophy

2023

THESIS: REGENERATING THE NUCLEUS PULPOSUS WITHIN THE INTERVERTEBRAL DISC WITH INJECTABLE CELL-SEEDED BIOMATERIALS

Rebecca Jade Williams

A thesis submitted in partial fulfilment of the requirements of University of Sheffield for the degree if Doctor of Philosophy

Oncology and Metabolism Department

Medical School

The University of Sheffield

July 2023

DEDICATION

This thesis is dedicated to millions of suffers of chronic pain related to disc degeneration. You are acknowledged and I hope that this fantastic spine research community can one day restore the life that you enjoy doing the things that you enjoy in life.

This thesis is also dedicated to my family.

ACKNOWLEDGEMENTS

First and foremostly I would like to thank my fantastic supervisory team Christine Le Maitre and Joseph Snuggs. Christine your dedication to spine research is remarkable and unequivocable. The time that you have given to me throughout my PhD is hugely appreciated, it absolutely eased the stresses and workload that comes with completing a PhD. Joseph, your knowledge, assistance and advise has also helped me loads during my work. You both have continued to inspire me and helped my confidence. My fellow PhD peers at Sheffield Hallam University that I met during this period, the friendships and bonding over low and high periods that accompanies a PhD.

My family: Mum, Dad, Ashleigh, Heather, Hannah, and Jack. You started my passion for the human body and physical sports and supported my continued studies. I thank you for creating and moulding an ambitious, dedicated and perseverate set of individuals. No matter how many obstacles are put in our way, we always make it through stronger and more together than ever.

My partner Reuben, that has been my backbone and his undoubted patience throughout this PhD. Thank you for being by my side in our adventures, which has giving me much needed means of escapism. Thank you to Tom, Caroline, Hope and Holly for your continued interest in my studies and support that you have also given to me.

You have all contributed to the completion of this PhD.

This work also wouldn't have been possible without the funding from Horizon 2020 and the iPSpine project and all those involved within that project, specifically Marianna Tryfonidou and again Christine Le Maitre.

ABSTRACT

Chronic lower back pain affects millions of people year upon year and has a striking effect on quality of life. About 40% of chronic lower back pain is associated with the degeneration of the intervertebral disc. With the current standard of care is heavily focused on symptomatic relief, with the last resort of surgical intervention. There is a lack of clinically available therapies that target the prevention of Intervertebral disc degeneration. In the field of intervertebral disc research, increased focus has been shifted to defining promising new treatments to enable disc regeneration. The reintroduction of cells within a biomaterial has theoretical promise, regarding restoring the main characteristics of cell loss and extracellular matrix degradation that are observed in disc degeneration.

This body of work consists of 7 chapters, chapter 1 delves into the understanding of the disease pathology, and reviews potential cell sources that have been investigated for nucleus pulposus regeneration within current literature. Chapter 2 facilitates future research with the chosen cell source, notochordal cells (NC), by providing key recommendations and methodologies for NC isolation within key species, numeration, *in vitro* manipulation and culture, and characterisation. The following chapter initiates research of screening biomaterials for cytocompatibility with primary porcine NCs (pNCs). The NC and biomaterial constructs were reviewed on the ability of biomaterials to maintain NC viability, phenotype and extracellular matrix synthesis and deposition. As pNCs wouldn't be an effective clinical cells source, an alternative NC-like cell source was utilised in Chapter 4. Which investigates biomaterial cytocompatibility with NC precursor cells, Mesendoderm progenitor cells derived from induced pluripotent stem cells (iPSC-MEPCs). Once more, this chapter aimed to identify a biomaterial which could enable the survival and differentiation of seeded iPSC-MEPCs into an NC-like phenotype with extracellular matrix synthesis and deposition. However, within chapter 4 issues were raised with the cryopreservation and thawing of iPSC-MEPCs, therefore chapter 5 analysed the method of differentiating iPSC into MEPCs and the effects of cryopreservation on cells was also investigated and directly compared to uninterrupted culture of MEPCs. With primary pNCs from Chapter 3 and iPSC-MEPCs from Chapter 5, Chapter 6 investigates the effect of external degenerative factors on these cell-seeded biomaterial constructs. The final chapter, Chapter 7, summaries the results of the chapters and includes some future work that would be beneficial to investigate in future research. As this research investigates cell-seeded biomaterials that has clinical potential as an application for disc degeneration therapy, the translational potential was reviewed, and a recommendation of which patient profile would most benefit from this treatment was discussed.

This thesis includes extensive research with NC and precursor NCs and reviews the cytocompatibility of a selection of biomaterials for this chosen cell source. The research was carried out *in vitro*, with culturing the cell-seeded biomaterials in environments mimicking

the disc and the degenerate disc. In conclusion, both cell sources survived *in vitro* culture of 4-weeks when seeded in select biomaterials, with some cells displaying regenerative properties. The number of available cells was a key limitation of this study and prevented an extensive multiple time point investigation. For future work with NCs, more research needs to be carried out in order to obtain a larger population ethically through primary sources or via stem cell differentiation.

CONTENTS

LIST OF FIGURES IN CHAPTER 1 TO 7

LIST OF TABLES IN CHAPTER 1 TO 6

ABBREVIATIONS

ABC	Avidin-Biotin-Complex
ACAN	Aggrecan
ADAMTS	A Disintegrin and Metalloproteinase with Thrombospondin Motifs
ADMSC	Adipose-Derived Mesenchymal Stromal Cells
AF	Annulus Fibrosus
AQP3	Aquaporin 3
AQP6	Aquaporin 6
ATMP	Advanced Medicinal Product
BMP	Bone Morphogenetic Proteins
BMSC	Bone marrow-derived Mesenchymal Stem Cells
BSA	Bovine Serum Albumin
BT-PEG	α,ω-Bisthio-Polyethylene Glycol
CA12	Carbonic Anhydrase 12
CAV1	Caveolin-1
CD	Chondrodystrophic
CD19	Cluster of Differentiation 19
CD24	Cluster of Differentiation 24
CD44	Cluster of Differentiation 44
CDH2	Cadherin 2
CEP	Cartilaginous endplates
CHIR	CHIR99021
CLBP	Chronic Lower Back Pain
COL2A1	Collagen Type II Alpha 1
COL6A1	Collagen Type VI Alpha 1
CS10	CryoStor® 10

DAB	3,3-Diaminobenzidine Tetrahydrochloride
DAPI	4',6-Diamidino-2-Phenylindole
DMEM	Dulbecco's Modified Eagle Medium
DMMB	1,9-Dimethylmethylene Blue
DMSO	Dimethylsulfoxide
DMTMM	4-(4,6-dimethoxy-1,3,5-triazin-2-yl)-4-Methyl-Morpholinium Chloride
DNA	Deoxyribonucleic acid
dNCM	Decellularised Notochordal Matrix
DPBS	Dulbecco's phosphate-buffered saline
DSTYK	Dual Serine/Threonine and Tyrosine Protein Kinase
ECM	Extracellular Matrix
EDTA	Ethylenediaminetetraacetic acid
ELISA	Enzyme-Linked Immunosorbent Assay
ESC	Embryonic stem cells
FACS	Fluorescent Activated Cell Sorting
FCS	Foetal calf serum
FGF	Fibroblast growth factors
FITC	Fluorescein Isothiocyanate
FOXA2	Forkhead Box A2
FOXF1	Forkhead Box F1
FOXJ1	Forkhead Box J1
GAGs	Glycosaminoglycans
GJA1	Gap Junction Protein Alpha 1
GLUT-1	Glucose Transporter Type 1
GLUT-1	Glucose Transporter Type 1
GMP	Good Manufacturing Practice
GSK3beta	Glycogen Synthase Kinase 3 β

HA	Hyaluronic Acid
HBSS	Hanks' Balanced Salt Solution
HIF-1α	Hypoxia-inducible Factor 1-alpha
HLA-DR	Human Leukocyte Antigen – DR isotype
HNA	Human Nuclear Antigen
hUCSC	human Umbilical Cord Stem Cells
ICM	Inner Cell Mass
IF	Immunofluorescence
IHC	Immunohistochemistry
IL-1β	Interleukin-1β
IMS	Industrial Methylated Spirit
iNC-LC	Induced Notochordal- Like Cells
iPSC	Induced Pluripotent Stem Cells
iPSC-MEPC	Induced Pluripotent Stem Cell derived Mesendoderm Progenitor Cells
ISVD	In-Straw Vitrification-Dilution
ITS	Insulin-Transferrin-Selenium
IVD	Intervertebral Disc
KLF4	Krüppel-like factor 4
KRT18	Cytokeratin 18
KRT19	Cytokeratin 19
KRT8	Cytokeratin 8
KSR	Knockout Serum
LBP	Lower Back Pain
LEF1	Lymphoid Enhancer Binding Factor 1
LEFTY1	Left-Right Determination Factor 1
LGALS3	Galectin 3
L-pNIPAM-co-DMAc	Laponite crosslinked poly N-isopropylacrylamide N, N' Dimethylacrylamide

LVE	Linear Viscoelastic
MA-HSA	Maleimido-Human Serum Albumin
MEPCs	Mesendoderm Progenitor Cells
MFAT	Micro Fragmented Adipose Tissue
MiPs	INSERM Induced Pluripotent Stem Cell Line
MMP-3	Matrix Metalloproteinase 3
MMPs	Matrix Metalloproteinases
MRI	Magnetic Resonance Imaging
mRNA	Messenger Ribonucleic Acid
MSC	Mesenchymal Stem Cells
NANOG	Nanog Homeobox
NC	Notochordal Cell
NCD	Non-Chondrodystrophic
NC-LC	Notochordal-Like Cells
NCM	Notochordal Cell Matrix
NOG	Noggin
NP	Nucleus Pulposus
NPC	Nucleus Pulposus Cell
NPgel	L-pNIPAM-co-DMAc Hydrogel Developed for Nucleus Pulposus Tissue
NPSC	Nucleus Pulposus-Derived Stem Cells
OCT 4	Octamer-Binding Transcription Factor 4
ODI	Oswestry Disability Index
PAX1	Paired Box 1
PBMC	Peripheral Blood Mononuclear Cells
PBS	Phosphate Buffered Saline
PDT	Population Doubling Time
PEG	Polyethylene Glycol

PEG/dNCM	Polyethylene Glycol with Decellularised Notochordal Matrix
PI	Propidium Iodide
PKH26	PKH26 Red Fluorescent Cell Membrane Labelling
pNC	Porcine Notochordal Cells
qRT-PCR	Quantitative Reverse Transcription Polymerase Chain Reaction
RIPK5	Receptor Interacting Protein 5
RNA	Ribonucleic Acid
ROCKi	ROCK Inhibitor Y-27632
SEM	Scanning Electron Microscope
SFRP2	Secreted Frizzled Related Protein 2
SHH	Sonic Hedgehog Signalling Molecule
SOX2	SRY-Box Transcription Factor 2
SOX5	SRY-Box Transcription Factor 5
SOX6	SRY-Box Transcription Factor 6
SOX9	SRY-Box Transcription Factor 9
SVF	Stromal Vascular Fraction
TBS	Tris-Buffered Saline
TBXT	Brachyury
TF	Thermofisher
Tie2	TEK receptor tyrosine kinase
TIMPS	Tissue Inhibitors of Metalloproteinase
UV	Ultraviolet
VAS	Visual Analogue Scale
Wnt	Wingless/Integrated
WPC	weeks post-conception
αMEM	Alpha Minimum Essential Medium

DISSEMINATION: SCIENTIFIC PUBLICTAIONS

PUBLISHED

Williams, R. J., Tryfonidou, M. A., Snuggs, J. W., & Le Maitre, C. L. (2021). **Cell Sources Proposed for Nucleus Pulposus Regeneration**. *JOR Spine*, 4(4), e1175. https://doi.org/10.1002/jsp2.1175

IN PRESS

Accepted June 2023, JOR Spine: **Recommendations for Intervertebral Disc Notochordal Cell Investigation: From Isolation to Characterisation**

Authors: **Rebecca J. Williams**, *Lisanne T. Laagland, *Frances C. Bach, Lizzy Ward, Wilson Chan, Vivian Tam, Adel Medzikovic, Shaghayegh Basatvat, Lily Paillat, Nicolas Vedrenne, Joseph W. Snuggs, Deepani W. Poramba-Liyanage, Judith A Hoyland, Danny Chan, Anne Camus, Stephen M. Richardson, Marianna A. Tryfonidou, Christine L. Le Maitre.

*These authors have contributed equally to the study

SUBMITTED

Submitted June 2023, eCells & Materials Journal: **Potential of Notochordal Cells Within Injectable Biomaterials to Promote Intervertebral Disc Regeneration**

Authors: **Rebecca J. Williams**, Shaghayegh Basatvat, Tara C. Schmitz, Ronak Janani, Chris Sammon, Karin Benz, Keita Ito, Mariana A. Tryfonidou, Joseph W. Snuggs, Christine Le Maitre.

IN PREPARATION

Potential Of Mesendoderm Progenitor Cells Within Injectable Biomaterials to Promote Intervertebral Disc Regeneration

Authors**: Rebecca J. Williams**, Georgina Targa Fabra, Julie Warin, Ronak Janani, Abhay Pandit, Chris Sammon, Anne Camus, Mariana A. Tryfonidou, Joseph W. Snuggs, Christine Le Maitre.

The Effects of External Disc Environment on Cell-Seeded Biomaterials for Disc Regeneration

Authors**: Rebecca J. Williams**, Shaghayegh Basatvat, Ronak Janani, Chris Sammon, Mariana A. Tryfonidou, Joseph W. Snuggs, Christine Le Maitre.

DISSEMINATION: CONFERENCE ABSTRACTS

PODIUM PRESENTATIONS

Britspine. Glasgow, UK. 18th-20th April 2023. **'Using Mesendoderm Progenitor Cells Seeded in Biomaterial to Regenerate the Intervertebral disc'**

International Combined Orthopaedic Research Societies. Edinburgh, UK. 7th-9th September 2022. '**An Analysis of Injectable Biomaterial for Delivery of Notochordal Cells for Intervertebral Disc Regeneration'**

Society of Back Pain Research. Warwick, UK. 30th June- 7th July 2022. '**An Analysis of Injectable Biomaterial for Delivery of Notochordal Cells for Intervertebral Disc Regeneration'**

POSTER PRESENTATIONS

Orthopaedic Research Society, The Philadelphia Spine Research Society. Philadelphia, USA. 6th-10th November 2022. **(Best Poster Award) 'Using Mesendoderm Progenitor Cells Seeded in Hydrogel Biomaterial to Regenerate the Intervertebral Disc'.**

eCells and Materials: Cartilage and Disc Repair and Regeneration. Davos, Switzerland. 15th-18th June 2022. '**An Analysis of Injectable Biomaterial for Delivery of Notochordal Cells for Intervertebral Disc Regeneration'**

Orthopaedic Research Society. Florida, USA. 4th- 8th February 2022. '**An Analysis of Injectable Biomaterial for Delivery of Notochordal Cells for Intervertebral Disc Regeneration'**

POSTERS

Tissue Engineering and Regenerative Medicine International Society. Maastricht, The Netherlands (Virtual Poster Presentation). 15th-19th November 2021. **'An Analysis of Injectable Biomaterial for Delivery of Notochordal Cells for Intervertebral Disc Regeneration'**

European Orthopaedic Research Society. Rome, Italy (Virtual Poster Presentation). 15th-17th September 2021. **'An Analysis of Injectable Biomaterial for Delivery of Notochordal Cells for Intervertebral Disc Regeneration'**

Tissue Engineering and Regenerative Medicine International Society. Manchester, UK (Virtual Poster Presentation). 26th-29th May 2020. **'Thermoresponsive Injectable Hydrogel for Delivery of Notochordal Cells for Intervertebral Disc Regeneration'**

Orthopaedic Research Society. Arizona, USA (Virtual Poster Presentation). 8th-11th February 2020. '**Thermoresponsive Injectable Hydrogel for Delivery of Notochordal Cells for Intervertebral Disc Regeneration'**

GRANTS

2023: **SBPR Travel Bursary**
£300 contribution for attending Britspine, Glasgow 2023 to present oral presentation.

SBPR Travel Fellowship Grant
£2,500 to visit AO institute Davos for experience in working with an Intervertebral Disc Bioreactor

2022: **ON/ICORS Education Grant**
£350 contribution for attending ICORS 2022 World Orthopaedic Congress

CHAPTER 1
INTRODUCTION

CONTEXT OF RESEARCH

The introduction is mainly based on the manuscript of a published literature review 'Cell Sources Proposed for Nucleus Pulposus Regeneration, JOR Spine (2021)', with an additional section introducing biomaterial carriers that was not in the published manuscript but added due to the importance to the thesis. The introduction describes lower back pain, the rationale behind generating a treatment and the association of lower back pain to the Intervertebral disc (IVD). The chapter then goes on to describe our understanding of disc degeneration and potential approaches that can regenerate the nucleus pulposus, with the focus being cells therapy. The body of chapter and the literature review's aim was to report current cell therapy for regeneration of nucleus pulposus; and to provide a critical appraisal of cell sources proposed for regeneration of the Nucleus Pulposus (NP) tissue. The review looked extensively through published papers over the last 26 years that have proposed the use of cells to regenerate a degenerative nucleus pulposus. The review systematically analysed each substantial cell type featured in the literature; highlighting the cells characteristics and rational for the potential to regenerate the disc, their handling proficiency with expansion capability and maintenance of phenotype *in vitro* and *in vivo*, the cells survival capacity in the harsh intervertebral disc environment, and finally reports of regenerative effect of the analysed cell type. The rational of the literature review and contribution to research was the perspectives on which cells could be the most promising and which *in vitro, ex vivo* or *in vivo* systems the cells have been tested in. The review highlights which cells have the most potential, for investigation for further enhancement of therapeutic approaches either alone or in combination with biomaterials and growth factors.

AUTHORS

Rebecca J. Williams[1], Marianna A. Tryfonidou[2], Joseph W. Snuggs[1], Christine Le Maitre[1]

AFFILIATIONS

[1] Biomedical Research Centre, Biosciences, Sheffield Hallam University, Sheffield S1 1WB, UK.
[2] Department of Clinical Sciences of Companion Animals, Faculty of Veterinary Medicine, Utrecht University, Utrecht, The Netherlands.

AUTHOR CONTRIBUTIONS

RJW, JWS, CLM, drafted the manuscript; All authors critically revised the manuscript for intellectual content; All authors approve the final version and agree to be accountable for all aspects of the work.

DETAILED CONTRIBUTION MADE

I performed the literature search and critically reviewed all literature involved in cell-based treatment for nucleus pulposus regeneration. I prepared the initial draft of the manuscript and completed alterations following feedback.

(PUBLISHED) Williams, R. J., Tryfonidou, M. A., Snuggs, J. W., & Le Maitre, C. L. (2021). Cell sources proposed for nucleus pulposus regeneration. JOR Spine, 4(4), e1175. https://doi.org/10.1002/jsp2.1175

MANUSCRIPT:
CELL SOURCES PROPOSED FOR NUCLEUS PULPOSUS REGENERATION

ABSTRACT

Lower back pain (LBP) occurs in 80% of adults in their lifetime, resulting in LBP being one of the biggest causes of disability worldwide. Chronic LBP has been linked to the degeneration of the intervertebral disc (IVD). The current treatments for chronic back pain only provide alleviation of symptoms through pain relief, tissue removal or spinal fusion; none of which target regenerating the degenerate disc. As nucleus pulposus (NP) degeneration is thought to represent a key initiation site of intervertebral disc (IVD) degeneration, cell therapy that specifically targets the restoration of the NP has been reviewed here. A literature search to quantitatively assess all cell types used in NP regeneration was undertaken. With key cell sources: NP cells; annulus fibrosus cells; notochordal cells; chondrocytes; bone marrow mesenchymal stromal cells; adipose derived stromal cells; and induced pluripotent stem cells extensively analysed for their regenerative potential of the NP. This review highlights: accessibility; expansion capability *in vitro;* cell survival in an IVD environment; regenerative potential; and safety for these key potential cell sources. In conclusion, whilst several potential cell sources have been proposed, induced pluripotent stem cells may provide the most promising regenerative potential.

INTRODUCTION

LOWER BACK PAIN AND TREATMENTS

Lower back pain (LBP) is the biggest cause of disability worldwide, around 80% of adults will suffer from LBP in their lifetime (Hartvigsen *et al.*, 2018; Traeger *et al.*, 2019). Most people experience mild pain and recover quickly; however, it is common for episodes of LBP to relapse contributing to a lifelong disability and a large societal burden (Maetzel and Li, 2002; Hartvigsen *et al.*, 2018). The current mainstay of treatments to combat LBP are split into pharmacological (opioids, non-steroidal anti-inflammatory drugs, antidepressants) and non-pharmacological (exercise, massage, manipulation, and self-management) (Qaseem *et al.*, 2017; Nice, 2018). Although these treatments are potentially helpful in acute LBP, there are limited therapies that are efficient in the management of chronic LBP (Phillips *et al.*, 2003; Bogduk, 2004; Steffens *et al.*, 2016; Foster *et al.*, 2018). For example, treatments available to relieve chronic LBP and recurrent onset back pain include an invasive operation to remove the disc and potentially fuse adjacent vertebrae, which can lead to the alteration of the normal physiological and biomechanical function of the spine (Berg *et al.*, 2009). The use of painkillers for the treatment of chronic LBP has also had repercussions; 24% of chronic LBP cases results in aberrant medication-taking behaviours (Martell *et al.*, 2007). Such behaviours are contributing to the opioid epidemic in the U.S (Manchikanti *et al.*, 2012) and the development of an opioid crisis in the UK and other countries (Häuser *et al.,* 2017). In the U.S. there were 70,237 opioid overdose deaths in 2017, which constituted 67.8% overall drug related overdoses (Scholl *et al.*, 2017). Therefore, there has been an emphasis to reassess the management of chronic LBP (Dowell *et al.,* 2016). Approximately 40% of all chronic LBP cases are associated with intervertebral disc (IVD) degeneration (Luoma *et al.*, 2000; Brinjikji *et al.*, 2015; Zheng and Chen, 2015). However, none of the treatments stated above address the underlying cause of IVD degeneration and target the restoration of the damaged IVD (Sakai and Andersson, 2015).

THE INTERVERTEBRAL DISC

The IVD is a complex structure, where the biomechanical functioning of the IVD relies on a balance between the three main tissues that compose it. The central aspect of the disc contains a glycosaminoglycan-rich gel-like tissue called the nucleus pulposus (NP), which is enclosed by the annulus fibrosus (AF). The third distinct region are the cartilaginous endplates (CEP), which are composed of cartilage and situated superiorly and inferiorly to the IVD, and act to separate and anchor the disc to the vertebrae via the bony end plates, the CEP also acts as a gateway for nutrient transport into the disc (Bae *et al.*, 2013; Tomaszewski *et al.*, 2015) (Fig. 1.1). The different compositions of the three areas of the IVD allow the support of spinal compressive loads, the NP osmotically exerts the swelling pressure whilst the AF constrains the NP, preventing it from protruding transversely and the CEP constrains the NP from bulging into the adjacent vertebrae; thus creating tensile stresses and absorbing the considerable hydrostatic pressure (Oegema, 1993; Tomaszewski *et al.*, 2015). A healthy disc requires

maintenance of this homeostatic environment, a simple shift in the matrix properties, cells, or molecular signals in these three areas of the IVD has implications to the distribution of the mechanical load and begins the cascade of IVD degeneration.

DISC DEGENERATION

The regulation of cellular turnover is vital to tissue homeostasis. In IVD degeneration the number of functional cells are decreased, through apoptosis and cellular senescence (Urban and Roberts, 2003; Le Maitre *et al.*, 2007; Bergknut *et al.*, 2013; Jiang *et al.*, 2013), with an accompanied phenotypic shift towards catabolism; which leads to altered NP matrix maintenance and an increase in catabolic responses by the IVD cells themselves (Le Maitre *et al.*, 2005; Le Maitre *et al.*, 2007; Erwin *et al.*, 2011; Hodgkinson *et al.*, 2019). NP matrix composition is regulated through cellular matrix synthesis and matrix degradation via the activity of matrix metalloproteinases (MMPs) and A disintegrin and metalloproteinase with thrombospondin motifs (ADAMTS), enzyme families, which can be inhibited by tissue inhibitors of metalloproteinases (TIMPS) (Le Maitre *et al.*, 2007). Healthy NP tissue contains a ratio of 27:1 glycosaminoglycan-to-hydroxyproline (collagen) ratio, and aggrecan and its associated glycosaminoglycans (GAGs) preserves the high-water content of the NP (Mwale *et al.*, 2004). During degeneration, NP matrix synthesis and degradation becomes dysregulated leading to the loss of proteoglycans and dehydration. The condensed NP and increase in intradiscal pressure results in reduced capacity of mechanical loading of the disc, leading to the creation of micro fissures throughout the IVD (Kadow *et al.*, 2015). Once the outer AF or CEP become ruptured, inflammatory cells can migrate into the disc which propagates an inflammatory cascade. Which together with the catabolic factors produced by the native disc cells, contributes to discomfort and the stimulation of pain sourced from the disc, also known as discogenic pain (Binch *et al.*, 2014; Kadow *et al.*, 2015). Although there is no definitive mechanism to explain the link between the IVD and the discogenic pain patients experience. The combination of structure disruption with the production of angiogenic and neurotrophic factors by NP and AF cells, stimulates angiogenesis and promotes neural ingrowth to the largely avascular and aneural disc (Freemont *et al.*, 1997; Binch *et al.*, 2014) (Fig. 1.1). The IVD cells also produce pain sensitising factors such as substance P, which can sensitize in-growing nerves and local nerve roots to pain (Freemont *et al.*, 1997; Ashton *et al.*, 2009). Thus, it is important to deduce a regenerative approach that will restore the balance of cells, extracellular matrix and the biomechanics of the disc and interrupt the viscous cycle of degeneration (Vergroesen *et al.*, 2015; De Vries *et al.*, 2019). In a clinical setting disc degeneration can be classified using the Pfirrmann grading system utilising a routine magnetic resonance imaging (MRI). The Pfirrmann grading system ranks discs from Grade I to V by accessing the MRI signal intensity, disc struct, distinction between nucleus and anulus, and disc height (Fig. 1.1). The signal loss of the disc on T2-weighted MRIs correlates with the progressive degenerative changes of the IVD shown in Figure 1.1, the signal brightness observed in the nucleus correlates directly with the proteoglycan concentration and not the water or collagen content (Pfirrmann *et al.*, 2001). Further assessment of disc hydration can

be analysed by quantitative MRI (Boos *et al.*, 1994). Pfirmann grading system lacks the changes observed in the vertebral body marrow adjacent to the IVD and thus can be characterised by Modic et al., (1988). Modic changes are classified also using an MRI and ranked from Type 1 to Type 3. Modic type 1: represents bone marrow oedema and inflammation visualised with high T-2 weighted MRI signal. Modic type 2: represents normal red haemopoietic bone marrow conversion into yellow fatty marrow as a result of marrow ischaemia visualised with isointense T-2 weighted MRI signal. Modic type 3: represents subchondral bony sclerosis visualised with low T2-weighted MRI signal (Modic *et al.*, 1988).

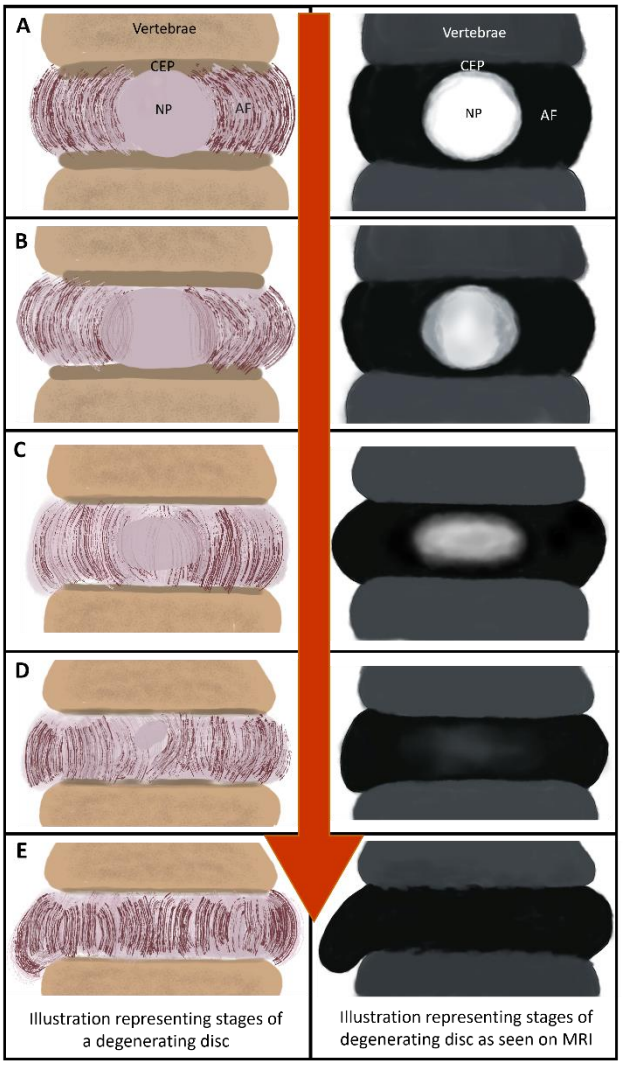

Figure 1.1. Stages of Intervertebral disc degeneration illustration to represent magnetic reasoning images (MRI). *(A) Represents grade I: The structure of the disc is homogeneous, with a bright hyperintense white signal intensity and a normal disc height. (B) Represents grade II: The structure of the disc is inhomogeneous, with a hyperintense white signal. The distinction between nucleus pulposus (NP) and annulus fibrosis (AF) is clear, and the disc height is normal, with or without horizontal grey bands. (C) Represents grade III: The structure of the disc is inhomogeneous, with an intermediate grey signal intensity. The distinction between nucleus and anulus is unclear, and the disc height is normal or slightly decreased. (D) Represents grade IV: The structure of the disc is inhomogeneous, with an hypointense dark grey signal intensity. The distinction between nucleus and anulus is lost, and the disc height is normal or moderately decreased. (E) Represents grade V: The structure of the disc is inhomogeneous, with a hypointense black signal intensity.*

POTENTIAL APPROACHES TO REGENERATE THE NUCLEUS PULPOSUS

There has been a focus for a tissue engineering approach to restore the appropriate cell and matrix content of the NP, which would benefit the function of the disc as a whole and thus resolve discogenic back pain (Risbud and Shapiro, 2011; Vadalà *et al.*, 2015; De Vries *et al.*, 2019). These studies have ranged from biomaterial-based to cellular approaches or a combination thereof. Some studies have investigated implanting biomaterials to stimulate the resident NP cells (Endres *et al.*, 2010; Chan *et al.*, 2013; Lin *et al.*, 2016), whilst others have used biomaterials to act as a combination of mechanical support and as a cell carrier system (Helen and Gough, 2008; Henriksson *et al.*, 2012; Thorpe *et al.*, 2016). As the pathological findings in IVD degeneration are mainly characterised by a progressive loss of viable cells and a shift to a catabolic phenotype, cell therapy has been proposed to restore the NP cell population (Aguiar *et al.,* 1999; Sakai, 2008; Smith *et al.*, 2018).

An important consideration in the choice of cell source for therapeutic use is the origin of cells of the IVD. Developmentally, the disc's unique structure is formed from cells of at least two embryonic origins: the notochord, which develops into the NP and the sclerotome which makes up all other connective tissue of the spine including the AF and vertebrae (Risbud and Shapiro, 2011; Alkhatib *et al.*, 2018). The notochord and sclerotome are derived from one of the three primary embryonic germ layers: the mesoderm (Fig. 1.1a) (Nieuwkoop, 1997; Smith *et al.*, 2011). Therefore, a cell-based therapy approach could be performed using cells that have the capacity to develop into, and from, the mesoderm-derived lineages (Fig. 1.1b). Such as differentiated cells: Notochordal cells (NC) (Bach *et al.*, 2018), NP cells (Colombier *et al.*, 2016, 2020), AF cells (Gao *et al.*, 2018), and chondrocytes (Ganey *et al.*, 2003; Gay *et al.*, 2019); adult stromal cells from bone marrow or adipose (Hoogendoorn *et al.*, 2008; Noriega *et al.*, 2017; Omlor *et al.*, 2018); embryonic stem cells (Ma *et al.*, 2008; Vadalà *et al.*, 2016), or more recently the use of induced pluripotent stem cells (iPSCs) has also been explored (Zhu *et al.*, 2017; Tang *et al.*, 2018; Sheyn *et al.*, 2019). However, this simple cell therapy strategy is made much more difficult by the fact that the microenvironment of the IVD is very harsh. The IVD environment has an acidic pH, due to high concentrations of lactate (Urban and Roberts, 2003), low concentrations of glucose and oxygen (Huang *et al.*, 2013), and fluctuating osmolality (Urban, 2002; Spillekom *et al.*, 2014; Li *et al.*, 2018); the degenerate disc also contains increased expression of catabolic cytokines (Le Maitre *et al.*, 2007; Phillips *et al.*, 2015), that further disrupt this harsh environment. Therefore, the cells will also need to be able to adapt and survive in the IVD niche.

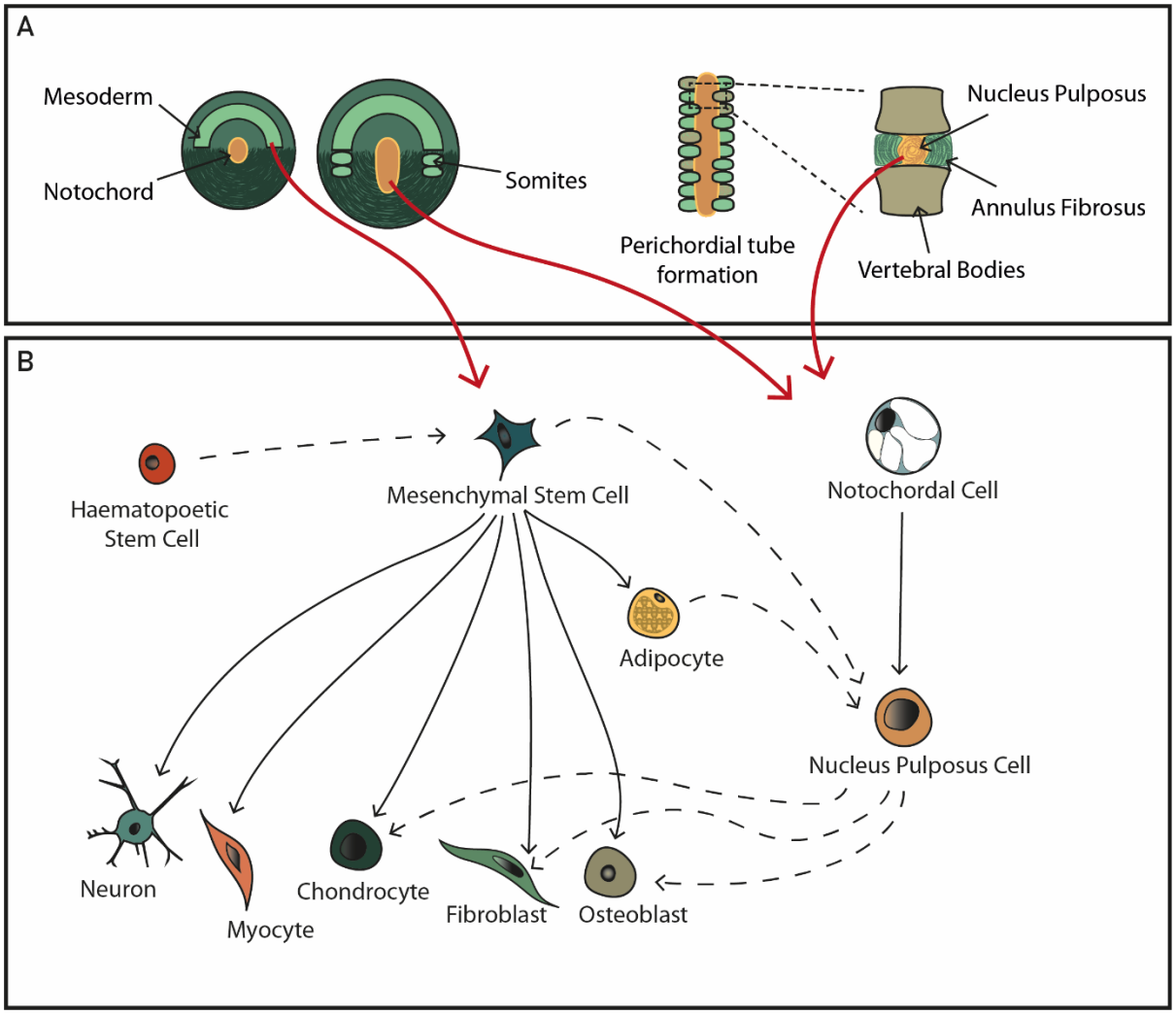

Figure 1.2. Cell sources and linages involved in cellular therapy in regenerating the intervertebral disc. (A) *Schematic illustration depicting key stages of intervertebral disc development, highlighting the mesodermal origin of the notochord and sclerotome that evolve into the nucleus pulposus, annulus fibrosus and vertebral bodies. Red arrows show the potential cell sources.* ***(B)*** *An illustration of the mesenchymal stem cell and notochordal cell differentiation lineages (black arrows). Under appropriate culture conditions trans-differentiation can be induced to develop different cell types (black dash arrows), which can interlink different cell lines.*

BIOMATERIAL CARRIERS

A complementary proposal for making sure cells survive the initial transportation into the NP, but also withstand the harsh environment associated with the IVD is to encapsulate cells into biomaterials. Seeding cells directly into a biomaterial scaffold can facilitate cell growth and/or favourable differentiation, additionally the biomaterial will also provide mechanical support and instantaneously restore disc structure (Peroglio *et al.*, 2012; Thorpe *et al.*, 2016). Ideally, biomaterials for NP repair should consist of the natural properties of NP such as: mechanical characteristics of swelling properties (Treffel *et al.*, 2016) and withstanding compress loading. The biological characteristics should be biocompatible and bioactive, potentially inhibiting degenerative process, inhibition of catabolic factors and cytokines, prevention of nerve and blood vessel ingrowth and stimulate regeneration through supporting the integration of

extracellular matrix. Furthermore, if intended for clinical use the biomaterial must also be sterile (F.D.A. Infection Control Devices Branch, 2016), durable, and generate minimal wear, be non-immunogenic and transmissible into the disc (injectable)(Schmitz *et al.*, 2020). With this in mind, soft biomaterials or hydrogel-based biomaterial carriers have previously been assessed for parameters to evaluate their for potential NP restoration (Bowles and Setton, 2017).

METHODS

There have been a wide range of potential cell sources explored for the repair and regeneration of the IVD which will be explored within this review. Specifically, this review will discuss the cell sources investigated for the regeneration of the NP, from terminally differentiated cell sources to the use of adult stem cells and recent studies investigating induced pluripotent stem cells (iPSCs).

PubMed was used as the principal database with a primary search of '((disc degeneration) OR (intervertebral)) NOT (retinal)) AND ((embryonic stem cells) OR (progenitor cells) OR (fibroblasts) OR (stem cells) OR (induced pluripotent stem cells) OR (adult stem cells) OR (mesenchymal) OR (adipose) OR (hematopoietic) OR (synovial) OR (disc stem cells) OR (disc cells) OR (nucleus pulposus) OR (chondrocytes) OR (notochordal) OR (notochord)) AND ((cell therapy) OR (regeneration) OR (therapy) OR (treatment))'. Clinical trials, *in vivo* and *in vitro* studies were all included, and the search was limited to the English language and published prior to 31st December 2020. These keywords were chosen to explore the different types of cell sources to be used as potential regenerative therapies for the IVD. This search generated a total of 3,566 publications. The title and abstracts were initially screened based on their relevance to cellular therapies for the regeneration of the NP region only. A total of 355 articles were identified.

TRENDS IN CELLULAR THERAPY RESEARCH FOR INTERVERTEBRAL DISC REGENERATION

There has been a gradual increase in the number of studies investigating potential cellular therapy to regenerate the NP, with the first studies reported in 1994. Over the last 10 years, a 50% increase has been seen (Fig. 1.2). Initial studies focused on the use of NP cells, either alone or augmented with growth factor stimulation or anti-catabolic therapies (Fig. 1.3). From 2003 onwards, initial studies were reported investigating the use of adult stem cells and alternative terminally differentiated cells (Fig. 1.3c). From then on bone marrow-derived mesenchymal stem cells (BMSC) have been the predominant cell choice, with 40% of the literature reporting studies using BMSC, followed by NP cells and then adipose derived stem cells (ADMSC) (Fig. 1.3b). From 2013 onwards the use of embryonic like cells with the use of human umbilical cord stem cells (hUCSC) and iPSC were first reported (Fig. 1.3). Most of the studies have utilised *in vitro* cell culture (42%) and *in vivo* small and large animal models (39%) (Fig. 1.4a, b), as organ and tissue culture models were only introduced in 2008 (Fig. 1.4c). One of the earliest *in vivo* studies was conducted in a dog model in 1994, after that smaller animal

models were favoured; in 2009, studies progressed to a higher incidence of large animal models, with the first clinical human trial implemented in 2006, 12 years after the first study on cell therapy. The first human clinical trial was reported using haematopoietic stem cells (Haufe and Mork, 2006); 9-fold more clinical trials have been conducted on humans than in dogs (Fig. 1.4c). Greater than 50% of the *in vivo* studies utilized small animal models, with rabbit being the dominant species (Fig. 1.5b); due to the ease of accessibility and cost implications (Thorpe *et al.*, 2018). Less than a quarter of studies utilized large animal models, with no studies using cow (Fig. 1.5a). Similarities between human and animal IVD disc have been previously reviewed by Alini *et al.,* (2008) and will not be part of the discussion of this review. However, it is worth noting that a significant limitation when analysing animal models for regenerative approaches is that many of the species utilised retain their immature NCs

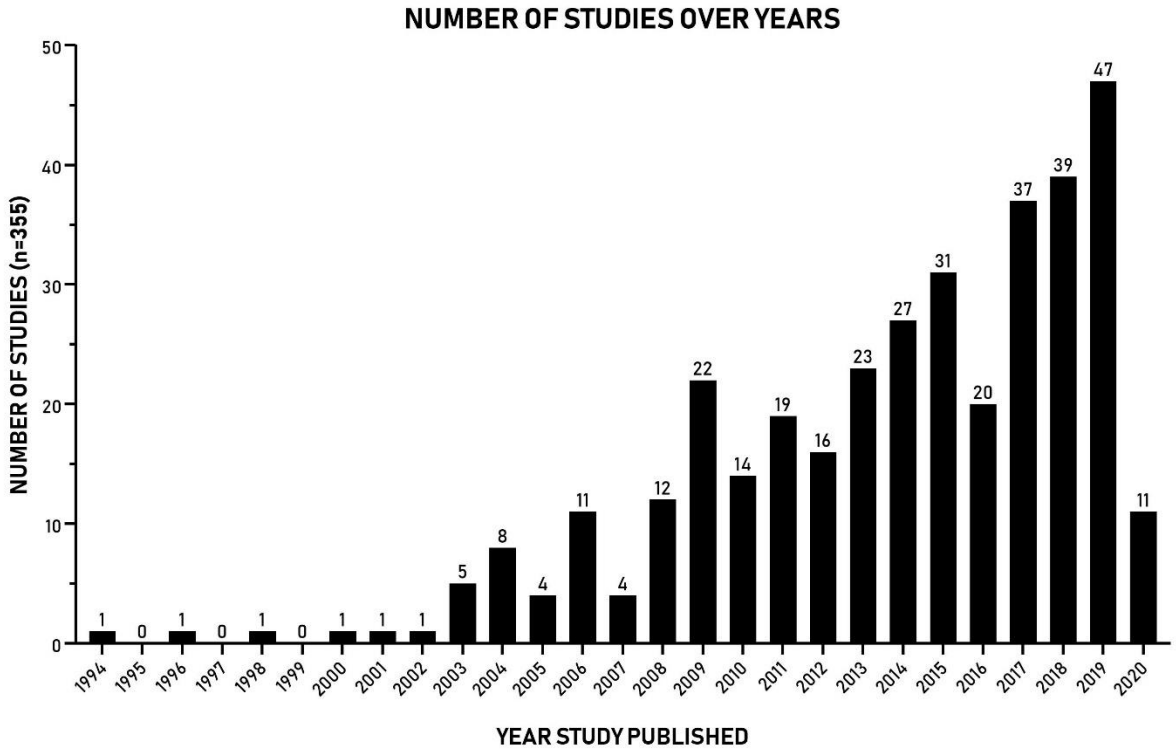

Figure 1.3. Publication intensity for cellular therapy for NP regeneration. *The number of studies investigating potential cellular therapy to regenerate the NP extracted from the literature review search expanding over 26 years (from January 1994 to December 2020).*

and thus have an increased regenerative capability which can skew results. Thus, model systems which lose NCs postnatally, such as sheep, rabbits, goats and chondrodystrophic dogs, would be more appropriate for investigations into regenerative approaches (Alini *et al.*, 2008).

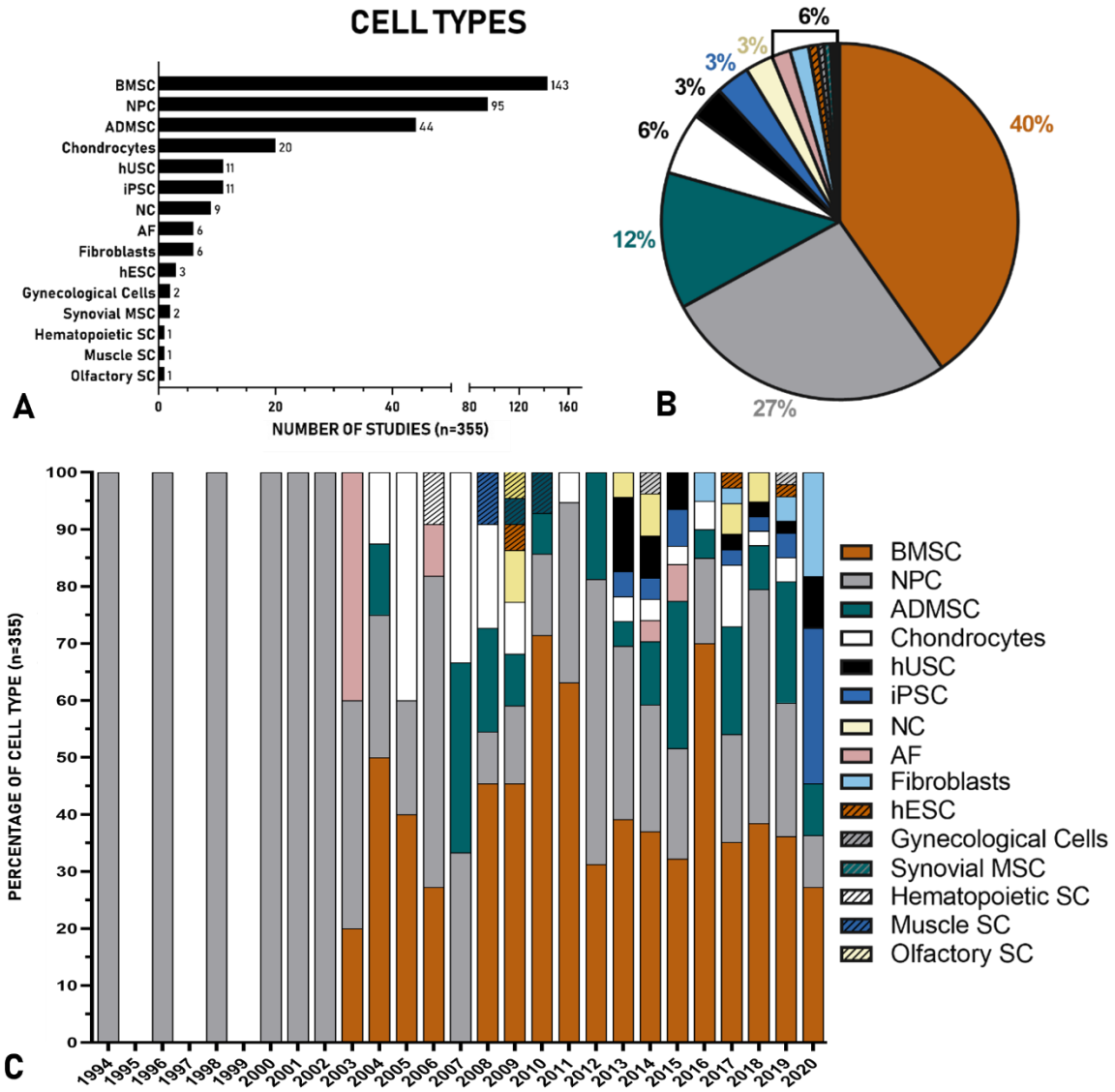

Figure 1.4. Cell sources proposed for NP regeneration: *Studies investigating potential cellular therapy to regenerate the NP expanding over 26 years (from January 1994 to December 2020) were classified according to cell source proposed: the number (A), percentage (B) of cell type and the percentage of cell type relative to the year (C) which used the following cell types: Adipose derived mesenchymal stem cells (ADMSC), annulus fibrosus (AF) cells, bone marrow derived mesenchymal stem cells (BMSC), Chondrocytes (subgroups include: endplate chondrocytes, hyaline chondrocytes, articular chondrocytes, nasal chondrocytes and auricular chondrocytes), fibroblast cells, gynaecological cells (subgroups include: menstrual blood derived stem cells and human amniotic cells), hematopoietic stem cells, human embryonic stem cells (hESC), human umbilical cord stem cells (hUSC; including placenta derived mesenchymal stem cells), induced pluripotent stem cells (iPSC), muscle derived stem cells, notochordal cells (NC), Nucleus pulposus cells (NPC), olfactory stem cells and synovial derived mesenchymal stem cells. (B) From the literature extracted: 40% used BMSC; 26% used NPC; 12% ADMSC; 6% used Chondrocytes; 3% used iPSC; 3% used hUSC; 3% used NCs; 2% used AF cells; 2% used Fibroblasts; <1% used hESC; <1% used Synovial MSC; <1% used Gynaecological cells; <1% used Olfactory SC; <1% used Muscle SC; <1% Hematopoietic SC.*

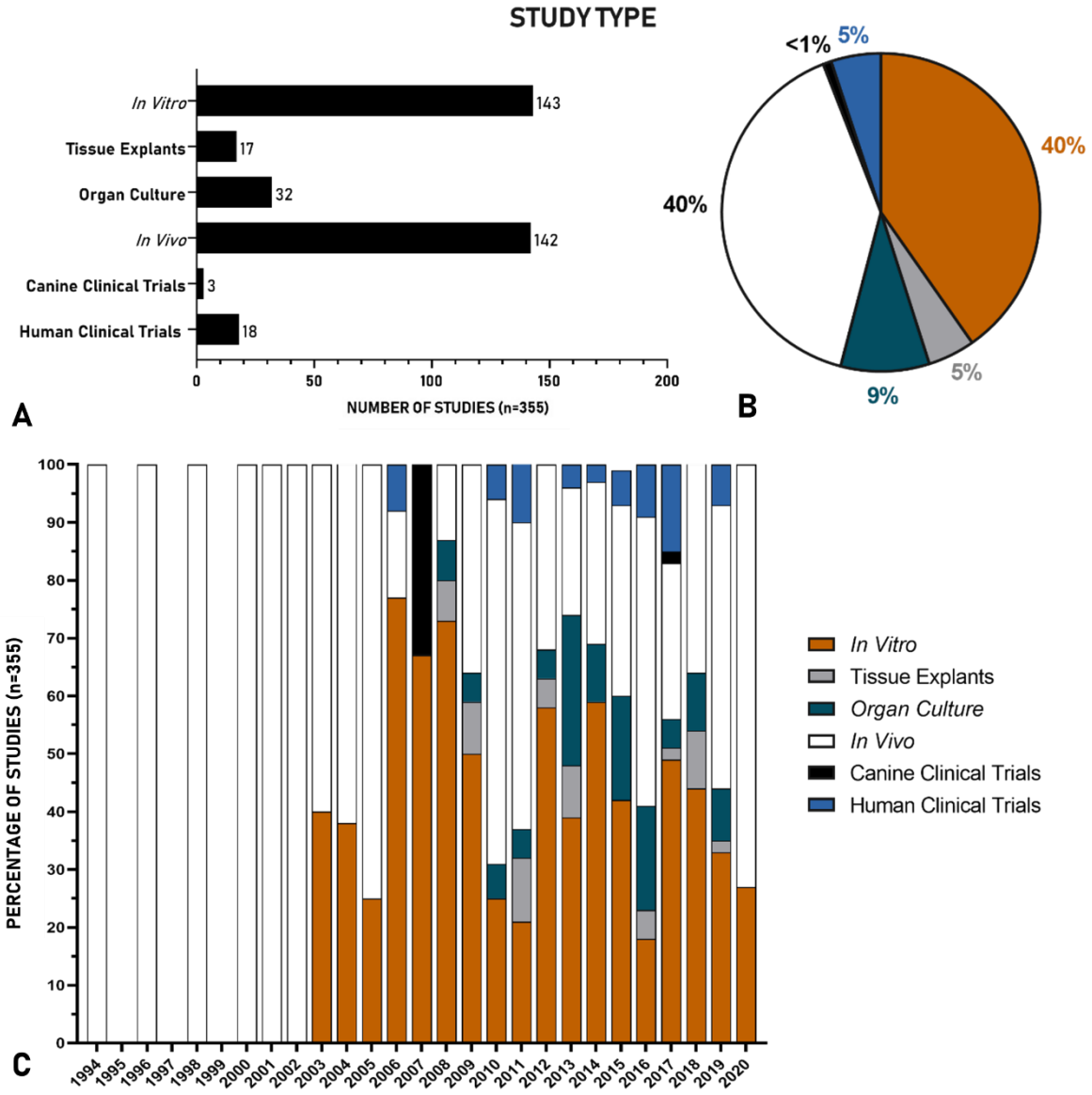

Figure 1.5. Study type utilised to investigate cellular regeneration of the NP. *Studies investigating potential cellular therapy to regenerate the NP expanding over 26 years (from January 1994 to December 2020) were classified according to the type of study performed; the number (A), percentage (B) of study type and the percentage of study type relative to the year (C) from the literature search that used the following model systems: in vitro (including 2D and 3D culture), tissue explants, organ culture, in vivo (subcutaneous or injected into a healthy or degenerate intervertebral disc), canine clinical trials and human clinical trials.*

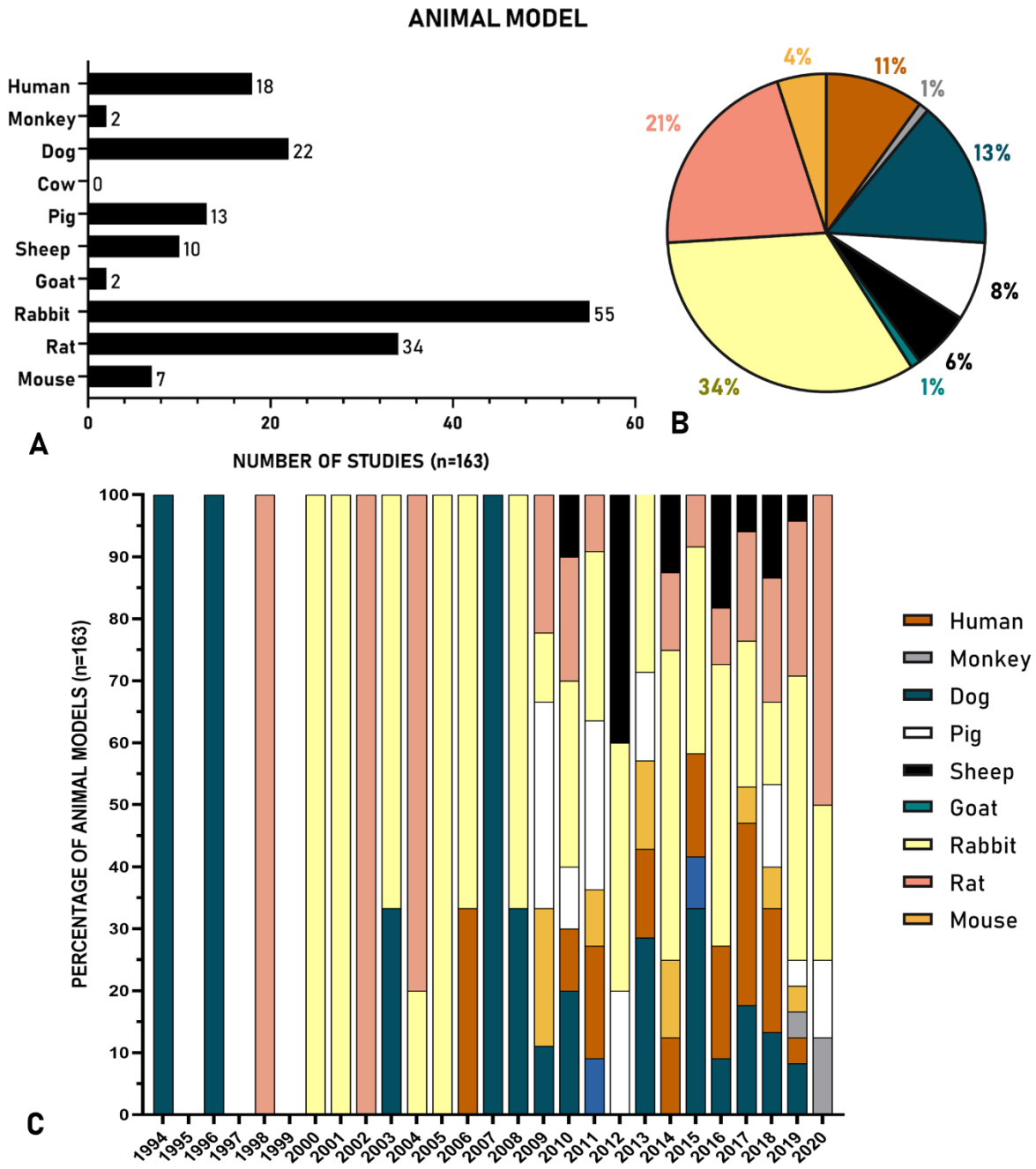

Figure 1.6. Animal model utilised for investigation of cell therapies for NP regeneration. *In vivo Studies investigating potential cellular therapy to regenerate the NP expanding over 26 years (from January 1994 to December 2020) were classified according to the animal model utilised; the number (A), percentage (B) of animal model used and the percentage of animal model used relative to the year (C) from the literature search that used the following animal model system: human, monkey, dog, cow, pig, sheep, goat, rabbit, rat and mouse.*

PROPOSED CELL SOURCES FOR NUCLEUS PULPOSUS REGENERATION

This review discusses the key cell types investigated for regenerative approaches and discusses their potential applicability for lower back pain. With a focus on native phenotype,

accessibility, survival, expansion capability and tolerance of the IVD environment. Leading to recommendations for potential cell sources for tissue regeneration approaches and their limitations. Cell types will be discussed in order of terminal differentiation, namely differentiated cells (NP, AF, NC, and chondrocytes); followed by adult stromal cells (BMSC, Adipose-derived mesenchymal stem cells (ADMSC), hUCSC); and finally, iPSCs. Other cell types were not further analysed as only a limited number of studies utilized them. These included: fibroblast cells (Chee *et al.*, 2016; Ural *et al.*, 2017; Shi *et al.*, 2019; Chen *et al.*, 2020), gynaecological cells (menstrual blood derived stem cells and human amniotic cells) (Hu *et al.*, 2014; Luo *et al.*, 2019), hematopoietic stem cells (Haufe and Mork, 2006), human embryonic stem cells (hESC) (Quintin *et al.*, 2009; Hang *et al.*, 2017; Diaz-Hernandez *et al.*, 2020), muscle derived stem cells (Vadalà *et al.*, 2008), olfactory stem cells (Murrell *et al.*, 2009) and synovial derived mesenchymal stem cells (Chen *et al.,* 2009; Miyamoto *et al.*, 2010). Cellular therapies have been proposed either as cells alone or together with instructive biomaterials or growth factors to support regenerative properties. This review, focuses on the choice of cell source for regenerative approaches and thus will not discuss the combinations with biomaterial and growth factors which have been reviewed elsewhere (Vadalà *et al.*, 2016; Tong *et al.*, 2017; Stergar *et al.*, 2019; Tendulkar *et al.*, 2019; Harmon *et al.*, 2020).

NUCLEUS PULPOSUS CELLS

NATIVE PHENOTYPE

NP cells within the mature human disc are rounded and situated within a lacunae[1], the NP cell produces abundant proteoglycans and collagen type II, with phenotypic makers of Forkhead Box F1 (FOXF1), Paired box 1 (PAX1), cytokeratin 19 (KRT19) amongst others (Risbud and Shapiro, 2011; Thorpe *et al.*, 2016; Chen *et al.*, 2016; Tang *et al.*, 2019; Wang *et al.*, 2019). NP tissue also contains a population of NP progenitor cells (Risbud *et al.*, 2007; Erwin, 2013; Chen *et al.*, 2016; Zhang *et al.*, 2020) which have been suggested to be NP-derived stem cells (NPSCs) although their full characterisation as stem cells has not been completed. NPSC *in vitro* are presented as elongated spindle shape cells (Liang *et al.*, 2017), which are positive for TEK receptor tyrosine kinase (Tie2) and express stem cell genes (e.g. Sox2, Oct3/4, Nanog, CD133, Nestin, and neural cell adhesion molecule) (Erwin *et al.*, 2013; Chen *et al.*, 2016; Zhang *et al.*, 2020). These NPSC were positive for CD73, CD90, CD105 (Wu *et al.*, 2018). NP cells show potential for osteogenic, adipogenic and, in comparison to AF and CEP cells, maintain the greatest chondrogenic potential (Wu *et al.*, 2018; De Luca *et al.*, 2020).

[1] ***Conclusion; Table 1.1. Accessibility of NP cells is ranked 1,*** *as these cells are situated in the NP within the IVD. Therefore, difficult to access and unable to use autologously.*

EXPANSION CAPABILITY AND MAINTENANCE OF PHENOTYPE

Human NP (hNP) cells are versatile, they can be harvested from cadavers, surgical samples (Tang *et al.*, 2019) and can be cryopreserved without altering cell integrity (Tanaka *et al.*, 2013). However, the numbers of cells retrieved are relatively low and *in vitro* expansion would be required to yield enough cells for further therapy. Furthermore, hNP cells extracted from degenerative discs undergo cellular senescence at an accelerated rate; and express a decreased replicative potential when compared to disc cells extracted from non-degenerate IVDs (Le Maitre et al., 2007)[2]. Rapid de-differentiation and phenotypic alterations of NP cells happen within the first passage of monolayer expansion or serial passaging in NP cells (Kluba *et al.*, 2005; De Luca *et al.*, 2020). Whereas continuous expansion (Rosenzweig *et al.*, 2017) and other three-dimensional culture systems such as NP pellet (Yung Lee *et al.*, 2001), alginates (Kluba *et al.*, 2005; Le Maitre *et al.,* 2005) or spheroid culture system (Zhang et al., 2020) leads to the maintenance and restores NP phenotype. Co-culture of hNP cells with other cell types can result in a positive effect on cell viability and proliferation e.g. doubling proliferation was seen when co-cultured with autologous hBMSC for 3 days (Mochida *et al.*, 2015).

CELL SURVIVAL IN THE INTERVERTEBRAL DISC ENVIRONMENT

Naturally, NP cells are adapted to survive within the harsh environment of the disc (Zhang *et al.*, 2020; Baumgartner *et al.*, 2021)[3], however when these cells are removed from the disc and cultured within monolayer in non-physiological conditions they may lose their adaptations to this environment. *In vitro* culture is often utilised when testing cells in IVD conditions as pH, osmolality and oxygen concentrations are easier to manipulate (Tao *et al.*, 2013; Han *et al.*, 2014; Suyama *et al.*, 2018). In altered pH conditions that resemble mild to severe degenerative IVD, NP cell viability and proliferation was sustained in low pH (Han *et al.*, 2014); rabbit NP (rNP) cells cultured in pH 7.4 displayed an increase in apoptosis and decrease in cell proliferation compared to pH 6.5, indicating that NP cells prefer mild acidic conditions. When directly comparing NP cells to ADMSC, it has been demonstrated that NP cells were less sensitive to acidic conditions and produced lower catabolic metabolism (Han *et al.*, 2014). It has previously been reported that matrix metabolic activity is also enhanced when cultured under acidic pH in bovine NP (bNP) cells (Neidlinger-Wilke *et al.*, 2012). This is an indication that bNP favours physiological conditions in comparison to hNP; high glucose also increased extracellular matrix gene expression in bNP cells compared to hNP cells (Rinkler *et al.*, 2010). A report of rabbit NPSC (rNPSC) cultured in IVD-like high osmolality using NaCl (400mOsm/kg) showed increased proliferation than isolated NP cells, whether under standard (280mOsm) or high osmolality conditions (400mOsm/kg) (Tao *et al.*, 2013).

[2] ***Conclusion; Table 1.1. Expansion capability of NP cells is ranked 2,*** *as these cells have low cell number from harvesting and inability to expand in monolayer culture conditions.*

[3] ***Conclusion; Table 1.1. Survival capability of NP cells in IVD environment is ranked 3,*** *as these cells are derived from the IVD and are adapted to survive in that physiological environment.*

However, hNP cells cultured in high osmolality increased proteoglycan production (Krouwels *et al.*, 2018). Low oxygen was not detrimental to matrix synthesis for either bNP or bAFs and even promotes the ideal NP phenotype, through an increase in aggrecan, and collagen type 2 markers (Mwale *et al.*, 2011). At low oxygen concentration Hypoxia-inducible factor -1 (HIF-1α) was mostly localised to NP cells, more so than other cells, including AF cells (Rajpurohit *et al.*, 2002; Risbud *et al.*, 2006). HIF-1α is a crucial physiological regulator in anaerobic metabolism and the constitutive expression of HIF-1α by a NP cell indicates their ability to survive and adapt to hypoxic conditions within the IVD (Ziello *et al.*, 2007).

IVD conditions of altered pH, osmolality and oxygen have a strong influence on metabolic rates, matrix production and cell survival (Bibby *et al.*, 2005). In monolayer NP and NPSC cells, can adapt and survive in IVD culture conditions, favouring altered pH, osmolality and oxygen to IVD physiological standards, which resulted in proteoglycan production. Given these findings NP cells seeded into a disc organ, have the potential to survive, proliferate and produce regenerative extracellular matrix. However, the culture of isolated cells prevents all cell-matrix interactions and signalling and thus, NP cells could act differently when cultured in *in vivo* systems (Bibby *et al.*, 2005)

NP cell transplantation into *in vivo* models have also been investigated and studies have shown that the transplanted NP cell remain viable for a number of weeks and months; allogeneic expanded rNP cells remained viable for 4 weeks in a rat model (Wang *et al.*, 2018); in a canine model, cryopreserved autologous cNP cells were observed at 12 weeks (Nukaga *et al.*, 2016) and 12 months of allogeneic expanded cNP cells (Ganey *et al.*, 2003); xenogeneic transplantation of a hNP established cell line were sustained in a rabbit model for 8 and 24 weeks (Iwashina *et al.*, 2006; Chen *et al.*, 2016), 12 weeks in a monkey model (Wang *et al.*, 2019) and 12 weeks in a canine model (Hiraishi *et al.*, 2018). Interestingly, transplanted NP cells were mainly localized in the injected zone, with cells migrating into the inner AF, suggesting that injected NP cells have the ability to migrate and integrate with native cells (Li *et al.*, 2014; Nukaga *et al.*, 2016). Once migrated to the inner AF, the cell takes upon the morphology of the native cell, such as an AF spindle-like shape. Whereas, the NP cells which stayed within the NP maintained their rounded shape (Wang *et al.*, 2018). Establishing that NP cells can remain viable and proliferate in most conditions and differing animal hosts.

REGENERATIVE EFFECT OF NUCLEUS PULPOSUS CELLS

hNP cells produced aggrecan and type II collagen and low levels of type I collagens, for up to 24 weeks when compared to the degenerate model in a number of *in vivo* systems (Ganey *et al.*, 2003; Iwashina *et al.*, 2006; Chen *et al.*, 2016; Silverman *et al.*, 2020)[4]. However, it has been observed that regenerative effects may differ depending upon the cell sources administered. Rosenzweig *et al*., (2017) observed a difference in proteoglycan expression of

[4] ***Conclusion; Table 1.1. NP cell's ability to produce extracellular matrix is ranked 3,*** *as these cells produce aggrecan and collagen type II, which are extracellular matrix physiologically found in the NP region of the disc.*

bNP and hNP cells; bNP cells resulted in higher expression of collagen type II and aggrecan (Rosenzweig *et al.*, 2017). Whereas, in expanded hNP cells protein expression was not preserved and less collagen type II and aggrecan were observed (Rosenzweig *et al.*, 2017). These differences may have been due to the hNP cells being taken from herniated degenerate discs, which would have higher levels of cellular senescence and increased inflammatory factors (Le Maitre *et al.,* 2007). There are reports that herniated cells have limited regenerative potential as they show signs of de-differentiation, degeneration and decreased aggrecan and collagen type II production (Le Maitre *et al.,* 2007; Hegewald *et al.*, 2011)[5].

hNP cells implanted into *in vivo* models, displayed partial regeneration of disc height (Hiraishi *et al.*, 2018), specifically, the results showed initial disc narrowing due to degeneration prior to implantation, followed by regenerated disc height of 14.8%, after 3 weeks analysed using MRI (Nukaga *et al.*, 2016), 18.91% and 9.7% after 4 weeks using X-ray (Iwashina *et al.*, 2006; Wang *et al.*, 2018), and 7-15% after 8 weeks using X-ray (Silverman *et al.*, 2020), in comparison to the degenerate control. Chen et al., (2016) reported that hNP and hNPSC injected into rabbit degenerate induced discs, and after 12 weeks there appeared to be no significant difference in the degenerate disc control and was actually significantly lower than in the normal 'healthy' disc (Chen *et al.*, 2016). An MRI analysis using relative signal intensity index suggested that the NPSC group restored disc height greater than the NP cell and degenerate control, however, in most studies the disc height was still less than that of a healthy disc (Iwashina *et al.*, 2006; Chen *et al.*, 2016; Nukaga *et al.*, 2016; Hiraishi *et al.*, 2018; Silverman *et al.*, 2020). Despite improvement to disc height seen in most studies and GAG production, NP cells used to regenerate the disc were able to halt further degeneration, but not significantly improve the degenerate condition in the context of Pfirrmann classification; which was reported at grade 2-3 (Mochida *et al.*, 2015; Nukaga *et al.*, 2016), whereas the degenerate discs displays progressive degeneration to grade 3-5 (Nukaga *et al.*, 2016).

CONCLUDING REMARKS

NP cells are able to demonstrate long term survival *in vivo* and display their ability to adapt to the IVD microenvironment, including differences to osmolality, oxygen and pH conditions, however NPSC also have this ability and further displayed regenerative effectiveness; recently, NPSC (or NP progenitor cells) have been successfully expanded from NP cell populations following spheroid culture system (Zhang *et al.*, 2020). It was reported that animal NP cells differed in responsiveness and bNP cells were less representative of hNP cells. NP cells demonstrated their ability to produce GAG for regenerating a degenerate disc, with slight restoration. However, the main issue with the use of native NP cells in a regenerative approach is the sourcing of these cells as harvesting from a normal disc would induce disc degeneration, but if cells are harvested from an already degenerate or herniated disc, these

[5] ***Conclusion; Table 1.1. The potential adverse effects of using NP cells is ranked 2,*** *as NP cells used from a degenerative disc source resulted in less regeneration of disc and an increase in inflammatory factors. Subjecting patients through treatments that may result in no significant improvement.*

cells would show increased catabolism and thus reduced regenerative capacity, although sourcing from cadavers could be a possibility. Such cells are currently in clinical trials (Discogenic Ltd.) and thus the results of these studies will be interesting to follow (Tschugg *et al.*, 2016).

ANNULUS FIBROSUS CELLS

NATIVE PHENOTYPE

AF cells in the inner AF are rounded, chondrocyte-like cells. Progressing to the outer AF, cells are more elongated in morphology, similar to fibroblasts (Pattappa *et al.*, 2012). The outer AF is mechanically strong matrix composed of a higher ratio of collagen type I to type II, resulting from expression of COL5A1, a gene that regulates collagen type I assembly (Poiraudeau *et al.*, 1999; Sato *et al.*, 2003; Colombier *et al.*, 2016).

EXPANSION CAPABILITY AND MAINTENANCE OF PHENOTYPE

The expansion capability for AF cells is very similar in some ways to NP cells. The same method of cell isolation[6] and expansion is often used (Colombini *et al.*, 2015; De Luca *et al.*, 2020) which extracts, per grams of tissue, roughly the same low density yield of cells as NP (Roughley *et al.*, 2006; Torre *et al.*, 2019)[7]. AF cells also share a similar phenotype: positive for CD44, CD73, CD90, CD105, CD151 and CD166 and negative for CD34, CD45, CD146, and similar transcriptome profiling to NP cells (Power *et al.*, 2011). However, Van den Akker *et al.,* (2020) published a set of novel membrane-associate markers for NP and AF cells, thus distinguishing the few markers specific for AF, e.g. Secreted Frizzled Related Protein 2 (SFRP2) and COL1A1 (Van den Akker *et al.*, 2020). Similar to NP cells, AF cells show osteogenic and chondrogenic potential, but with a greater number of highly expressed stemness genes (De Luca *et al.*, 2020).

CELL SURVIVAL IN THE INTERVERTEBRAL DISC ENVIRONMENT

As AF cells are native to the IVD environment, it is no surprise that when transplanted into *in vivo* rabbit IVDs, >90% of allogeneic AF cells were viable 12 weeks post-transplantation (Sato *et al.*, 2003)[8].

---

[6] ***Conclusion; Table 1.1. Accessibility of AF cells is ranked 1****, as these cells are situated in the AF within the IVD. Therefore, difficult to access and unable to use autologously.*

[7] ***Conclusion; Table 1.1. Expansion capability of AF cells is ranked 2,*** *as these cells have low cell number from harvesting.*

[8] ***Conclusion; Table 1.1. Survival capability of AF cells in IVD environment is ranked 3,*** *as these cells are derived from the IVD and are adapted to survive in that physiological environment.*

REGENERATIVE EFFECT OF ANNULUS FIBROSUS CELLS

The majority of studies utilising AF cells in this literature search were *in vitro* methods, with two papers studying AF cells in rabbit induced degeneration disc models (Sato *et al.*, 2003; Wang *et al.*, 2015). AF cells *in vitro* have been shown to produce elastin (Sato *et al.*, 2003; Sakai and Andersson, 2015; Bhunia *et al.,* 2018) and predominantly collagen type I, where collagen type II remained undetected (Helen and Gough, 2008; Colombini *et al.*, 2015; Frauchiger *et al.*, 2018). Even in different biomaterial culture conditions, AF cells favour the synthesis collagen type I, a characteristic of native fibrocartilaginous AF tissue (Helen and Gough, 2008; Colombini *et. al.*, 2015; Frauchiger *et. al.*, 2018)[9]. The two *in vivo* studies highlighted that collagen type II and aggrecan were upregulated (Wang *et al.*, 2015). The structure of the inner AF was significantly preserved (Wang *et al.*, 2015) and strong Safranin-O staining was observed in the AF cell-transplanted NP tissue, which is very histologically similar to hyaline-like cartilage and normal AF (Sato *et al.*, 2003).

CONCLUDING REMARKS

AF cells predominately produce an unfavoured collagen type I and cartilage-type matrix, which did not resemble the native extracellular matrix of the NP[10]. Thus, in the IVD regeneration field, AF cells in are mainly utilised for AF repair (Gebhard *et al.*, 2010; Yang *et al.*, 2016; Bhunia *et al.*, 2018; Frauchiger *et al.*, 2018; Nukaga *et al.*, 2019). There are a couple of reviews that have discussed large animal and clinical trials studies that target the 'sealing' of AF to prevent disc herniation which is outside the scope of the current review (Sloan *et al.*, 2018; Olivia M Torre *et al.*, 2019).

NOTOCHORDAL CELLS

NATIVE PHENOTYPE

Notochordal (NC) cells are distinct through their relatively large size (>20µm) and presence of vacuoles (Kim *et al.*, 2009; Ellis *et al.,* 2013)[11]. In many studies this classic phenotype was used to distinguish between other cell types (Gantenbein *et al.*, 2014).

[9] ***Conclusion; Table 1.1. AF cells ability to produce extracellular matrix is ranked 2,*** *as these cells produce cartilage like matrix, which is not phenotypic of the NP region.*

[10] ***Conclusion; Table 1.1. The potential adverse effects of using AF cells is ranked 2,*** *as using this cell source wouldn't result in a regeneration of the native matrix production, thus subjecting patients through treatments that results in no significant improvement.*

[11] ***Conclusion; Table 1.1. Accessibility of NCs is ranked 1****, as these cells are only situated in the NP region of certain species of animals and in humans under the age of 10.*

EXPANSION CAPABILITY AND MAINTENANCE OF PHENOTYPE

In standard monolayer culture, this distinct phenotypic characterisation of Notochordal cells (NC) were lost with expansion of porcine NC (pNC) cells after 28 days (Potier *et al.*, 2014; Potier and Ito, 2014) or within 1-3 passages (Gantenbein *et al.*, 2014); cNCs observed a loss in NC characterisation after 6 days in monolayer (Smolders, Meij, *et al.*, 2013). It was reported that NCs acquired a NP-like morphology (small, round cells) and became indistinguishable from NP cells (Gantenbein *et al.*, 2014; Potier and Ito, 2014). There are additional reports of a decrease in NC marker expression such as Brachyury (Gantenbein *et al.*, 2014), Keratin (KRT) 8, and KRT19 (Potier and Ito, 2014). Gantenbein *et al*., (2014) reported that when pNCs are cultured in monolayer, they are outcompeted by smaller (< 8µm) NP cells, despite the culture starting as 80% NC population. Kim *et al*., (2009) highlighted that NCs grown in monolayer culture had a significantly slower growth rate of 135 hours population doubling time (PDT) compared to NP cells which showed a growth rate of 23 hours PDT. This is in conjunction with the observation that single isolated NCs morphologically differentiated into 3 distinct cell types: vacuolated NCs, giant cells, and small NP cells (Kim *et al.*, 2009; Spillekom *et al.*, 2014). As a result, alternative methods such as co-culturing NCs with other cells and culturing in 3D *in vitro* culture models have been investigated. When canine NCs (cNCs) are cocultured with cMSC, an increase in proteoglycan production and maintenance of NC phenotype was observed (Arkesteijn *et al.*, 2015). NCs were shown to have high cell viability for up to 42 days in alginate bead culture (Purmessur *et al.*, 2013; Arkesteijn *et al.*, 2017), with one study reporting up to 80% cell viability at 10 days (Kim *et al.*, 2009), and Gantenbein *et al*., (2014) reported that a higher fraction of around 50% of pNCs were recoverable after 34 days of culture when compared to the identical cell population grown in monolayer. Providing evidence that keeping NCs in 3D cultures, which would resemble their *in vivo* cluster form, rather than completely isolating them in monolayer, could preserve the NC phenotype better during *in vitro* culture (Gantenbein *et al.*, 2014; Spillekom *et al.*, 2014; Humphreys *et al.*, 2018)[12].

CELL SURVIVAL IN INTERVERTEBRAL DISC ENVIRONMENT

NCs are sensitive to culture conditions. Osmolality has been shown to affect NC phenotype, Spillekom *et al*., (2014) cNCs cultured in Minimum Essential Medium α (αMEM) at 400mOsm/kg contained more vacuolated cells and showed significantly higher Brachyury expression compared with high glucose Dulbecco's Modified Eagle Medium (DMEM)/F12 and αMEM both at 300mOsm/kg. Guehring *et al*., (2009) established that NC are also highly metabolically active; consuming more oxygen and glucose and producing more lactate compared to NP cells. Thus, NC exhibit a strong nutrient dependency (Arkesteijin *et al.,* 2017;

[12] ***Conclusion; Table 1.1. Expansion capability of NCs is ranked 1,*** *as there's limited experience in handling these cells in research and the few research has shown that NCs are problematic in monolayer and in continuous expansion culture conditions.*

Gantenbein *et al*., 2014), which resulted in some studies altering the culture condition when culturing NCs: such as adding 10% foetal calf serum (FCS) supplement (Gantenbein *et al.*, 2014), whilst other studies co-culturing NC and other cells at a lower ratio of 30:70 (Arkesteijn *et al.,* 2017) as seeding the disc with a high cell density may lead to the cell death (Arkesteijn *et al.*, 2017). Further, NCs were more sensitive to nutrient deprivation than other disc cells and were found to not survive under conditions which NP cells were still viable and interestingly, the porosity of the cartilage endplate is correlated with the nutrient supply and presence of NCs (Urban *et al.,* 1978; Urban *et al.*, 2001; Hunter *et al.,* 2004; Guehring *et al.*, 2009). Despite NC sensitivity in nutrient deprivation, culture preference is with low glucose media αMEM at 400mOsm/kg (Spillekom *et al.*, 2014). Finally, oxygen content as Gantenbein *et al*., (2014) observed, also plays a role in NC marker expression. Brachyury and CD24 was only expressed in the 2% oxygen conditions and downregulated in the 20% oxygen, indicating that NCs were functional only in physioxia conditions (Erwin, 2013; Gantenbein *et al.*, 2014). Despite these findings, to date there appears to be no ideal culture conditions established for NCs. IVDs are subject to other stimuli which could impede NC's ability to regenerate the disc, such as mechanical loading exerted *in vivo* and its effect on the NC metabolism and biosynthesis. Purmessur *et al.,* (2013) used an *ex vivo* model of pNC-rich NP tissue loaded into a hydrostatic pressure chamber and subjected the tissue to a daily load of 0.5 to 2MPa at 0.1Hz for 2 hours (Purmessur *et al.*, 2013). Despite the reported increase in proteoglycan accumulation observed in the daily loading control, the histological images show the cell population transitions from ~75% of large NCs being observed in the control to ~25% in the daily pressurization control. Which together with the lack of evidence of apoptosis, supports potential differentiation into small NP cells under load. The study concluded that NCs were able to withstand the hydrostatic loading, with the daily loading regime causing little effect on cell viability in comparison to the controls, but the results showed that the large vacuolated morphology of NCs decreased under load, suggesting alteration in cell phenotype[13].

REGENERATIVE EFFECT OF NOTOCHORDAL CELLS

Due to the loss of NC phenotype in culture, efforts have been made to improve regenerative effects by co-culturing NP cells with other cells or 3D culture. Most studies investigated NCs with a co-culture of NP cells. A significant increase in the GAG/ Deoxyribonucleic acid (DNA) ratio at 7 days, irrelevant of oxygen concentration was observed with the co-culture of pNCs and bNP (Gantenbein et al., 2014), which after 14 days GAG/DNA ratio was only significantly increased in specifically the 2% oxygen control. However, other studies observed only slight increase in GAG or insignificant change in extracellular matrix content when cNC and cNP were co-cultured (Arkesteijn *et al.*, 2015); and pNC and bNP cells were co-cultured (Arkestejin

[13] ***Conclusion; Table 1.1. Survival capability of NCs in IVD environment is ranked 3,*** *as these cells are derived from the IVD and are adapted to survive in that physiological environment.*

et al., 2017; Potier *et al.,* 2014). In respect of specific extracellular gene expression: Arkesteijn *et al.,* (2017) demonstrated the inhibitory potential of NCs on collagen type I expression, as an increased expression in collagen type I was significantly increased in the degenerative control and not in the pNCs control (Arkesteijn *et al.* 2017). Aggrecan was upregulated in the co-culture pNCs and bNP at 14 days (Gantenbein et al., 2014) and cNCs cultured in αMEM 400mOsm/kg conditions at 28 days (Spillekom *et al.*, 2014). In Arkesteijn *et al.,* (2017) and Potier and Ito, (2014) there was no significant increase in collagen type II reported in *in vitro* NC controls, however both studies also documented the loss of NC morphology (Arkesteijn *et al.* 2017; Potier and Ito, 2014), whereas Spillekom et al., (2014) observed collagen type II in cNC cultured at 28 days in higher osmolality and lower glucose conditions (Spillekom *et al.*, 2014). A major limitation with the co-culture of NC and NP cells, is that, as previously discovered, both cells proliferate at different rates and thus NCs could be overcrowded by the proliferation of NP cells (Potier *et al.*, 2014; Spillekom *et al.*, 2014), and NC demanding dependency of culture conditions. NCs show constant DNA content throughout culture and can display an increase in proteoglycan production through a high GAG/DNA ratio, thus demonstrating an efficient phenotype for producing extracellular matrix within the limited nutrient environment of the IVD. Furthermore, Cappello *et al*., (2006) reported cNCs could produce proteoglycans at a 1.5-fold greater rate of synthesis than cNP cells; thus, indicating that the extracellular matrix produced by NCs is assembled in a distinct manner different to NP cells, as proteoglycans secreted from NCs migrate and aggregate quicker compared to NP cell synthesized proteoglycans (Cappello *et al.*, 2006)[14]. The next question would be: is the extracellular matrix produced by NCs more favourable to regenerating the degenerative disc *in vivo*?

There have been limited use of NCs *in vivo* models, however the studies that have used NCs for regeneration of degenerative discs have shown promising results. Liu *et al.,* (2018) used rNCs in a rat model in which degeneration was induced via puncture, where NCs restored the loss of proteoglycans and maintained NP/AF boundary (Liu *et al.*, 2018). Collagen type II was significantly increased when compared to the degenerative control and the rNP : rNC combined. As a result, disc height was increased compared to degenerative controls and a disc injected with rNC and rNP cells (Liu *et al.*, 2018).

CONCLUDING REMARKS

NCs are highly viable in the conditions related to the IVD and have been shown to upregulate collagen type II and down-regulate collagen type I, however limited studies have been able to preserve their large vacuolated morphology and most suggest that they differentiate into small NP-like cells when they are cultured in the harsher degenerative disc conditions (Purmessur *et al.*, 2013; Potier *et al.*, 2014; Gantenbein *et al.*, 2014; Spillekom *et al.*, 2014;

[14] ***Conclusion; Table 1.1. NCs ability to produce extracellular matrix is ranked 3,*** *as these cells produce proteoglycans at a higher fold than NP cells and extracellular matrix at the same physiological GAG/DNA ratio.*

Humphreys *et al.*, 2018). There are inconclusive results for the ideal culture conditions of NCs, the general consensus is that due to their *in vivo* cluster form, 3D alginate bead culture is preferred; however, from all the studies extracted from the literature review, no studies have investigated NCs in biomaterials to date. The lack of progression with NCs in studies could be explained by species-specific difference[15], but also, and most likely, by variances in isolation protocols and/or in culture conditions. As stated above, a valuable characteristic of NCs is their anti-angiogenic effects; the natural IVD conditions and mechanical stimuli promote vascular growth, which if unchecked may lead to a worsened state of IVD degeneration and contribute to the symptoms of pain (Purmessur *et al.*, 2013; Kwon *et al.*, 2017). The anti-angiogenic molecules produced by NCs have the potential to prevent such unfavourable consequences. However, a key limitation of utilising NCs is obtaining a suitable cell source as human discs do not retain NCs beyond adolescence; xenografts would need to be deployed which also have limitations. Furthermore, the difficulties seen in NC expansion/culture, but the advantageous characteristics has led to alternative approaches of developing human derived NCs through autologous iPSCs (Tang *et al.*, 2018; Sheyn *et al.*, 2019; Colombier *et al.*, 2020; Zhang *et al.*, 2020) (see section on iPSCs) or non-cell based therapy with the introduction of NC-conditioned media and the potential use of NC matrix or growth factors derived from NCs (De Vries *et al.*, 2019).

CHONDROCYTES

NATIVE CHARACTERISTICS, EXPANSION CAPABILITY AND MAINTENANCE OF PHENOTYPE IN AN INTERVERTEBRAL DISC ENVIRONMENT

Chondrocytes harvested from different sources[16] are able to adapt their phenotype and differentiate into a spherical shape with well-formed lacunae irrelevant of their *in-situ* culture system, for example, nasal chondrocytes in *in vitro* 3D pellet culture (Gay *et al.*, 2019), alginate beads (Vedicherla and Buckley, 2017) or in hydrogel (Tsaryk *et al.*, 2017), and auricular chondrocytes *in vivo* rabbit IVD (Gorenšek *et al.*, 2004). Numerous reports evaluated the following cell surface proteins as potential markers of chondrogenesis, namely CD29 in combination with CD49, CD146, and CD166 (Vinod et al., 2018), with Sox9 being the strongest indicator of chondrocytic lineage (Janssen *et al.,* 2018; Koelling *et al.,* 2009*)*.

As chondrocytes also exhibit favourable properties for cartilage repair, there are systematic reviews that have collated information on the culture and expansion capability of

[15] ***Conclusion; Table 1.1. The potential adverse effects of using NCs are ranked 3,*** *as NCs used are xenogenous and could pose a rejection reaction.*

[16] ***Conclusion; Table 1.1. Accessibility of Chondrocyte cells is ranked 2,*** *as these cells can be harvested from multiple sources in the body, however they are invasive procedures and could lead to injury at the site of cell source.*

chondrocytes; highlighting that chondrogenic phenotype can be maintained using low glucose and hypoxic conditions (Vinod, *et al.,* 2020). Chondrocytes retain good expansion capability with Fellows *et. al.,* (2017) reporting human chondrocytes retained good viability after passage 9 (Fellows, *et. al.,* 2017; Vinod, *et. al.,* 2020)[17]. Gay *et al*., (2019) conducted an insightful study comparing articular and nasal chondrocytes, with the chondrocytes harvested from the same animal model. The study investigated how the cell types respond to different environments that are associated with the IVD, such as altered oxygen and glucose concentrations, within an *in vitro* pellet culture model. In this study nasal chondrocytes were the cell type that displayed an increase in DNA content in each condition, indicating that nasal chondrocytes can survive, adapt, and proliferate favourably when directly compared to articular chondrocytes (Vedicherla and Buckley, 2017; Gay *et al.*, 2019). *In vivo* chondrocytes demonstrated the potential for long-term survival of transplanted cells; transplanted autologous auricular chondrocytes were shown to survive for at least 6 months in a rabbit model (Gorenšek *et al.*, 2004), and porcine articular cartilage remained viable at 12 months post injection into a porcine model (Acosta *et al.,* 2011)[18]. Throughout the studies using chondrocytes for cell therapy for IVD regeneration, the cells were shown to be tolerant to the disc environment, most probably due to its similarities to the condition of cartilage the chondrocytes are derived, and remain viable post-transplantation in small animal models (Gay *et al.*, 2019).

REGENERATIVE EFFECT OF CHONDROCYTES

With the confirmation of sustained cell viability, most studies also investigated potential for restoration of the IVD through analysing matrix production. In normal conditions of 21% oxygen in a monolayer, articular chondrocytes were able to up-regulate aggrecan, type I and type II collagen messenger ribonucleic acid (mRNA), when compared to AF cells in the same conditions (Kuh *et al.*, 2009). In conditions related to the IVD (hypoxic and low glucose), nasal chondrocytes and articular chondrocytes were both capable of producing GAGs and collagen type I and type II (Kuh *et al.*, 2009). Furthermore, in the IVD conditions nasal chondrocytes produced a ratio of low collagen to high GAG content, whereas articular cells produced a less favourable high collagen content (Vedicherla and Buckley, 2017). However, when acidic and inflammatory cytokines were introduced to represent a degenerative disc environment, neither articular chondrocytes nor nasal chondrocytes stained for GAGs (Gay *et al.*, 2019).

[17] ***Conclusion; Table 1.1. Expansion capability of Chondrocyte cells is ranked 2,*** *as these cells can be easily expanded in different in vitro culture systems, whilst still maintaining good viability after several passages. However, they are limited by senescence.*

[18] ***Conclusion; Table 1.1. Survival capability of Chondrocyte cells in IVD environment is ranked 3,*** *as it has been demonstrated that these cells can survival and proliferate in in vitro IVD environment and survive in the IVD of in vivo animal models.*

In vivo transplantation of auricular and articular chondrocytes within the degenerative NP resulted in the production of proteoglycans for up to 12 months in a porcine model (Acosta *et al.*, 2011) and tissue formation which resembled hyaline-like cartilage was apparent in a rabbit model (Gorensek *et al*., 2004). Despite the chondrocytes' ability to express extracellular matrix components, it was duly noted that the values were not in the same range of magnitude as native tissue, with native healthy NP tissue having a unique biochemical composition with a GAG to collagen ratio of 27 : 1 (Mwale *et al.*, 2004)[19]. Studies also assumed that the filling of the degenerate disc with matrix produced from the chondrocytes, were deemed 'restored' and did not review how the composition, for example of type I and type II collagens (which are usually understood to be an unfavourable structure of scar tissue in knee joints), would fare in restoring the biomechanical properties of the disc. Therefore, it would be logical to favour a cell source which can accumulate a similar, if not equal, amount and type of extracellular matrix as a healthy NP (Gay *et al.*, 2019).

CONCLUDING REMARKS

Several different sources of chondrocytes have been utilised in studies were regenerating the IVD is proposed, including articular chondrocytes, nasal chondrocytes, endplate chondrocytes and auricular chondrocytes. Signifying chondrocytes are readily available from multiple sources and could be autologous, although some sources are more accessible than others. The ultimate issue with using chondrocytes as cell therapy, refers to the fact that they maintain their chondrocyte phenotype in the disc. This is not the characteristic we want to observe in the NP, as chondrocytes produce cartilage and extracellular matrix that is macroscopically more solid in comparison to the gelatinous healthy NP (Gorenšek *et al.*, 2004), and does not contain the same composition as native NP (Sato *et al.*, 2003). Despite these limitations, studies investigating chondrocytes for IVD regeneration, identify a cell type that is reliable and stable, easy to expand *in vitro* and remains viable under the harsh conditions of the IVD. Throughout these studies there was no evidence of necrotic change, unfavourable bone growth, transplanted cell migration, nor were there any active signs of tissue vascularization (Ganey *et al.*, 2003; Gorenšek *et al.*, 2004; Meisel *et al.*, 2007)[20]. In fact, Acosta *et al.,* (2011) demonstrated that chondrocyte treated discs produced high levels of the anti-angiogenic/neurogenic factor, chondromodulin-I, which lasted for at least 12 months post injection (Acosta *et al.,* 2011). Potentially making chondrocytes a viable option for regeneration, if the correct IVD phenotype can be reproduced by transplanted cells.

[19] ***Conclusion; Table 1.1. Chondrocyte cell's ability to produce extracellular matrix is ranked 2,*** *as these cells were shown to be able to produce extracellular matrix in vitro and in vivo models, however it did not resemble the phenotypic matrix observed in the NP.*

[20] ***Conclusion; Table 1.1. The potential adverse effects of using Chondrocyte cells is ranked 2,*** *as using this cell source wouldn't result in a regeneration of the native matrix production, thus subjecting patients through treatments that results in no significant improvement.*

ADULT STROMAL CELL SOURCES

Adult stromal cells are favourable for their self-renewal properties and have a much greater interest than embryonic stem cells (ESCs) because of several disadvantages of ESCs. hESC show notable tumorigenic properties, through an increase of telomerase activity, leading to high proliferation and potential formation of teratomas. Additionally, using embryonic cells is surrounded by several ethical issues, therefore it is a less preferable option for future IVD regeneration approaches (Oehme *et al.*, 2015). Adult stromal cells can be isolated from various tissues including umbilical cord, bone marrow, and adipose tissue (Chun *et al.*, 2012).

BONE MARROW STROMAL CELLS

NATIVE CHARACTERISTICS, EXPANSION CAPABILITY AND MAINTENANCE OF PHENOTYPE

BMSC display similar fibroblastic morphologies, with an apparent marginally extending cytoplasm in monolayer culture, indicating plastic adhesion ability (Pattappa *et al.,* 2012; Shim et al., 2016; Yang *et al.,* 2019; Li et al., 2020). BMSC express cell surface markers, including CD29, CD44, CD73, CD90, CD105 and CD166 and are negative for typical markers of haematopoietic stem cells, CD34, leukocytes, CD45 and endothelial cells such as CD14 (Bucher et al., 2013; Mwale *et al.*, 2014; Tsaryk *et al.*, 2017; li et al., 2020). BMSC can maintain cell markers in 90% of cells after passage 4/5 (Henriksson *et al.*, 2009; Tsaryk *et al.*, 2017); however, this cell type favours high-glucose condition (4.5g/L) independent of oxygen concentration (Gay et al., 2019). BMSC are easily manipulated, if exposed to the appropriate stimuli *in vitro,* they can differentiate into osteogenic, chondrogenic and adipogenic lineages (Mwale *et al.*, 2014; Tsaryk *et al.*, 2017; Yang *et al.,* 2019; Li et al., 2020)[21].

CELL SURVIVAL IN THE INTERVERTEBRAL DISC ENVIRONMENT

In vitro, altered hypoxic conditions resulted in an increase in cell viability in rBMSC (Wuertz *et al.*, 2008; Wang *et al.*, 2018) and reports of no change in metabolic activity hBMSC (Binch et al., 2019; Gay *et al.,* 2019; Peroglio *et al.,* 2013). An observation that pro-inflammatory cytokine stimulation does not change the hBMSC metabolic and cell activity (Binch et al., 2019). In contrast, when BMSC were cultured in IVD-like pH (6.8) or osmolality of 485mOsm, cell proliferation and expression of matrix proteins were strongly decreased in rBMSC (Wuertz *et al.*, 2008) and in hBMSC (Gay et al.,2019). Suggesting that acidic conditions and high osmolality were critical factors that reduced biosynthesis and proliferation of BMSC *in vitro*. In a degenerated animal disc models *in vivo,* hBMSC have been reported to remain viable and

[21] ***Conclusion; Table 1.1. Expansion capability of BMSCs is ranked 3,*** *as these cells can be easily maintained after multiple passages and are easily manipulated into different cell lineages.*

survive in porcine IVDs for 6 months (Henriksson *et al.*, 2009), rabbits for 3 months (Papadimitriou et al., 2015), rats for 6 weeks (Wei et al. 2007), and bovine for 3 weeks (Mwale *et al.*, 2014). Reports from *in vitro* and *ex vivo* analysis show that when BMSC are subject to IVD-conditions they differentiate towards NP-cell like phenotype (Wei et al., 2009; Henriksson et al., 2009), with elevated SRY-Box Transcription Factor 9 (SOX9) gene expression after 7 days (Le Maitre et al., 2009) and 14 days *in vitro* (Gay *et al.,* 2019; Kumar *et al.*, 2014; Shim *et al.,* 2016), and after 1 month (Wei et al., 2009) and 3 to 6 months *in vivo* (Henriksson et al., 2009)[22]. Recently more efforts have been made to differentiate BMSC into NP cells *in vitro,* utilising the IVD environment, such as using NP conditioned medium and hypoxia (Sinkemani et al., 2020) or co-cultured with NC-rich NP tissue (Li et al., 2020).

REGENERATIVE EFFECT OF BONE MARROW STEM CELLS

Human aspirated BMSC is frequently used to inject into degenerative induced models of rabbit (Papadimitriou et al., 2015), rat (Wei et al., 2009), porcine (Henriksson *et al.*, 2009) and bovine (Chan *et al.*, 2013; Mwale *et al.*, 2014; Pereira *et al.*, 2016), and are one of a few cell types that has been established in human clinical trials (Henriksson *et al.*, 2009; Orozco *et al.*, 2011; Elabd *et al.*, 2016; Centeno *et al.*, 2017; Noriega *et al.*, 2017; Pettine *et al.*, 2017; Blanco *et al.*, 2019; Binch *et al.*, 2021). The introduction of hBMSC in animal models resulted in increased collagen type II and aggrecan expression (Mwale et al., 2014; Henriksson et al., 2009; Pereira et al., 2016), collagen type I (Henriksson *et al.*, 2009; Pereira et al., 2016) was also observed in small areas of NP, increased compared to degenerative controls but less than healthy discs. Interestingly, proteoglycans were expressed throughout the NP region in hBMSC treated disc controls, even in areas void of cells (Mwale et al., 2014). Analysis using transmission electron microscopy displayed degenerative discs treated with hBMSCs preserved some lamellar organization, as well as a denser matrix in both AF and NP, resembling the healthy disc control group (Pereira *et al.*, 2016). These results could be due to the observation that after the injection of hBMSC studies have shown that the expression of SOX9 was detected in the injected cells, indicating that when hBMSC are subject to the IVD environment they tend to differentiate towards disc-like cells (Henriksson *et al.*, 2009; Peroglio et al.,2013; Wei et al., 2009)[23]. However, BMSC have been shown to have potentially adverse characteristics of migrating away from the injected site. Henriksson et al., (2009) reported areas of tissue with limited injected hBMSC cells and many studies have observed that BMSC migrate away from the injection site; BMSC have been found distributed throughout the NP region (Mwale et al., 2014), in the border zone between NP and AF

[22] ***Conclusion; Table 1.1. Survival capability of BMSCs in IVD environment is ranked 2,*** *as in vitro IVD conditions effected BMSCs biosynthesis and proliferation ability, however these cells were able to survive in vivo animal models as they differentiated towards NP-like cells.*

[23] ***Conclusion; Table 1.1. BMSC's ability to produce extracellular matrix is ranked in IVD environment is ranked 3,*** as in in vivo animal studies BMSCs that differentiate into NP-like cells have shown their ability to produce NP native matrix, resulting in some disc regeneration.

(Henriksson *et al.*, 2009), and cells seeded onto the CEP migrated into the NP (Pereira *et al.*, 2016; Wangler et al., 2019)[24]. Animal studies have demonstrated hBMSC capability to differentiate into an NP-like phenotype, display matrix producing properties and with no adverse bone mineralization being detected in large animal models (Henriksson *et al.*, 2009), therefore BMSC have transitioned to clinical trials on human patients which has been reviewed recently (Kim and Yang, 2012; Meisel *et al.*, 2019).

Patients used for BMSC clinical trials were selected based on lower back pain diagnosed with disc degeneration (Centeno et al., 2017; Orozco et al., 2011; Noriega et al., 2017; Pettine et al., 2017), lumbago (Yoshikawa et al., 2010) or their candidacy for spinal fusion or total discectomy (Pettine et al., 2017). More specifically, the inclusion symptoms were pain (Yoshikawa *et al.*, 2010; Elabd *et al.*, 2016; Centeno *et al.*, 2017; Noriega *et al.*, 2017; Pettine *et al.*, 2017), the presence of a posterior disc bulge or small protrusion (Elabd *et al.*, 2016; Centeno *et al.*, 2017) or disc height loss (Noriega et al., 2017; Pettine et al., 2017). Interestingly, two clinical studies requested an intact annulus fibrosus ring capable of holding cells (Noriega et al., 2017; Orozco et al., 2011). Only one study injected allogeneic hBMSC (Noriega et al., 2017), while the rest used patient derived autologous hBMSC. The allogeneic therapy posed no safety concerns and was concluded to be a valid and a more convenient alternative to autologous BMSC-treated patients (Noriega et al., 2017). Quality control tests of karyotyping the BMSC were monitored and displayed that the injected BMSC characteristics remained stable over time (Orozco *et al.*, 2011), with no adverse effects being reported in either allogeneic (Noriega *et al.*, 2017) or autologous BMSC injection, also demonstrating safety (Elabd *et al.*, 2016). The methods that were used to analyse the regenerative effects of BMSC treatment differed between each clinical trial. In one study, 40% of patients improved 1 modified Pfirrmann grade, with no radiographic worsening (Pettine *et al.*, 2017). MRI analysis was used to assess the visual bulging of the treated disc. Reports of the reduction of the IVD posterior bulge by an average of 23% after 6-month post-treatment (Centeno et al., 2017), and another study observed 4 out of 5 patients posterior protrusion reduced by 20%, 43%, 40% and 48%, with one patient displaying mild progression and a 25% increase in size of their posterior protrusion, after 4-6 year post-treatment (Elabd *et al.*, 2016). Water content was also analysed through MRI; BMSC treatment resulted in an observed increase in water content in the disc in patients after 12 months post-treatment (Orozco *et al.*, 2011; Noriega *et al.*, 2017) and visualised after 2-year post-treatment (Yoshikawa *et al.*, 2010). Orozco et al., 2011 reported that despite the increase in water content, disc height was not recovered through treatment (Orozco *et al.,* 2011). Throughout clinical trials the assessment of pain and disability was the method of analysing regeneration. However, studies

[24] ***Conclusion; Table 1.1. The potential adverse effects of using BMSCs is ranked 2,*** *as in in vivo animal studies BMSCs have shown to migrate away from the injected site, posing a risk of bone formation in unwanted areas of the IVD. Additionally, BMSCs are used in clinical human trails which has shown no overall significant change to LBP patients, as the use of BMSC resulted in slowing down the degeneration of the disc and not regenerating the disc.*

had differing methods of scoring and analysing pain and disability, with some patients self-reported overall quality of life improvements despite reports of continued disc degeneration (Elabd *et al.*, 2016). Four clinical trials utilised the Oswestry Disability Index (ODI) to assess disability and visual analogue scale (VAS) to evaluate pain; disability was reduced 3 months post-treatment, which was maintained till 12 months (Noriega *et al.*, 2017), 12 months post-treatment (Blanco *et al.*, 2019) and a slight reduction in disability was observed (Noriega *et al.*, 2017). Lumbar pain was acutely reduced 3 months post-treatment, followed by minimal difference to 12 months (Noriega *et al.*, 2017), or patients that reported >25% reduction of posterior bulge also reported lower pain score at 6 months post-treatment (Centeno et al., 2017). Sciatic pain improved at 6 - 12 months post-treatment (Orozco *et al.*, 2011) and 4-year post-treatment lumbar and radicular pain improved (Blanco *et al.*, 2019).

CONCLUDING REMARKS

BMSC are easily sourced[25] and easy to differentiate *in vitro,* once in an IVD environment BMSC commonly differentiate towards NP-cell like phenotype, expressing NP markers CD24, KRT19, SOX9, aggrecan, collagen type II and produce proteoglycans. These characteristics transition into large animal models. However, *in vivo* BMSC were not able to produce enough matrix to reverse the degenerated disc, as BMSC which were used to investigate regeneration of enzyme induced degeneration in an animal model with a complete digested NP showed an inability to survive. Whilst in a less harsh degenerative disc model, injected BMSC were unable to produce enough matrix comparable to a healthy disc. One major limitation was the ability of BMSC to migrate, as demonstrated when BMSC appeared in the NP despite being seeded onto the CEP; BMSC migrating from the CEP into the vertebrae may give rise to BMSC differentiating into osteophytes, which has been reported of BMSC leakage into adjacent vertebrae in a rabbit model (Vadalà *et al.*, 2012). Despite these potential adverse effects, clinical trials demonstrate the safety and efficacy of autologous and allogeneic BMSC implantation (Noriega et al., 2017; Elabd et al., 2016; Orozco et al., 2011; Pettine et al., 2017; Blanco et al., 2019). MRI displayed BMSC treatment improved moisture content, disc bulges were reduced, but no significant difference to height of the disc was observed. An acute decrease of pain and disability was reported post-treatment with BMSC, followed by modest additional improvements. In one study 23% of patients elected to proceed with surgery within 3 years post-treatment, as after 1-3 years ODI reduced to moderate disability (Noriega et al., 2017; Blanco et al., 2019). All in all, in most cases BMSC treatment was effective at slowing down degeneration but not regenerating the disc[26]. Further useful research may involve NP

[25] ***Conclusion; Table 1.1. Accessibility of BMSCs is ranked 2,*** *as these cells are easily sourced from the bone marrow, however it is a painful and invasive procedure.*

[26] ***Conclusion; Table 1.1. The potential adverse effects of using BMSCs is ranked 2,*** *as in in vivo animal studies BMSCs have shown to migrate away from the injected site, posing a risk of bone formation in unwanted areas of the IVD. Additionally, BMSCs are used in clinical human trails which has shown no overall significant change to*

regeneration in animal models with natural occurring IVD degeneration, which includes all of the degenerative disc chemical, physical and mechanical microenvironment (as *in vitro,* BMSC were observed to undergo apoptosis in IVD-like acidic conditions) (Wuertz *et al.*, 2008; Smith *et al.*, 2018); to evaluate and improve transplanted BMSC differentiation, regenerative effects and safety (Urits *et al.*, 2019).

ADIPOSE DERIVED MESENCHYMAL STROMAL CELLS

NATIVE CHARACTERISTICS, EXPANSION CAPABILITY AND MAINTENANCE OF PHENOTYPE

Isolated hADMSC grow as adherent monolayers with a spindle-shaped and fibroblast-like morphology *in vitro* (Gimble and Guilak, 2003; Marfia *et al.*, 2014; Kumar *et al.*, 2017) and exhibit high proliferation capability in appropriate culture conditions (Marfia *et al.*, 2014; Zhou *et al.*, 2020). When maintained in standard culture conditions hADMSC expressed mesenchymal stem cell markers CD73, CD90 and CD105, and lacked expression of hematopoietic cell markers CD14, CD34 and CD45, and the immunological cell markers CD19 and Human Leukocyte Antigen – DR isotype (HLA-DR) (Marfia *et al.*, 2014; Zhou et al., 2020). Similar to BMSC, these cells have the ability to differentiate into osteogenic, chondrogenic and adipogenic lineages (Marfia *et al.*, 2014; Comella *et al.,* 2017; Zhou *et al.*, 2020; wang et al., 2019)[27]

CELL SURVIVAL IN INTERVERTEBRAL DISC ENVIRONMENT

In a 2D *in vitro* culture system, degenerate conditions such as low acidity and high osmolality impaired the viability and proliferation of rADMSC (Han *et al.*, 2014; Zhang et al., 2020) and in hADMSC (Li et al., 2012; Liang et al., 2012). Interestingly, despite hyperosmolality leading to lower cell viability and proliferation, 400mOsm/kg resulted in the highest expression of SOX9, aggrecan, collagen II in comparison to 300 and 500mOsm/kg (Zhang et al., 2020). The effect of inflammatory factors resulted in hADMSC producing more pro-inflammatory cytokines and also enhanced osteogenesis (Borem et al., 2019). Low oxygen has also been shown to trigger hADMSC to produce angiogenic and neurotrophic factors which would be detrimental for IVD regeneration (Binch et al., 2019). In degenerate models *in vivo* hADMSC have been observed after 2 weeks (Jeong *et al.*, 2010), 10 weeks (Chun et al., 2012) and 12 weeks post-injection (Marfia *et al.*, 2014) in small animal models and 16 weeks in Porcine animal model (Zhou et al., 2020)[28].

LBP patients, as the use of BMSC resulted in slowing down the degeneration of the disc and not regenerating the disc.

[27] ***Conclusion; Table 1.1. Expansion capability of ADMSCs is ranked 3,*** *as these cells can be easily maintained in different culture conditions and are easily manipulated into different cell lineages.*

[28] ***Conclusion; Table 1.1. Survival capability of ADMSCs in IVD environment is ranked 1,*** *as the IVD conditions effected the proliferation and viability of ADMSCs. Additionally, the hypoxic conditions resulted in these cells releasing adverse factors, which would further disc degeneration.*

REGENERATIVE EFFECT OF ADIPOSE DERIVED STROMAL CELLS

hADMSC have been studied in small animal models, using genetically defective biglycan mice (Marfia *et al.*, 2014), rats and rabbit models subject to needle puncture injury (Jeong *et al.*, 2009; H.-J. Chun *et al.*, 2012; Hua *et al.*, 2019; Ma *et al.*, 2019), in one large animal model (Zhou et al., 2020) and in a human clinical trial (Comella et al., 2017). hADMSC diffused throughout the discs (Marfia *et al.*, 2014). Degenerative discs injected with hADMSC demonstrated an improvement to GAG content with positive staining of collagen type II and aggrecan at 2–6-week post-injection in rat discs (Jeong et al., 2009), at 12-week post-injection in mice discs (Marfia et al., 2014) and in rabbits at 18-week post-injection (Chun *et al.*, 2012). Structural organisation of the degenerative discs was improved at 4 weeks post-injury in rabbit models (Ma *et al.*, 2019), at 12 weeks post-injection in a mouse model (Marfia et al., 2014) and 16 weeks in rat and rabbit models (Hua *et al.*, 2019; Chun et al., 2012). Despite the effect of ADMSC demonstrating some regenerative properties throughout all these studies, only partial regeneration of the disc was demonstrated. Furthermore, the presence of small chondrocytes within the NP was observed in a rabbit model (Chun *et al.*, 2012) and fibrous connective tissues were observed, which was also present in degenerative controls (Hua *et al.*, 2019). hADMSC displayed limited proliferation capability *in vivo,* as 12 weeks post-injection hADMSC were negative for the proliferation marker, Ki67 (Marfia *et al.*, 2014), and human nuclear antigen (HNA). HNA was expressed at 2 weeks yet had disappeared by the 4–6-week immunohistochemistry (IHC) analysis (Jeong *et al.*, 2009).

αThere was a lack of larger animal studies that used hADMSC, however analysis of the few studies demonstrated that the effects of hADMSC did not change the level of aggrecan, or collagen type II in a porcine model, but did result in a greater expression of Sox 9 in comparison to a degenerative disc control at 21 days (Zhou et al., 2020)[29]. This study also analysed the effect of human micro fragmented adipose tissue (hMFAT) seeded into the porcine model; MFAT contains a mixture of cells including ADMSCs and growth factors (Comella et al., 2017). MFAT resulted in a homologous distribution of extracellular matrix and cells, additionally, it showed the partial regeneration of the degenerate NP. Specifically, proteoglycans and collagen type II were easily detected, and GAG content was comparable to normal non-degenerate controls (Zhou *et al.*, 2020). MFAT has the same composition as stromal vascular fraction (SVF) of subcutaneous adipose tissue which has been used in human clinical trials (Comella *et al.,* 2017); the difference between the SVF and MFAT is the enzymatic and mechanical techniques used for isolation (Zhou *et al.*, 2020). In human clinical trials, autologous SVF injection has improved pain, analysis with (VAS) after 6 months post-treatment in 15 patients with degenerative disc disease (Comella *et al.,* 2017) and after 12 months post-treatment on chronic LBP patients (Kumar *et al.*, 2017). In 3 patients who

[29] ***Conclusion; Table 1.1. ADMSC's ability to produce extracellular matrix is ranked 2,*** *as in in vivo small animal models resulted in improved matrix deposit, however in larger animal models no difference in extracellular matrix production was observed.*

experienced improvement of pain and disability, also simultaneously displayed increased water content on MRI 12 months post-treatment (Kumar *et al.*, 2017). In human clinical trials there was no reports of adverse events, including osteophyte formation or incidence of infection (Comella et al., 2017; Kumar *et al.*, 2017)[30].

CONCLUDING REMARKS

ADMSCs can be obtained by a simple surgical procedure which is routinely used in cosmetic surgery; one clinical trial reported patients were discharged 4 hours from the start of harvesting autologous ADMSCs until after cell transplantation. Harvesting of cells also ascertains large quantities of cells, with additional ease in proliferation *in vitro* under standard tissue culture condition[31]. *In vivo,* ADMSC results in partial regeneration of the disc mainly through extracellular matrix production, and there was no report of adverse events. However, injection of ADMSC demonstrated evidence of low cell survival in IVD-like environments *in vitro* which translated to poor survival *in vivo* animal model studies. Moreover, ADMSC are very angiogenic by nature (Comella *et al.,* 2017) and increased the expression of proinflammatory molecules and promoted inflammation in Nucleus pulposus cell (NPC) (Zhou *et al.*, 2020; Borem et al., 2019), which could contribute further to degeneration.

UMBILICAL CORD STEM CELLS

NATIVE CHARACTERISTICS, EXPANSION CAPABILITY AND MAINTENANCE OF PHENOTYPE

The umbilical cord Wharton's jelly tissue contains stem cells similar to adult Mesenchymal stem cells (MSC) (Breymann *et al.,* 2006; Zhang *et al.*, 2015). *In vitro* hUCSC displays adherent growth, ability to form cell colonies and exhibits fibroblast-like morphology (Chon *et al.*, 2013; Zhang *et al.*, 2015; Beeravolu *et al.*, 2018: Choi et al., 2020). They expressed typical MSC markers CD29, CD44, CD73, CD90 and CD105, but were negative for CD14, CD34, and CD45 (Chon *et al.*, 2013; Zhang *et al.*, 2015; Zeng et al., 2020; choi et al., 2020); with 98-99% of cells positive for these MSC after 5 passages, with the exception of CD105 which was positive in 75% of cells (Chon *et al.*, 2013). hUCSC have self-renewing capability, leading to high proliferation and have also demonstrated multi-differentiation capacity (Pang *et al.,* 2014; Zhang *et al.*, 2015), differentiating into cells such as osteogenic, chondrogenic and adipogenic cell lines (Wang et al., 2004; Mueller *et al.*, 2014; Zeng et al., 2020; Choi et al., 2020), including

[30] ***Conclusion; Table 1.1. The potential adverse effects of using ADMSCs is ranked 2,*** *as even though there were no reports of ADMSC differentiation into unwanted bone formation, transplanted ADMSC had low survival rate reducing the potential of regeneration and increasing the risk of ADMSCs excreting detrimental factors, thus subjecting patients through treatments that would result in no significant improvement.*

[31] ***Conclusion; Table 1.1. Accessibility of ADMSCs is ranked 3,*** *as an abundance of cells are collected in a simple surgical procedure.*

muscle cells (Zatz *et al.*, 2011), neural cells (Leite *et al.*, 2014) and disc cells (Zhang *et al.*, 2015)[32].

CELL SURVIVAL IN THE INTERVERTEBRAL DISC ENVIRONMENT

In vitro cultured within a hypoxic environment irrelevant of culture serum, hUCSC demonstrated NP differentiation, cells displayed a clustering morphology, deposited GAGs, and expressed extracellular matrix proteins (Chon *et al.*, 2013). Exposure of NP cells taken from a degenerate disc to hUCSC conditioned media, has been shown to restore degenerative NP cells to multipotent and self-renewing NP precursor cells that expressed Tie 2+, OCT4 and Nanog (Zeng et al., 2020). Furthermore, it has been observed that mechanical IVD stimuli results in hUSC anti-apoptotic effects; when co-cultured with hNP cells undergoing compressive stress, the compression-induced apoptosis of NP cells was supressed (Zhao et al., 2020). hUCSC were influenced to differentiate towards NP cells with upregulation of ACAN, COL2A1, FOXF1 and KRT19 at higher levels *in vivo* than *in vitro* (normal culture conditions; DMEM, 37^{o}C, 5% CO_2) (Beeravolu *et al.*, 2018). hUCSC survived in rabbit IVD explants for 4 weeks (Anderson *et al.*, 2013), *in vivo* rabbit degenerative discs 8 weeks post-injection (Beeravolu *et al.*, 2018) and canine degenerative discs 24 weeks post-injection (Zhang *et al.*, 2015)[33].

REGENERATIVE EFFECT OF UMBILICAL CORD STEM CELLS

hUCSC have been used in *in vivo* rabbit models (Beeravolu et al., 2018; Perez-Cruet et al., 2019; Anderson et al., 2013), rat models (Choi et al., 2020) and larger dog models (Zhang et al. 2015). In degenerate animal disc models, treatment with hUCSC demonstrated partial preservation of the NP region and increased structure in both the rabbit (Leckie *et al.*, 2013; Beeravolu *et al.*, 2018) rat (Choi et al., 2020) and canine models (Zhang et al., 2015). Aggrecan, type II collagen, and SOX9 increased in hUCSC injected groups when compared to the degenerate controls (Beeravolu et al., 2018; Leckie et al., 2013; Zhang et al., 2015; Choi et al., 2020), which also translated into an increase of matrix gene expression (Zhang et al., 2015). Interestingly collagen type I was downregulated in the hUCSC injected group (Zhang *et al.*, 2015) as well as inflammatory cytokines to levels comparable to healthy controls (Choi et al., 2020)[34].

MRI analysis of the NP displayed increased disc height and water content in a rabbit degenerate model 8-weeks post-injection (Beeravolu *et al.*, 2018) and in canine models 8-,

[32] ***Conclusion; Table 1.1. Expansion capability of hUCSCs is ranked 3,*** *as these cells can be easily maintained in different culture conditions and are easily manipulated into different cell lineages.*

[33] ***Conclusion; Table 1.1. Survival capability of hUCSCs in IVD environment is ranked 2,*** *as these cells were able to survive in vitro IVD conditions and in vivo animal models as they differentiate towards NP-like cells. However, they have not yet been investigated in a degenerate environment.*

[34] ***Conclusion; Table 1.1. hUCSCs ability to produce extracellular matrix is ranked 2,*** *as in in vivo animal models these cells were able to produce extracellular matrix native to the NP, which resulted in partial regeneration.*

12- and 24-weeks post-injection (Zhang et al., 2015). However, there was no reported difference in MRI analysis after 12 weeks post-injection (Leckie et al., 2013), and MRI signals remained lower than in healthy control discs (Zhang et al., 2015). One major limitation observed in Beeravolu *et al.,* (2018), was human specific markers were observed in the AF of the injected IVD. Either transplanted cells were not fully placed into the NP during injection or like BMSC they were capable of migrating out of the NP region (Beeravolu *et al.*, 2018)[35]. The mixed MRI analysis from *in vivo* testing were also reiterated in a small clinical trial with hUCSC. Two patients that presented with chronic low back pain were treated with hUCSC (Pang *et al.,* 2014). After a 2- year follow up post-treatment pain and function improved in both patients; the first patient showed an immediate effect of pain relief (VAS), followed by sustained effect up to 24 months, this was also observed in their disability report (ODI), and translated into a greater MRI signal intensity compared to pre-treatment, indicating higher water content in the NP. In the second patient there was an acute regeneration with an improved pain (VAS) and disability (ODI) score at 6 months post-treatment, however the scores progressively worsened following 12 and 24 months. Also correlating to no notable increase of MRI signal intensity (Pang *et al.,* 2014).

CONCLUDING REMARKS

hUCSC are harvested from the umbilical cord or placenta, which is non-invasive, and readily available in blood banks; umbilical cord displays low incidence of graft vs host disease and can be used allogeneically[36]. However, social, and ethical issues have been recognised surrounding the practice of blood collection, due to obtaining consent and that blood banking is becoming more commercialised; a case story of a private biotechnology company that enforced obstetricians to halt blood collection to certain banks due to alleged patent infringement, highlights these concern of commercialising (Kurtzberg *et al.,* 2005). As with MSC, hUCSC have the capability of high proliferation rates and differentiating into multiple lineages, including NP cells, especially in the IVD environment. In smaller animal models and larger animal models, hUCSC demonstrated partial regeneration of NP degeneration; aggrecan and collagen type II was deposited with a downregulation in collagen type I and cytokines. However, there are some limitations with the migration ability of hUCSC, which could lead to safety concerns. hUCSC have been tested in human clinical trials in 2 patients, one showed improvement to pain and disability, which was reflected in an MRI analysis of water retention. The other patient displayed overall improvement to pain and disability but was starting to relapse and MRI did not show regeneration. No adverse events were found in the human patients (Pang et al., 2014), however, this study was limited by only using two

[35] ***Conclusion; Table 1.1. The potential adverse effects of using hUCSCs is ranked 1,*** *as some reports of transplanted cells migrating away from treatment site, and human clinical trials have shown limited regeneration with the use of hUCSCs.*

[36] ***Conclusion; Table 1.1. Accessibility of hUCSCs is ranked 3,*** *as these cells are externally sources and there is an abundance of hUCSCs in blood banks.*

patients; more clinical studies are needed to identify a reliable outcome for the use of hUCSC for regenerative purposes.

INDUCED PLURIPOTENT STEM CELLS

NATIVE CHARACTERISTICS, EXPANSION CAPABILITY AND MAINTENANCE OF PHENOTYPE

Induced pluripotent stem cells (iPSC) can be generated from almost any type of somatic cell by introducing a combination of several reprogramming transcription factors, such as Oct3/4, Sox2, Krüppel-like factor 4 (KLF4) and c-Myc (Takahashi and Yamanaka, 2006; Okita and Yamanaka, 2011)[37]. Human iPSC for use in NP regeneration has been generated from normal dermal fibroblasts (Sheyn *et al.*, 2019; Colombier *et al.*, 2020) and nucleus pulposus cells (Zhu *et al.*, 2017). IPSC have a distinct morphology with a prominent nucleolus and a high nucleus to cytoplasm ratio. Pluripotency is characterised with the expression of OCT4, SRY-Box Transcription Factor 2 (SOX2), c-MYC, KLF4 and Nanog Homeobox (NANOG). IPSCs have an unlimited proliferation capacity and maintain normal karyotype in culture (Zhu *et al.*, 2017; Sheyn *et al.*, 2019). IPSC can differentiate into cells of all germ layers (Zakrzewski *et al.*, 2019)[38]. However, rapid cell growth and high plasticity allow iPSC to form teratomas *in vivo* (Zhu *et al.*, 2017), which are used to demonstrate iPSC pluripotency but would not be favourable for treatment approaches (Zhu *et al.*, 2017; Sheyn *et al.*, 2019). Thus, for applicability for regeneration it is essential to differentiate the iPSCs to the cell type of choice for regeneration prior to injection *in vivo.*

DIFFERENTIATION INTO NOTOCHORDAL -LIKE CELLS

To generate induced NC- like cells (iNC-LC), iPSC can be subject to differentiation via different methods; the most common method is firstly differentiating iPSC towards primitive streak mesoderm, followed by plasmid transfection with NC transcription factors such as Brachyury, FOXA2 or NOTO to differentiate into an NC phenotype (Tang *et al.*, 2018; Sheyn *et al.*, 2019; Colombier *et al.*, 2020; Zhang *et al.*, 2020); Xia *et al.,* (2019) differentiated hiPSC towards mesoblastic cells, followed by differentiation into NP-like cells with the influence of TeSR-E8 Basal Medium (STEMCELL Technologies) (Xia *et al.*, 2019); Hu *et al.,* (2015) used GDF5 transfection to differentiate hiPSC (Hu *et al.*, 2020); and hiPSC was successfully differentiated into NC-like cells under the influence of native devitalized porcine NP matrix powder (Liu *et al.*, 2015). iNC-LC have been shown to express typical notochordal markers of Brachyury, KRT-8, KRT-19, collagen type II, collagen type I and aggrecan (Liu *et al.*, 2015; Xia *et al.*, 2019). iNC-LC has been demonstrated to survive in IVD retain phenotype of NC for up to 8 weeks post-

[37] ***Conclusion; Table 1.1. Accessibility of iPSCs is ranked 3,*** *as these cells are generated from almost any somatic cell and then stored in abundance in iPSC banks.*

[38] ***Conclusion; Table 1.1. Expansion capability of iPSCs is ranked 3,*** *as these cells can be easily maintained, expanded in culture conditions, and are easily manipulated into different cell lineages.*

injection in a small (Zhang *et al.*, 2020) and large degenerative animal model (Sheyn *et al.*, 2019)[39].

REGENERATIVE EFFECT OF INDUCED PLURIPOTENT STEM CELLS

In vitro iNC-LC upregulated NP tissue related genes including Sox9 and collagen type II (Y. Liu *et al.*, 2015). After 28 days in culture, histological analysis displayed an abundance of proteoglycans present with the staining of collagen type II and aggrecan, demonstrating the ability of differentiated hiPSC co-cultured with pNP matrix powder to generate NP-like tissue *in vitro* (Liu *et al.*, 2015). When iNC-LC were translated into animal models, collagen type II and aggrecan proteins were present following 8 weeks (Zhang *et al.*, 2020) and 16 weeks post-injection in rat models (Xia *et al.*, 2019), leading to increased proteoglycan production and restored NP region[40]. In these small animal models, there was an observed disc height increase at 8 weeks (Zhang *et al.*, 2020) and 24 weeks post-injection (Xia *et al.*, 2019). Interestingly, the injection of iNC-LC resulted in an increase in intradiscal pH, 12 weeks post-injection in a porcine model, indicating the cells were able to influence their surroundings to produce a less degenerate environment and potentially play a protective role (Sheyn *et al.*, 2019).

CONCLUDING REMARKS

iPSCs are potentially an abundant cell source, as they can be obtained through reprogramming somatic cells of the patient to generate autologous stem cells. IPSC also have an unlimited proliferation ability and the capacity to differentiate into a chosen cell. Studies using iPSC have differentiated these stem cells into NC-like cells and to date no studies have investigated differentiation to mature NP cells. Once iNC-LC are generated, these cells upregulate NP markers *in vitro* and increase collagen type II and aggrecan expression *in vitro* and *in vivo.* Which, in turn has shown a decrease in disc degeneration in animal models. However, iPSC ability to form teratomas in the disc is a cause for concern, however no teratoma formation was reported in these initial studies (Sheyn *et al.*, 2019; Zhang *et al.*, 2020), which may be the result of stable phenotype of iNC-LC once differentiated into a committed cell lineage[41]. In conclusion, the study of iPSC in animal models is novel and no iPSCs are used clinically at present, but preliminary results of seeding iNC-LC into degenerate discs in animal models shows promising results, with no safety issues highlighted to date.

[39] ***Conclusion; Table 1.1. Survival capability of iPSCs in IVD environment is ranked 2,*** *as these cells were able to survive in vitro IVD conditions and in vivo animal models as they differentiate towards NC-like cells.*

[40] ***Conclusion; Table 1.1. IPSC's ability to produce extracellular matrix is ranked 3,*** *as in in vivo animal models these cells were able to produce extracellular matrix native to the NP, which resulted in disc regeneration.*

[41] ***Conclusion; Table 1.1. The potential adverse effects of using iPSCs is ranked 1,*** *as there is potential of iPSCs to form teratomas, however there have been no reports in the few initial in vivo studies with these cells.*

DISCUSSION & CONCLUSIONS

A key challenge of cell therapy is choosing an appropriate cell source that can not only survive within the natural harsh environment of the IVD, but is also safe to use and produces appropriate extracellular matrix to restore biomechanical and biological function of the disc. One accommodating factor about the IVD is the avascular nature (although this does change during degeneration); therefore, is considered immunoprivileged and should tolerate autologous or allogeneic cells (Sun et al., 2013; Sun et al., 2020). The key characteristics of the ideal cell source are assessed on their ability to proliferate *in vitro*, to obtain sufficient number of cells for preparation as a therapeutic model, survive in the IVD environment, regenerate the NP through the analysis of extracellular matrix production and assure safety and long-term effectiveness.

The first and most logical cells to regenerate the NP with would be utilising disc cells themselves, NP, and AF cells. NP and AF cells can survive in the NP and produce extracellular matrix *in vivo* (Meisel *et al.*, 2007). However, AF cells produce extracellular matrix that does not resemble the native extracellular matrix of the NP, and the harvesting of NP cells involves a difficult invasive procedure, which results in a limited cell number and inefficient expansion capacity limits the use of NP and AF cells as a cell source potential greatly. Although cadaveric sources are currently in clinical trials (Silverman *et al.*, 2020). In addition, NP cells exposed to the degenerated disc may result in NP cellular senescence and contribute to an inability to produce proteoglycans (Roberts *et al.*, 2006; Le Maitre *et al.,* 2007); as this is a key factor in initial stages of disc degeneration. NP cells display similar phenotypic characteristics to chondrocytes, sharing similar morphology and some gene expression. Chondrocytes are readily available from multiple sources, can be expanded *in vitro* and remain viable in IVD condition. However, *in vivo* they retain their chondrocytic phenotype and produce extracellular matrix that involves a slightly different composition compared to NP extracellular matrix (Sato *et al.*, 2003; Gorenšek *et al.*, 2004), thus affecting the biomechanical properties of the disc. Another NP-like cell is IVD disc derived NCs; these cells are of notochordal origin and are pre-existing cells in the NP region of the human IVD prior to adulthood. NCs are capable of synthesizing a proteoglycan-rich matrix and play a protective role in a catabolic environment; however, they are hampered by difficulties in handling them. In particular the difficulties in maintaining phenotype in monolayer culture *in vitro* (Gantenbein *et al.*, 2014; Potier and Ito, 2014; Spillekom *et al.*, 2014), together with difficulties in harvesting sufficient numbers due to difficulties with amplification *in vitro* (Kim *et al.*, 2009; Potier *et al.*, 2014; Spillekom *et al.*, 2014).

Alternatives are to utilise adult stromal cell differentiation into NP-like cells. BMSC have good differentiation capacity and are easily accessible. Animal model and clinical trials showed promising results for partial regeneration of NP. However, the differentiation fluidity resulted in adverse events such as osteophyte formation (Vadalà *et al.*, 2012) and capacity of BMSC to migrate, applies a reason for concern with unwanted bone formation if injected alone. Whilst

BMSC are the target of many clinical trials, results to date are limited to short term follow up and thus longer-term results are awaited. Another source of MSC is ADMSC, harvesting these cells is less invasive and can result with larger cell quantities than BMSC extraction (Jeong *et al.*, 2010). *In vitro* they are grown easily under standard conditions. Despite promising *in vitro* results, and some extracellular matrix production observed *in vivo,* ADMSC survival rates in IVD conditions *in vitro* and *in vivo* are low, triggered by the hypoxic and inflammatory host environment (Marfia *et al.*, 2014; Kumar *et al.*, 2017). BMSC and ADMSC generally proliferate when exposed to inflammatory conditions, especially where there is also oxidative stress; this response is valuable in normal healing conditions and protects from apoptosis (Borem et al., 2019; Blanc and Mougiakakos, 2012). However, in the context of the degenerative disc, the increase in cells could result in depleting the already limited nutrient supply of the disc and thus may not provide regeneration. MSC derived from perinatal tissues have less limitations than using BMSC and ADMSC; hUCSC are more primitive and display a lower risk of rejection (Arufe *et al.*, 2011), making these cells available for allogeneic transplants. HUCSC offers good differentiation capabilities and can be subject to differentiation into NP-like cells in IVD conditions. In smaller and larger animal models, hUCSC demonstrated partial regeneration of degenerate NP tissue, yet their observed migration ability is a limitation, which may lead to safety concerns. In human clinical trials, overall, there was an improvement in self-assessment of pain and disability and some reports of NP regeneration through MRI analysis. There were no adverse events reported, displaying the safety of hUCSCs in humans. However, this was a small cohort, and more studies are needed.

The final cells proposed are iPSCs, which could be used to generate NP-like cells. As there are no established precursors of NP cells, differentiating iPSC into iNC-LC is used to regenerate the disc in the literature to date. IPSC can be generated from any somatic cell; therefore, they are highly accessible and have an unlimited proliferation ability. As iPSC have been used to differentiate into iNC-LC, they survive in IVD conditions and have been shown to produce extracellular matrix *in vivo*, although investigation of the true degenerate environment has not been performed to date. However, safety issues with these cells still need to be evaluated, iPSC can form teratomas and the safety of viral transfection, used to induce iPSC differentiation, on the cells' karyotype also needs to be assessed. Based on the evaluation of all cell types (Table 1.1), iPSC may provide the highest overall potential for cellular therapy to regenerate the NP. If the safety of iPSC can be established, then utilizing iPSC for cell therapy would provide improved accessibility compared to NP, AF, NC, BMSC and ADMSC; increased proliferation compared to NP, AF, and NCs; and at least in principle would be on par with the ability of NC and NP cells to survive within the IVD environment and produce the desired extracellular matrix. The next question would be which cell type would possess the greatest regenerative potential in a degenerate disc? Whereas injecting NP cells could cause the injected cells to contribute to degeneration, limited knowledge is known about the regenerative effects of NCs.

Table 1.1. Heat map showing the conclusion of cell type use to regenerate the degenerative nucleus pulposus of the intervertebral disc*; nucleus pulpous cells (NP), annulus fibrosis (AF) cells, notochordal (NC) cells, chondrocytes, bone marrow stem cells (BMSC), adipose derived stem cells (ADMSC), umbilical cord stem cells (UCSC) and induced pluripotent stem cells (iPSC). These cell types were ranked 1-3, 1 being inefficient and 3 being efficient at accessibility of harvesting the cell type, expansion capability in vitro, the ability of the cell type to survive in an intervertebral disc environment, the ability of the cell to produce extracellular matrix and the potential adverse event that could potentially happen; deeming a safety issue.*

	Accessibilty	Expansion capability *in vitro*	Survival in IVD	ECM	Potentital adverse effects	Overal Rating
NP	1	2	3	3	2	11
AF	1	2	3	2	2	10
NC	1	1	3	3	3	11
Chondrocytes	2	2	3	2	2	11
BMSC	2	3	2	3	2	12
ADMSC	3	3	1	2	2	11
hUCSC	3	3	2	2	1	11
IPSC	3	3	2	3	1	12
	1= difficult to harvest 3= easy to harvest	1= difficult to expand 3= easy to expland	1= cell death in IVD 3= survival in IVD	1= no ECM production 3= NP specific ECM production	1= potential hazards 3= safe	

This report concentrates on cell sources; however, there are other important considerations that have an extensive influence on cell behaviour, such as the addition of biomaterials and growth factors. Biomaterials are used as cell carriers, cell anchoring, a guide for extracellular matrix synthesis and mechanical support; reviews have discussed cell-biomaterial approaches of intervertebral disc tissue engineering (Stergar et al., 2019; Huang et al., 2018; Bowles and Setton, 2017). These materials could be utilised to provide instructive cues and protection to cells and thus must be considered in combination for future therapies. Bowles and Setton (2017) have reviewed bioengineering advances to treat IVD regeneration. Interestingly this biomaterial review concludes too, that the regeneration of IVD must take into consideration biological processes (Bowles and Setton, 2017). Growth factors can also be implemented to facilitate correct differentiation, or regenerative properties (Bucher et al., 2013; Hu et al., 2020; Xu et al., 2020; Hua et al., 2019; Clarke et al., 2014). For example, GDF5 gene transferred BMSC upregulated aggrecan and SOX9 and KRT19 compared to non-transfected cells, which was reported to lead to partial recovery of GAGs in bovine degenerated disc (Bucher *et al.*, 2013); also pre-treated ADMSCs with smoothened agonist resulted in the improved disc height, water content, extracellular matrix content, and structure of degenerated IVDs *in vivo* (Hua et al., 2019). Few of the studies cited in this review compared the treatment of cells only and cells with biomaterials, there is evidence that when cells are used in conjunction with a biomaterial, it can result in an enhanced regenerative effect on the disc (Choi et al., 2020;

Zhang et al., 2020). Combining cells, biomaterial and growth factors is the principle of a tissue engineering review by Tendulkar et al., (2019), whose analysis focuses on the repair of NP utilizing tissue engineering approach of injectable hydrogels, cells, and growth factors (Tendulkar *et al.*, 2019).

In summary, a rational discussion of potential cell sources proposed for NP tissue regeneration, based on accessibility, expansion capability *in vitro,* cell survival in the IVD environment, regenerative effects of cells alone, and potential safety of the cells. We propose that the use of iPSC-NC-like cells as a cell source could have the potential for regenerating the NP in degenerate discs and requires further study to assess their regenerative ability and safety.

UPDATED LITERATURE FOLLOWING REVIEW PUBLICATION

The PubMed search conducted in this literature review was repeated with a primary search of '((disc degeneration) OR (intervertebral)) NOT (retinal)) AND ((embryonic stem cells) OR (progenitor cells) OR (fibroblasts) OR (stem cells) OR (induced pluripotent stem cells) OR (adult stem cells) OR (mesenchymal) OR (adipose) OR (hematopoietic) OR (synovial) OR (disc stem cells) OR (disc cells) OR (nucleus pulposus) OR (chondrocytes) OR (notochordal) OR (notochord)) AND ((cell therapy) OR (regeneration) OR (therapy) OR (treatment))'. Clinical trials, *in vivo* and *in vitro* studies were all included, and the search was limited to the English language, with the dates changed from between 1st January 2021 and 26th May 2023. To explore papers that have been published after the date when this literature review was written. This search generated a total of 9 publications and the title and abstracts were initially screened based on their relevance to cellular therapies for the regeneration of the NP region only. A total of 3 articles were identified.

Two of the studies were previously analysed in the literature utilised BMSC for human clinical trials prolonged the investigations for a longer-term follow-up report (Noriega *et al.*, 2021; Gomez-Ruiz *et al.*, 2023). Of the first study, an initial 5-year study performed by Blanco et al., (2019) summarised radiological solid fusion was obtained in 9 out of 11 cases, with ODI, acute relief of pain and disability was improved after the initial 5-year study of utilising autologous BMSC (Blanco *et al.*, 2019). In the later manuscript, the study analysed outcome after 10-years, highlighting the most important finding for the longer-term study was that no adverse events were observed. The events included evaluating radiological evaluation of local tumoral transformation, infections, and lumbar ossification, with radiograph showing solid fusion at the 10-year follow-up in 100% of the patients (n=11). This study analysed that pain intensity, VAS, ODI and physical functioning questionnaire were all improved in comparison to the pre-intervention scores. From the second study the initial report was a 1-year follow-up of using allogeneic BMSC, summaries that patients displayed acute improvement to pain and

disability, however this improvement was followed by modest improvement after 3-months and was restricted to 40% of the cohort (n=24) (Noriega *et al.*, 2017). In the 3.5-year follow-up study, no serious adverse effects were reported, with the initial early pain and disability improvement observed in the 1-year being maintained persisted into the longer-term follow-up. The study experienced two subpopulations of patients, with one subpopulation results demonstrate 'perfect treatment' with improvement from BMSC treatment, whilst the second subpopulation showed no improvement to VAS and ODI score when compared to control group. MRI analysis demonstrated the decrease Pfirrmann grading that was observed in 1-year was also sustained after 3.5 years (Noriega *et al.*, 2021).

A study utilising adult allogeneic mesenchymal precursor cell in combination with Hyaluronic acid (HA) was used in 100 patients with moderate disc degeneration (Pfirrmann score 3-6) for up to 3-year follow-up post injection. The results demonstrate that the treatment patients experienced improved VAS and ODI scores throughout the 36-month period, however the MRI assessed Pfirrmann score was not improved in any subject. The procedure with these cells were shown to be tolerable and no immune response was observed (Amirdelfan *et al.*, 2021).

These 3 studies have reiterated and demonstrated safety and efficacy of stem-like cell implantation within the degenerative disc after 3–10-year follow-up reports. With evidence of improved pain and disability score that was acutely improved upon injection but sustained or gradually improved through the long-term period. Interestingly, the MRI score of degenerative discs was not improved with these cell treatments, with the 10-year study resulting in disc fusion.

AIMS AND OBJECTIVES

The overall project aim was to test the hypothesis that NC-like cells once seeded within a biomaterial system has the capability of retaining NC phenotype and regenerative properties of extracellular matrix production. The NC-like cell seeded biomaterial construct imitates an injectable therapeutic treatment which could be utilised to regenerate a degenerative intervertebral disc.

SPECIFIC OBJECTIVES

1. Characterise NCs phenotype and behaviour *in vitro* and optimse extraction and culture methodology (Chapter 2).
2. Investigate the phenotype and behaviours of porcine NCs seeded into biomaterials (Chapter 3).
3. Investigate the phenotype and behaviours of iPSC generated mesendoderm progenitor cells (MEPCs) in biomaterials (Chapter 4).
4. Assess the alternative differentiation methods of attaining iPSC generated MEPCs (Chapter 5).

5. Determin the influence of cryopreservation of iPSC-MEPCs to assess compatibility with clinical application (Chapter 5).
6. Investigate the effect of environments that mimic the degenerative disc on the porcine NC or iPSC derived MEPCs seeded biomaterial constructs when cultured *in vitro,* for up to 4 weeks in differing physiological conditions to related the *in vivo* setting of the IVD (Chapter 6).

CHAPTER 2
RECOMMENDATIONS FOR INTERVERTEBRAL DISC NOTOCHORDAL CELL INVESTIGATION: FROM ISOLATION TO CHARACTERISATION

CONTEXT OF RESEARCH

Notochordal cells are precursor cells of the nucleus pulposus within the Intervertebral disc and as shown in Chapter 1, they have potential as a regenerative cell source. However, in research there has been a limited use of NC *in vitro* and therefore recommendations, methodologies and standard operation procedures are severely lacking for facilitating the use of this cell source. Thus, this chapter contributes to research by providing key recommendations and consensus methodologies for NC isolation, numeration, *in vitro* manipulation, and characterisation. As this information will support future research into NC physiology and their utility in regenerative therapies.

AUTHORS

Rebecca J. Williams [1,2], *Lisanne T. Laagland[3], *Frances C. Bach[3], Lizzy Ward[4], Wilson Chan[5], Vivian Tam[5], Adel Medzikovic[3], Shaghayegh Basatvat [1,2], Lily Paillat[6], Nicolas Vedrenne[6], Joseph W. Snuggs [1,2], Deepani W. Poramba-Liyanage[3], Judith A Hoyland[4,7], Danny Chan[5], Anne Camus [6], Stephen M. Richardson[4], Marianna A. Tryfonidou[3], Christine L. Le Maitre [1,2]

*These authors have contributed equally to the study

AFFILIATIONS

[1]Department of Oncology and Metabolism, Medical School, The University of Sheffield, Beech Hill Road, Sheffield, S10 2RX, UK. [2] Biomolecular Sciences Research Centre, Sheffield Hallam University, Sheffield, S1 1WB, UK. [3]Department of Clinical Sciences, Faculty of Veterinary Medicine, Utrecht University, Utrecht, the Netherlands. [4]Division of Cell Matrix Biology and Regenerative Medicine, School of Biological Sciences, Faculty of Biology, Medicine and Health, The University of Manchester, Stopford Building, Oxford Road, Manchester, M13 9PT, United

Kingdom. [5]School of Biomedical Sciences, The University of Hong Kong, Hong Kong. [6]Nantes Université, Oniris, CHU Nantes, INSERM, Regenerative Medicine and Skeleton, RMeS, UMR 1229, F-4400 Nantes, France. [7]NIHR Manchester Biomedical Research Centre, Central Manchester Foundation Trust, Manchester Academic Health Science Centre, Manchester, United Kingdom.

AUTHOR CONTRIBUTIONS

AC, MAT, CLLM, contributed to conception of the study; RJW, LTL, FCB, AC, MAT, CLLM, contributed to the design of the study; RJW, LTL, FCB, LW, SB, WC, JWS, LP contributed to acquisition of laboratory data (RJW: Porcine and Rat isolation, numeration studies, characterisation and culture; LTL: Canine and porcine isolation, characterisation; FCB: human, canine and porcine isolation; LW: human isolation; SBL porcine isolation; WC: mouse isolation; JWS: rat isolation, monolayer culture, characterisation; LP: mouse isolation); RJW, LTL, FCB, SB, SMR, WC, JWS, LP, MAT, CLLM performed data analysis; RJW, LTL, FCB, LW, WC, VT, AM, LP, JWS, DWP, JAH, DC, AC, SMR, MAT, CLLM contributed to interpretation of the data; RJW, LTL, FCB, LW, WC, VT, AM, SB, NV, JWS, DWP, DC, AC, MAT, CLLM drafted the manuscript; All authors critically revised the manuscript for intellectual content; All authors approve the final version and agree to be accountable for all aspects of the work.

DETAILED CONTRIBUTIONS MADE

I refined the digestion protocol for harvesting NCs from pig tissue (Table 2.1). I performed a comparison of NC extraction yields collected from porcine spines and tails (Fig. 2.6). I designed and performed the methodology experiment for dissociating NCs and optimised the numeration studies (Fig. 2.7 and 2.8). I contributed to the histological, immunohistochemistry and immunofluorescence staining and imaging of porcine discs (Fig. 2.10, 2.11, 2.12). I contributed to the optimisation of IHC antibodies used in the characterisation of pigs (Table 2.2). I performed immunofluorescence staining and imaging of NC *in vitro* with rat and porcine cells (Fig. 2.13). I contributed to statistical analysis and interpretated the data. I contributed to the digestion protocol from porcine IVDs, I drafted parts of the manuscript, specifically the abstract, second part of the introduction, cryopreservation of NCs, characterising the phenotype of NCs, conclusion and was actively involved in script editing throughout the drafting process.

(IN PRESS) Williams, R. J., Laagland, L. T., Bach, F. C., Ward, L., Chan, W., Tam, V., Medzikovic, A., Basatvat, S., Paillat, L., Vedrenne, N., Snuggs, J. W., Poramba-Liyanage, D. W., Hoyland, J. A., Chan, D., Camus, A., Richardson, S. M., Tryfonidou, M. A., & Le Maitre, C. L. (2023). Recommendations for Intervertebral Disc Notochordal Cell Investigation: From Isolation to Characterisation. JOR Spine, *In Press*

MANUSCRIPT: RECOMMENDATIONS FOR INTERVERTEBRAL DISC NOTOCHORDAL CELL INVESTIGATION: FROM ISOLATION TO CHARACTERISATION

ABSTRACT

Background: Lineage-tracing experiments have established that the central region of the mature intervertebral disc, the nucleus pulposus, develops from the embryonic structure called “the notochord”. However, changes in the cells derived from the notochord which form the nucleus pulposus (i.e., notochordal cells (NCs)), in terms of their phenotype and functional identity from early developmental stages to skeletal maturation are less understood. These key issues require further investigation to better comprehend the role of NCs in homeostasis and degeneration as well as their potential for regeneration. Progress in utilising NCs is currently hampered due to poor consistency and lack of consensus methodology for *in vitro* NC extraction, manipulation, and characterisation. Methods: Here, an international group has come together to provide key recommendations and methodologies for NC isolation within key species, numeration, *in vitro* manipulation and culture, and characterisation. Results: Recommended protocols are provided for isolation and culture of NCs. Experimental testing provided recommended methodology for numeration of NCs. The issues of cryopreservation are demonstrated, and a panel of immunohistochemical markers are provided to inform NC characterisation. Conclusions: Together we hope this article will provide a road map for *in vitro* studies of NCs to support advances in research into NC physiology and their potential in regenerative therapies.

INTRODUCTION

The notochord is a mesodermal midline structure (also called the axial mesoderm) located along the anterior-posterior axis at the ventral surface of the neural tube and dorsal to the gut, characteristic of chordates (Balmer *et al.*, 2016; De Bree *et al.*, 2018). It is a transient signalling structure involved in the regionalization and fate of the surrounding embryonic tissues (Camus *et al.*, 2000; Yamanaka *et al.*, 2007). In vertebrates, the notochord plays a key role in signalling and coordinating the development of the vertebral column (Lawson and Harfe, 2017; Williams *et al.*, 2019). During development, the notochordal plate folds to develop into the neural tube forming the notochord (ventrally), which is flanked by the paraxial mesoderm and ectoderm (dorsally) (Copp *et al.*, 2003; McCann and Séguin, 2016). The paraxial mesoderm goes on to form the somites, which further differentiate into skeletal muscle, connective tissue, dermis, and the sclerotome. The latter eventually gives rise to the ribs, vertebral bodies, cartilaginous end plates (CEPs) and the annulus fibrosus (AF) of the intervertebral disc (IVD) (McCann and Séguin, 2016; Ward *et al.*, 2018; Wopat *et al.*, 2018; Tani *et al.*, 2020). Whilst lineage tracing studies in mouse models have demonstrated that the founder cells of the nucleus pulposus (NP), the core of the IVD, originate in the embryonic notochord (Choi *et al.*, 2008; McCann *et al.*, 2012). Once the notochord regresses, notochordal cells are restricted to within the NP, and excluded from the forming vertebral bodies (Lawson and Harfe, 2015).

Substantial changes in the cytomorphology and function of notochordal cells are observed throughout morphogenesis, growth, and maturation of the IVD, from its initial state as a notochord primordium to its mature state: the NP of the adult disc. A consensus terminology is currently lacking for defining the notochordal derived cells within the NP from development to adulthood. Here, we adopt the terminology utilised in Bach *et al.,* (2022), where notochordal cells from the embryonic notochord are defined as embryonic notochordal cells (eNCs), whilst those within the central region of the IVD are termed notochordal cells (NCs) (Bach *et al.*, 2022).

As well described, at an early stage, the embryonic notochord is composed of large eNCs packed within the peri-notochordal sheath consisting of extracellular matrix proteins (mainly laminin, proteoglycans and collagen). eNCs synthesize and secrete collagens and proteoglycans (containing chondroitin 4-sulphate, chondroitin 6-sulphate and heparan sulphate GAG) which accumulate in the peri-notochordal sheath (Paavola *et al.*, 1980; Smits and Lefebvre, 2003; Choi and Harfe, 2011). Once these eNCs mature within the NP they exhibit multiple large cytoplasmic vacuoles and eventually differentiate into the NCs. With further NP maturation a transition in cell phenotype takes place from large vacuolated NCs, present in clusters, to smaller and more dispersed non-vacuolated NP cells (NPCs), although the timing of this differs considerably by species (Fig. 2.1). The NPCs are phenotypically characterized by their ability to synthesize the appropriate matrisome (Tam *et al.*, 2020) and can to some extent be identified by specific gene biomarkers (Hunter *et al.*, 2004; Gilchrist *et al.*, 2011; Hwang *et*

al., 2014; Risbud *et al.*, 2015). Although differential gene markers are difficult to identify between the vacuolated NCs and mature non-vacuolated NPCs, the advent of single-cell transcriptomic analysis of these cells provides new perspectives and potential markers (Rodrigues-Pinto *et al.*, 2016, 2018; Peck *et al.*, 2017; Richardson *et al.*, 2017; Wymeersch *et al.*, 2019). Thus, further research into developmental studies and NC biology is essential to provide insights into NC related pathogenesis of IVD degeneration and to understand their potential in IVD regeneration (McCann and Séguin, 2016; Colombier *et al.*, 2020; Zhang *et al.*, 2020; Gan *et al.*, 2021; Tessier and Risbud, 2021; Jiang *et al.*, 2022).

The NC population in the NP undergoes species-specific changes (Fig. 2.1). In humans, NCs start to decline before birth (Fig. 2.1 and 2.2), with complete loss based on their vacuolated morphology by teenage years. Richardson *et al.,* (2017), reported the presence of NC remnants within adolescent human IVDs (Richardson *et al.*, 2017). Similarly, mature NPs from sheep, goats, and cows contain no NCs, while in mice, rabbits, rats, and pigs, the NC population is maintained until much later in life (Fig. 2.1 and 2.3) (Hunter *et al.*, 2004; Alini *et al.*, 2023). In dogs, NCs are lost at about one year of age in chondrodystrophic breeds (CD) (e.g. Beagles and Dachshunds), but remain in the NP until middle/old age in non-chondrodystrophic (NCD) breeds (e.g. Shepherds and Mongrels) (Fig. 2.1 and 2.3) (Hunter *et al.*, 2004; Smolders, Bergknut, *et al.*, 2013; Smolders, Meij, *et al.*, 2013).

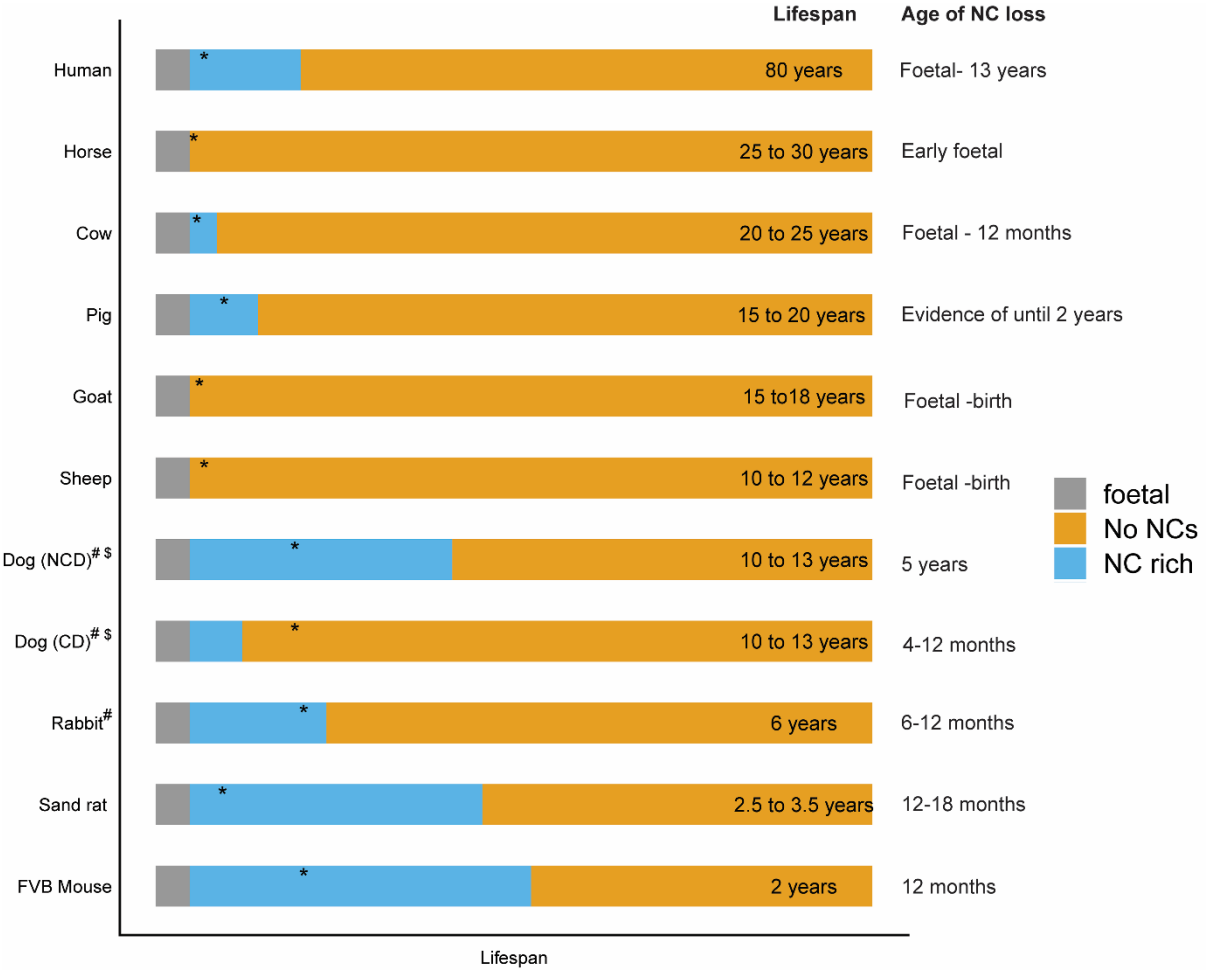

Figure 2.1. Comparison of the age at which notochordal cells are lost from the intervertebral disc. *Lifespan refers to approximate lifespan in captivity and can vary depending on environmental factors and other variables. * Indicates time of skeletal maturity (human 20 years; horse: 2 years; cow: 2-3 years; pig: 12 months; goat: 2-3 years; sheep: 2-3 years; dog (NCD) and dog (CD): 1-2 years; rabbit: 10 months; sand rat: 2 months; FVB mouse: 4 months). #Depends on breed and genetic background. $loss of NCs can depend on breed, genetic background, diet, obesity and injury. In the human, sheep and cow, NC loss begins at foetal stages, with NCs seen at birth. Horse discs in later stages of foetal development are devoid of NCs and none are seen at birth. NC: notochordal cells, CD: chondrodystrophic, NCD: non-chondrodystrophic. (References: Human (Trout et al., 1982; Nerlich et al., 1997; Weiler et al., 2010; Pattappa et al., 2012; Bach et al., 2015; Richardson et al., 2017; Gan et al., 2021); Horse (Bergmann et al., 2022); Goat (Hoogendoorn et al., 2007); Sheep* (Hunter *et al.*, 2004; Shu *et al.*, 2013; Constant *et al.*, 2022)*; Cow (Aguiar et al., 1999; Panebianco et al., 2021); Dog (CD) (Hansen, 1951); Dog (NCD)* (Hansen, 1951; Smolders, Bergknut, *et al.*, 2013)*; Rabbit* (Scott *et al.*, 1980; Hunter *et al.*, 2004; Guehring *et al.*, 2010)*; Sand rat (Adler et al., 1983); FVB mouse (Winkler et al., 2014)).*

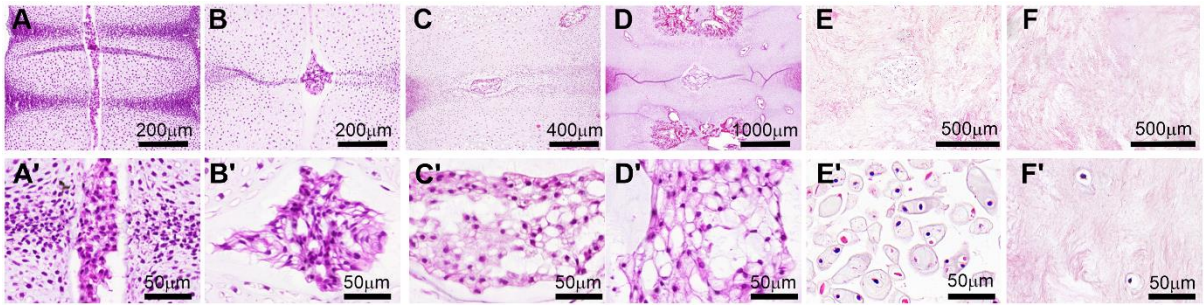

Figure 2.2. Notochordal cells within Human Intervertebral discs. *Haematoxylin and eosin (H&E) stained human IVD tissue during development, shown at low and high magnification. Staining demonstrates large vacuolated morphology of cells within the developing NP region at (A) 7-weeks post-conception (WPC), (B) 8.5 WPC, (C) 10 WPC and (D) 17 WPC. (E) shows retention of clusters of large cells within the NP region in a 10-year-old IVD, while (F) shows presence of only single, smaller mature NP cells within the NP region in a 17-year-old IVD.*

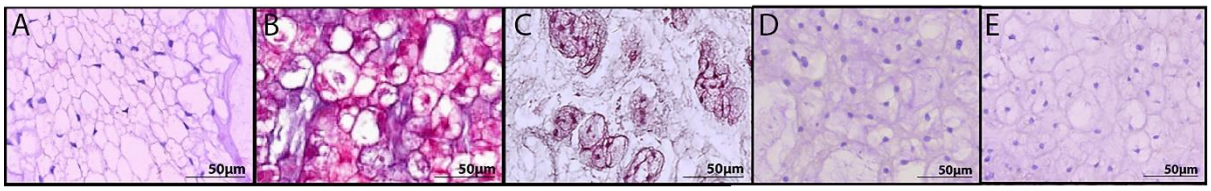

Figure 2.3. Notochordal cells are maintained in mature discs of Mice (A), Rats (B), Rabbits (C), Pigs (D) and some breeds of Dogs (E). *Images shown are from Rodents and Pigs < 3 months of age, Dog image is from a mixed breed non-chondrodystrophic dog at 1 year of age. Haematoxylin and eosin (H&E) stained images, Scale bar = 50μm.*

The loss of the NC population in certain species (*e.g.* CD dogs) coincides with the development of IVD degenerative changes and clinical disease (Bergknut *et al.*, 2013), indicating that NCs may play a role in maintaining healthy NP tissue. Several studies (Aguiar *et al.*, 1999; Gantenbein-Ritter and Chan, 2012; Gantenbein *et al.*, 2014) have determined the regenerative potential of NCs and found that they may be a promising target for regenerative and/or symptom modifying therapies for IVD disease which has been reviewed recently (Bach *et al.*, 2022). However, less than 3% of papers reporting the potential use of cells to promote regeneration of the disc, utilised NCs as the cell choice (Williams *et al.*, 2021), whereas a larger emphasis has been on other cell types such as bone marrow-derived mesenchymal stem cells, and mature NP or AF cells. Studies investigating the use of NCs have sourced these from pigs (Devina Purmessur *et al.*, 2013; Gantenbein *et al.*, 2014; Potier and Ito, 2014; Arkesteijn *et al.*, 2017), rats (Miyazaki *et al.*, 2009; Kwon *et al.*, 2017; Li *et al.*, 2018), rabbits (Miyazaki *et al.*, 2009), and dogs (Cappello *et al.*, 2006). The studies mainly utilised 3D *in vitro* culture, where the phenotype could be maintained at least partially, with a distinct lack of progression into clinical studies. Their limited use in research so far has been due to the difficulties in their utilisation *in vitro*. In particular, maintaining phenotype in monolayer culture *in vitro* is problematic (Gantenbein *et al.*, 2014; Potier and Ito, 2014; Spillekom *et al.*, 2014) and due to

their limited capacity to proliferate without loss of phenotype, it is often difficult to harvest sufficient numbers for *in vitro* manipulation (Kim *et al.*, 2009; Potier *et al.*, 2014; Spillekom *et al.*, 2014) and extraction itself often leads to disruption of normal phenotype (Wang *et al.*, 2001). To date, there is a lack of consensus for the extraction, numeration, *in vitro* culture and characterisation of NCs. Discrepancies observed in results could be explained by species-specific differences, however large variations in methodological approaches are likely a major contributor. Thus, this paper aims to provide key recommendations and methodologies for NC isolation, numeration, *in vitro* manipulation, and characterisation to support research into NC physiology and potential in regenerative therapies.

RECOMMENDED METHODOLOGY FOR EXTRACTION OF NOTOCHORDAL CELLS FROM THE NUCLEUS PULPOSUS OF MULTIPLE SPECIES

RECOMMENDATIONS FOR DISSECTION AND ASEPTIC ISOLATION OF INTERVERTEBRAL DISC/NUCLEUS PULPOSUS TISSUE

NCs are regularly sourced from several species for *in vitro* investigations. These include small rodents such as mice and rats where lumbar and caudal (tail) discs are commonly used, however, caudal discs within mice are often preferred due to their higher numbers and ease of accessibility, whilst lumbar and caudal discs are often sourced from rats. However, given the size of rodent IVDs, isolation of pure NP tissue can be problematic and may require downstream fluorescent activated cell sorting (FACS). Furthermore, generating sufficient cells for downstream analysis normally requires the pooling of discs. Large species such as non-chondrodystrophic dogs (IVDs ~20 mm depending on the breed), and pig (IVDs ~30mm at 3 months) provide large NP tissue sources which are easier to isolate. Within species which lose their NCs during development, i.e., humans and chondrodystrophic dogs, foetal (7-25 weeks post conception (wpc) human) or young dog discs are sourced dependant on age of the donor, the separation of NP and AF may not be possible in the case of earlier stages of development, like pre segmentation spines, and thus FACS is recommended to ensure pure populations for study.

ASEPTIC ISOLATION OF THE SPINE/TAIL

This method outlines the procedure for dissecting the spine or tail (where appropriate) into intact spinal units. However, as some samples, e.g., human samples obtained from early pregnancy terminations, are not always received intact, adaptation of this procedure may be required based on the state of the tissue on arrival. To ensure sterility external surfaces such as whole mice, rats or pig tails/lumbar sections received from the animal house or external sources (i.e., abattoirs) remove first any debris and blood and clean with 70% ethanol (note: only use 70% ethanol if there are tissues external to the IVDs). For isolation of the spinal column of whole cadavers where available, eviscerate and cut off the limbs as close to the

spine as possible and dissect the spinal column according to the procedure described in detail by Lee *et al.,* (2021). For isolation of caudal discs, a longitudinal incision along the dorsal side of the tail is performed to reveal the underlying tissues. Dissect away the skin, muscles and other tissues exposing the IVDs, whereafter the exterior of the spine/tail is aseptically cleaned according to surgical protocol (2 times with Hibiscrub (chlorhexidine gluconate 40 mg/mL)) via spraying with chlorhexidine for 2 times both followed by 3 min incubation.

DISSECTION OF THE INTERVERTEBRAL DISC FROM THE SPINE/TAIL

For the isolation of IVDs from small specimens, e.g., mouse, rat, young dogs, and human foetal samples, IVDs can be seen as bright white stripes between the more translucent vertebral bodies (Fig. 2.4a). It is recommended to use a dissection microscope or binocular glasses to aid with the isolation of the IVD, starting at the most anterior disc. While holding the spine with the fine forceps, use for dissection a microsurgical knife (*e.g.,* nr 11 scalpel knife for larger IVDs) or ophthalmic knives (Beaver® Optimum™ Knives) or an equivalent such as micro blades or a stab knife for small discs such as mouse caudal discs. The stab knife is recommended because discs from mice are very small ~2 mm in diameter and the standard #10/#11 scalpel blades are too large and could lead to accidental cutting into the IVD, immediate depressurization of the NP and loss of the tissue (Fig. 2.4b). Cut transversely along the plane of the anterior side of the disc, cutting off the vertebral body adjacent to it (Fig. 2.4c). The disc/vertebral body boundary should be a natural line of least-resistance. For younger donors (foetal <18wpc in humans) where the AF and NP tissues have not undergone segmentation or the vertebrae are not entirely calcified, it may not be possible to isolate the NP tissue from surrounding tissues. In such a case the whole IVD is dissected, and a mixed population of cells isolated which may include NC, AF and CEP cells which could then be separated using FACS (See extraction of whole disc segments below).

For older donors of NC-rich discs where the NP and AF tissues can easily be distinguished, the AF is seen as a white ring surrounding a translucent jelly-like NP (Fig. 2.4c and d). For mouse discs use a pair of fine curved forceps to ‘spoon out’ but it is essential you do not pinch the NP tissue from the disc (*pinching via standard forceps application will traumatise the tissue and diminish cell viability) (Fig. 2.4di) and place this onto the wall of an empty sterile Eppendorf tube on ice (Fig. 2.4ei). Whilst for larger discs such as young dog and foetal human (>~18wpc) discs the NP and AF are separated manually using a curettes size A (World Precision Instruments, 501773) (Fig. 2.4dii). Mouse NCs retain high viability in a sealed empty tube on ice, or room temperature for up to one hour. Collect multiple levels of the NP as required into the same tube to minimise variation of the digestion time (Fig. 2.4f) and proceed to digestion of the tissue (Fig. 2.4g and h). A freshly extracted NP is observed as a clump of cells, but after 20 minutes digestion, are separated into single cells (Fig. 2.4i and j). For larger IVD such as those from adult non-chondrodystrophic dogs and pig IVDs, open the IVD-space with a sterile no 22 blade at the border of the cranial endplate. Distract the IVD-space with the aid of a Hohmann retractor (approaching the spinal canal from the adjacent opened IVD). Collect the

gel-like NP with the aid of a curette and transfer into a 50mL tube with 10-15mL αMEM + 1 % P/S.

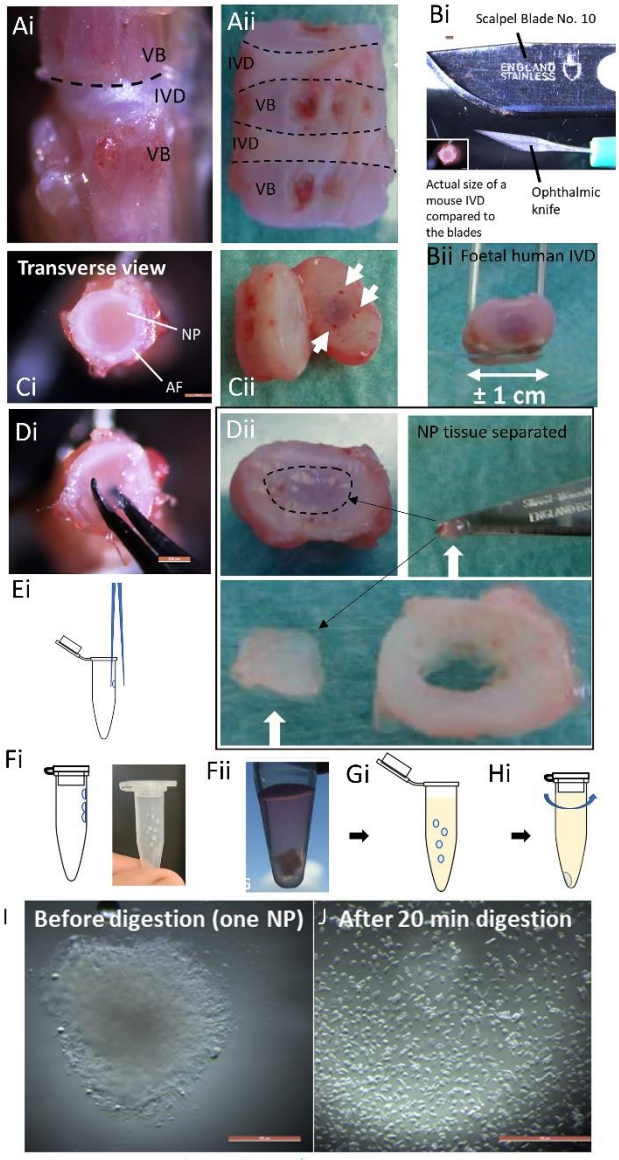

Figure 2.4. Dissection of mouse and stillborn foetal human lumbar spine (21 weeks of gestation). *Ai: Mouse motion segment and Aii: Human foetal L3, L4, and L5 vertebrae with IVDs L3-L4 and L4-L5. Bi: Ophthalmic knife and scalpel blade no 10 in comparison to whole mouse IVD demonstrating importance of use of ophthalmic or stab knife for extraction. Bii Whole foetal human IVD isolated for scale (1cm in diameter). C: The IVD should be excised by cutting at the junction between endplate and AF shown for mouse (Ci) and human (Cii) IVDs, noted within human foetal IVD end plates with blood vessels (white arrows) can be clearly seen. D: The NP region is carefully removed from the IVD in the mouse (Di) this is spooned out with curved forceps, whilst human NP (Dii) can be carefully separated with a nr 11 scalpel blade separating out from the AF and EP tissue. E: The tissue of the mouse IVD is placed carefully in the edge of an Eppendorf tube and F multiple NP tissue samples can be combined together for mouse (Fi) or individual NP tissue may be collected separately for human (Fii) dependant on size. The sample can further be processed by enzymatic digestion (G) prior to centrifugation and resuspension in resuspension media (H). I: Mouse NP tissue shown pre digestion and J: after digestion. Scale bar = 500µm.*

RECOMMENDATIONS FOR DIGESTION OF NUCLEUS PULPOSUS TISSUE AND NOTOTCHORDAL CELL EXTRACTION

Following dissection, the NP tissue is placed in a 50mL tube with 10-15mL αMEM + 1% Penicillin/Streptomycin (P/S), or 15ml centrifuge tube for smaller discs (e.g., mouse) with 5ml media. Centrifuge at 500*g* for 5 min at room temperature (RT) and discard the supernatant. Of note is that contrary to degenerate NP tissue, NC-rich NP tissue is gel-like and generates a relatively loose pellet upon centrifugation requiring caution during removal of the supernatant. Incubate the collected NP tissue in digestion enzyme as per species specific methodology (Table 2.1). Place the tube on an orbital shaker at 37°C, 300 rpm during enzyme digestion. It is expected that after shorter term digestion periods, there will be a small number of remaining cell clumps, however, these can be readily dispersed by gently pipetting the cells with wide bore 1mL tips. Centrifuge at 500*g* for 5 min at room temperature and discard the supernatant. The expected outcome of this protocol is obtaining both single cells and clusters. Filter the sample over a 40-µm cell strainer (the filtered solution will contain the non-clustered cells). Collect the NC clusters by washing the filter upside down with resuspension media (Table 2.1). After centrifugation at 500*g* for 5 minutes, resuspend the cells in αMEM with 1% P/S and count (See numeration section). The < 40-µm fraction will contain single cells and smaller clusters, whereas the > 40µm fraction will contain the larger clusters of predominantly NC-like cells with vacuoles, 25–85µm in diameter.

Table 2.1. Digestion protocols*. Note: for mouse, young dog and foetal human NP extraction enzymatic digestion with pronase, higher concentrations of collagenase, or longer digestion times considerably decreases NC viability and is not necessary because of the loose extracellular matrix. Collagenase (Worthington, LS004177), Dispase (Worthington, LS02109), and Pronase (11459643001, Roche Diagnostics), are filtered with a 0.22µm membrane filter to ensure sterility, all incubations are performed at 37°C.*

Tissue type	**Digestion enzymes**	**Resuspension medium**
Mouse tissue	20 minutes in HBBS with 850 U/mL Collagenase II and 2.6 U/mL Dispase	HBSS + 2% BSA
Rat tissue	30 minutes with 7 U/mL pronase followed by 4 hours digestion with 125 U/mL collagenase type II	αMEM + 1% P/S
Young dog tissue	1 hour in αMEM with 37.5 U/mL collagenase type II	αMEM + 1% P/S + 2% BSA
Adult dog tissue (NCD)	30 minutes in αMEM with 7 U/mL pronase followed by 4 hours with 125 U/mL collagenase type II	αMEM + 1% P/S
Pig tissue	30 minutes in αMEM with 7 U/mL pronase followed by 4 hours digestion with 125 U/mL collagenase type II	αMEM + 1% P/S
Foetal human tissue	30 minutes in αMEM with 37.5 U/mL collagenase type II	αMEM + 1% P/S

Of note, mouse NC digestion was particularly sensitive to digestion time, with an increase of digestion time from 20 to 30 min resulting in lower cell viability (Fig. 2.5). Furthermore, the addition of 2% v/v BSA in Hanks' Balanced Salt Solution (HBSS) during digestion improved cell viability compared to HBSS alone (Fig. 2.5), which has also been found for puppy NC isolation, whilst this was not necessary for NC isolation from other species. A small study was conducted to compare harvested NCs from pig spines versus tail IVD which are often waste material from the meat industry. More NP tissue was extracted from pig spines than tail IVDs in line with the larger IVDs within the spine (Fig. 2.6). However, no difference was observed in the total number of NCs harvested per disc (Fig. 2.6) with greater number of NCs per gram of tissue in NP tissue taken from the smaller tail IVDs compared to larger spine IVDs. Furthermore, isolation from tails was experienced as simpler; IVD exposure was more straightforward than spines where collection is hampered by the facet joints and transverse processes. These results provide the opportunity to refine and reduce waste material, as tails can be sourced from waste material from the meat industry whilst the use of spines often wastes the associated meat joints, this is in line with 3Rs (replace, reduce, refine) (Thorpe *et al.*, 2018; Hubrecht and Carter, 2019).

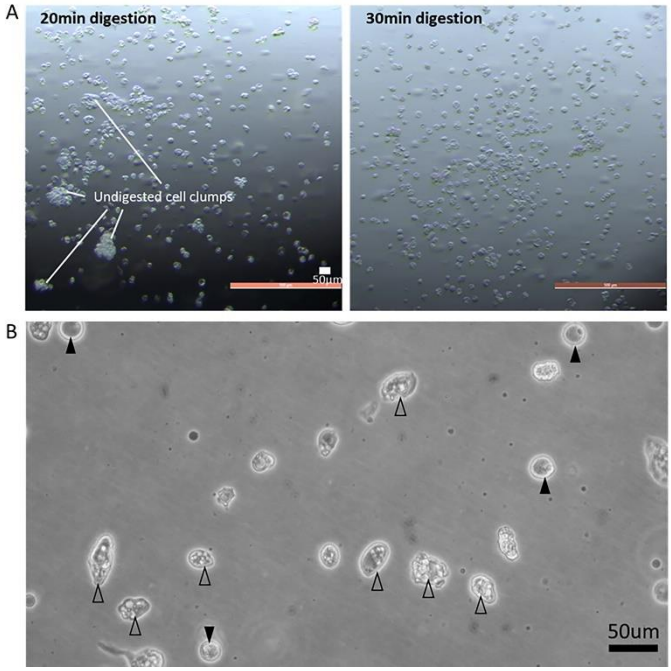

Figure 2.5. Shortened digestion times for mouse NC digestion result in better cell viability. *After 20 minutes digestion, there will be some undigested cell clumps remaining which can be dispersed by gentle pipetting with a wide bore pipette, whilst increased incubation time to 30 minutes results in increased levels of cell lysis which are observed as more transparent cells (A). Morphology of healthy NP cells includes both notochordal-like cells (Δ) which exhibit an irregular shape and contain vacuoles, and round chondrocyte-like cells (▲) (B).*

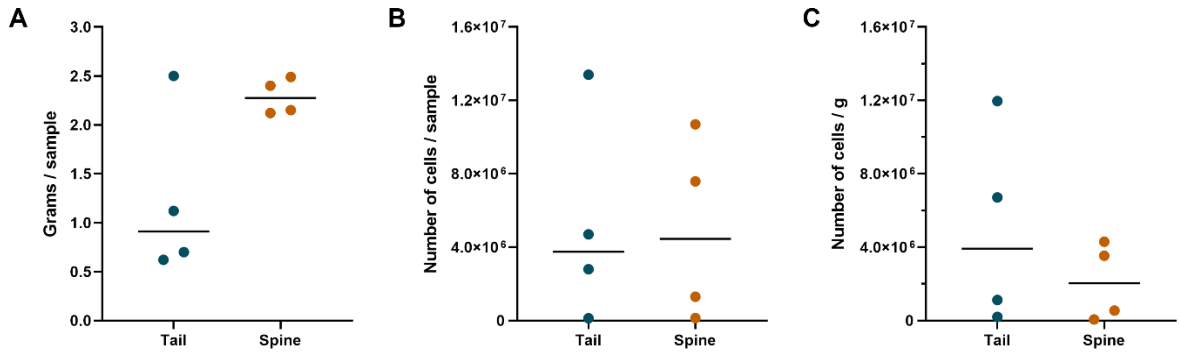

Figure 2.6. NC extraction yields from porcine spines and tails. *NP tissue harvested from porcine spinal and lumbar IVDs, comparing the weight and NC density from the extracted tissue. (A) the weight of NP tissue usually extracted from a porcine spine or tail specimen, (B) the total number of NC extracted from a porcine spine or tail specimen (C) The amount of NC counted per gram of NP tissue from the spine or tail IVDs. N=4, Mann Whitney test performed to evaluate statistical significance.*

DIGESTION OF WHOLE INTERVERTEBRAL DISC TISSUE WHERE NUCLEUS PULPOSUS ISOLATION IS NOT POSSIBLE (E.G. HUMAN FOETAL IVDS (<18 WPC))

Note: The enzyme concentration and centrifugation steps reported in the section below were designed to rapidly isolate cells and maximise the number of cells collected for RNA/protein extraction, thus further optimisation may be required to ensure high cell viability (see "*Digestion of NP tissue*" as a guide).

Transfer the IVD to a petri dish containing phosphate buffered saline (PBS) to remove blood cells from the sample, which may contaminate the collected NC population during FACS. Using fine forceps (scoop do not pinch), transfer the IVDs to 50mL Falcon tube containing 15mL 62.5U/mL Collagenase Type II (Gibco®, 17101-015) and 150U/mL type I-S hyaluronidase (Sigma-Aldrich®, H3506) in αMEM media containing 1% antibiotic/antimycotic solution. Incubate on an orbital shaker at 37°C for 2 hours. Centrifuge at 500*g* for 5 minutes at room temperature and discard the supernatant. Suspend the cell-pellet in a pre-warmed non-enzymatic cell dissociation solution (e.g., Sigma, C1419) and incubate on the orbital shaker at 37°C for 10 minutes to help dissociate further cell aggregates. Centrifuge at 2000*g* for 5 minutes at room temperature and discard the supernatant. Resuspend in 1mL sterile PBS and pipette gently to disperse the pellet. Thereafter, the cells are strained to remove cell aggregates or debris that would interfere with downstream FACS with 50µm cup type Filcon® (BD Biosciences, 340629). The Filcon® cup is pre-wet with 500µL PBS, before the application of the 1mL cell suspension. Following washing with 500µL PBS, the cell suspension is centrifuged at 500*g* for 5 minutes at 4°C and FACS can be conducted as reported previously (Rodrigues-Pinto *et al.*, 2018). The notochordal population is typically 5-20% of total viable cells (NC, AF and CEP cells) from the digested IVD (Rodrigues-Pinto *et al.*, 2018).

CALCULATING CELL NUMBER

The characteristics of NCs contribute to creating an increasingly difficult cell type to count, due to the large cytoplasmic vacuoles, freshly isolated NCs range from 10 to 40 µm in diameter(Hunter *et al.*, 2004; Snuggs *et al.*, 2019) and NCs exist as a network of large cell clusters, containing 10 to 400 cells (Hunter *et al.*, 2003; Spillekom *et al.*, 2014); with multiple tight cell to cell adhesions (Hunter *et al.*, 2003; Hunter *et al.*, 2004b; Hwang *et al.*, 2015). Furthermore, these large cell clusters are surrounded by a thin layer of matrix (notochordal sheath) which physically separates one cluster from another (Hunter *et al.*, 2003). Whilst several techniques and specialist cell counters have been developed to count clusters of cells (Kothari *et al.*, 2009), they often fail to accurately enumerate single cells. In order, to gain the most efficient and reliable cell count, the cell clusters must be dissociated.

The customary methods of dissociation include using enzymatic approaches, such as: trypsin, TrypLE, dispase and accutase (Ellerström *et al.*, 2007; Wallman *et al.*, 2011; Beers *et al.*, 2012; Lin *et al.*, 2013; Ohnuma *et al.*, 2014; Diaz-Hernandez *et al.*, 2020; Zhang *et al.*, 2020); and/or mechanical approaches, such as: filters, chopping techniques, microfluidic devices and various ways of pipetting (Jager *et al.*, 2016). Jager *et al.,* (2016) compared different ways of dissociating human induced pluripotent stem cells, which are grown in large clusters (17,000 μm^2) if left untreated and therefore difficult to dissociate without cells loss (Ohnuma *et al.*, 2014; Jager *et al.*, 2016). They demonstrated that none of the mechanical methods of dissociation produced single cells or small cell clusters. Whereas the combination of TrypLE followed by trypsin/ Ethylenediaminetetraacetic acid (EDTA) digestion produced dissociated samples where the individual cells could be easily distinguishable (Jager *et al.*, 2016).

Within the current study, enumeration methods were investigated to enable efficient and reliable dissociation of NC clusters which has not previously been reported. A comparison of dissociation methodologies was investigated to determine influence on cell count, viability and resulting diameter, utilising an automated cell counter (NucleoCounter® NC-200™ (Chemometec, Gydevang, Denmark)). Freshly extracted NC clusters were harvested from a single donor pig spine, as described above, and 500µL of NC suspension in αMEM + 1% P/S (allowing for triplicate repeats) was used to undergo different cell dissociation reagents. Dissociation reagents included either a) solution 10 lysis buffer (Chemometec); b) Solution A100 and B (Chemometec); c) Accutase (Sigma); d) Trypsin/EDTA (Thermofisher, Gibco); e) TrypLE (Thermofisher, Gibco); and lastly f) TryLE followed by Trypsin. For solution 10 lysis buffer method; 100µL NC suspension was directly added to 100µL solution 10 lysis buffer (Chemometec). The Solution A100 and B methods was conducted by taking 100µL NC suspension sample and directly adding Solution A100 lysis buffer (Chemometec), leaving the NC sample in 100µL solution A100 for 0, 2, 5, and 10 minutes, before next adding 100µL of solution B stabilizing buffer (Chemometec). The Accutase method involved adding 1mL of accutase (Sigma) directly to 100µL of NC suspension, incubated for 10 minutes at 37^{o}C, prior to being centrifuged for 1 minute at 400*g* and resuspended in 1mL αMEM + 1% P/S.

Trypsin/EDTA method involved adding 1mL of Trypsin/EDTA (Thermofisher) directly to 100µL of NC suspension, incubated for 10 minutes at 37^{o}C, prior to being centrifuged for 1 minute at 400*g* and resuspended in 1mL αMEM + 1% P/S. Finally, TrypLE method also involved adding 1mL of TrypLE (Thermofisher) directly to 100µL of NC suspension, incubated for 10 minutes at 37^{o}C, prior to being centrifuged for 1 minute at 400*g* and resuspended in 1mL αMEM + 1% P/S. After dissociating NC suspension was counted using the NucleoCounter® NC-200™.

A combined analysis of images captured, and the cell count (Fig. 2.7) demonstrated that solution A100 and B could produce accurate cell counts and displayed visible NC dissociation, with the observation of single cells, whilst accutase, Trypsin, TrypLE and TrypLE + trypsin resulted in reduced cell counts (Fig. 2.7). Repeatability, linearity and range was further tested with the Solution A100 and B. The method of dissociating NC clusters with Solution A100 followed by the stabilizing solution B buffer after 2 minutes, showed the most promising method of dissociation (Fig. 2.8). Prolonged incubation of NC clusters in solution A100 for more than 2 minutes caused the release of 'sticky' DNA from neighbouring dying cells causing the observation of cell clumps (Fig. 2.8), whilst addition of solution A100 followed by immediate analysis (0 minutes) did not dissociate NCs into single cells (Fig. 2.8). Linearity studies demonstrated excellent linearity with a slope of 1.047 and R2 of 0.9979 compared to expected cell number (Fig. 2.8). Thus, the recommended methodology for numeration is to add 100µL of solution A100 lysis buffer (Chemometec) to 100µL of cell suspension and incubate for 2 minutes at room temperature. Following incubation 100µL of stabilising buffer (Solution B (Chemometec)) should be added. The resulting cell suspension with solution A100 and B is then loaded into the Via1-Cassette™ (Chemometec) and read with the NucleoCounter® NC-200™ to provide a NC count allowing for the 1 in 3 dilutions of the original cell suspension due to addition of 1:1:1 cell suspension, solution A100 and solution B. If a NucleoCounter® is not available we would recommend following the dissociation method described above and proceed to simple cell count using a manual haemocytometer, whilst automatic counting decreases subjective counting and user error and increases throughout.

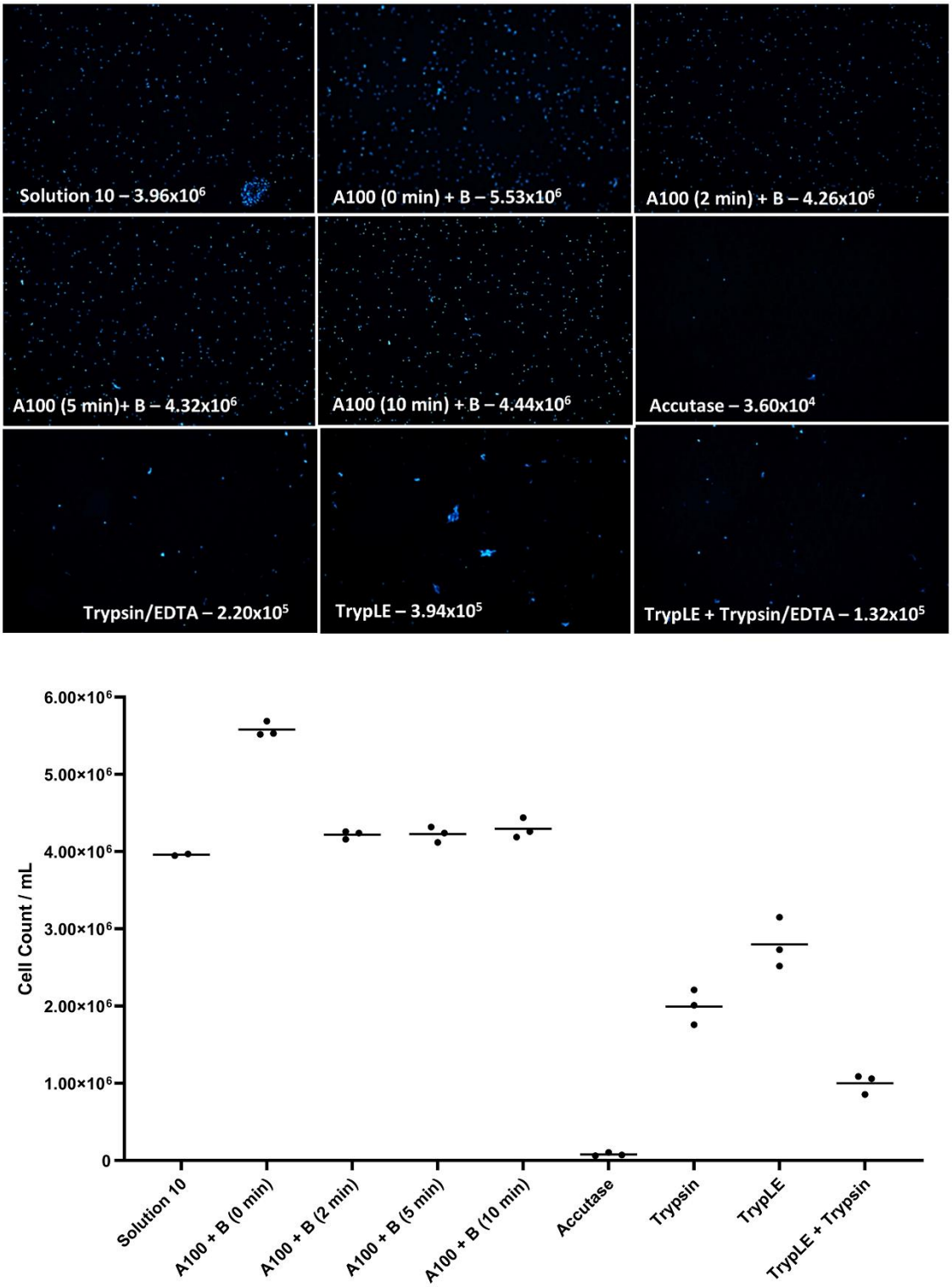

Figure 2.7. Differential dissociation methods to enable numeration of notochordal cells from porcine NP tissue. *Nucleocounter images and total cell counts/ml obtained using dissociation methodology: Solution 10 lysis buffer (Chemometec) (n=2), Solution A100 Lysis Buffer (Chemometec) with differential incubation times (0-10 minutes) followed by solution B stabilizing buffer (Chemometec) (n=3), Acutase (Sigma) (n=3), Trypsin/EDT (Thermofisher) (n=3), TrypLE (Thermofisher) (n=3) or TryLE followed by Trypsine EDTA (n=3).*

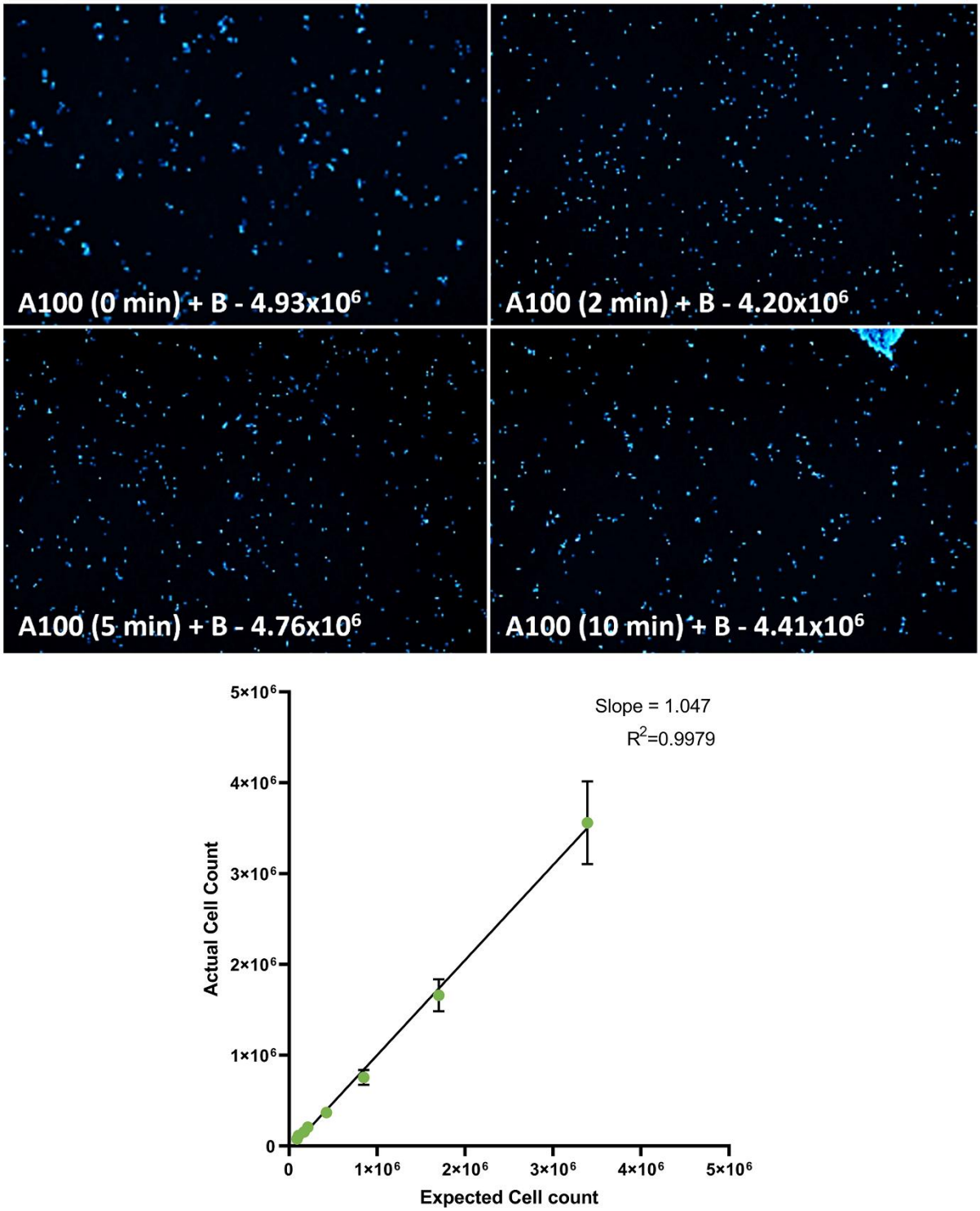

Figure 2.8. Numeration methodology for NCs using Chemometec nucleocounter*. Dissociation of NCs was performed using solution A100 lysis buffer for 0,2,5 or 10 minutes prior to addition of Solution B stabilising buffer (n=3). Similar total cell counts were observed, however at 0 minutes cell clusters were still present and if A100 was left on for 10 minutes larger clumps could be visualised. Thus a 2-minute incubation time was selected for further linearity testing. Linearity studies comparing expected cell number via serial dilution was confirmed with a slope of 1.047 and R2 of 0.9979. Statistics performed with in GraphPad prism v9.5.1 to calculate the coefficient of variation.*

CRYOPRESERVATION OF NOTOTCHORDAL CELLS

Cryopreservation of NCs in the presence of a cryoprotective agent comes with anecdotal challenges in achieving a high cell viability after thawing. During freezing, the intracellular water molecules can form ice crystals which can damage cell membranes and other organelles and result in cell death. Cryoprotective agents prevent the formation of these ice crystals (Tamagawa *et al.*, 2022), nonetheless the effectiveness therefore may depend on the cell type. Mature NPCs have been shown to maintain high viability after cryopreservation with the use of Dimethylsulfoxide (DMSO) and FCS as cryoprotective agents (Nukaga *et al.*, 2016; Croft *et al.*, 2021), and is the most utilised methodology in the spine field (Basatvat *et al.*, 2023). Yet, there is little information on the cryopreservation of NCs. One of the key challenges relates to the NC vacuoles thought to contain a high-water content making NCs more susceptible to the formation of ice crystals in comparison to non-vacuolated NPCs.(Hunter *et al.*, 2007) In addition, NCs are present in cell clusters, which could prevent the cryoprotective agents from entering cells within the centre of large cell clusters.

To determine whether NCs could be cryopreserved and the optimal method to maintain viability and phenotype, different types and concentrations of cryoprotective agents were examined. The NCs were extracted from 10-week-old pig spines (*n*=3) and cryopreserved in a) 20% v/v FCS in αMEM with different percentages of DMSO (0, 5, 10 or 20%), b) 10% glycerol+90% FCS, or c) using a commercially available cryoprotective agent: CryoStor® CS10 (07930, Stemcell Technologies). Freshly isolated NCs were cryopreserved in a pre-cooled (4°C) Mr. Frosty™ Freezing Container which was put in -80°C overnight. Sixteen hours thereafter, the NCs were transferred to liquid nitrogen (-196°C). After one week, the NCs were thawed in a water bath (37°C) and the number and viability of the NCs were determined using the NucleoCounter® NC-200™.

Since NCs can be compared to oocytes because of their large size and high-water content and oocytes are successfully cryopreserved with in-straw vitrification-dilution (ISVD), this method was also tested for NC cryopreservation. Straws were prepared as described by Inaba *et al.,* (2011). As handling medium, αMEM was used and as a diluent solution αMEM + 0.5 M sucrose. Both single NCs (<40µm fraction) and clusters (>40µm fraction) were resuspended in 1.6M ethylene glycol and incubated for 5-15 minutes at room temperature to adjust to the isotonic volume. After centrifugation, the cells were resuspended in 75µL vitrification solution (1M sucrose + 10% glycerol in αMEM) (Mahmoud *et al.*, 2010). Three times 25µL cell suspension was taken up per straw, whereafter the straws were sealed using a heat-sealing machine. The straws were frozen directly in liquid nitrogen and stored at -196°C. The ISVD straws were thawed by holding them in the air for 5 seconds, whereafter they were swirled in a water bath (37°C, 8s). The straws were placed in a vertical position for 1 minute to mix the different contents, whereafter they were placed horizontally for 5 minutes to allow the cells to calibrate to their osmotic environment and temperature. Next, the sealed parts were cut

off and the cells were transferred to empty tubes. After centrifugation (500*g*, 5 min) cell viability was assessed using the NucleoCounter® NC-200™.

The viability of the NCs directly after extraction was high (>70%) (Fig. 2.9), however, following cryopreservation low viability levels were seen (between 5 to 20% in all the different concentrations of DMSO and the 10% glycerol + 90% FCS solution) (Fig. 2.9). IVSD cryopreservation failed to yield viable NCs after thawing. Interestingly, NCs cryopreserved in CS10 had a much higher viability (50-60%) than the NCs cryopreserved in all other cryoprotective agents (Fig. 2.9). In conclusion, to date all tested cryopreservation methods resulted in large loss in NC viability. CS10 showed highest viability levels with only 50% NCs remaining viable, but as a commercial product the content of this solution is unknown and further work would be required to determine phenotype following cryopreservation. It is thus currently recommended that NCs are utilised directly from extraction and not cryopreserved.

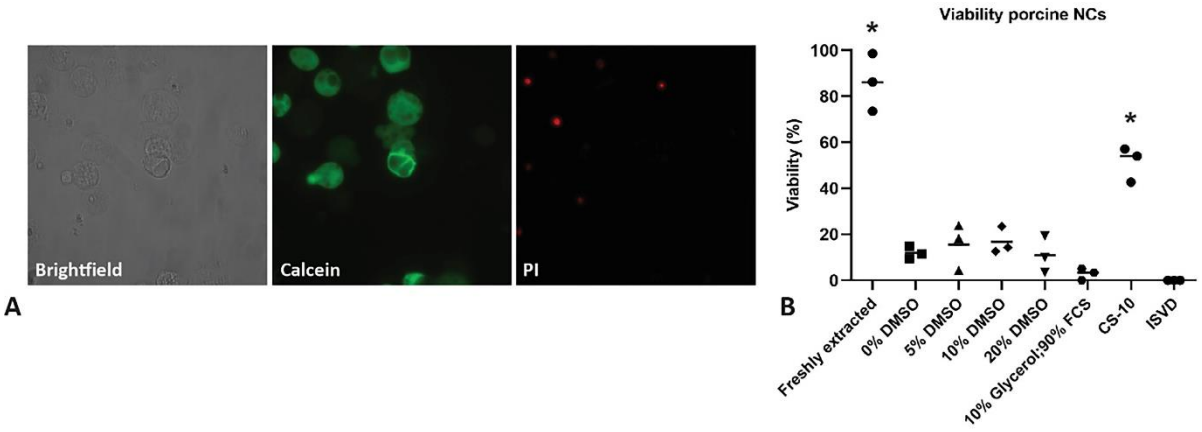

Figure 2.9. Viability of porcine NCs following cryopreservation testing: *(A) Brightfield and Calcein-AM and Propidium Iodide staining images of freshly extracted porcine NCs. (B) Viability of NCs directly after extraction, after cryopreservation using different methods (n=3 donors). *: p≤0.05 from all other conditions except condition with same symbol. Statistics performed with IBM SPSS statistics, Mann-Whitney U test, corrected for multiple comparisons (Benjamini-Hochberg posthoc test).*

CHARACTERISING THE PHENOTYPE OF NOTOCHORDAL CELLS

Characterisation of the phenotype of NCs residing in the IVD is essential to understand whether this phenotype can be maintained during culture. The morphological appearance of NCs, in particular the large vacuolated NCs, are distinctive and can be identified via numerous histological stains as described previously (Lee *et al.*, 2021) and showcased in Figure 2.10.

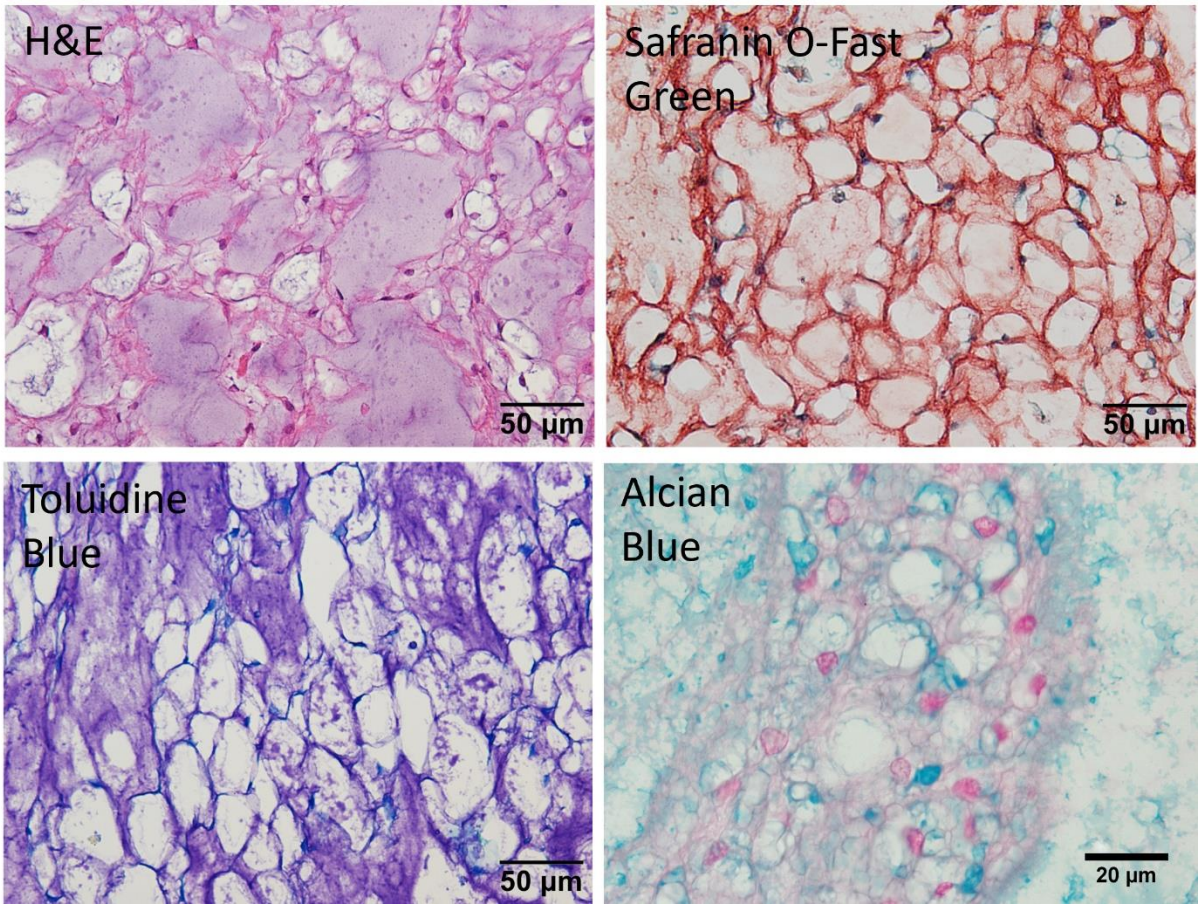

Figure 2.10. Histological appearance of NC rich pig disc: *NCs can be visualised clearly within a rich matrix of collagens and proteoglycans. NCs can be seen in large clusters of cells and display a vacuolated morphology. Which can be visualised with a variety of histology stains including H&E, Safranin O-Fast green, Toluidine Blue and Alcian Blue-Picrosirius Red.*

Here, we describe potential markers which can be useful to investigate key phenotypic and functional features of NCs, and whilst these are not all specific to NC phenotype, together they form a picture of cell status (Table 2.2). Cells that reside within the NP experience dynamic changes of gene transcription profiles throughout postnatal cell proliferation, differentiation, IVD growth, ageing and degeneration. The recent review by Bach *et al.,* (2022) discussed potential markers which can be utilised to aid in the characterisation of eNCs, NCs to NP cells highlighting key issues with identification of NC/NP specific markers and differential results between studies (Bach *et al.*, 2022). Whilst a number of key markers have been suggested to identify NC and NP cells, the evidence for NC specific markers are currently lacking, with cross expression across multiple cell types (Table 2.2). Expression of certain previously proposed NP markers (Sonic Hedgehog Signalling Molecule, SHH; Brachyury, TBXT; KRT18/19; CA12; CD24; HIF-1α; Glucose Transporter Type 1, GLUT-1) (Risbud *et al.*, 2015) are lost in older mature NPCs and hence could be useful to separate NCs from mature NP cells. Considering that the NC-rich NP can be properly isolated, the use of these markers is not complicated by the fact that they are also expressed by other similar cell types such as

articular chondrocytes (Thorpe *et al.*, 2016). Interestingly many markers which have been described have not yet been investigated at protein level within most/any species, demonstrating a need for further characterisation (Table 2.2).

In this context, key factors involved in normal NC physiology provide useful functional characterisation markers for NCs (Table 2.2). Furthermore, NCs are distinguished from the smaller mature NP cells by the presence of vacuoles and the formation of large cell clusters, which are surrounded by a rich extracellular matrix (ECM) NC sheath and thus key markers for these characteristics could be useful additional factors. Although cellular clusters are also observed during human disc degeneration(Johnson *et al.*, 2009; Brown *et al.*, 2018; Lama *et al.*, 2019; Le Maitre *et al.*, 2021), and thus additional markers in addition to clustering is essential to separate the juvenile NC and a cluster of NP cells from degenerate discs. The NC **vacuoles** express high levels of aquaporins (AQP) on the membrane (Snuggs *et al.*, 2019), with AQP6 demonstrating high intensity, which could be utilised to aid in vacuole identification (Fig. 2.11). Dual serine/threonine and tyrosine protein kinase (DSTYK) also known as Receptor interacting protein 5 (RIPK5) is required for notochord vacuole biogenesis and integrity, DSTYK mutants in zebrafish causes scoliosis-like phenotype in fish, and overexpression leads to vacuole formation in sheath cells (Parsons *et al.*, 2002; Pollard *et al.*, 2006; Gansner and Gitlin, 2008; Corallo *et al.*, 2013; Garcia *et al.*, 2017; Bagwell *et al.*, 2020). To date, limited studies have investigated the presence or role of RIPK5 within mammalian NCs and therefore its expression is investigated here within 3-month-old pig NCs. RIPK5 was identified within porcine NCs, mainly around large NC clusters and thus could be a useful additional marker of NCs (Fig. 2.12).

The **large NC clusters** are supported by multiple cell adhesion molecules, including gap junction proteins and cadherins. The presence of functional gap junctions anchored to the actin cytoskeleton, specifically connexin-43, have been shown in NC clusters from non-chondrodystrophic dog NP (Hunter *et al.*, 2003; Hunter *et al.*, 2004b) Furthermore, cadherins which are membrane-spanning macromolecular complexes responsible for cell-cell adhesion (Maître and Heisenberg, 2013; Hwang *et al.*, 2015), regulate the stability and cell contact formation. NC-rich NP tissues, including juvenile human discs and other animals, express high levels of CDH2 (N-cadherin, CD325) with a decrease in CDH2 correlating with the disappearance of cell clustering during ageing, as NCs are replaced by widely separated NPCs. Microarray and immunostaining have also implicated the membrane protein CAV1 (caveolin 1), an essential regulator of cell adhesion and migration, and is decreased during differentiation of NC to NPCs (Smolders, Meij, *et al.*, 2013; Bach *et al.*, 2016) and associated with progression of degeneration (Bach *et al.*, 2016).

The **NC sheath** has been shown to be highly important in the homeostasis of the developing spine within zebrafish, with scarce studies investigating this in mammals. The NC sheath is responsible for segmental patterning of the spine (Garcia *et al.*, 2017; Wopat *et al.*, 2018). Structurally the NC sheath is composed of three different layers that are comprised of laminin,

fibrillin, fibronectin, proteoglycan and collagen (Parsons *et al.*, 2002). Studies that used zebrafish deficient in α1α4 or α1α5 chain of laminin (Pollard *et al.*, 2006), the B1 and y1 chains of laminin-1 (Parsons *et al.*, 2002), Emilin-3 (Corallo *et al.*, 2013), Collagen 8 (Gansner and Gitlin, 2008) and Collagen 9α2 (Garcia *et al.*, 2017; Bagwell *et al.*, 2020) disrupt the sheath layer leading to a kinked spine and less vacuoles in NCs, which has also been linked to RIPK5 expression.

Table 2.2. Detection of key phenotypic markers in the embryonic notochord cells (eNC), notochordal cells (NCs) and the non-vacuolated nucleus pulposus cells (NPCs). *Evidence for expression identified at protein level based on immunostains, reporter expression, mass spectrometry or FACS. Confirmed protein expression is indicated for the cells residing within the notochord (eNCs) and the core of the intervertebral disc (NCs and NPCs). Within individual species:*

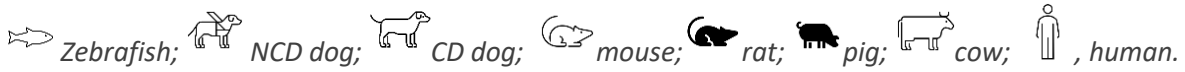

Blue icons indicate examples presented in the current manuscript (Fig. 2.11 and 2.12).

Note that immunopositivity is largely dependent on the antibodies employed and tissue processing methods and the absence of expression may indicate a lack of data and technical difficulties in protein detection. In the absence of protein expression data, evidence from in situ hybridization indicates the localization of gene expression in their cellular environment (Boxed symbols). Gene descriptions refer to data from https://www.genecards.org/.

Marker gene	Description	eNC	NC	NPC	References
TBXT (T, Brachyury)	T-Box Transcription Factor T. Involved in the transcriptional regulation of genes required for mesoderm formation and differentiation.	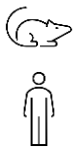	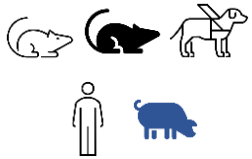		(Risbud *et al.*, 2010; Dahia *et al.*, 2012; Maier *et al.*, 2013; Hwang *et al.*, 2016; Rodrigues-Pinto *et al.*, 2016; Richardson *et al.*, 2017; Snuggs *et al.*, 2019)
CAV1	Caveolin-1. Acts as a scaffolding protein within caveolar membranes				(Heathfield *et al.*, 2008; Bach *et al.*, 2016; Paillat *et al.*, 2023)
CD24	Cluster of differentiation 24. Cell surface sialoglycoprotein expressed at the surface of immune as well as epithelial, neural, and muscle cells.				(Rodrigues-Pinto *et al.*, 2016; Richardson *et al.*, 2017)

DSTYK/ RIPK5	Dual Serine/Threonine and Tyrosine Protein Kinase. NC Sheath protein				(Bagwell *et al.*, 2020)
FOXA2	Forkhead box protein A2. Transcription factor involved in embryonic development, establishment of tissue-specific gene expression and regulation of gene expression in differentiated tissues.				(Maier *et al.*, 2013)
FOXF1	Transcription factor involved in embryonic development, establishment of tissue-specific gene expression and regulation of gene expression in differentiated tissues.				(Kalinichenko *et al.*, 2003; Thorpe *et al.*, 2016; Richardson *et al.*, 2017)
FOXJ1	Forkhead Box J1. Transcription factor specifically required for the formation of motile cilia.				(Beckers *et al.*, 2007)
KRT18	Keratin 18. Encodes the type I intermediate filament chain.		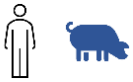		(Weiler *et al.*, 2010; Rodrigues-Pinto *et al.*, 2016; Richardson *et al.*, 2017)
KRT19	Keratin 19. Smallest known acidic cytokeratin specifically expressed in the periderm, the transiently superficial layer that envelopes the developing epidermis.		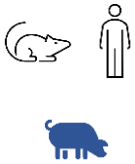		(Dahia *et al.*, 2012; Rodrigues-Pinto *et al.*, 2016; Richardson *et al.*, 2017)
LGALS3	Galectin 3. Encodes advanced Glycation End-Product Receptor.				(Götz *et al.*, 1997; Weiler *et al.*, 2010; Rodrigues-Pinto *et al.*, 2016; Richardson *et al.*, 2017)

NOG	Noggin. Inhibitor of bone morphogenetic proteins (BMP) signalling which is required for growth and patterning of the neural tube and somite.				(McMahon *et al.*, 1998)
NOTO	Notochord homeobox. Transcription regulator acting downstream of both FOXA2 and Brachyury during notochord development.				(Ben Abdelkhalek *et al.*, 2004; McCann *et al.*, 2012; Maier *et al.*, 2013)
SHH	Sonic Hedgehog Signalling Molecule. Encodes a protein that is instrumental in patterning the early embryo.				(McMahon *et al.*, 1998; Dahia *et al.*, 2012; Maier *et al.*, 2013; Peck *et al.*, 2017; Bach *et al.*, 2019)
SOX5	SRY-Box Transcription Factor 5. Involved in the regulation of embryonic development and in the determination of the cell fate.				(Smits and Lefebvre, 2003; Takimoto *et al.*, 2019)
SOX6	SRY-Box Transcription Factor 6. Involved in several developmental processes, including neurogenesis, chondrocytes differentiation and cartilage formation				(Smits and Lefebvre, 2003; Takimoto *et al.*, 2019)
SOX9	SRY-Box Transcription Factor 9. Transcription factor involved in chondrocytes differentiation and skeletal development.				(Sive *et al.*, 2002; Le Maitre *et al.*, 2004; Gruber *et al.*, 2005; Barrionuevo *et al.*, 2006; Dahia *et al.*, 2012; Takimoto *et al.*, 2019; Xu *et al.*, 2020)
ACAN	Aggrecan. Major proteoglycan component of the IVD extracellular matrix .				(Götz *et al.*, 1997; Hayes *et al.*, 2001; Le Maitre *et al.*, 2004; Roughley *et al.*, 2014; Hwang *et al.*, 2015; Peck *et al.*, 2017; Kudelko *et al.*, 2021)

AQP6	Aquaporin 6. Encodes for a membrane protein that functions as a water and solute channel in cells. Shown to clearly highlight vacuoles in NCs			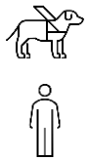	(Snuggs *et al.*, 2019)
CA12	Carbonic Anhydrase 12. Member of the large family of zinc metalloenzymes that catalyse the reversible hydration of carbon dioxide.				(Richardson *et al.*, 2017)
CDH2 (CD325, N-CADHERIN)	Cadherin 2. Encoded preproprotein is proteolytically processed to generate a calcium-dependent cell adhesion molecule which plays a role in the establishment of left-right asymmetry, development of the nervous system and the formation of cartilage and bone.				(Hwang *et al.*, 2016; Palacio-Mancheno *et al.*, 2018)
COL2A1 and COL2A2	Collagen Type II Alpha 1 Chain and Collagen Type II Alpha 2 Chain.		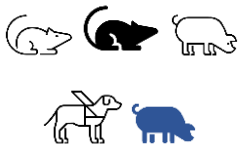	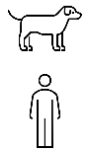	(Le Maitre *et al.*, 2004; Bach *et al.*, 2015, 2018; Hwang *et al.*, 2016; Peck *et al.*, 2017)
COL6A1	Collagen Type VI Alpha 1 Chain				(Perris *et al.*, 1993; Nerlich *et al.*, 1997, 1998; Aulisa *et al.*, 1998; Hayes *et al.*, 2001; Peck *et al.*, 2017)
GJA1 (CX43, Connexin-43)	Gap Junction Protein Alpha 1. Encoded protein is a component of gap junctions, which are composed of arrays of intercellular channels that provide a route for the diffusion of low molecular weight materials from cell to cell.				(Palacio-Mancheno *et al.*, 2018; Kudelko *et al.*, 2021)
GLUT-1 (SLC2A1)	Glucose Transporter Type 1/ Solute Carrier Family 2 Member 1. Encodes a major glucose transporter				(Rajpurohit *et al.*, 2002; Richardson *et al.*, 2008; Tsingas *et al.*, 2020)

HIF-1α	Hypoxia-inducible factor 1-alpha. Regulates genes that enable cell survival in a hypoxic environment, including those involved in glycolysis, angiogenesis, and expression of growth factors.				(Rajpurohit *et al.*, 2002; Thorpe *et al.*, 2016)
KRT8	Keratin 8. Typically dimerizes with keratin 18 to form an intermediate filament in simple single-layered epithelial cells. Plays a role in maintaining cellular structural integrity and also functions in signal transduction and cellular differentiation.				(McCann *et al.*, 2012; Richardson *et al.*, 2017)
PAX1	Paired Box 1. Involved in pattern formation during embryogenesis and may be essential for development of the vertebral column.				(Thorpe *et al.*, 2016; Richardson *et al.*, 2017; Takimoto *et al.*, 2019; Xu *et al.*, 2020)
TEK (TIE 2)	TEK Receptor Tyrosine Kinase. Encodes a protein that acts as cell-surface receptor for ANGPT1, ANGPT2 and ANGPT4. Regulates angiogenesis, endothelial cell survival, proliferation, migration, adhesion and cell spreading, reorganization of the actin cytoskeleton, but also maintenance of vascular quiescence.		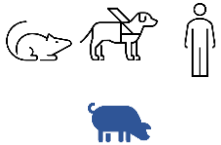	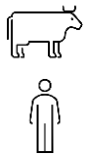	(Sakai *et al.*, 2012, 2018; Tekari *et al.*, 2016)

As a showcase immunohistochemistry was utilised to determine the expression and localisation of key proposed NC/NPC phenotypic markers within the NC-rich pig disc. Freshly extracted discs of juvenile pigs were formalin fixed and paraffin embedded, 4µm sections were utilised for IHC (Table 2.3) using previously published IHC protocols (Binch *et al.*, 2020). NP tissue within the NC-rich pig discs were shown to express positive immunohistochemical staining for a number of potential NC markers including: TBXT, SOX9, HIF-1α, FOXF1, PAX1, TIE-2 and pan-cytokeratin (Fig. 2.11). Furthermore ECM markers collagen type II and aggrecan were identified both within the ECM and cellular expression (Fig. 2.11). Vacuoles within NCs could be clearly seen using both AQP6 and CAV1 markers (Fig. 2.11), whilst CDH2 was also highly expressed (Fig. 2.11). Immunofluorescence was also utilised to identify expression of DSTYK/RIPK5 within native porcine discs and was shown to be highly expressed by NCs, particularly located around large NC clusters (Fig. 2.12), in a similar pattern to the NC sheath seen in zebrafish. Immunofluorescence also enables co-staining of cell and ECM markers, with the showcase demonstrated for AQP6 and COL2 (Fig. 2.12).

Table 2.3. Immunohistochemical procedures utilised for phenotypic characterisation of pigs – show case.

Antibody	Clonality	Optimal dilution	Antigen retrieval
Aggrecan Abcam, (ab3778)	Mouse monoclonal	5.58 µg/mL	Heat
AQP6 (Abcam, ab191061)	Rabbit Polyclonal	2.5 µg/mL	Enzyme
Caveolin-1 (BD Biosciences, 610406)	Mouse monoclonal	2.5 µg/mL	Heat
Collagen Type II (Sigma, maB1330)	Mouse monoclonal	5 µg/mL	Enzyme
FOXF1 (Abcam, ab168383)	Rabbit monoclonal	6.9 µg/mL	Heat
HIFα (Abcam, ab16066)	Mouse monoclonal	10 µg/mL	None
CDH-2 (Abcam, ab76011)	Rabbit polyclonal	10 µg/mL	Heat
panKRT (8, 18, 19) (Abcam, ab41825)	Mouse monoclonal	0.25 µg/mL	Enzyme
Pax 1 (Abcam, ab203065)	Rabbit polyclonal	2.5 µg/mL	Enzyme
RIPK5 (Abcam, ab234736)	Rabbit polyclonal	5 µg/mL	Heat
TBXT (Abcam, ab20680)	Rabbit polyclonal	10 µg/mL	None
Tie2 (Santa Cruz, sc-324)	Rabbit polyclonal	4 µg/mL	Heat

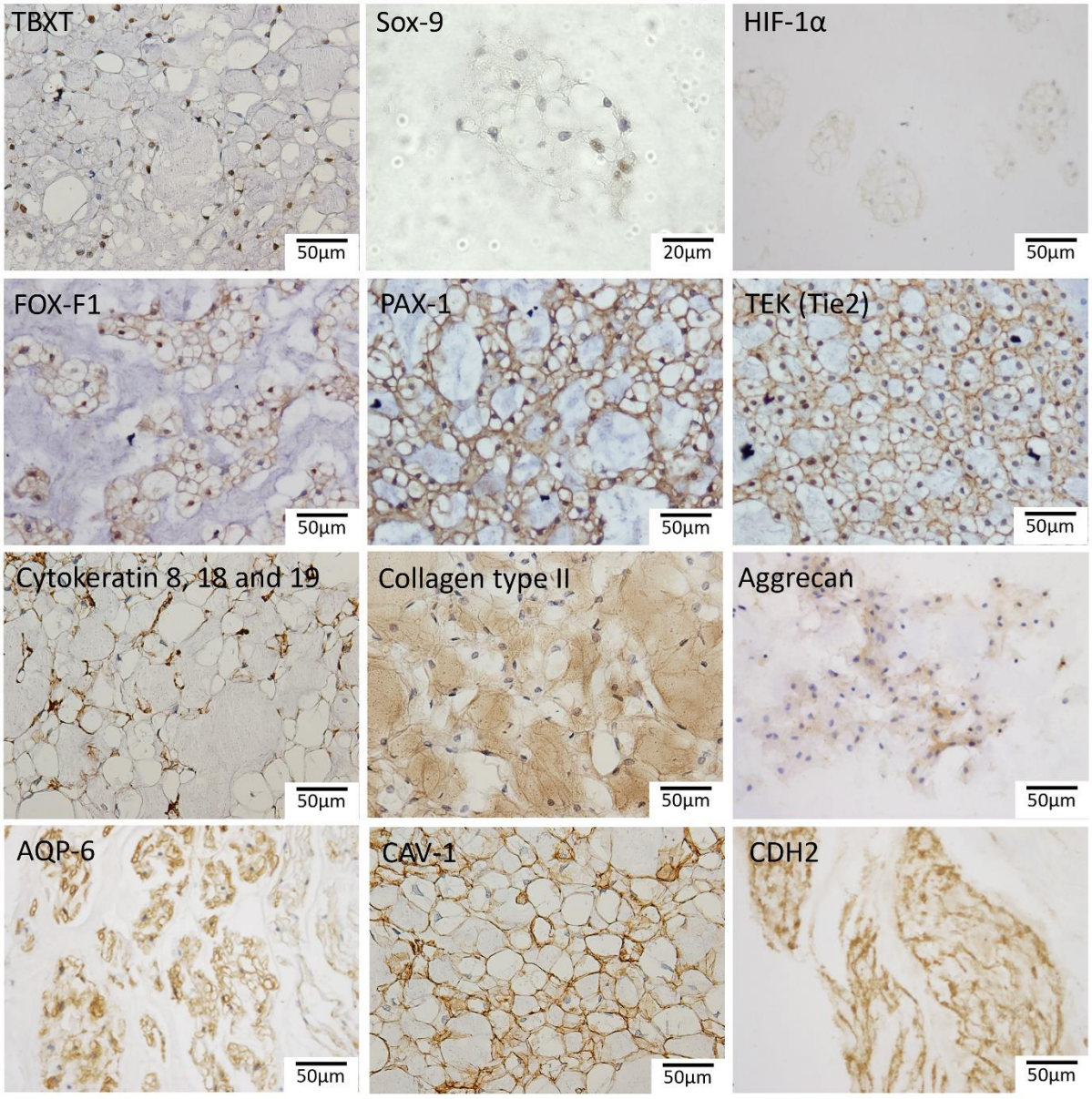

Figure 2.11. Immunohistochemical staining of NC rich pig and dog NP tissue: *Immunohistochemistry was utilised to identify localisation for potential characterisation markers of NCs. TBXT, SOX9, HIF -1α, FOXF1, PAX1, TEK (Tie 2), Pan Cytokeratin (8,18,19) Collagen type II, Aggrecan, CAV-1, and CDH2 were all observed within the NC rich regions of the NP of pig discs. AQP6 staining was shown for dog discs. Scale bars = 50µm except for SOX9 which is shown at higher magnification and 20µm scale bar.*

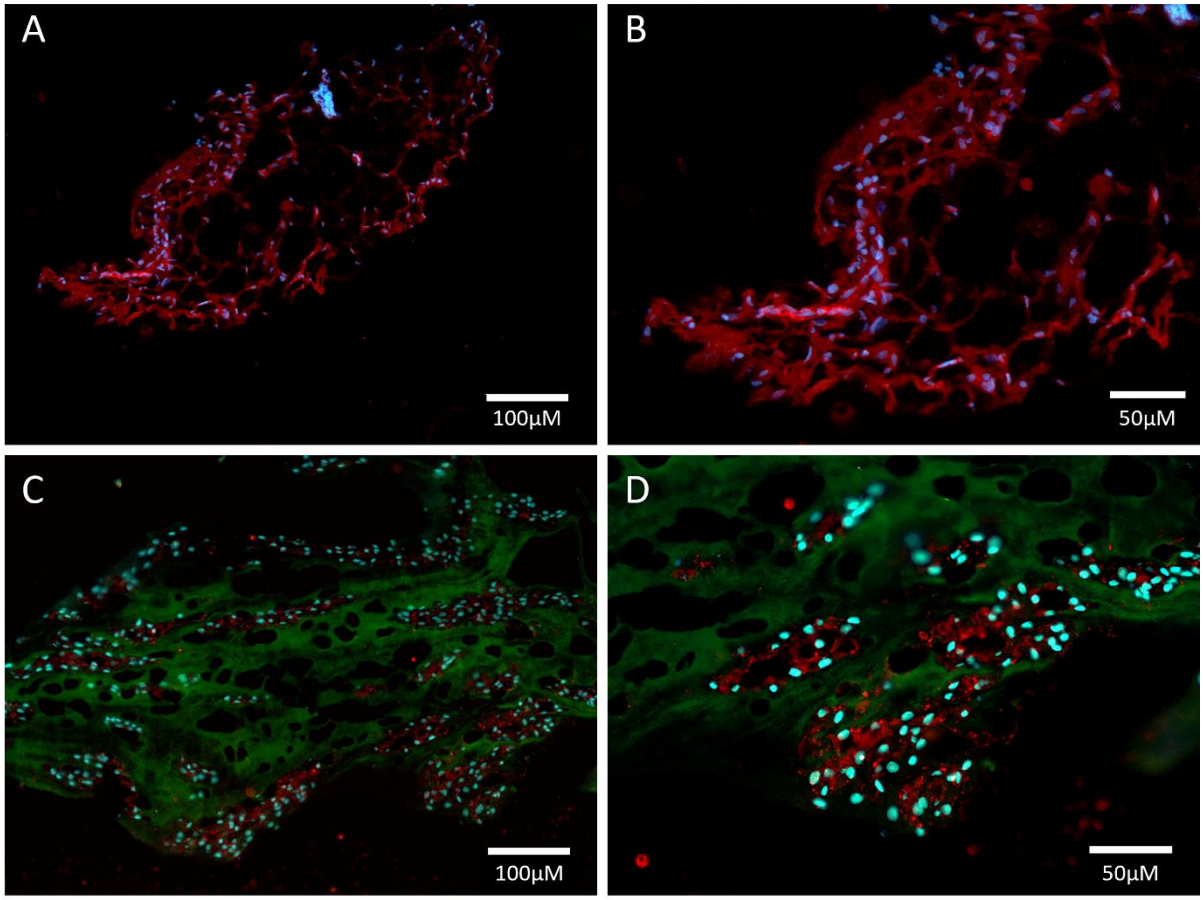

Figure 2.12. Immunofluorescence staining for NC rich pig NP tissue*. Immunofluorescence staining for DSKY-5 (A&B), and co-staining for AQP6 (red) and collagen type II (green) (C&D). Scale bar as stated 100µm or 50µm.*

In conclusion, the characterization of NC-specific markers, conserved across species and of physiological relevance, that can be utilized to define stage-specific cell types found in the notochord and later in the NP from eNCs to NCs and then NPC is still subject to discussion by experts in the field and remains to be fully resolved (see review; Bach *et al.*, 2022). Advances in "omic" technologies and in particular single cell or spatial profiling approaches hold promise to enable NC marker discovery and improve characterising and benchmarking the NC and NP cells phenotypic changes across species during their life journey (Peck *et al.*, 2017; Wymeersch *et al.*, 2019). Based on current knowledge particularly evidence from immunopositivity and the expression profile of potential markers which can be deployed to characterise NCs (Table 2.3; Fig. 2.11 and 2.12). However, given that many of the markers are expressed through eNCs, NCs and NPCs to discriminate between these cell types and to evidence NC phenotype co-expression at the level of single cells should be aimed using techniques such as co-immunostaining analysis.

CELL EXPANSION AND CULTURE WHILST MAINTAINING PHENOTYPE

The expansion and culture of freshly isolated vacuolated NCs, whilst also maintaining their *in vivo*-like phenotype, remains challenging. If cultured within a standard monolayer system, NCs

rapidly lose their clustered, vacuolated phenotype between 6-28 days or between 1-3 passages, and present morphologically as smaller, singular, non-vacuolated cells (Fig. 2.13), a phenomenon reported across multiple species (Smolders, Meij, *et al.*, 2013; Gantenbein *et al.*, 2014; Potier and Ito, 2014; Potier *et al.*, 2014). During this change in morphology, it has been observed that the expression of NC markers TBXT, KRT8/19, are decreased indicating that the smaller, non-vacuolated cells are phenotypically distinct from the originally extracted vacuolated NCs (Gantenbein *et al.*, 2014; Potier and Ito, 2014). In addition, vacuolated cells are quickly outcompeted by small, non-vacuolated cells in monolayer culture, as their growth rate is significantly slower (Kim *et al.*, 2009; Gantenbein *et al.*, 2014).

Therefore, specialised techniques have been developed which utilise several environmental cues, for the retention of the vacuolated NC phenotype during *in vitro* culture and expansion. It has been well established that 3D alginate bead culture helps to maintain the *in vivo* phenotype of mature non-vacuolated cells (Wang *et al.*, 2001). When vacuolated cells are cultured within alginate beads viability and culture duration was increased, their clustered, vacuolated morphology was retained, when compared to monolayer culture, with most studies to date using αMEM media (Kim *et al.*, 2009; Devina Purmessur *et al.*, 2013; Gantenbein *et al.*, 2014; Arkesteijn *et al.*, 2017). This indicates 3D alginate bead culture is an appropriate method that enables retention of native phenotype. In addition, alginate bead culture under physioxic (2% pO_2) (Gantenbein *et al.*, 2014) and physiological osmolality (400 mOsm/kg in αMEM media) (Spillekom *et al.*, 2014), increased vacuolated cell marker expression and clustering. Furthermore, there is evidence that the vacuolated cell phenotype can be retained under specific culture conditions *in vitro*. Initial short-term alginate culture caused some loss of phenotype, yet this was restored after 28 days in culture, indicating the initial NC vacuolated phenotype may be lost after isolation, but then at least partially recovered following extended 3D culture under appropriate osmotic culture conditions (Spillekom *et al.*, 2014).

3D culture systems such as alginate fail to enable expansion of NCs, thus alternative substrate surfaces together with environmental conditions have been investigated in the attempt to maintain phenotype whilst enabling expansion. Humphreys *et al.,* (2018), investigated retention of the vacuolated cell phenotype of pig NCs in 2D culture, with the use of cell culture substrate coatings, oxygen concentration, osmolality and surface stiffness (Humphreys *et al.*, 2018). The greatest levels of cell adhesion and proliferation, morphology and expression of NC phenotypic markers (CD24, KRT8, KRT18, KRT19 and TBXT) was observed with the use of laminin-521-coated surfaces with 0.5 kPa stiffness and αMEM media, under 2% pO_2, 400 mOsm/kg culture conditions, where highest number of vacuolated NCs (around 70%) were retained (Humphreys *et al.*, 2018). This indicates that the vacuolated NC phenotype can also be maintained under specific 2D culture conditions, where at least some population doubling is possible (Humphreys *et al.*, 2018). However, culture within such conditions can be difficult to obtain across laboratories and thus where proliferation of NCs is not required we

recommend that clusters of isolated NCs are maintained as clusters and cultured within alginate beads in αMEM media, under physiological O_2 concentration (1-5%) and osmolality (400 mOsm/kg), in FCS free media such as that described for alginate culture of NP cells with the inclusion of Insulin-transferrin-Selenium (ITS), Albumax and L-Proline (Basatvat *et al.*, 2023), as this enables the retention of their *in vivo* morphology (Fig. 2.13) and maintained the expression of NC phenotypic markers, including TBXT, CDH2, PAX1, HIF-1α, pan KRT, COL2, ACAN, AQP6 and RIPK5 (Fig. 2.13).

Recent micromass cultures have also been investigated for a simple and reproducible 3D culture model of NCs, to study basic biology and function, isolated from mouse immature NP tissue (Paillat *et al.*, 2023). Culture conditions were optimized to enable growth of self-organized micromasses of NCs in suspension. This 3D model system successfully preserves the phenotype of mouse NCs, which was determined by maintenance of the intracytoplasmic vacuoles, the expression of NC characteristic markers (TBXT; SOX9) and the synthesis of proteins related to their function (CD44; CAV1; AQP3; Patched-1) (Fig. 2.14). However, this remains to be confirmed for other species and mature NCs.

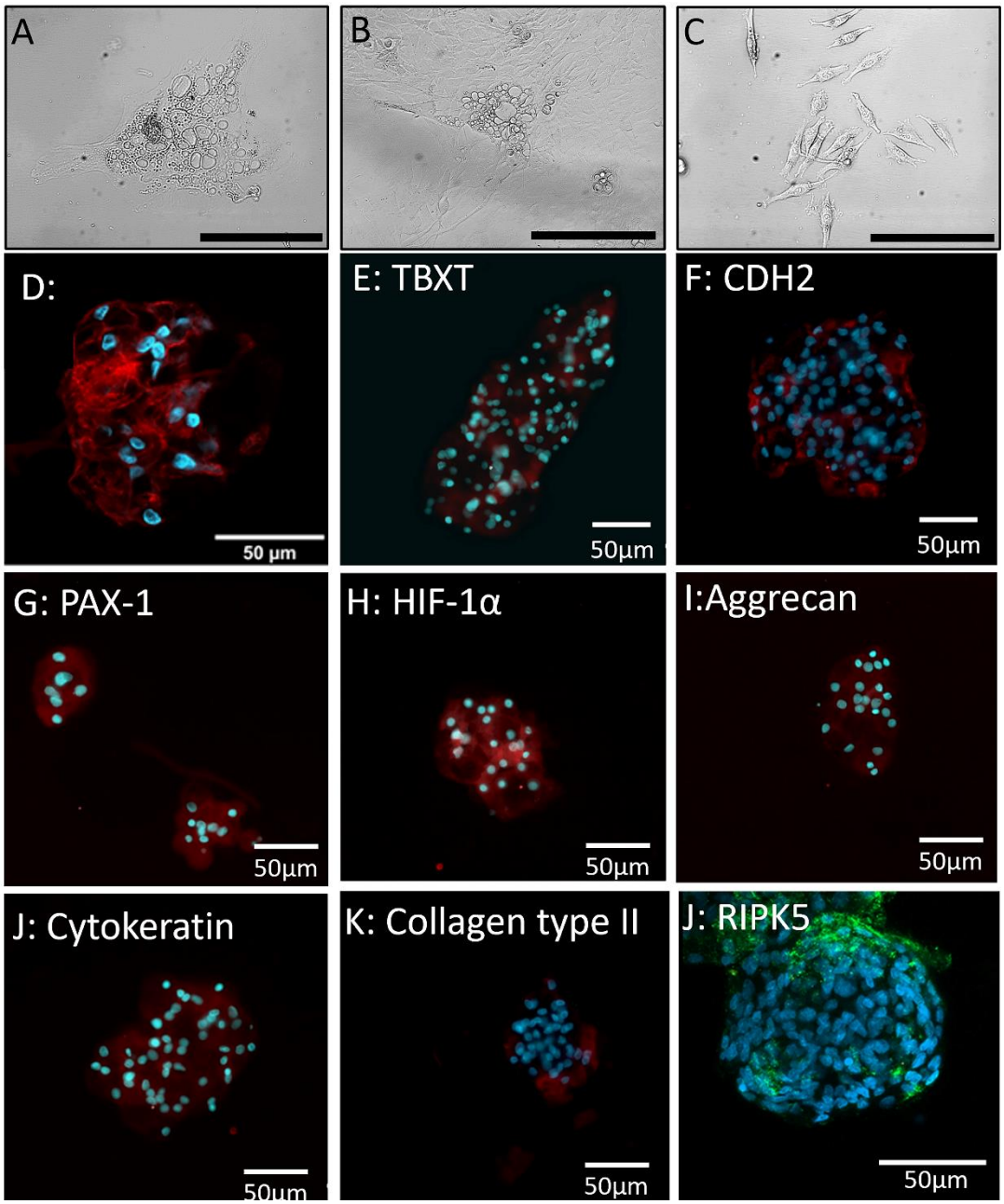

***Figure 2.13. NC morphology and phenotype within in vitro culture**. A-C: Monolayer culture and morphology of cells directly extracted from rat nucleus pulposus tissue. (a) Clusters of large, vacuolated NCs are the main cell type present during 2D in vitro culture 1d after extraction from rat NP tissue, although some smaller, non-vacuolated cells are also present. (b) After 7d in 2D in vitro culture, the number of clustered, vacuolated cells has reduced, whereas the number of smaller, non-vacuolated cells has increased. The remaining clusters of vacuolated cells are surrounded by smaller, non-vacuolated cells. (c) At 10d post extraction, the clusters of large, vacuolated cells have almost completely been replaced by or differentiated into smaller, non-vacuolated cells. Scale bar 50µm. D: Rat NCs cultured in alginate in 400mOSM/L αMEM maintained clusters and vacuolated morphology as shown by Phalloidin and DAPI staining following 1 day in culture. E-L: Immunofluorescence staining for NC characterisation markers in rat NCs cultured in alginate for 4 days. E: TBXT, F: CDH2, G: PAX1, H: HIF-1α, I: Aggrecan, J: Pan Cytokeratin (8,9,19), K: Collagen type II. L: DSKY-5 immunofluorescence staining in porcine NCs cultured in alginate for 14 days. Scale bars = 50µm.*

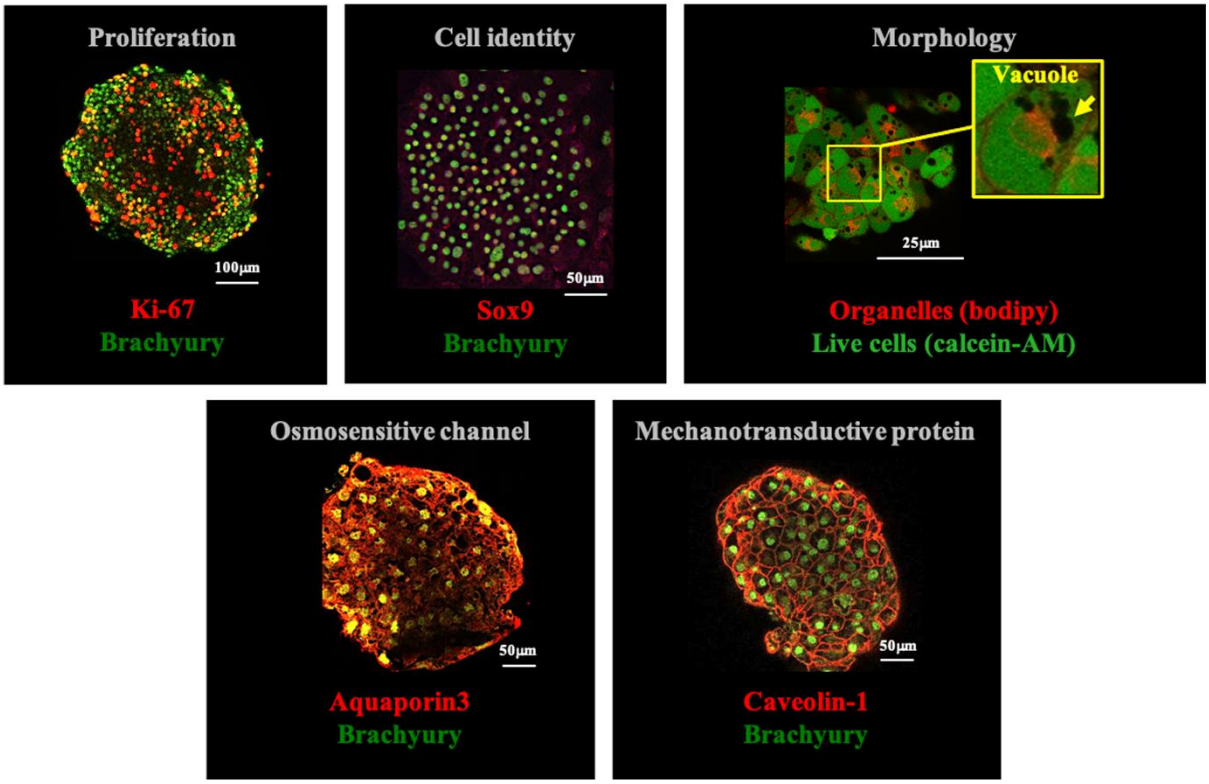

***Figure 2.14. Micromass culture of mouse NC Immunofluorescence co-localisation**: Immunofluorescence images showing Ki-67+/Brachyury+ proliferative NCs, coexpressing SOX9+/Brachyury+, AQUAPORIN3+/Brachyury+, and Caveolin-1+/Brachyury+ NC-specific markers respectively and showing vacuoles within the cytoplasm where the calcein-AM fluorophore is excluded (yellow arrowhead).*

CONCLUSIONS

This article aims to provide key recommendations for the extraction of NCs from multiple species from mice to humans. Providing tips and tricks to harvest maximal viable cells to enable downstream studies and analysis with differential methodology particularly for foetal tissues. Considerations for numeration of NCs are provided with a recommended methodology which enables accurate counting despite the challenges of the tight NC clusters. The issues associated with cryopreservation of these cells are discussed and further work is required to identify whether these cells can be cryopreserved. Recommendations are provided for NC characterisation: whilst to date no marker is specific to NCs, by utilising a phenotypic panel approach their characterisation is possible. New insights in phenotypic markers using single cell transcriptomics, which many groups are currently working on, will in the future provide for improved characterisation methodologies to further understand these fascinating cells. Together we hope that this article will provide a road map for *in vitro* studies using NCs derived from a range of commonly utilised species, which can enable acceleration of research.

Table 2.4. Key recommendations for the use of Notochordal Cells (NCs). *The conclusion of key findings extracted from this chapter, that will be utilised for further research with porcine NCs, and NC-like cells derived from induced pluripotent stem cells of human origin within this thesis.*

Key recommendations for the use of Notochordal cells (NCs)

	Porcine	**Foetal Human Tissue**
Tissue harvest	Notochordal cells can be harvested from Nucleus pulposus of the intervertebral discs in the Lumbar region and tails. NC loss begins at 2 years (Fig. 2.1)	Notochordal cells can be harvested from Nucleus Pulposus tissue of the intervertebral disc. NC loss begins at foetal stages (Fig. 2.1)
Digestion methods	30 minutes in αMEM with 7 U/mL pronase followed by 4 hours digestion with 125 U/mL collagenase type II (Table 2.1)	30 minutes in αMEM with 37.5 U/mL collagenase type II (Table 2.1)
Method for numeration	Recommended methodology for numeration is to add 100µL of solution A100 lysis buffer (Chemometec) to 100µL of cell suspension and incubate for 2 minutes at room temperature. Following incubation 100µL of stabilising buffer (Solution B (Chemometec)) should be added. The resulting cell suspension with solution A100 and B is then loaded into the Via1-Cassette™ (Chemometec) and read with the NucleoCounter® NC-200™ to provide a NC count allowing for the 1 in 3 dilution of the original cell suspension due to addition of 1:1:1 cell suspension, solution A100 and solution B (Fig. 2.8).	
Cryopreservation	All tested cryopreservation methods resulted in large loss in porcine NC viability. CS10 showed highest viability levels with only 50% NCs remaining viable, but as a commercial product the content of this solution is unknown and further work would be required to determine phenotype following cryopreservation. It is thus currently recommended that NCs are utilised directly from extraction and not cryopreserved (Fig. 2.9).	
Culture	If cultured within a standard monolayer system, NCs rapidly lose their clustered, vacuolated phenotype between 6-28 days or between 1-3 passages, and present morphologically as smaller, singular, non-vacuolated cells (Fig. 2.13). Isolated NCs are maintained as clusters and cultured within 3D alginate beads in αMEM media, under physiological O_2 concentration (1-5%) and osmolality (400 mOsm/kg), in FCS free media with the inclusion of Insulin-transferrin-Selenium (ITS), Albumax and L-Proline, enables the retention of their in vivo morphology (Fig. 2.13) and maintained the expression of NC phenotypic markers.	

Expansion	3D culture systems such as alginate fail to enable expansion of NCs, thus alternative substrate surfaces together with environmental conditions have been investigated in the attempt to maintain phenotype whilst enabling expansion.	
Characteristic	The morphological appearance of NCs, are large vacuolated NCs and present in large clusters. NC can be identified via numerous histological stains such as Haematoxylin and eosin, Safranin O-fast Green, Toluidine Blue and Alcian Blue (Fig. 2.10) and by markers below.	
Phenotypic Markers	TBXT (Brachyury), CAV1, FOXF1, pan KRT, SOX9, ACAN, CDH2, COL2A1, HIF-1α, PAX1 and TIE 2 (Fig. 2.13 and Table 2.2)	TBXT (Brachyury), CD24, FOXF1, pan KRT, LGALS3, SOX9, ACAN, AQP6, CA12, COL2A1, COL6A1, HIF-1α, PAX1 and TIE 2 (Fig. 2.13 and Table 2.2).

ACKNOWLEDGEMENTS

This publication has received funding from the European Union's Horizon 2020 research and innovation program (iPSpine; grant agreement number 825925, with RW, FCB, LTL, AM, SB, NV, JS, DWPL, AC, MAT, CLM involved); it is also part of the project NC-CHOICE (with project number 19251 of the research programme TTW which is partly financed by the Dutch Research Council (NWO). The financial support of the Dutch Arthritis Society (LLP22) is greatly appreciated. DC received funding from the RGC European Union - Hong Kong Research and Innovation Cooperation Co-funding Mechanism (E-HKU703/18). AC received funding from Region Pays de la Loire, RFI BIOREGATE (CAVEODISC) and the French Society of Rheumatology (Spherodisc). The Authors would like to thank the other members of the spine community whom contributed to early discussions of the manuscript planning whom are authors from the prior NP methods paper (Basatvat *et al.*, 2023).

CONFLICT OF INTEREST

The authors have no relevant conflicts of interest to declare in relation to this article.

CHAPTER 3
POTENTIAL OF NOTOCHORDAL CELLS WITHIN INJECTABLE BIOMATERIALS TO PROMOTE INTERVERTEBRAL DISC REGENERATION

CONTEXT OF RESEARCH

The context of Chapter 3 involves investigating the regenerative potential of notochordal cells (NCs) once seeded within a selection of three injectable biomaterials, which intentionally represent natural, semi-synthetic and synthetic properties. The contribution to research is the novel culturing of porcine NCs into biomaterials *in vitro* for 4 weeks under disc physiological conditions of 5% O_2, 5% CO_2. With particular interest of screening the biomaterials that enables liquid injection followed by *in situ* gelation, with additional attributes of biocompatibility, mechanical stability, compliance with regulatory pathway approvals and to determine if biomaterials would facilitate the maintenance of porcine notochordal phenotype as a first stage to develop a biomaterial delivery system for the IVD.

AUTHORS

Rebecca J. Williams[1,2], Shaghayegh Basatvat[1,2], Tara C. Schmitz[3], Ronak Janani[4], Chris Sammon[4], Karin Benz[5], Keita Ito[3], Mariana A. Tryfonidou[6], Joseph W. Snuggs[1,2], Christine Le Maitre[1,2]

AFFILIATIONS

[1] Department of Oncology and Metabolism, University of Sheffield, UK. [2] Biomolecular Sciences Research Centre, Sheffield Hallam University, UK. [3] Orthopaedic Biomechanics, Department of Biomedical Engineering, Eindhoven University of Technology, The Netherlands. [4] Materials Engineering research Institute, Sheffield Hallam University, UK. [5]TETEC Tissue Engineering Technologies AG, Germany. [6] Department of Clinical Sciences, Faculty of Veterinary Medicine, Utrecht University, The Netherlands.

AUTHOR CONTRIBUTIONS

RJW, CLM, JWS and MAT contributed to conception and design of the study; RJW, JS, RJ, TS and SB contributed to acquisition of laboratory data; RJW performed most of the data analysis; RJW, CLM, JS, KB, MT, CS, KI, TS contributed to interpretation of the data; RJW, CLM and JWS drafted the manuscript; All authors critically revised the manuscript for intellectual content; All authors approve the final version and agree to be accountable for all aspects of the work.

DETAILED CONTRIBUTIONS MADE

I conducted experiments: optimising cell seeding density with Alcian Blue staining (Fig. 3.2), the initial investigation of porcine NCs in biomaterials with live cell images (Fig. 3.3), immunofluorescence (Fig. 3.4), histology (Fig. 3.6) and counting the cell cluster size (Fig.3.7). I investigated the characterisation and phenotypic analysis of porcine NCs in biomaterials, immunohistochemistry (Fig. 3.8 and 3.9) and the analysis of glycosaminoglycan release from culture media (Fig. 3.10). I preformed all data analysis and statistical analysis relating to these experiments and drafted the entire manuscript excluding the data associated with the rheological properties.

(SUBMITTED, ECM JOURNAL) Potential of Notochordal Cells Within Injectable Biomaterials to Promote Intervertebral Disc Regeneration. Rebecca J. Williams, Shaghayegh Basatvat, Tara C. Schmitz, Ronak Janani, Chris Sammon, Karin Benz, Keita Ito, Mariana A. Tryfonidou, Joseph W. Snuggs, Christine Le Maitre.

ABSTRACT

Low back pain is the leading cause of disability worldwide and is strongly associated with degeneration of the intervertebral disc (IVD). During degeneration the nucleus pulposus (NP) in the core of the IVD, is affected by altered matrix synthesis, increased degradation, and cell loss. Strategies combining regenerative cell sources with injectable biomaterials could provide a therapeutic approach to treating IVD-degeneration related back pain. The juvenile cells of the NP, known as notochordal cells (NC), could provide both anabolic and anti-catabolic responses for disc regeneration. However, their behaviour within biomaterial delivery systems has not previously been investigated. Here, porcine NCs were incorporated into three injectable hydrogels: Albugel (an albumin/ hyaluronan hydrogel), NPgel (a L-pNIPAM-co-DMAc hydrogel) and NPgel with decellularized Notochordal cell-matrix (dNCM). The NCs and biomaterial constructs were cultured for up to 4 weeks under 5% oxygen (n=3 biological repeats). The ability of biomaterials to maintain NC viability, phenotype and extracellular matrix synthesis and deposition was investigated through histological, immunohistochemical and glycosaminoglycans analysis. NCs survived in all three biomaterials after 4 weeks and maintained cell clustering, whilst phenotype and cell clustering were maintained to a greater extent in NPgel and Albugel. Thus, these biomaterials could facilitate maintenance of the NC phenotype, support matrix deposition and be a basis for future IVD regeneration strategies.

KEYWORDS

IVD degeneration, disc degeneration, biomaterial, notochordal cells, hydrogels, hyaluronic acid

INTRODUCTION

LOWER BACK PAIN AND INTEREVRTEBRAL DISC DEGENERATION

Low back pain (LBP) is the biggest cause of disability worldwide; around 80% of adults will suffer from LBP in their lifetime (Hartvigsen *et al.*, 2018; Traeger *et al.*, 2019). Most people experience mild pain and recover quickly, however, in some cases LBP lasting longer than 6 weeks progresses to chronic LBP (CLBP) which can contribute to a lifelong disability and a societal burden (Maetzel and Li, 2002; Hartvigsen *et al.*, 2018). Current treatments to combat LBP may be pharmacological or non-pharmacological, such as: non-steroidal anti-inflammatory drugs, opioids, anti-depressants, exercise, massage, and manipulation (Qaseem *et al.*, 2017; Nice, 2018). Whilst CLBP can be tackled with surgery in some situations, but this is invasive, expensive, and only targets the end-stage of disease in the spine having limited effectivity to manage CLBP in many patients (Phillips *et al.*, 2003; Bogduk, 2004; Steffens *et al.*, 2016; Foster *et al.*, 2018). In around 40% of cases, the underlying cause of CLBP is associated with degeneration of the intervertebral disc (IVD) (Luoma *et al.*, 2000; Sakai and Andersson, 2015). Importantly, none of the current treatments target the regeneration of the IVD.

INTERVERTEBRAL DISC AND NOTOCHORDAL CELLS

The IVD permits range of motion and supports biomechanical forces applied to the spine (Risbud and Shapiro, 2011). The core of the disc contains an aggrecan-rich gel-like tissue called the nucleus pulposus (NP), which is enclosed circumferentially by the ligamentous annulus fibrosus (AF). The composition of the NP changes as a human IVD matures. The NP of a neonate is populated by notochordal (NC) cells, which are large, vacuolated, and morphologically distinct cells. In humans, some canine breeds, and other species, such as ovine and caprine, large vacuolated NCs (morphotypic NCs) gradually disappear during disc maturation, substituted by more smaller NP cells as the primary cell type (Chapter 2)(Sheyn *et al.*, 2019; Bach *et al.*, 2022). However, certain species, retain morphotypic NCs within the NP region throughout most of their lifespan, including porcine, leporine, and murine species (Alini *et al.*, 2008; Sheyn *et al.*, 2019). Interestingly, an association between morphotypic NC loss and the onset of disc degeneration has been highlighted, where natural degeneration is only seen in species which lose their morphotypic NCs prior to adulthood (Urban and Roberts, 2003; Bergknut *et al.*, 2012; McCann and Séguin, 2016). As a result, NCs have become a trending research topic regarding their promise for therapeutic application to mediate disc regeneration (Humphreys *et al.*, 2018; Bach *et al.*, 2022).

REGENERATING THE INTERVERTEBRAL DISC WITH CELL-BIOMATERIAL TREATMENTS

Of the cell types which have been considered for the purposes of regenerating a degenerative IVD, less than 3% of the papers utilised NCs as the choice of regenerative cell source in a recent review (Williams *et al.*, 2021). The review highlights that NCs have been successfully extracted from several species, however, these studies have mainly focused on 3D *in vitro* culture, with

a distinct lack of progression into *in vivo* studies (Williams *et al.*, 2021). The limited use in studies so far may have been due to the difficulties in NC handling, such as: the inability to maintain their phenotype in monolayer culture (Gantenbein *et al.*, 2014; Potier and Ito, 2014; Spillekom *et al.*, 2014), harvesting insufficient numbers due to limited amplification and inability to passage whilst maintaining phenotype (Chapter 2) (Kim *et al.*, 2009; Potier *et al.*, 2014; Spillekom *et al.*, 2014). Nonetheless, NCs could provide an excellent cell source for regenerating the degenerate IVD, due to their capabilities of synthesising extracellular matrix, being highly viable in the conditions within the IVD and producing anti-angiogenic, and anti-catabolic effects (Devina Purmessur *et al.*, 2013; Gantenbein *et al.*, 2014; Potier *et al.*, 2014; Spillekom *et al.*, 2014), for a recent review on the potential of NCs please see Bach et al., (2022).

The limitation of NCs being maintained only in 3D culture models can be addressed by the seeding of cells directly into a biomaterial scaffold, facilitating cell growth and/or favourable differentiation, to provide mechanical support and aid the delivery of the cells into the disc (Peroglio *et al.*, 2012; Thorpe *et al.*, 2016). A proposed biomaterial that enables liquid injection followed by *in situ* gelation, with additional attributes of biocompatibility, mechanical stability, compliance with regulatory pathway approvals and facile translation from research to future medical application, would be an ideal candidate for a therapeutic treatment.

Hydrogel-based biomaterial carriers that have previously been developed for NP regeneration, were investigated in this study to support NCs. The first biomaterial selected was a polyethylene glycol-crosslinked serum albumin/ hyaluronan hydrogel, referred to as Albugel, which has been previously shown to support the survival of disc cells and disc healing and has been shown safe to use in human clinical trials regarding cartilage therapy in knee joints (Benz *et al.*, 2010, 2012; Niemeyer *et al.*, 2022). The second selected biomaterial was a synthetic Laponite® crosslinked poly N-isopropylacrylamide-co-N, N- dimethylacrylamide (NPgel) biomaterial (Boyes *et al.*, 2021) which has been previously reported to induce human bone marrow progenitor cell differentiation into an NP-like phenotype with matrix deposition that mimics the native NP tissue (Thorpe *et al.*, 2016a; Thorpe *et al.*, 2016b; Vickers *et al.*, 2019), and can restore degenerate discs in a goat organ culture model (Snuggs *et al.*, 2023). The importance of cells to retain their NP phenotype will facilitate the regenerative potential of the cells, such as NP cell production of extracellular matrix. This hydrogel system has also undergone *in vivo* safety studies in rats, where it was demonstrated to not show any adverse events within a subcutaneous implantation model (Thorpe *et al.,* 2018). The third and final biomaterial was selected to investigate whether the inclusion of the native extracellular matrix from the NC-rich NP tissue improved phenotypic maintenance. Notochordal cell matrix (NCM)-based materials have been previously shown to promote anabolism within NP cells and degenerated IVD tissue (de Vries *et al.*, 2019; Schmitz *et al.*, 2022). Thus, here the hypothesis that the supplementation of the synthetic NPgel with the NCM would provide additional cues to the NCs supporting their phenotype (Cornejo *et al.*, 2015; Bai *et al.*, 2017;

Bach *et al.*, 2018; Vickers *et al.*, 2019), specifically a decellularised NCM (dNCM) was utilised creating a bioactive functional biomaterial (NPgel/dNCM).

Altogether, this study investigated the use of porcine NCs (pNCs) in combination with three potential injectable biomaterials: Albugel, NPgel and NPgel/dNCM that were intentionally representative of either synthetic (NPgel), semi-synthetic (NPgel/dNCM) or primarily based on natural components (Albugel), as a first translation step of NC-based therapeutic strategies.

METHODS

EXPERIMENTAL DESIGN

Following initial biomaterial rheology characterisation, optimisation experiments were firstly performed by seeding pNCs into a readily available biomaterial, which has been extensively characterised (NPgel). These initial optimisation studies were used to determine optimal seeding density, and viability. Thereafter, pNCs were harvested from three independent biological porcine donors, and seeded into three different injectable biomaterials in at least duplicate per donor, total replicates: Albugel (n=8), NPgel (n=8) and NPgel/dNCM (n=6), with all output measures performed on every sample. Cell-biomaterial constructs were cultured for 4 weeks at IVD conditions in relation to physioxia. Following culture viability was assessed using Calcein/Hoechst staining. Morphology was investigated using scanning electron microscopy (SEM) and histology. Finally, phenotype and matrix production were assessed using immunohistochemistry and histological staining.

ALBUGEL PREPARATION

Albugel (an albumin/ hyaluronan hydrogel) was prepared by firstly creating hyaluronic acid (HA) solution; HA solution was constructed with 35% v/v Ostenil Plus® (TRB Chemedica, Newcastle-under-Lyme, UK) and αMEM base media. This was then combined with 11% v/v chemically modified human serum albumin (maleimido-human serum albumin; MA-HSA; TETEC, Germany), 18% v/v cell suspension. Using a dual syringe with mixing head, the HA, MA-HSA and cell mixture was combined with the crosslinker α,ω-bisthio-polyethylene glycol (BT-PEG; Laysan Bio Inc. Arab, AL, USA) at 1:5 ratio.

NPGEL PREPARATION

Laponite® crosslinked pNIPAM-co-DMAc (NPgel) biomaterial was prepared as previously described (Thorpe *et al.*, 2016). In short, a 10mL exfoliated suspension of 0.11g Laponite® clay nanoparticles (25-30nm diameter, <1nm thickness) (BYK Additives Ltd, UK) in 18mΩ deionized H_20 was prepared. To the 10mL exfoliated Laponite® clay suspension, 0.87g N-isopropylacrylamide 99% (NIPAM) (KJ Chemicals, Japan), 0.13g N-dimethylacrylamide (DMAc) (Sigma, UK), and 0.01g 2-20-azobisisobutyronitrile (AIBN) (Sigma, UK) were added, mixed well, and filtered through a 5 to 8µm pore filter paper. Polymerization was performed at 80°C overnight. NPgel suspension was cooled to ~38 - 39°C prior to cell incorporation.

NPGEL WITH DNCM PREPARATION

Decellularized NCM powder (dNCM) was prepared as previously described (Schmitz *et al.*, 2022). Briefly, NC-rich NP tissue was harvested from 12-week-old porcine donors and processed by firstly freeze drying in a lyophilizer (Labconco, Kansas City, US) overnight at −80°C, then for >7 hours at ≤ −50°C. The sample was then decellularized using a 200U/mL benzonase (Merck KGaA, Darmstadt, Germany) in 50mM Tris-HCl buffer (Sigma, Zwijndrecht, The Netherlands), pH 7.5, 2.5mM $MgCl_2$ (Sigma, Zwijndrecht, The Netherlands) at 0.01mL buffer/mg dry weight tissue for 48 hours at 37°C on a roller at 2rpm; followed by pulverization to obtain a powder that can be kept a -80^{o}C. The dNCM was then sterilized using Ultraviolet (UV) light and 0.5% w/v was stirred to dispersed within NPgel just prior to cell seeding, a single batch of dNCM was utilised for these studies.

RHEOLOGICAL CHARACTERISATION

The rheological behaviour of the biomaterials at different degrees of deformation was characterised using an Anton Paar 301 rheometer in parallel plates configuration. Circular samples were prepared using bespoke PTFE moulds (20 mm in diameter, 2 mm in height) and immersed in low glucose DMEM, with pyruvate pH adjusted to 6.8 to mimic the degenerate disc environment for up to 24 hours at 37 °C. To prevent sample slippage during measurement, sandpaper was attached to the measuring plates. A constant load of 1 N was applied on the sample throughout the measurement to maintain good contact between the sample and the top plate. Amplitude sweep measurements were conducted on the hydrogels between 0.1-50% strain at 1 Hz frequency after 2 and 24 hours of immersion in media. A minimum of three replicates were conducted for each sample and the average moduli values are reported here. For samples that suffered from shrinkage, the resultant moduli values were corrected by the factor $(\frac{d}{d_{sample}})^4$ where d is the diameter of the upper plate and d_{sample} is the diameter of the measuring sample (Bron *et al.*, 2009).

NOTOCHORDAL CELL EXTRACTION

pNC were obtained from lumbar IVDs harvested from young pigs (<15 weeks old) (Medical Meat supplier, UK; Marr Grange Butchers, UK). Following the protocol from Chapter 2 (Recommendations for digestion of Nucleus Pulposus tissue and Notochordal cell extraction), the spines were dissected, and the NP harvested under sterile conditions and digested following a sequential treatment in 7U/mL pronase (Roche Diagnostics, UK) in Minimum Essential Medium α (αMEM modified with ribonucleosides, deoxyribonucleosides, phenol red, L-glutamine; Life technologies, UK) with 1% v/v Penicillin-Streptomycin (P/S; Life Technologies, UK) for 30 minutes at 37^{o}C. Followed by a 16 hour digestion in 125U/mL collagenase type II (Life technologies, UK) in αMEM at 37^{o}C. The clusters of pNC were captured in a 40µm cell strainer and further cultured as described below.

INCORPORATION OF NOTOCHORDAL CELLS INTO BIOMATERIALS AND CULTURE

pNC clusters were counted post harvesting using a NucleoCounter® NC-200™ (Chemometec, Allerod, DK), as previously described in Chapter 2 (Calculating cell number). For seeding, harvested pNC were centrifuged at 200*g* for 5 minutes, the supernatant was removed, and the NC pellet was resuspended in 10% v/v extraction media, prior to adding the biomaterials to the Eppendorf. Cell density optimisation studies investigated $1x10^6$, $4x10^6$, $1x10^7$ and $2x10^7$ cells/ml within NPgel for 2 weeks in culture. From which a final cell density of $4x10^6$ cells/mL of pNC was selected for further studies and seeding into the three injectable biomaterials: Albugel, NPgel and NPgel/dNCM. In addition, parallel acellular biomaterial controls were established. Each 300µL pNC and biomaterial constructs were extruded through a 27-gauge needle to mimic injection into the disc into 48 well culture plate, left to gel at 37^{o}C for 5 minutes. Five hundred microliters of complete NC culture media was then added to the well: αMEM (life technologies, Paisley, UK) containing P/S 50U/mL (Life Technologies UK), amphotericin B 2.5ug/mL (Sigma, Dorset, UK), L-ascorbic acid 25ug/mL (Sigma, Dorset, UK), 1% Insulin-transferrin-Selenium v/v (ITS-X), 1% L-glutamine v/v (Life technologies, UK), L-proline 40ug/mL (Life technologies, UK) and Albumax 1.25mg/mL (Life technologies, UK) (Basatvat *et al.*, 2023), leaving the outer wells of the plate void of constructs, but hydrated with phosphate buffered saline (PBS; Gibco, UK). Triplicate biological repeats of cellular and acellular controls were cultured for up to 4 weeks in a physiological disc environment of 5% v/v O_2, with 5% v/v CO_2 at 37°C using a hypoxia glove box (Coy Laboratory Products, USA). Complete media was replaced in the hypoxia glove box three times per week during the culture period.

To assess initial cell viability, constructs were stained with 10µM Calcein-AM (Invitrogen™, UK) and Hoechst 33342 (Invitrogen™, UK). Constructs following culture were firstly washed in PBS, next, cells were stained with 10µM of Calcein-AM for 30 minutes at 37°C, washed three times with PBS, followed by 5pg/mL of Hoechst for 15 minutes at 37°C. After staining culture media was re-added, and a small piece of the construct was taken and constrained between a microscope slide and coverslip and visualised on an Olympus BX60 microscope using 494nm filter (fluorescein isothiocyanate, FITC) and 361nm filter (4',6-Diamidino-2-Phenylindole, DAPI) for visualising Calcein-AM and Hoechst stains, respectively. After the culturing for up to 3 weeks constructs were harvested for assessment of cell morphology, matrix deposition and analysis of cellular phenotypic markers, along with acellular controls.

SCANNING ELECTRON MICROSCOPY

Triplicate samples were removed from culture and flash frozen with liquid N_2 and stored at -80°C. The sample was freeze dried overnight using a freeze dryer (FD-1A-50; Boyikang, Beijing, China) at -50°C under vacuum. The sample was then fractured to expose the interior surface morphology, attached onto an aluminium stub, and then using a Quorum Technology 150 Q TES system coated with gold (20mA sputter current for 120 s with a 2.7 tooling factor). The fracture surfaces were examined and captured using a FEI NOVA nano SEM 200. Secondary

electron images were obtained using accelerating voltage 5kV at various magnifications ranging from 600x to 6,000x.

HISTOLOGICAL ANALYSIS

NC phenotype and matrix deposition was investigated in acellular controls and cellular constructs following 2 and 4 weeks in culture. Triplicate samples per biomaterial were removed from culture and fixed in 10% w/v neutral buffered formalin for 20 minutes and processed to wax using the TP1020 tissue processor (Leica Microsystems, Newcastle, UK). Following fixing and embedding, all samples were sectioned at 6µm and mounted to X-tra® adhesive positively charged slides (Leica Microsystems, Newcastle, UK). Sections were dewaxed in Sub X (Leica Microsystems, Newcastle, UK) three times for 7 minutes and rehydrated in industrial methylated spirit (IMS; Fisher, Loughborough, UK; 10552904) for three times for 7 minutes and hydrated in running tap water for 5 minutes prior to histological staining. Sections were assessed using histological stains. H&E: Mayer's Haematoxylin (Leica Microsystems, Newcastle, UK) for 1 minute, before being 'blued' in running water for 5 minutes and immersed in Eosin (Leica Microsystems, Newcastle, UK) for a further 1 minute; Alcian Blue (pH 2.5): for 30 minutes (Leica Microsystems, Newcastle, UK) followed by counter stain of Nuclear fast red (Leica Microsystems, Newcastle, UK) for 10 minutes; Masson's Trichrome (Atom Scientific, UK): according to the manufacturer's instructions; Safranin O/ Fast green: sections are stained with Weigert's Haematoxylin for 5 minutes, followed by 0.4% v/v aqueous Fast green (Sigma, Dorset, UK) for 4 minutes, rinsed with 1% v/v acetic acid (Sigma, Dorset, UK) and counter stained with 0.125% w/v Safranin O (Sigma, Dorset, UK). After specific histological staining, sections were dehydrated three times for 10-minute washes in IMS, cleared in Sub-X three times for 10-minute and mounted in Pertex (Leica Microsystems, Newcastle, UK). All slides were examined with an Olympus BX51 microscope and images captured by digital camera and Capture Pro OEM v8.0 software (Media Cybernetics, UK). Histological sections were analysed, and representative images captured to document their histological appearance and cellular staining patterns.

IMMUNOHISTOCHEMISTRY AND IMMUNOFLUORESCENCE ANALYSIS

Immunohistochemistry (IHC) and immunofluorescence were also performed on porcine disc samples and pNCs cultured in biomaterials. Specific antibodies were used to target antigens in relation to NP matrix, NC and NP phenotype (Table 3.1). Samples embedded in paraffin wax were dewaxed in Sub X for three times for 7 minutes and rehydrated in IMS for three times for 7 minutes. For IHC, as previously reported (Binch et al., 2020), endogenous peroxidase activity was blocked for 30 minutes using IMS containing 3% w/w H_2O_2 (Sigma, Dorset, UK) and 5 drops of 37% hydrochloric acid. Followed by three times for 5 minutes washes in tris-buffered saline (TBS; 20mM tris (Fisher, Loughborough, UK), 150mM sodium chloride (Fisher, Loughborough, UK), pH 7.5). Sections were subjected to antigen retrieval methods as detailed in Table 3.1. For heat antigen retrieval, sections were immersed in pre-heated (60^{o}C) antigen retrieval buffer (0.05M tris, pH 9.5) and irradiated for 5 minutes at 40% power in a microwave

oven (Sanyo 800 Watt) and then again for 5 minutes at 20% power. Sections were left to stand at room temperature for 15 minutes. For enzyme antigen retrieval, sections were placed in a preheated (37^{o}C) TBS buffer with 0.01% w/v α-chymotrypsin (Sigma, Dorset, UK) in 0.1% w/v $CaCl_2$ for 30 minutes at 37^{o}C; or no retrieval was required. Sections were washed in TBS and blocked for 2 hours with normal serum from which the animal in which the secondary antibody was raised in; 5% v/v bovine serum albumin (BSA; Sigma, Dorset, UK)) w/v in 75% TBS and 25% normal serum v/v (Table 3.1). Primary antibody was applied overnight at 4^{o}C according to Table 3.1 alongside equivalent concentration IgG controls. On the second day, the sections were washed in TBS followed by appropriate biotinylated secondary antibody for 30 minutes. Sections were subject to avidin-biotin-complex (ABC) elite reagent for 30 minutes (Vector Laboratories, CA, USA), 3,3-diaminobenzidine tetrahydrochloride (DAB) solution (Sigma, Dorset, UK) for 20 minutes and washed in running tap water for 5 minutes prior to counterstaining with Mayer's Haematoxylin for 1 minute and blued in running tap water for 5 minutes. Sections were dehydrated in IMS three times for 10 minutes, cleared in Sub-X three times for 10 minutes, and mounted in Pertex.

Table 3.1. Immunohistochemical procedures utilised for phenotypic characterisation of porcine notochordal cells. *Primary antibody target, clonality, dilutions optimised and antigen retrieval. Along with the Secondary antibodies and dilutions, which were used for immunohistochemical staining the staining methods.*

Primary Antibody	Target	Clonality	Optimal dilution	Antigen retrieval	Technique	Secondary Antibody	Optimal dilution
Aggrecan (Abcam, ab3778)	NP matrix	Mouse monoclonal	1:100	Heat	IHC	Rabbit Anti-Mouse (Abcam, ab6727)	1:500
Brachyury (Abcam, ab20680)	NC/NP marker	Rabbit polyclonal	1:100	None	IHC	Goat Anti-Rabbit (Abcam, ab6720)	1:500
Collagen Type II (Sigma, maB1330)	NP matrix	Mouse monoclonal	1:200	Enzyme	IHC	Rabbit Anti-Mouse (Abcam, ab6727)	1:500
KRT 8/18/19 (Abcam, ab41825)	NC/NP marker	Mouse monoclonal	1:400	Enzyme	IHC	Rabbit Anti-Mouse (Abcam, ab6727)	1:500

DIMETHYLMETHYLENE BLUE ASSAY

Media samples were collected during every media change during the culture of the pNC in biomaterial constructs and stored at -80^{o}C. DMMB reagent was generated with 1,9-dimethylmethylene blue (Sigma, Dorset, UK), formic acid (Sigma, Dorset, UK), and sodium formate (Sigma, Dorset, UK), adjusted to pH 6.8 and diluted so that the ODI measured between 0.38 and 0.41 with a blank sample. Once ready to perform a DMMB assay, media was thawed at room temperature, 50µl of construct sample was added to 96 well plate (Thermofisher, Waltham, USA) followed by 20µl of guanidinium chloride solution (2.16M

Guanidium Chloride (Sigma, Dorset, UK) diluted in papain buffer (0.1M sodium acetate (Sigma, Dorset, UK), 0.01M L-cysteine hydrochloride (Sigma, Dorset, UK), 0.05M disodium EDTA (Sigma, Dorset, UK), 0.2M NaCl (Sigma, Dorset, UK) adjusted to pH 6.0), adjusted to pH 6.8, followed by 200µl of DMMB reagent. The plate was set to orbital shake for 5 seconds followed by a 3 minutes reast before being read at 520nm absorption using a CLARIOstar® Microplate Reader (BMG Labtech, Aylesbury, UK).

STATISTICAL ANALYSIS

Statistics were performed in GraphPad prism v9.5.1. The normality of the data was assessed using the Shapiro-Wilk test. The cell distribution when seeded within the biomaterials was not normally distributed, therefore analysed with a Kruskal-Wallis test followed by the Dunn's multiple comparisons test for reviewing statistical differences between the biomaterial groups (pNC & Albugel v pNC & NPgel v pNC & NPgel/dNCM). When analysing percentage of pNC positive for a phenotype marker, an Kruskal-Wallis test was performed, followed by Dunn's post hoc test to compare each group (pNC & Albugel v pNC & NPgel v pNC & NPgel/dNCM). For the statistical analysis of GAG production data was normally distributed therefore a one-way ANOVA was performed, followed by the recommended Tukey's multiple comparisons test to compare each acellular biomaterials (Albugel v NPgel v NPgel/dNCM) and the equivalent cellular construct (Albugel v pNC & Albugel; NPgel v pNC & NPgel; NPgel/dNCM v pNC & NPgel/dNCM). Statistical significance was accepted at $p \leq 0.05$.

RESULTS

RHEOLOGICAL PROPERTIES

Storage moduli of the three biomaterials (post-gelation) were monitored over a range of strain values (Fig. 3.1). During the strain sweep (or amplitude sweep) experiment, all three hydrogels behaved like a viscoelastic solid characterised by a higher storage modulus (G') than loss modulus (G"). A gradual downturn of G' can be seen in every sample as the strain was increased. However, the elastic portion of these materials prevailed the viscous portion throughout the strain range tested here (no G' and G" crossover). In both NPgel and NPgel/dNCM systems, the storage moduli increased after 24 hours, reaching an average G' of ~14kPa and ~3kPa (at 1 Hz) for the NPgel and NPgel/dNCM systems, respectively. These two hydrogel systems exhibited modest shrinkage (up to 20%) after 24 hours of media immersion. The slight change in volume was associated with the release of water as a result of interaction with the media, creating a denser scaffold with higher G'. Albugel did not display shrinkage during the 24-hour period and maintained a G' value of ~0.8kPa at both time points. The strain-independent region of an amplitude sweep, also known as the linear viscoelastic (LVE) region, describes the limits within which a viscoelastic material can be deformed non-destructively. Whilst all three biomaterials displayed linear viscoelastic properties within

physiological strain ranges. The LVE limit of Albugel (40% strain) exceeded that of NPgel (7%) and NPgel/dNCM (10%) (Fig. 3.1).

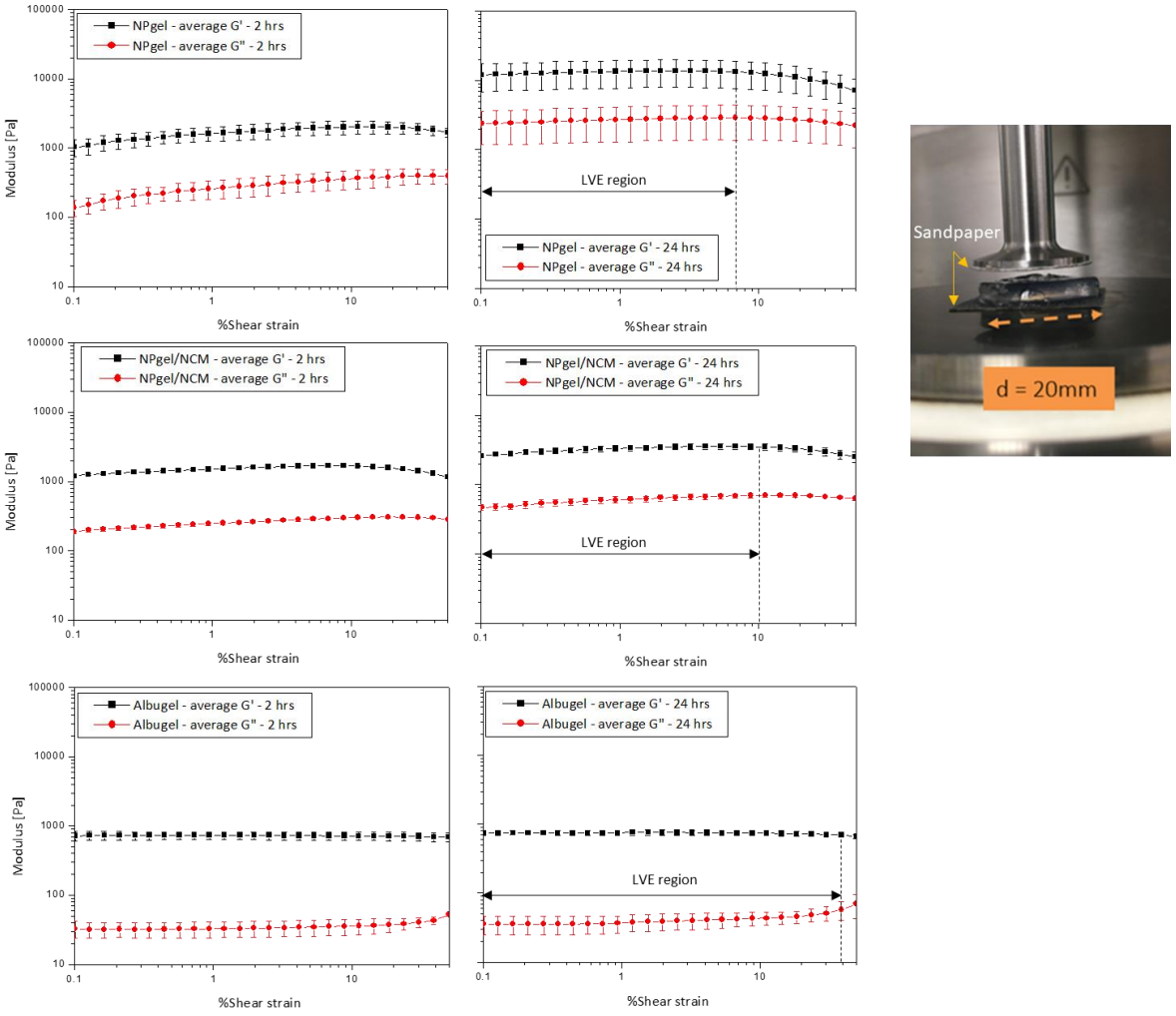

Figure 3.1. Storage moduli of the three biomaterials (post-gelation). *Amplitude sweeps of the NPgel, NPgel/dNCM and Albugel after 2- and 24-hours immersion in culture media (n=3 technical repeats). Experimental setup is shown on the right-hand side.*

OPTIMISING CELL SEEDING DENSITY WITHIN NPGEL AS AN EXAMPLE BIOMATERIAL

An initial optimisation experiment was conducted to determine seeding density and to observe if different cell densities influenced the morphology and survival of pNC *in vitro* following 2 weeks culture within NPgel as the example biomaterial. Cells were visible in the $1x10^6$ cells/mL constructs, but they were sparse, and presented as single cells (Fig. 3.2). Cell clustering was observed in biomaterial constructs seeded with $4x10^6$ cells/mL, $1x10^7$ cells/mL and $2x10^7$ cells/mL. There was no observable difference between the $4x10^6$ cells/mL and $1x10^7$ cell/mL, and in the constructs seeded at $2x10^7$ cells/mL displayed smaller clusters with dispersed single cells (Fig. 3.2). As clusters were first observed in $4x10^6$ cells/mL, further experimental set ups were performed with $4x10^6$ cells/mL seeding density in biomaterials.

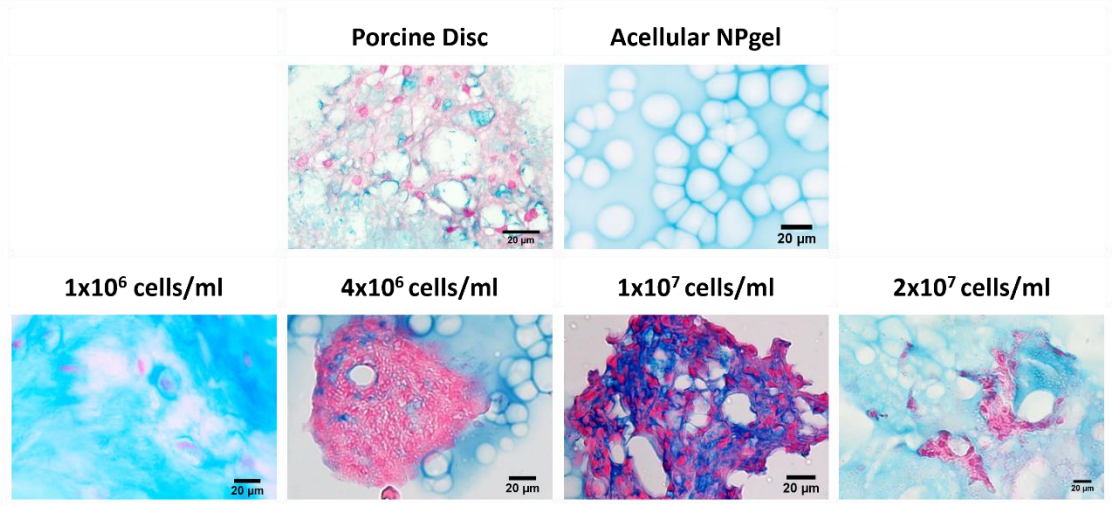

Figure 3.2. Optimised seeding density of cells into biomaterials. *Porcine notochordal cells seeded at different densities; $1x10^6$, $4x10^6$, $1x10^7$, and $2x10^7$ before culturing for up to 2 weeks at 5% v/v oxygen, 37°C and stained with Alcian Blue (n=3 technical repeats). Scale bar 20µm.*

ISOLATED NOTOCHORDAL CELL MORPHOLOGY IN NPGEL

Optimisation experiments were conducted to determine whether pNCs could be maintained within a biomaterial system. Phase contrast images demonstrated the presence of large cell clusters within NPgel, with predominant vacuoles seen up to 2 weeks in culture, which are still visible at 3 weeks (Fig. 3.3; vacuoles indicated by black arrow heads).

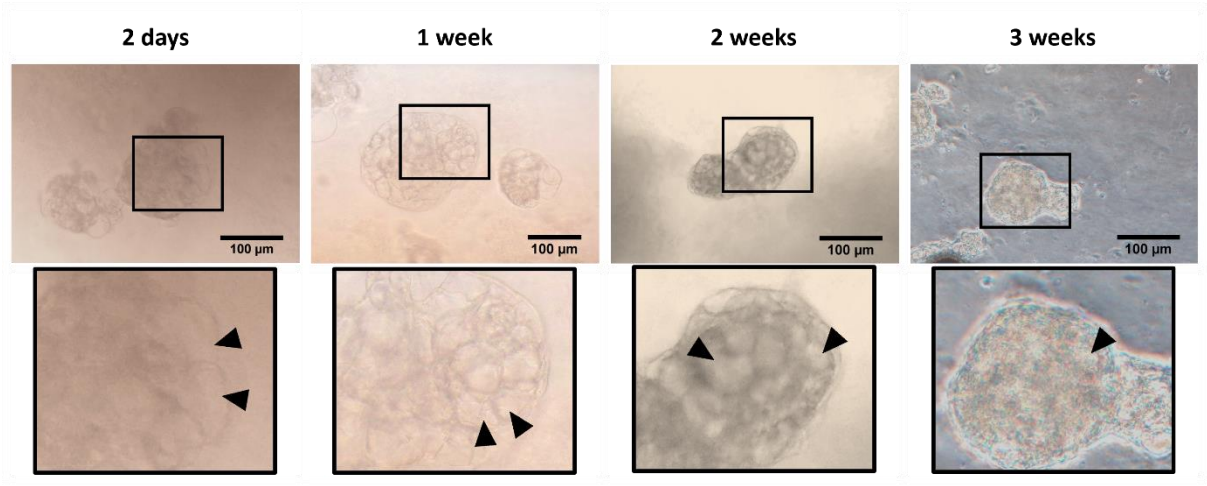

Figure 3.3. Brightfield live cell imaging of porcine notochordal cells cultured in NPgel*, for up to 3 weeks in a hypoxia unit of 5% v/v oxygen at 37°C. Scale bar 100µm. Black arrow heads indicate vacuoles (n=3 biological repeats).*

PORCINE NOTOCHORDAL CELLS IN ABLUGEL, NPGEL AND NPGEL/DNCM

Live-cell imaging with Calcein-AM and Hoechst staining, demonstrated that pNCs remained present and viable up to 2 weeks in all biomaterials. The maintenance of NC morphology and the retention of vacuole-like structures (indicated with white arrows) were observed in the 1-week NPgel and up to 2-week in the Albugel samples seeded with pNCs (Fig. 3.4). NPgel/dNCM with pNC showed less notochordal-like morphological phenotype with no vacuoles present at any timepoints (Fig. 3.4).

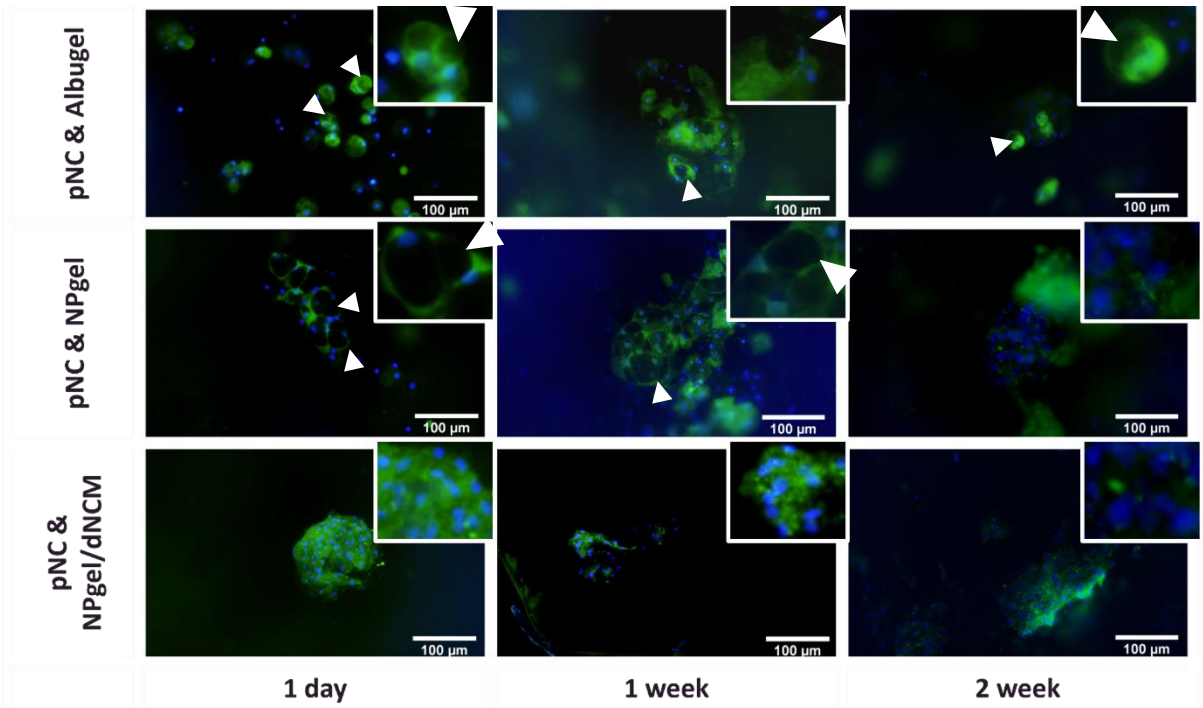

Figure 3.4. Immunofluorescence staining of live cell imaging of porcine notochordal cells cultured in NPgel, NPgel/dNCM and Albugel, *for up to 2 weeks in a hypoxia unit of 5% v/v oxygen (n=3 biological repeats). Images were captured using Calcein-AM and Hoechst 33342. White arrow heads indicate vacuoles.*

Constructs were further cultured for an extended 4-week culture. Scanning electron microscopy was utilised to investigate morphology of acellular and cellular biomaterials. Furthermore, histological stains: H+E, Alcian Blue, Masson's Trichrome and Safranin O/ Fast green were used to determine the morphology and matrix deposition by the cells in the biomaterials.

SCANNING ELECTRON MICROSCOPY MORPHOLOGY

SEM analysis of acellular constructs demonstrated a porous structure within all biomaterials. Albugel demonstrated a dense structure with fibrous pores (Fig. 3.5a). Whilst NPgel displayed a more honeycomb porous structure (Fig. 3.5c), which following inclusion of dNCM showed the appearance of thinner strands (Fig. 3.5e). Whilst constructs containing pNCs demonstrated apparent cellular structures within all gel systems, although constructs were heterogeneous, with some areas filled with cellular structures, whilst other areas were devoid of cells (Fig. 3.5b, d, e), suggesting an uneven distribution of pNCs within the constructs. The majority of cells within all three biomaterials were seen in small clusters (Fig. 3.5b, d, e), although some single/duplicate cells were observed in Albugel constructs (Fig. 3.biii). Within NPgel constructs some clusters displayed a visible 'membrane' which appeared to wrap the entire pNC cluster (Fig. 3.5d; white arrow heads).

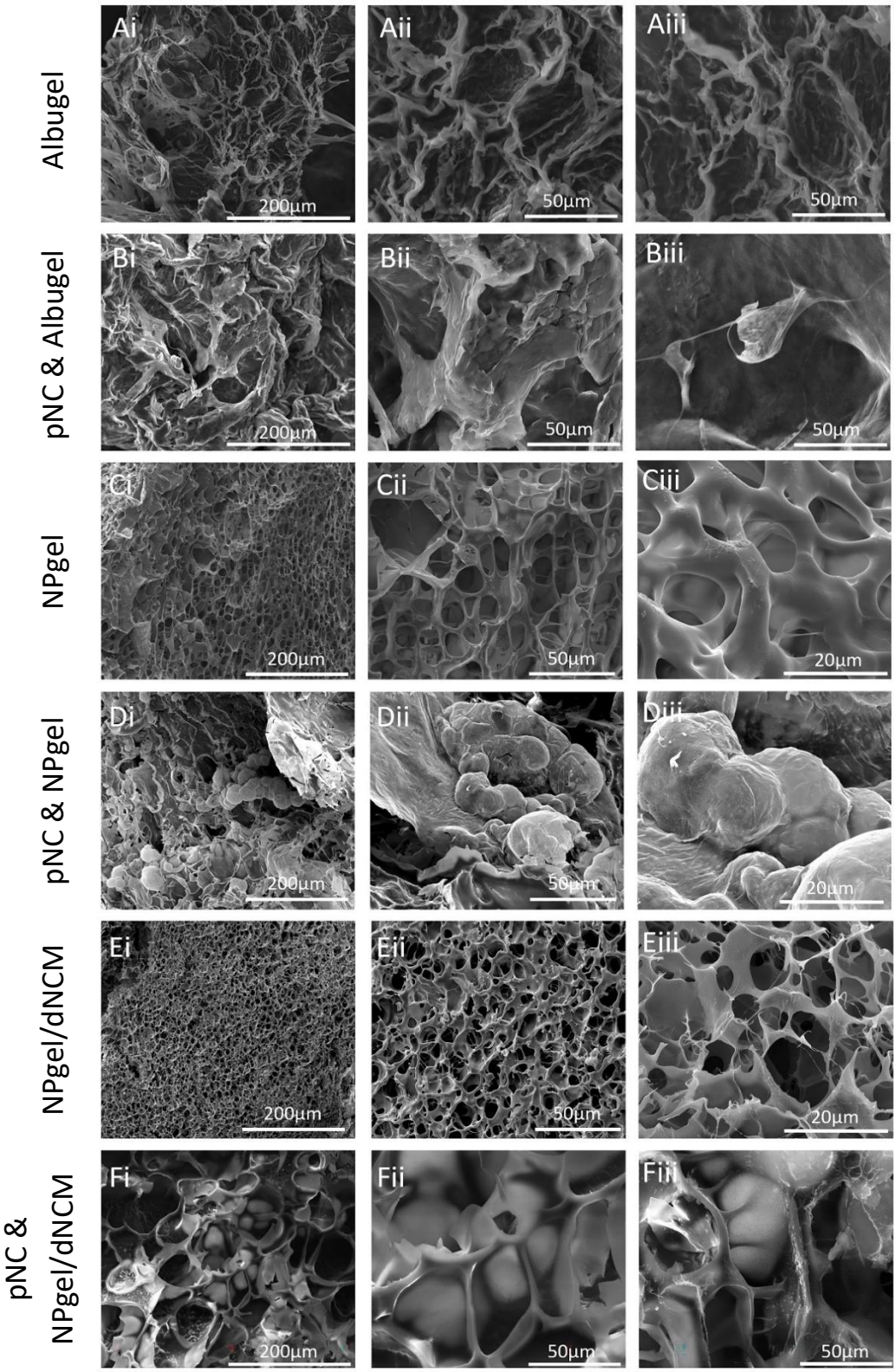

Figure 3.5. Scanning electron microscope images acellular biomaterials and those containing porcine notochordal cells (pNC), *cultured for 2 weeks in a hypoxia unit at 5% v/v oxygen, 37°C. A: Acellular Albugel, B: pNC cultured in Albugel; C: Acellular NPgel; D: pNCs cultured in NPgel; E: Acellular NPgel / dNCM; F: pNCs cultured in NPgel/dNCM (n=3 biological repeats). Scale bars as indicated (20, 50 or 200µm).*

ISOLATED NOTOCHORDAL CELL BEHAVIOUR AND MORPHOLOGY IN NOVEL BIOMATERIALS

H+E staining of pNC & NPgel and pNC & NPgel/dNCM demonstrated the seeded cells remained in cluster formation, whereas the pNCs in the Albugel construct appeared more dispersed (Fig. 3.6). Alcian Blue demonstrated GAG staining around the cell clusters (stained blue) in pNC & NPgel constructs (Fig. 3.6). In the NPgel and NPgel/dNCM constructs (Fig. 3.6) Masson's Trichrome blue staining surrounding the cells indicates collagen expression in the surrounding material (Fig. 3.6). Collagen expression is also indicated in Safranin Orange stain by pericellular green/turquoise staining (Fig. 3.6). Albugel constructs failed to demonstrate clear matrix indication when stained with Alcian Blue or Masson's Trichrome, however Safranin Orange stain indicated slight green/turquoise staining surrounding the pNC (Fig. 3.6).

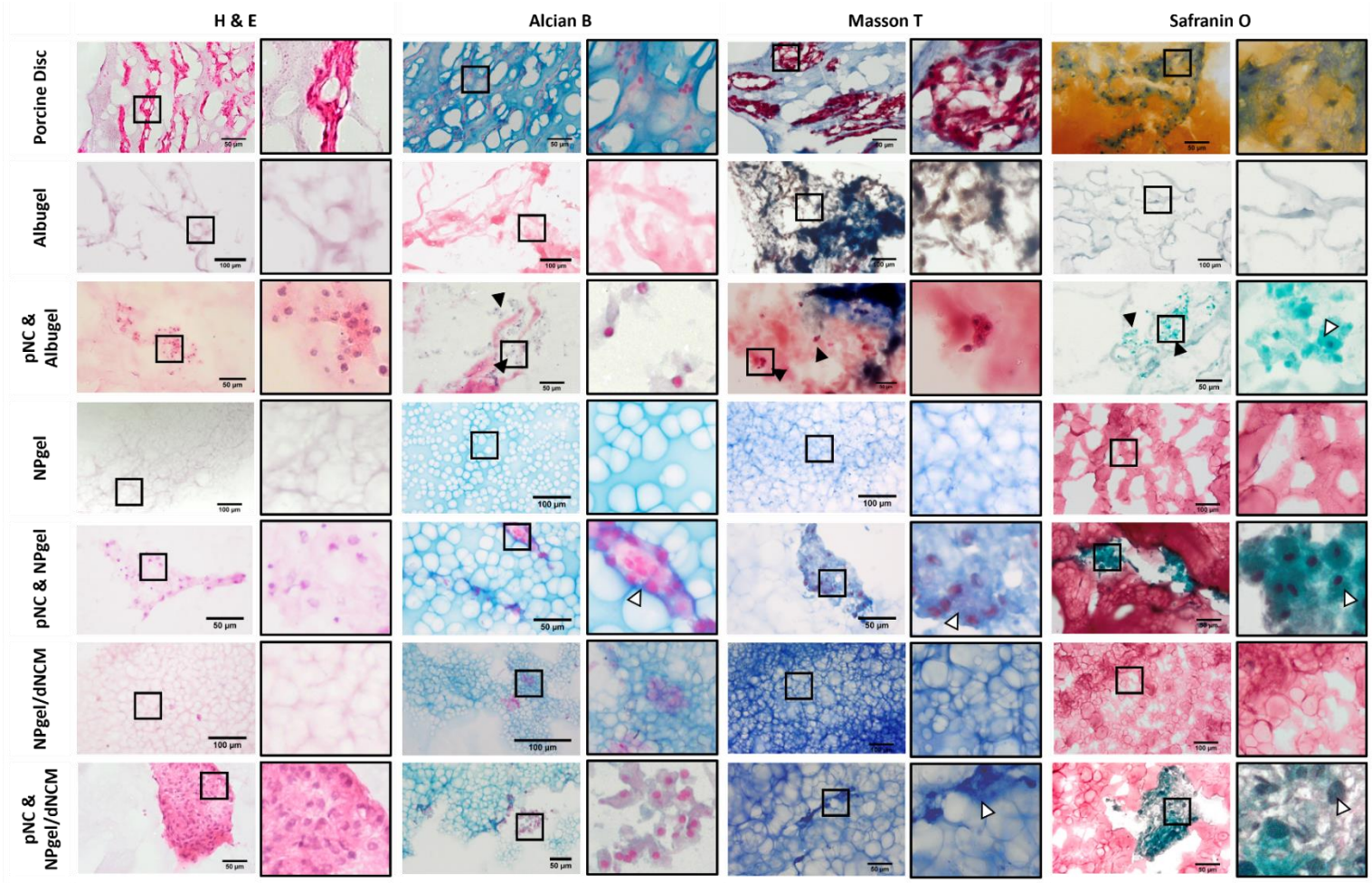

Figure 3.6. Porcine notochordal cell (pNC) morphology when cultured in Albugel (pNC & Albugel), NPgel (pNC & NPgel) and NPgel/dNCM (pNC & NPgel/dNCM) with acellular controls (Albugel; NPgel; NPgel/dNCM), *for up to 4 weeks at 5% v/v oxygen, 37°C. Haematoxylin and Eosin (H+E), Alcian Blue (Alcian B), Masson's Trichrome (Masson's T) and Safranin Orange (Safran O) (n=3 biological repeats). Black arrows highlight where cells are present. Images with black outline are high magnification regions of cellular constructs, white arrows indicate extracellular matrix deposition. Porcine disc and cellular constructs are scale bar 50µm, acellular constructs scale bar 100µm.*

The number of cells per cluster was determined following 4 weeks in culture. The number of cells in clusters were significantly different between each biomaterial, with the number of pNCs in clusters when cultured in NPgel, were significant greater when compared to NPgel/dNCM ($p \leq 0.01$) and significantly greater when compared to Albugel ($p \leq 0.0001$); NPgel/dNCM were significantly greater when compared to Albugel ($p \leq 0.001$; Fig. 3.7). With the highest number of cells observed per cluster of 40 cells in NPgel, 26 in NPgel/dNCM and 14 cells in Albugel, with the median number of cells observed per cluster was 5 in NPgel, 2 in NPgel/dNCM and 1 in Albugel (Fig. 3.7). Altogether, this demonstrated that pNCs present themselves in larger clusters in NPgel and NPgel/dNCM biomaterials, whereas in Albugel they were mostly single cells.

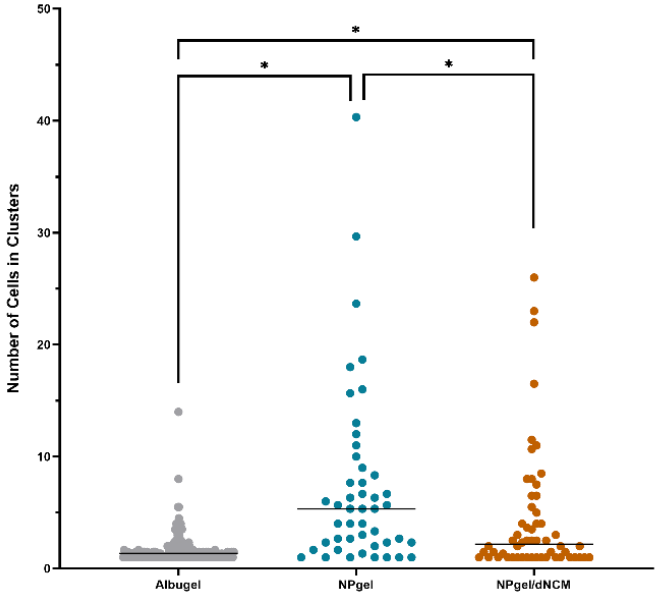

Figure 3.7. Porcine notochordal cell (pNC) cluster size when seeded into biomaterials; *NPgel, NPgel/dNCM and Albugel after 4 weeks in culture at 5% v/v oxygen, 37°C (n=3 biological repeats). A single dot represents a cluster of pNCs. Statistics performed with in GraphPad prism v9.5.1, Kruskal-Wallis test, followed by the Dunn's multiple comparisons test * p≤0.05.*

NOTOCHORDAL CELL CHARACTERISATION AND PHENOTYPIC ANALYSIS WITHIN NOVEL BIOMATERIALS

Immunohistochemical staining was further used to analyse and characterise the pNC that were cultured in the biomaterials for 4 weeks (Fig. 3.8a). The pNCs seeded into all three biomaterials showed nuclear and cytoplasmic positive staining for the NC/NP cell markers Brachyury and cytokeratin 8/18/19, which when quantified showed no significant difference in expression between the biomaterials ($p>0.05$) (Fig. 3.8b). Extracellular immunohistochemical staining for aggrecan was shown in the pNCs seeded into Albugel, NPgel and NPgel/dNCM, with extracellular immunohistochemical staining for collagen type II only distinguishable in the pNC & NPgel constructs (Fig. 3.9). However, staining was also observed in the acellular NPgel and NPgel/dNCM construct, due to nature of biomaterials retaining DAB (Fig. 3.9).

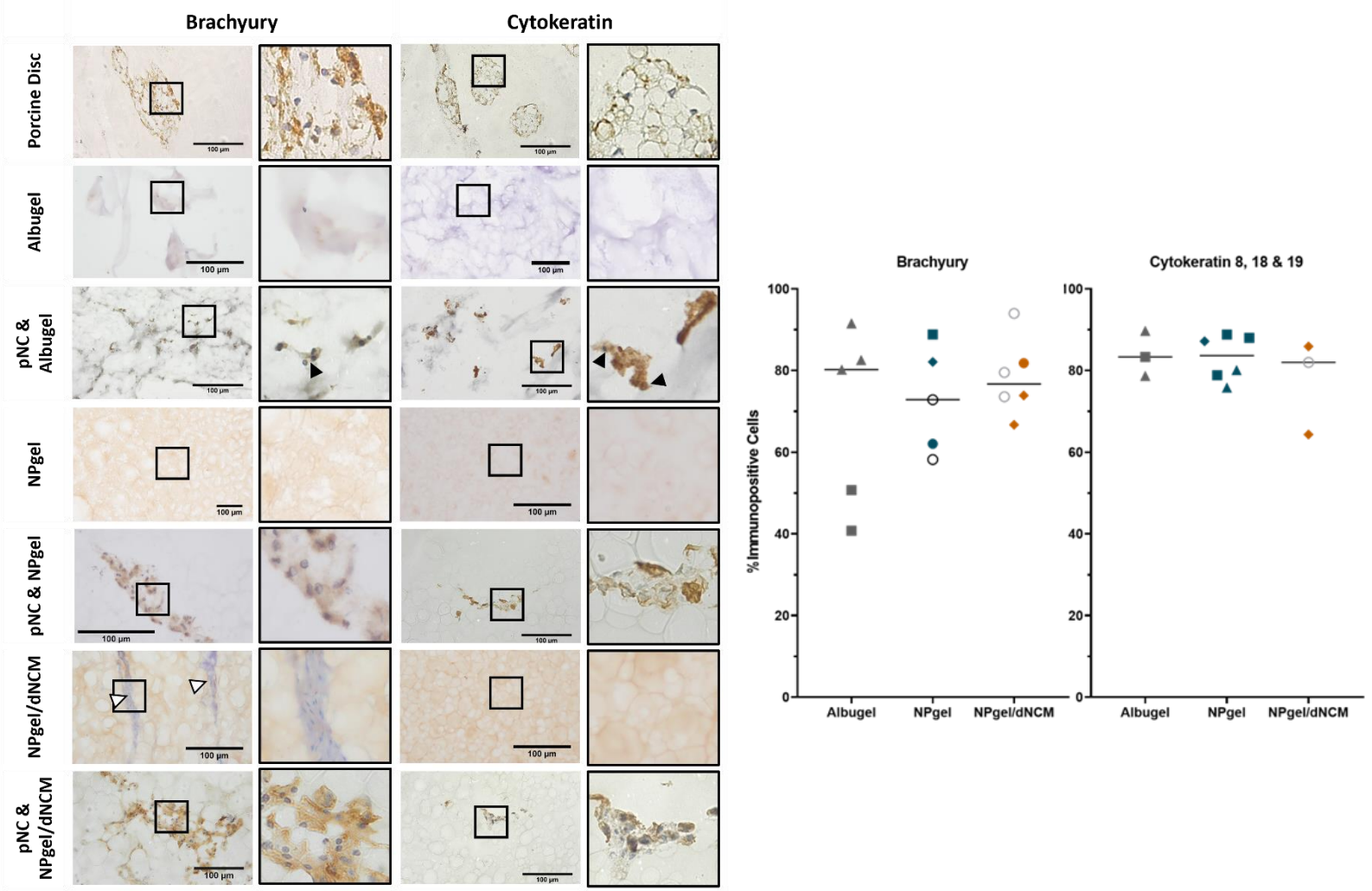

Figure 3.8. Porcine notochordal cell phenotype when cultured in three biomaterials. (A) *Immunohistochemistry staining of porcine notochordal cells (pNC) seeded in biomaterials Albugel (pNC & Albugel), NPgel (pNC & NPgel) and NPgel/dNCM (pNC & NPgel/dNCM) and cultured for up to 4 weeks in 5% v/v oxygen at 37°C, including acellular controls (Albugel; NPgel; NPgel/dNCM) and porcine disc. Stained with Brachyury, Cytokeratin 8/18/19 (pan Cytokeratin). Black boxed images represent zoomed in images of pNC in biomaterials and porcine disc. Black arrows highlight pNC. White arrows highlight residual cellular staining from dNCM. Scale bar 100µm.* ***(B)*** *Quantitative analysis of the percentage of Brachyury and cytokeratin 8/18/19 immunopositive cells in pNC & Albugel (Albugel) (n=2 biological repeat), pNC & NPgel (NPgel) (n=4 biological repeat) and pNC & NPgel/dNCM (NPgel/dNCM) (n=3 biological repeat). Each shape represents a different biological repeat. Statistics performed with in GraphPad prism v9.5.1, Kruskal-Wallis test, followed by the Dunn's multiple comparisons test, not significant.*

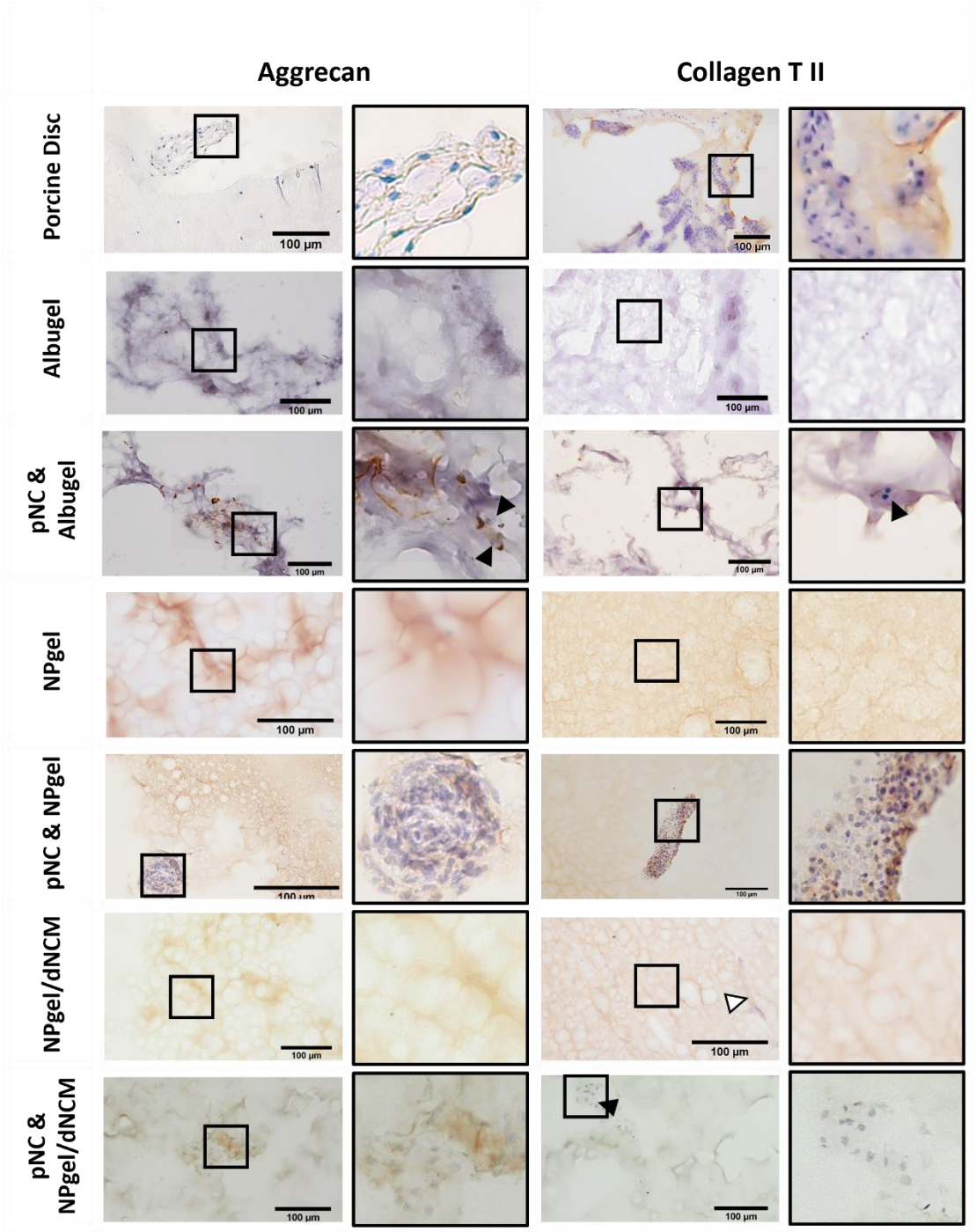

Figure 3.9. Porcine notochordal cell (pNC) extracellular matrix expression when seeded in biomaterials*. Immunohistochemistry staining of pNCs seeded in biomaterials Albugel (pNC & Albugel), NPgel (pNC & NPgel) and NPgel/dNCM (pNC & NPgel/dNCM) and cultured for up to 4 weeks in 5% v/v oxygen at 37°C, including acellular controls (Albugel; NPgel; NPgel/dNCM) and porcine disc (n=3 biological repeats). Stained with Aggrecan and Collagen type II (Collagen T II). Black boxed images represent zoomed in images of pNC in biomaterials and porcine disc. Black arrows highlight pNC. White arrows highlight residual cellular staining from dNCM. Scale bar 100µm.*

GAGs released into the culture media from pNC, and biomaterial constructs was assessed throughout the 4-week culture period and analysed using DMMB assay (Fig. 3.10). The acellular NPgel/dNCM constructs had a significantly higher GAG release into the culture media compared to acellular NPgel and Albugel biomaterials at 1 week (NPgel/dNCM v Albugel, $p \leq 0.001$; NPgel/dNCM v NPgel, $p \leq 0.001$), 2 week (NPgel/dNCM v Albugel, $p \leq 0.0001$; NPgel/dNCM v NPgel, $p \leq 0.01$) and 3-week (NPgel/dNCM v Albugel, $p \leq 0.01$; NPgel/dNCM v NPgel, $p \leq 0.01$) culture time points but was reduced following 4 weeks in culture ($p > 0.05$). This may suggest release of the natural GAGs coming from the dNCM within the biomaterial, with no further increase of GAG release into media within NPgel/dNCM materials seeded with pNCs. No significant difference in GAG release was observed between acellular controls and pNC-containing constructs at any time-point (Fig. 3.10).

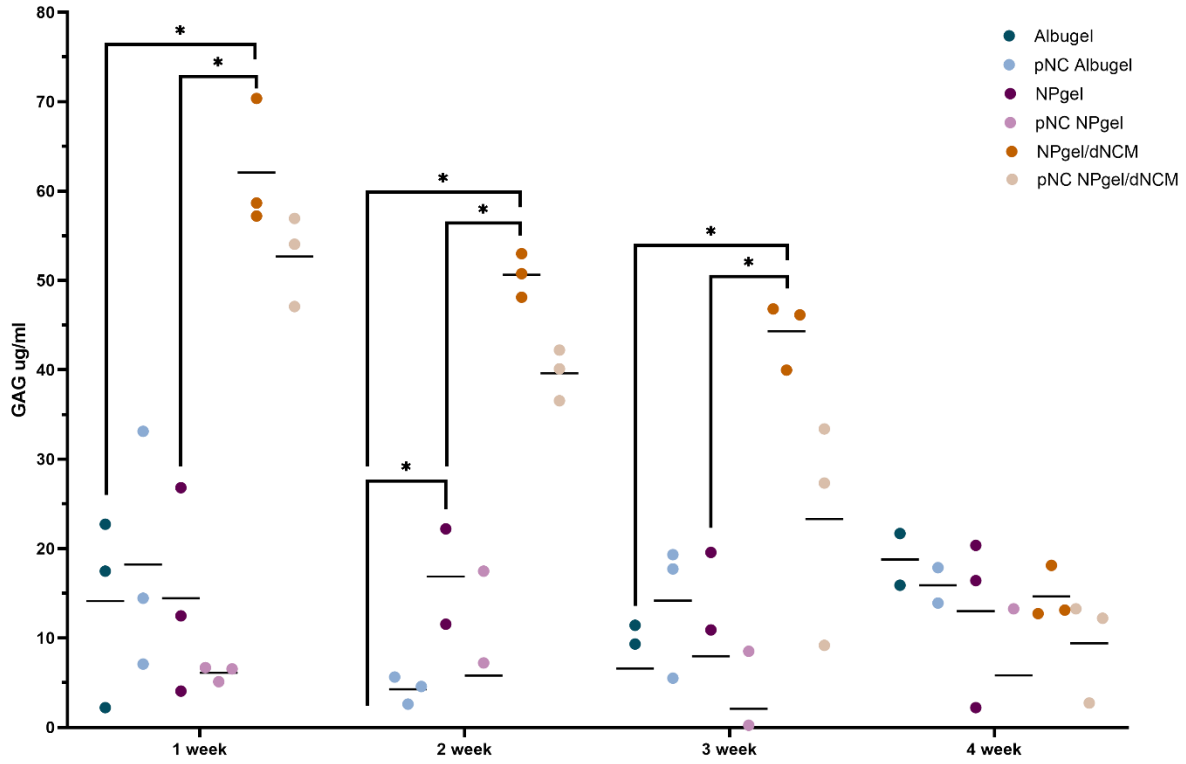

Figure 3.10. Porcine notochordal cell glycosaminoglycan (GAG) release during culture in biomaterials. *GAG release was measured using 1,9-Dimethylene blue (DMMB) assay in media collected over 4 weeks of acellular biomaterials (Albugel, NPgel and NPgel/dNCM) and porcine notochordal cells (pNC) seeded in Albugel, NPgel and NPgel/dNCM biomaterials at $4x10^6$ cells/ml and cultured at 5% v/v oxygen, 37°C for up to 4 weeks (n=3 biological repeats). Statistics performed with in GraphPad prism v9.5.1, one-way ANOVA test, followed by the Tukey's multiple comparisons test *p ≤0.05.*

DISCUSSION

NCs have attracted considerable interest due to their potential application for regeneration of the intervertebral disc (Bach *et al.*, 2022), but to date, no studies have investigated the potential of biomaterials to support their viability and phenotype, with studies purely investigating simple 3D culture systems to maintain phenotype purely for *in vitro* applications. This study investigated three potential biomaterials which are all injectable and could provide excellent mechanical support to the IVD whilst delivering the regenerative cell source. Biomaterials were selected representing a naturally inspired cross linked hydrogel (Albugel), a fully synthetic hydrogel which gels based on entanglement of polymer chains (NPgel) (Boyes *et al.*, 2021), and the supplementation of the synthetic hydrogel with naturally derived dNCM (NPgel/dNCM) (Schmitz *et al.*, 2022). All three biomaterials demonstrated they retained linear viscoelastic properties within the physiological strain rates observed for IVDs. NPgel exhibited a higher gel strength (characterised here by G') compared to NPgel/dNCM and Albugel. Furthermore, NPgel and to a lesser extent NPgel/dNCM showed an increase in G' following 24hrs in culture media which mimics the degenerate IVD. The G' of NPgel following 24hrs in degenerate media reached ~14KPa which is similar to that of human NP tissue reported previously of 7-21kPa (Iatridis *et al.*, 1996, 1997). We have previously reported other rheological properties of NPgel including its gelation kinetics (Boyes *et al.*, 2021).

Initial studies with pNCs utilised NPgel to determine the seeding density for future studies. Porcine NCs were seeded at different cell densities ranging between $1x10^6$ cells/mL to $2x10^7$ cells/mL into NPgel, where pNCs presented mainly in clusters and easier to identify within sectioned materials at $4x10^6$ cells/mL and $1x10^7$ cells/mL. Whilst lower densities of $1x10^6$ cells/mL displayed mainly single cells and the highest cell density of $2x10^7$ cells/mL displayed both clustered and single cells but showed no advantage over lower seeding densities. The native cell density of the NP has been reported to be $1.3x10^5$cells/cm^3 in non-chondrodystrophic dogs (Hunter, Matyas, *et al.*, 2003), and $4x10^6$ cells/cm^3 in humans (Maroudas *et al.*, 1975). The importance of preservation the pNC clusters phenotype was also hypothesised to support NC survival and function (Aguiar *et al.,* 1999; Hunter *et al.,* 2003; Gantenbein *et al.*, 2014; Spillekom *et al.*, 2014; Humphreys *et al.*, 2018). Additional, NCs are also reported to be highly metabolically active and sensitive to nutrient deprivation (Guehring *et al.*, 2009; Spillekom *et al.*, 2014), therefore the optimum cell density was selected as $4x10^6$ cells/mL, as cluster formation was retained without excessive cell density which could provide nutrient deprivation over long term culture and is also in agreement with the cell density reported in human NP (Maroudas *et al.*, 1975; Roughley, 2004). However, a study by Liebscher et al., (2011) elucidated cell density and total cell numbers of human IVDs and concluded that the cell density of NCs in NP tissue harvested from 0-1 year old donors had a cell density of $5.6 \pm 4.3x10^6$ cells/cm^3 (Liebscher *et al.*, 2011). Indicating that the $4x10^6$ cells/cm^3 figure which was taken from a referenced NP tissue populated with NP cells could be lower than NC densities; perhaps native porcine tissue should have been analysed and quantified to generate a cell density of NCs. Based on brightfield images pNCs showed clear cluster and vacuoles

structures up to at least 2 weeks in culture, thus following these successful initial results, the complete screening experiment was performed, seeding pNC into three biomaterials that have shown potential for disc regeneration.

RETENTION OF NOTOCHORDAL CELL CYTOMOPHOLOGY IN BIOMATERIALS

From the histological images, it was promising to observe that pNCs survived for up to 4 weeks in all three biomaterials, however the morphotypic pNC was not retained in all biomaterials. In Albugel, Calcein-AM images, SEM and histology, showed a lack of large clusters, with most cells observed in single cells. However, some preservation of vacuole-like structures was observed after 2-weeks and key NC/NP markers were retained, including Brachyury and keratin 8/18/19. In native NP tissue, single cells are usually smaller and resemble more the mature NP cells often seen in a more mature and degenerate disc (Hunter, John R. Matyas, *et al.*, 2003; Chen *et al.*, 2006), suggesting that the pNC in Albugel were differentiating into these mature NP cells. Within the literature their remains some debate to whether the population of smaller mature NP cells are derived from the juvenile NCs or replaced from alternative progenitor cells (Kim *et al.*, 2009), whereas these results supports the perspective that NCs have the capability to differentiate into mature NP cells, which can retain their expression of Brachyury and cytokeratin (Minogue *et al.*, 2010; Risbud *et al.,* 2010). In NPgel, the pNCs predominately presented in clusters and contained vacuolated structures evident in Calcein-AM stained live-cell images, within this biomaterial clusters containing up to 40 cells per cluster were maintained. However, following long term culture of 4-weeks the vacuole-like phenotype was lost despite the pNC remaining in clusters. Similar findings were also observed during a longer-term culture of NCs in alginate beads, despite the maintenance of phenotypic markers, the morphology of the cells changed from large NC clusters to NCs with smaller vacuoles and mature NP cells (Arkesteijn *et al.,* 2015). The loss of vacuole morphology along with loss of phenotypic markers was also noted when NC were cultured in monolayer (Arkesteijn *et al.,* 2015) and when injected directly into NP tissue (Arkesteijn *et al.,* 2017). In NPgel/dNCM, histological images, SEM and cell cluster size analysis demonstrated the presence of clusters and vacuole like structures were observed, although this was not visualised within live-cell imaging.

RETENTION OF NOTOCHORDAL CELL PHENOTYPE IN BIOMATERIALS

The histological and IHC images demonstrated the indication of pericellular matrix deposition containing aggrecan staining observed in the pNC & Albugel, pNC & NPgel and pNC & NPgel/dNCM constructs, which also corresponded to the turquoise GAG stain within Safranin O staining (Leung *et al.*, 2009). Interestingly, collagen type II staining was only strongly observed in pNC cultured within NPgel. IHC demonstrated the retention of Brachyury and cytokeratin NC/NP phenotypic markers. Studies using NCs in alginate beads have also shown cell survival during culture, which corresponded with Brachyury and cytokeratin expression and an increase in GAG detection (Aguiar *et al.,* 1999; Gantenbein-Ritter and Chan 2012; Arkesteijn *et al.,* 2017). Within the current study there was limited GAG release evidenced

from pNCs cultured within the biomaterials, with only Albugel demonstrating a difference between acellular and cellular constructs. Potentially suggesting the hyaluronic acid within the Albugel increases GAG production. Alternatively, the lack of GAG release into the media in NPgel constructs could indicate greater GAG retention in the NPgel constructs containing pNCs, as histological staining did display cellular GAG staining using both Alcian Blue and Safranin O. Whilst NPgel supplemented with dNCM demonstrated high secretion of GAGs into the media even in acellular controls over the first 3 weeks, this decreased after 4 weeks in culture. Suggesting loss of the dNCM (which is GAG rich) into the media over the initial time course. The decreased GAG content in the media after 4 weeks may indicate exhaustion of the GAG content from the dNCM or potentially the formation of a more complex matrix network leading to the trapping of the GAGs at later time course. However, given the low collagen staining observed both with Masson's Trichrome staining and immunohistochemical staining for collagen type II it is more likely the dNCM had all leached out over the first 3 weeks. The incorporation of dNCM into NPgel is based on a physical entanglement rather than any physical cross linkages and thus it may be necessary to develop biomaterials which enable chemical cross linking of NCM into the materials to ensure longer term retention. Furthermore, when such a system is injected into the NP tissue space in a whole IVD the GAG release would likely be retained in the disc and thus this leaching out may not be a detriment following IVD injection. Alternative methods of assessing extracellular matrix production by the seeded cells, such as the use of tagging cellular GAG production as used by Baskin *et al.,* (2007), would enable a better understanding whether the observed matrix staining was produced from the pNCs themselves rather than a remnant from the biomaterial.

VACUOLES WITHIN CULTURED NOTOCHORDAL CELLS

The seeding of pNC in the three biomaterials resulted in the presentation of morphologically different cells, which was characterised by the gradual loss of vacuoles, but a retention of NC marker expression. The purpose of NC vacuolation in embryonic development of the spine is focused on retaining hypertonic tension (Hunter *et al.*, 2007). Taking NCs into an *in vitro* setting does have the limitation of altering the cells environment; in this study the constructs were maintained in physiologically relevant hypoxic conditions of 5% oxygen (Soukane *et al.,* 2005; Chen *et al.*, 2014), and using media recommended for IVD 3D culture (Basatvat *et al.*, 2023). Nevertheless, with the isolation of cells, there is a change of environment such as the loss of mechanical stress and extracellular matrix which otherwise would have promoted water retention, although by maintaining cell clusters the pericellular matrix should be retained (Urban *et al.,* 1978; Oegema, 1993). All three biomaterial systems investigated here are hydrogel-based biomaterials, which have high water-soluble polymeric materials. In the biomaterial that contains NC matrix, (NPgel/dNCM), there was potentially the retention of vacuole-like structures. In previous studies where altered media osmolality has been tested, from standard 300 to 500mOsm/kg resulted in a sustained canine NPC population with improved phenotype, irrespective of oxygen conditions (Spillekom *et al.*, 2014; Laagland *et al.*, 2022), suggesting that there could be many factors that can affect the NC phenotype. It

may be that the lack of external mechanical and hydrostatic tension caused the difference in NC morphology, as vacuoles function to withstand compression forces (Ellis *et al.*, 2013; Wang *et al.*, 2017; Hong *et al.*, 2018; Bagwell *et al.*, 2020). Although compression loading has also been shown to be detrimental to NC health (Guehring *et al.*, 2010; Spillekom *et al.*, 2014; Yurube *et al.*, 2014; Hong *et al.*, 2018), whilst other studies have shown no effect on NC viability and phenotype (Saggese *et al.*, 2020). Thus, it would be important to investigate if these pNC seeded biomaterial constructs subjected to physiological compression and loading, would affect morphological NC and their phenotype.

CONCLUSION

Three biomaterials, Albugel, NPgel and NPgel/dNCM represents differing classes of natural (Albugel), synthetic (NPgel), and semi-synthetic (NPgel/dNCM) biomaterials were investigated, to determine if they would maintain pNCs phenotype as a first stage to develop a biomaterial delivery system for the IVD. The results determined that pNC can retain viability and maintain NC markers in biomaterials, Albugel, NPgel and NPgel/dNCM for up to 4 weeks in physiological 5% v/v oxygen, however loss of clustering was observed within Albugel and loss of the morphotypic vacuolated NC phenotype was lost or decreased in all three biomaterials. Therefore, the biomaterials selected have the potential to harness NC regenerative properties, however future work is needed to determine whether retention of the morphotypic phenotype is required to provide regenerative properties.

ACKNOWLEDGMENTS

This work was supported by the funding received from the European Union's Horizon 2020 research and innovation programme [grant agreement No 825925]. MAT is financially supported by the Dutch Arthritis Society (LLP22).

CONFLICT OF INTEREST

CLM and CS are named inventors on the patent for NPgel, KB is named inventor on the patent for the albumin/ hyaluronan hydrogel.

CHAPTER 4
POTENTIAL OF MESENDODERM PROGENITOR CELLS WITHIN INJECTABLE BIOMATERIALS TO PROMOTE INTERVERTEBRAL DISC REGENERATION

CONTEXT OF RESEARCH

As porcine notochordal cells (NCs) are less likely to be clinically applicable (Chapter 1, Table 1.1), in this Chapter the use of iPSC derived Mesendoderm progenitor cells (iPSC-MEPCs), seeded into injectable biomaterials, as an alternative cell source was investigated. IPSC-MEPCs were recovered and seeded into previously assessed biomaterials: Albugel, NPgel and NPgel/dNCM (Chapter 3), with the addition of another two biomaterials: alginate and Polyethylene glycol with dNCM (PEG/dNCM; a leading biomaterial from a collaborating University). The contribution to the research field was the novel culturing of iPSC-MEPCs within biomaterials *in vitro* for 4 weeks under IVD physiological conditions of hypoxia. With particular interest of analysing the survival of iPSC-MEPCs in 3D culture, with the potential to initiate differentiation into NC-like cell lineage when cultured in these selected biomaterials.

AUTHORS

Rebecca J. Williams[1,2], Georgina Targa Fabra[3], Julie Warin[4], Tara C. Schmitz[5], Ronak Janani[6], Abhay Pandit[3], Karin Benz[7], Keita Ito[5], Chris Sammon[6], Anne Camus[4], Mariana A. Tryfonidou[8], Joseph W. Snuggs[1,2], Christine Le Maitre[1,2]

AFFILIATIONS

[1] Department of Oncology and Metabolism, University of Sheffield, UK. [2] Biomolecular Sciences Research Centre, Sheffield Hallam University, UK. [3] CÚRAM Centre for Research in Medical Devices, University of Galway, Ireland. [4] Regenerative Medicine and Skeleton, University of Nantes, Nantes, France. [5] Orthopaedic Biomechanics, Department of Biomedical Engineering, Eindhoven University of Technology, The Netherlands. [6] Materials Engineering research Institute, Sheffield Hallam University, UK. [7] TETEC Tissue Engineering Technologies

AG, Germany. [8] Department of Clinical Sciences, Faculty of Veterinary Medicine, Utrecht University, The Netherlands.

AUTHOR CONTRIBUTIONS

RJW, CLM, JWS and MAT contributed to conception and design of the study; JW and AC generated the iPSC-MEPCs; GTF, TCS, RJ, AP, KB, KI, CS, JWS contributed to biomaterial synthesis; RJW, GTF contributed to acquisition of laboratory data; RJW performed most of the data analysis; RJW, CLM, JWS contributed to interpretation of the data; RJW, CLM and JWS drafted the manuscript.

DETAILED CONTRIBUTIONS MADE

I conducted experiments: recovering iPSC-MEPCs that were generated and cryopreserved from INSERM and the University of Nantes. Investigating their viability and cell counts (Fig. 4.4, 4.5, 4.6 and 4.7). I performed all laboratory work investigating behaviour of the iPSC-MEPCs within NPgel, Albugel and NPgel/dNCM (Fig. 4.8, 4.9, 4.10, 4.11 and 4.12). During comparison studies investigating the leading biomaterials alongside GFT and CLM, we seeded MEPC into alginate (CLM), PEG/dNCM (GFT) and NPgel (RW). I maintained all the biomaterials in culture for the 4 weeks investigated, harvested, fixed, and processed wax and sectioned. I performed the Histological assessments and cell counts (Fig. 4.15 and 4.19), and the majority of immunohistochemical staining (GFT performed Sox9 and FOXA2) whilst the rest were performed by myself (Fig. 4.16, 4.17 and 4.18), I also assessed glycosaminoglycan production (Fig. 4.20). I preformed all data analysis and statistical analysis relating to these experiments and drafted the entire manuscript.

(IN PREPARATION) Potential of Mesendoderm Progenitor Cells Within Injectable Biomaterials to Promote Intervertebral Disc Regeneration. Rebecca J. Williams, Georgina Targa Fabra, Julie Warin, Ronak Janani, Abhay Pandit, Chris Sammon, Anne Camus, Mariana A. Tryfonidou, Joseph W. Snuggs, Christine Le Maitre.

ABSTRACT

Low back pain is the leading cause of disability worldwide and is strongly associated with degeneration of the intervertebral disc (IVD). During degeneration the nucleus pulposus (NP) in the core of the IVD, is affected by altered matrix synthesis, increased degradation, and cell loss. Strategies combining regenerative cell sources with injectable biomaterials could provide a therapeutic approach to treating IVD degeneration-related to back pain. Whilst several potential cell sources have been proposed, induced pluripotent stem cells (iPSCs) provide a promising regenerative potential, due to their accessibility; expansion capability *in vitro,* and the capacity to differentiate into a chosen cell. Differentiating iPSC into notochordal cells (NC), which are juvenile cells of the NP, could provide both anabolic and anti-catabolic responses for disc regeneration. Unfortunately, high yield, pure populations of iPSC-derived NCs proved challenging to generate, therefore iPSC-derived Mesendoderm progenitor cells (iPSC-MEPCs) were utilised to investigate the ability of biomaterials to drive the differentiation into mature NC or NP like cells. MEPCs have not previously been investigated within biomaterial delivery systems for the regeneration of the IVD. Here, a three-phase biomaterial investigation was conducted; Phase I investigated iPSC-MEPC survival when cultured within cytocompatible biomaterials Albugel (an albumin/ hyaluronan hydrogel) and NPgel (a L-pNIPAM-co-DMAc hydrogel) for 5-days under 5% oxygen. Phase II investigated MEPC characterisation and phenotypic analysis within biomaterials Albugel, NPgel and NPgel with decellularized NC-matrix powder (dNCM); and were cultured for up to 2 weeks under 5% oxygen (n=3 biological repeats). Phase III investigated MEPC characterisation and phenotypic analysis within biomaterials alginate, polyethylene glycol with dNCM (PEG/dNCM) and NPgel; and were cultured for up to 4 weeks under 5% oxygen (n=3 biological repeats). This study aimed to identify a biomaterial which could enable the survival and differentiation of seeded iPSC-MEPCs into an NC-like phenotype with extracellular matrix synthesis and deposition, which was investigated through histological, immunohistochemical and glycosaminoglycan analysis. It was concluded that some biomaterials enabled initial MEPC cell encapsulation and facilitated MEPC survival. The PEG/dNCM and NPgel biomaterial showed most potential due to the observation of MEPC survival and the demonstration of regenerative properties through positive extracellular matrix staining and iPSC-MEPCs expressing NC-like phenotype. The MEPC cultured in biomaterials analysed could have potential to be utilised as an injectable delivery system of iPSC-MEPCs into the disc, if they continue to differentiate into NC-like cells.

INTRODUCTION

LOWER BACK PAIN AND INTERVERTEBRAL DISC DEGENERATION

Lower back pain is a prevalent health problem in western society with 60-80% of adults experiencing this common medical condition (Hartvigsen *et al.*, 2018), LBP can often manifest as chronic pain and disability, which can have a debilitating effect to sufferers' quality of life (Smith and Osborn 2007; Phillips et al. 2003). Lower back pain has been strongly associated with the degeneration of the intervertebral disc (IVD) (Luoma *et al.*, 2000); a complex fibrocartilaginous organ that connects adjacent vertebral bodies to permit the movement of the spine and absorbs biomechanical forces (Shapiro and Risbud, 2014). IVD degeneration is coupled with the failure of the IVD structure and with the natural ageing of tissue, which presents as fissures and herniation, markers of impaired disc function (Adams and Roughly, 2006). IVD degeneration is linked to initial deterioration of the core of the IVD, the nucleus pulposus (NP), during which degradation of extracellular matrix production and increased proinflammatory cytokines, and a change in NP cell phenotype, is observed (Phillips et al. 2015; Le Maitre et al. 2007; Bergknut et al. 2013). These structural defects of the IVD are closely related to pain associated with IVD degeneration, and is often initiated with the altered microenvironment and biological disorganization of the IVD (Ito and Creemers, 2013; Binch *et al.*, 2015).

CELL-BASED THERAPY FOR INTERVERTEBRAL DISC DEGENERATION

Treatments for lower back pain induced with IVD degeneration, attempt to alleviate the pain or remove the herniated IVD tissue with microdiscectomy or decompression (Malik *et al.*, 2013; Fujii *et al.*, 2019), rather than targeting the repair of the degenerated disc. Cell-based therapies are considered the most promising for IVD repair, as this method targets the repopulation and regeneration of biomechanical tissue function, allowing the restoration of spinal movement, flexibility and integrity (Binch *et al.*, 2021; Williams *et al.*, 2021). However, the ideal cell source is an important consideration; several cell types have been used in research for the potential to regenerate the NP (Williams *et al.*, 2021). This review highlighted that bone marrow stromal cells and induced pluripotent stem cells (iPSC) shows the most potential, through their ability to produce appropriate extracellular matrix and could theoretically withstand the harsh IVD environment (if iPSC were to differentiate into a more disc-like cell) (Williams *et al.*, 2021; Bach *et al.*, 2022). Previous studies have successfully used iPSC to differentiate into notochordal (NC) like cells (Chen *et al.*, 2013; Liu *et al.*, 2014; Liu *et al.*, 2015 Liu *et al.*, 2015; Tang *et al.*, 2018; Sheyn *et al.*, 2019; Xia *et al.*, 2019; Xia *et al.*, 2019; Colombier *et al.*, 2020; Zhang *et al.*, 2020; Kamatani *et al.*, 2022; Seki *et al.*, 2022), in which some studies have resulted with matrix expressing cells and shown promising regenerative potential in animal models (Zhu *et al.*, 2017; Sheyn *et al.*, 2019; Xia *et al.*, 2019).

USING INDUCED PLURIPOTENT STEM CELLS GENERATED MESENDODERM PROGENITOR CELLS AS A CELLULAR-BIOMATERIAL TREATMENT

Generating NC can be implemented with harnessing the utility of induced pluripotent stem cells (iPSCs) (Takahashi *et al.*, 2007). Stable NC-like cells have been generated via a two-step process of differentiating iPSC *in vitro*, which have the characteristics of the embryonic immature NCs (Colombier *et al.*, 2020). In brief Colombier *et al.,* (2020) initiated the first step of activating the Wingless/Integrated (Wnt)/B-catenin pathway by CHIR99021 stimulation, which generates Mesendoderm progenitor cells (MEPCs) (Lindsley et al., 2006). MEPCs (positive for Brachyury and FOXA2) are recognised as an antient biopotential germ layer of cells, as they gives rise to both endoderm (positive for FOXA2) and mesoderm linages (positive for Brachyury, SOX9) (Fig. 4.1) (Kimelman and Griffin, 2000; Rodaway and Patient, 2001; D'amour *et al.*, 2005; Yasunaga *et al.*, 2005; Takenaga *et al.*, 2007; Sumi *et al.*, 2008). Mesendoderm generation occurs in the primitive streak and is controlled by serval signalling pathways, including Nodal, Wnt and Fibroblast growth factor (FGF), with Nodal signalling being the most important influencer of the expression of Mesendoderm transcription factors (Kimelman & Griffin, 2000; Zorn & Wells, 2007). In Colombier *et al.,* (2020) the second step was to drive the differentiation of MEPCs to NC-like cells through synthetic mRNA coding notochordal transcription factor NOTO. However, from this method, a mixed cell population was produced, which included a small population of NC-like cells, but unfortunately many other off-target cell linages were also observed. Other studies that have developed strategies of differentiating iPSCs into NC-like cells have also observed low percentage yield of NC-like cell reported as: 14% (Zhang *et al.*, 2020), 25% (Tang *et al.*, 2018), 24% (J. Chen *et al.*, 2013) of cell population, demonstrating heterogeneous populations with current technologies (J. Chen *et al.*, 2013; Sheyn *et al.*, 2019), which would have limited potential for regulatory approval.

As these results highlighted difficulties in generating a large amount of purified iPSC-NC-like cells, an alternative would be to regress back to using progenitor cells, specifically the MEPCs, to determine whether MEPCs will differentiate further following seeding in biomaterial or *in vivo.* Therefore, not only will the inclusion of biomaterials provide a carrier system for cells, but additionally they may also facilitate differentiation, provide mechanical support and enable cell survival (Peroglio *et al.*, 2012; Thorpe *et al.*, 2016). To test the hypotheses that the seeding of iPSC-derived MEPCs (iPSC-MEPCs) into the novel biomaterials will augment differentiation into NC-like cells, a three-phase study was carried out; the first two phases involved, running a pilot investigation of iPSC-MEPCs survival after a short 5-day culture, then a prolonged 2-week culture. Both involved seeding iPSC-MEPCs into biomaterials that have been previously tested with porcine NC; Albugel, NPgel and NPgel/dNCM (Chapter 3). With the conclusion that the novel biomaterials Albugel, NPgel and NPgel/dNCM have the capacity to cultivate NC harvested from porcine origin and maintain their phenotype of expressing Cytokeratin 8, 18 and 19 and Brachyury in a 4-week culture period (Chapter 3). Additionally in this study, the last phase of the experiment utilising novel biomaterials that have been selected from two laboratories as the leading biomaterial for disc regeneration: a cross-linked

Polyethylene glycol (PEG) in combination with dNCM (PEG/dNCM), NPgel and alginate was also investigated as a potential 3D culture control. The use of PEG hydrogels in research has demonstrated biocompatibility and shown to promote tissue regeneration (Mellott *et al.,* 2001; Martin *et al.*, 2020). In this study PEG was combined with dNCM to generate a more highly crosslinked hydrogel in comparison to NPgel/dNCM, as the inclusion of dNCM into NPgel via physical entanglement failed to maintain the dNCM within the material for long term culture, with release into media seen via DMMB assay over the first 3 weeks of culture (Chapter 3). Alginate was included as a gold standard control in the phase-two study. Alginate has been utilised for cell encapsulation since the 1990s (Smidsrød and Skjåk-Bræk, 1990) and commonly used natural hydrogel for culturing cells in 3D (Andersen *et al.,* 2015). This study aimed to identify a biomaterial which could enable the survival and differentiation of seeded iPSC-MEPCs. In this study, iPSC-MEPCs were recovered and seeded into injectable biomaterials. The iPSC-MEPCs and biomaterial constructs were analysed for cell phenotype, morphology and the expression of extracellular matrix markers using histological and immunohistochemical staining. This study focused on the investigation whether MEPCs have the potential to demonstrate initial regenerative potential including retention of viability, and production of extracellular matrix.

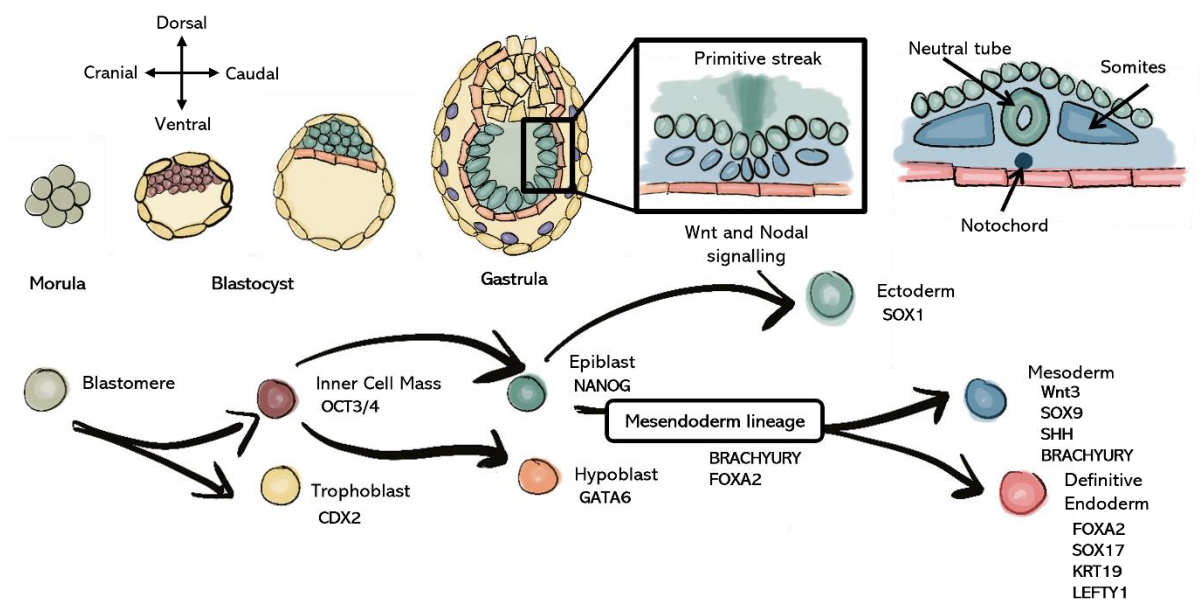

Figure 4.1. The origin of the Mesendoderm. *Illustration showing the stages of embryogenesis, displaying the progression the morula, comprising of a few totipotent blastomere cells, which then undergoes cavitation and compaction to transform into the blastocyst, consisting of an outer shell of trophoblasts and an inner collection of dense cells termed the inner cell mass (ICM). The outer trophoblast structures will eventually develop into the uterine lining and placenta that will provide nutrients to the embryo (Marikawa and Alarcon 2009; Zhange and HIIragi 2018). The ball of ICM spreads and differentiates into a bilayer of epiblast and hypoblast cells, creating a bilaminar disc (Niu et al., 2019). Decreased Oct4 and SOX2 signify the exit of pluripotency (kreuzer et al., 2020). The next developmental process is called gastrulation, and results in the important development of the three germ layers: Ectoderm, Mesoderm and Endoderm. Gastrulation is initiated with the formation of a primitive streak through TGFB, Wnt, Nodal and BMPs factors at the cranial end of the epiblast layer. Cells from specific regions of the epiblast are recruited and ingress into the primitive streak, during which, the migrating epiblast epithelial cells transition into mesenchymal cells. The cells integrate into the hypoblast layer to form the endoderm, fill the space in-between the endoderm and epiblast layer, forming the mesoderm. This is where the bipotential population of Mesendoderm (Brachyury, FOXA2) are created, which gives rise to through Nodal and Wnt signals to the definitive endoderm (SOX17, GATA6, FOXA2) and mesoderm (Brachyury, Nodal, SOX9, BMP4, FGF2, GATA4) (Kimelman and Griffin, 2000; Rodaway and Patient, 2001; Sumi et al. 2008; D'amour et al., 2005; Yasunaga et al., 2005; Takenaga et al., 2007)). The mesoderm derivatives have the potential to differentiate into chondrocytes (Umeda et al., 2012; Wu et al., 2013), cardiomyocytes (Kadari et al., 2015; Nguyen et al., 2014) or skeletal muscle cells (Kim et al., 2017; Mizuno et al., 2010); and the definitive endoderm derivatives can differentiate into hepatocytes, pancreatic cells, alveolar cells, thyroid, and the epithelial lining of the alimentary intestines and respiratory tract (Kubo et al., 2004; Lu et al., 2001; Wells & Melton, 2003). The remaining cells of the epiblast forms the Ectoderm (SOX1), it is known as the default pathway as neural linages develop without the need of the BMP, Wnt or Nodal signalling form the primitive streak (Kubo et al., 2004; Thompson 2011).*

METHODS

EXPERIMENTAL DESIGN

iPSC lines included in this study were derived from 3 iPSC lines: iPSC cell lines produced in Nantes (MiPs; University of Nantes, France), peripheral blood mononuclear cells (PBMC) taken from a patient undergoing disc trauma surgery (University of Bern) which are Sendai-viral reprogramed with four factors: OCT4, SOX2, KLF4 and c-MYC by INSERM (INSERM, France) (collectively referred to as OSKM) generating a patient derived cell line (Takahashi and Yamanaka, 2006; Takahashi *et al.*, 2007; Fusaki *et al.*, 2009) and a commercially available iPSC cell line from Thermofisher (TF). Differentiation was then implemented to generate Mesendoderm progenitor cells (MEPCs) through the activation of the Wnt/B-catenin pathway by CHIR99021 stimulation (Lindsley et al., 2006) at the University of Nantes. Which involved culturing the iPSC for 48 hours with mTeSR™ Plus Medium (supplemented with 10µM ROCK inhibitor Y-27632 for the first 24 hours) (Fig. 4.2; Step 1) and at day 3 the media was changed to N2B27 media (Table 4.1) supplemented with CHIR99021 (3µM; 130-106-539, Miltenyi, Surrey, UK) for an additional 48 hours (Fig. 4.2; Step 2).

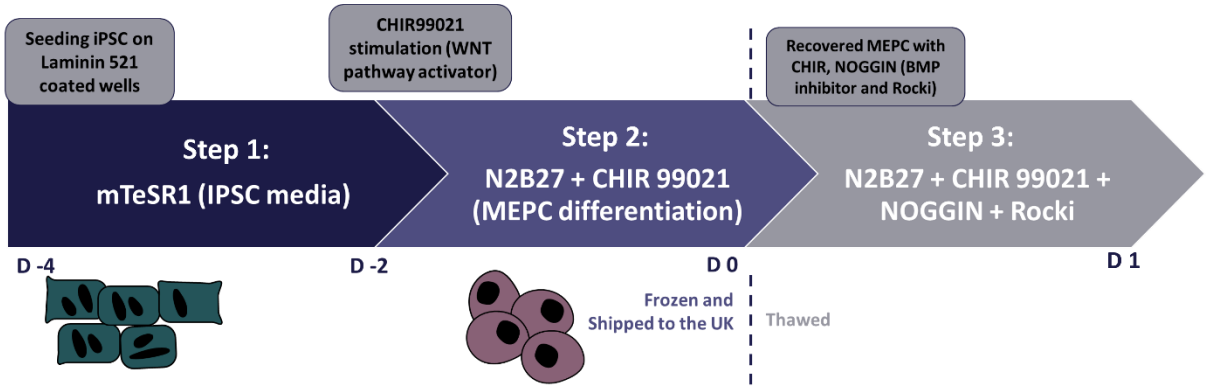

***Figure 4.2. Illustration displaying the method used to differentiate iPSC into MEPCs**: involving culturing iPSC for 48 hours with mTeSR™ Plus Medium supplemented with 10µM ROCKi on Laminin-521 wells, and at day 3 (D-2) change the media to N2B27 media supplemented with CHIR99021 (3µM; Miltenyi, Surrey, UK) for an additional 48 hours. Theses MEPCs were then cryopreserved and shipped to then be recovered for 24 hours with N2B27 media supplemented with CHIR99021, Noggin and ROCKi at 21% v/v oxygen, 37^{o}C.*

Following the generation of MEPCs, cells were cryopreserved at 2 million cells per cryovial and shipped to our laboratory on dry ice and used to study their behaviour within novel biomaterials to investigate the potential induction of differentiation towards NC-like cells. Several biomaterials were selected for this investigation, which divided the study in three phases: Phase I involved seeding MiPs derived iPSC-MEPCs into established and cytocompatible biomaterial Albugel (n=3) and NPgel (n=3) for 5 days. Phase II involved seeding TF derived iPSC-MEPCs also into Albugel (n=3), NPgel (n=3) and NPgel/dNCM (n=3) for 2 weeks. Phase III involved seeding PBMC derived iPSC-MEPCs into alginate (n=3), PEG/dNCM (n=3) and NPgel (n=3) for 1-week, 2-week, and 4-week. All culture conditions mimicked IVD conditions in relation to physioxia. Following culture, viability was assessed using

Calcein/Hoechst staining. Morphology was investigated using and histology, phenotype and matrix production was assessed using immunohistochemistry and histological staining (Fig. 4.3).

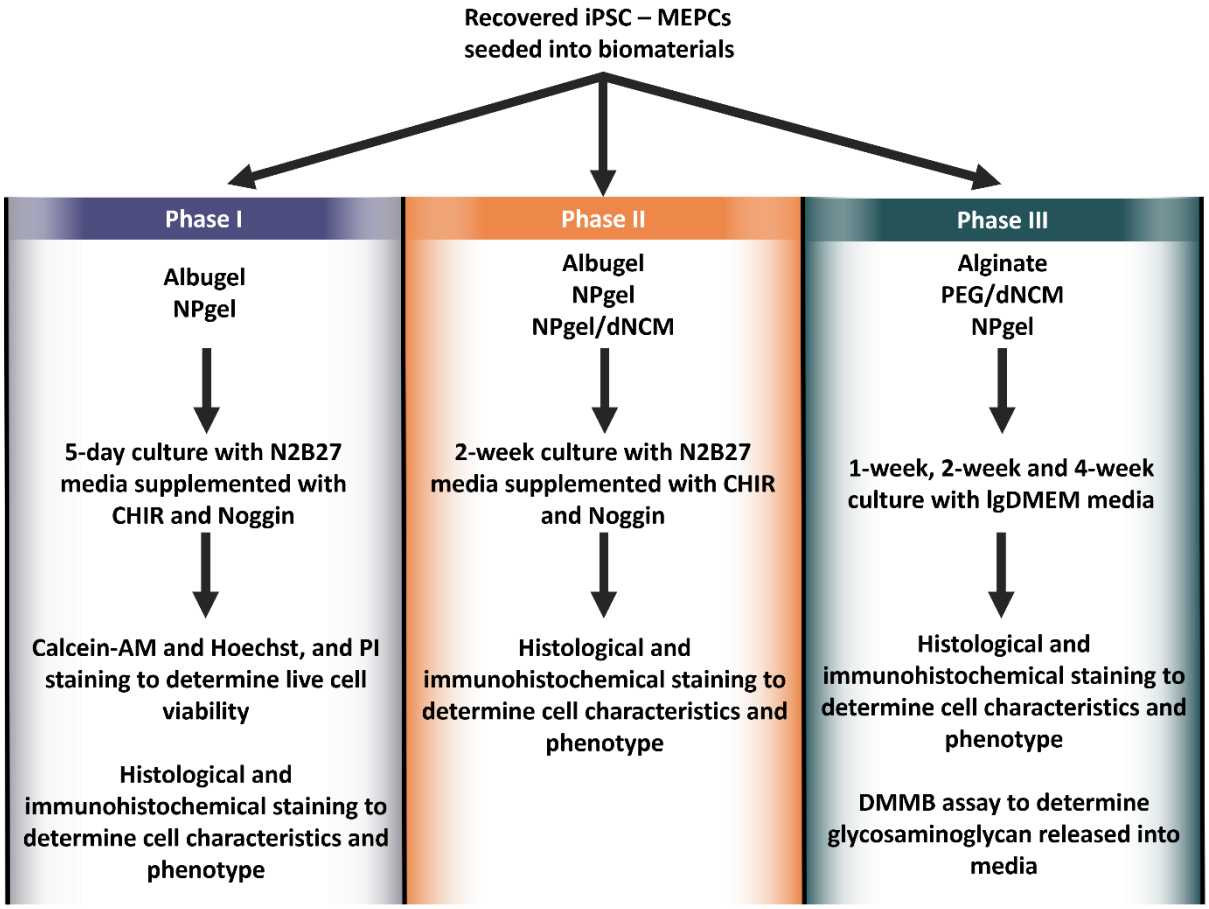

Figure 4.3. Illustration representing the experimental design. *Following the recovery, induced pluripotent stem cell derived mesendoderm progenitor cells (iPSC-MEPCs) were seeded into biomaterials. The study was split into three phases: Phase I, which involved seeding iPSC-MEPCs into Albugel and NPgel biomaterials, and culturing for 5 days with N2B27 media supplemented with CHIR99021 (3µM), Noggin (100ng/mL) at 5% v/v oxygen, 37°C. Phase II, which involved seeding iPSC-MEPCs into Albugel, NPgel and NPgel biomaterials, and culturing for 2 weeks with N2B27 media supplemented with CHIR99021 (3µM), Noggin (100ng/mL) at 5% v/v oxygen, 37°C. Phase III, which involved seeding iPSC-MEPCs into alginate, PEG/dNCM and NPgel biomaterials, and culturing for 1, 2 and 4 weeks with lgDMEM (DMEM, low glucose, glutaMAX™ (life technologies, Paisley, UK) containing P/S 50U/mL (Life Technologies UK), amphotericin B 2.5ug/mL (Sigma, Dorset, UK), L-ascorbic acid 25ug/mL (Sigma, Dorset, UK), 1% Insulin-transferrin-Selenium v/v (ITS-X), 1% L-glutamine v/v (life technologies, UK), L-proline 40ug/mL (Life technologies, UK) and Albumax 1.25mg/mL (Life technologies, UK)) at 5% v/v oxygen, 37°C. Each phase shows the downstream analysis and staining that was performed on the MEPCs and biomaterial constructs.*

THAWING MESENDODERM PROGENITOR CELLS

A cryo-vial of 2 million iPSC-MEPCs was thawed rapidly using a sterile 37°C water bath and gently resuspended in 1mL of N2B27 media (Table 4.1) with supplements of CHIR99021 (3µM; 130-106-539, Miltenyi, Surrey, UK) and Noggin (100ng/mL; 130-103-455, Miltenyi, Surrey, UK),

so that a single piece of ice remains, before transferring to a 15mL falcon tube containing 10mL of N2B27 media with supplements CHIR99021 (3µM) and Noggin (100ng/mL). The iPSC-MEPCs suspension was then centrifuged at 200*g* for 5 minutes at room temperature and resuspended in N2B27 media supplemented with CHIR99021 (3µM), Noggin (100ng/mL) and ROCK inhibitor Y-27632 (10µM; 72307, StemCell technologies, Cambridge, UK). IPSC-MEPCs were plated at $6.87x10^4$cells/cm^2 into 6 well plates (353046, Corning, Flintshire, UK) precoated with 5µg/mL Laminin-521 (354223, Corning, Flintshire, UK) in PBS Ca^{2+} / Mg^{2+} (D8662, Sigma, Dorset, UK). Plates were gently swirled prior to placing into the incubator to ensure an even distribution of cells and placed into a 21% v/v O_2, with 5% v/v CO_2 at 37^{o}C incubator.

Table 4.1. Composition of N2B27 media, used for Mesendoderm progenitor cells thawing and culture*. Stating what reagents are used, at what working concentration, with an example of volume of reagents needed to produce 500mL of N2B27 media.*

'N2 B27' Media	Final concentration	QSP 500mL of N2B27 media
DMEM F-12 High Glucose (1133057, Life technologies, Paisley, UK)	-	480mL
MEM non-essential amino acid (11140050, Life technologies, Paisley, UK)	1% v/v	5mL
Glutamax (35050061, Life technologies, Paisley, UK)	1% v/v	5mL
Beta-mercaptoethanol (31350010, Life technologies, Paisley, UK)	0.16% v/v	800µL
N2 Supplement (17502048, Life technologies, Paisley, UK)	0.5% v/v	2.5mL
B27 Supplement (17504044, Life technologies, Paisley, UK)	1% v/v	5mL
Bovine Albumin (A1595, Sigma, Dorset, UK)	0.05% w/v	250µL

MESENDODERM PROGENITOR CELL DISSOCIATION AND CELL COUNT

Twenty-four hours after thawing, iPSC-MEPCs were visualised using Olympus IX81 motorized inverted system microscope (Olympus Europa GMBH, Germany) to investigate cellular morphology (Fig. 4.4). The media was aspirated and washed twice with PBS w/o Ca^{2+} / Mg^{2+}, prior to detaching cells with TrypLE (12605010, Life technologies, Paisley, UK) at 21% v/v O_2, with 5% v/v CO_2 at 37^{o}C for 3 minutes. Knockout Serum (KSR) media (Table 4.3) was added to inhibit the action of TrypLE, and suspended iPSC-MEPCs were transferred to a 15mL falcon tube prior to centrifugation at 200*g* for 5 minutes. A cell count was performed with a sample of iPSC-MEPCs suspension using a NucleoCounter® NC-200™ (910-0002, Chemometec, Allerod, DK) as previously described in Chapter 2 (Calculating cell number).

Table 4.2. Composition of Knockout serum (KSR) media, *used during Mesendoderm progenitor cells dissociation and inhibiting TrypLE reaction. Stating what reagents are used, at what working concentration, with an example of volume of reagents needed to produce 500mL of KSR media.*

'KSR' Media	Final concentration	QSP 500mL of KSR media
DMEM F-12 High Glucose (1133057, Life technologies, Paisley, UK)	-	489mL
Knockout Serum (10828010, Life technologies, Paisley, UK)	2% v/v	100mL
MEM non-essential amino acid (11140, Life technologies, Paisley, UK)	1% v/v	5mL
Glutamax (35050, Life technologies, Paisley, UK)	1% v/v	5mL
Beta-mercaptoethanol (31350, Life technologies, Paisley, UK)	0.16% v/v	800µL

CELL LABELLING WITH PKH26

PKH26 Red Fluorescent cell membrane labelling kit (PKH26GL, Sigma, Dorset, UK) was performed on $4.5x10^5$ cells/mL of iPSC-MEPCs to check viability and count post recovery and post staining with red cell dye tracker PKH26. The labelling of iPSC-MEPCs with PKH26 was performed as per the manufacturer's instructions. In brief, cells were placed into a 1.5mL Eppendorf and washed with PBS w/o Ca^{2+} / Mg^{2+}, and centrifugation at 200*g* for 5 minutes. Prior to staining dye solution was prepared to generate $4x10^{-6}$M (4µL of PKH26 to 1mL Diluent C). The supernatant was removed and 1mL of diluent C added, mixed by gentle pipetting. Next, centrifuged for 200*g* 5 minutes, supernatant removed, and dye solution added for 2-minute incubation at room temperature. Cells were again pelleted via centrifugation at 200*g* for 5 minutes and washed twice with PBS w/o Ca^{2+} / Mg^{2+}. Cell count and viability was assessed using the NucleoCounter® NC-200™ as previously described in Chapter 2 (Calculating cell number).

PHASE I AND PHASE II BIOMATERIAL PREPARATION

Albugel, NPgel/dNCM and NPgel were generated as previously described in Chapter 3 (Albugel preparation; NPgel preparation; NPgel with dNCM preparation).

SEEDING MESENDODERM PROGENITOR CELLS INTO PHASE I AND II BIOMATERIALS

For seeding, suspended iPSC-MEPCs were centrifuged at 200*g* for 5 minutes, the supernatant was removed, and the iPSC-MEPCs pellet was resuspended in 10% v/v extraction media, prior to seeding into biomaterials. IPSC-MEPCs were seeded at cell density of $4x10^6$ cells/mL into the injectable biomaterials, and 300µL constructs created extruding the biomaterial/ iPSC-MEPC suspension through a 27-gauge needle to mimic injection into the disc into a 48 well culture then left to set at 5% v/v O_2, with 5% v/v CO_2 at 37°C for ~5 minutes. Triplicate technical

repeats of iPSC-MEPCs were seeded into Albugel and NPgel for 5 days and triplicate technical repeats of iPSC-MEPCs were seeded into Albugel, NPgel and NPgel/dNCM for 2 weeks. Five hundred microlitres of N2B27 media supplemented with CHIR99021 (3µM), Noggin (100ng/mL) was added per well. Outer wells were left void of constructs but hydrated with phosphate buffered saline (PBS; Gibco, UK). Triplicate technical repeats were cultured in a physiological disc environment of 5% v/v O_2, with 5% v/v CO_2 at 37°C using a hypoxia glove box (Coy Laboratory Products, USA). Complete N2B27 media was replaced three times a week during the culture period.

PHASE III BIOMATERIAL PREPARATION

Alginate was prepared as described in Basatvat et al., (2023), in brief cells expanded in monolayer (see below) cultured at 21% v/v O_2, with 5% v/v CO_2 at 37^{o}C were resuspended in sterile-filtered 1.2% w/v medium viscosity alginic acid (A2033, Sigma-Aldrich) in 0.15M NaCl and filter sterilised through 0.22µm syringe filter.

PEG/dNCM contains 2-(N-morpholino) ethanesulfonic acid (MES) buffer at pH 7.2 by crosslinking 8-arm PEG-amine (JenKem technology, Plano, TX, USA) with dNCM via covalent bonds between carboxylic groups found in dNCM's sGAGs and the PEG's terminal amine groups using 4-(4,6-dimethoxy-1,3,5-triazin-2-yl)-4-methyl-morpholinium chloride (DMTMM). For preparation of the PEG/dNCM, prior to combining, the components (dNCM, DMTMM and PEG) were sterilized under UV light for 10-15 minutes and stored on ice for the mixing process. To combine, first 0.1M MES buffer was added to 21mg/mL PEG; next, 0.1M MES buffer was added to 15mg/mL DMTMM. The generated DMTMM solution was then combined with 15mg/mL dNCM with a vortex and combined the PEG solution to the newly mixed DMTMM/dNCM with a vortex to produce PEG/dNCM. Cells were then seeded at this stage as described below.

SEEDING MESENDODERM PROGENITOR CELLS INTO PHASE III BIOMATERIALS

For seeding, suspended iPSC-MEPCs were centrifuged at 200*g* for 5 minutes, the supernatant was removed, and the iPSC-MEPCs pellet was resuspended in 10% v/v extraction media, prior to seeding into biomaterials. IPSC-MEPCs were seeded at cell density of $4x10^6$ cells/mL into the injectable biomaterials: alginate, PEG/dNCM and NPgel to create 50µL constructs, the iPSC-MEPC and biomaterial constructs were extruded through a 27 gauge needle to mimic injection into the disc into a 96 round bottom well plate, then left to set at 5% v/v O_2, with 5% v/v CO_2 at 37^{o}C, 30 minutes for PEG/dNCM and ~5 minutes for NPgel, whilst alginate constructs were carefully overlayed with 0.2M $CaCl_2$ and polymerised for 10 minutes at 37^{o}C, $CaCl_2$ was removed and constructs washed twice in 0.15M NaCl, and twice in lgDMEM Smaller constructs were created to ensure three technical repeats of each biomaterial: iPSC-MEPC cultured in alginate, PEG/dNCM and NPgel could be prepared at three different time points: 1-week, 2-week and 4-week were created with the limited iPSC-MEPCs that were attainable due to decreased cell availability. For the Phase III, iPSC-MEPC cultured in alginate, PEG/dNCM

and NPgel constructs 200µL of lgDMEM media (DMEM, low glucose, glutaMAX™ (life technologies, Paisley, UK) containing P/S 50U/mL (Life Technologies UK), amphotericin B 2.5ug/mL (Sigma, Dorset, UK), L-ascorbic acid 25ug/mL (Sigma, Dorset, UK), 1% Insulin-transferrin-Selenium v/v (ITS-X), 1% L-glutamine v/v (life technologies, UK), L-proline 40ug/mL (Life technologies, UK) and Albumax 1.25mg/mL (Life technologies, UK)) as described previously as culture media for 3D disc cells (Basatvat *et al.*, 2023) adjusted to 400mOsm/kg using N-Methyl-D-glutamine HCL 37.5mM (NaCl homologue; Santa Cruz Biotechnology, Germany), to mimic more closely the disc environment and previously demonstrated to maintain NC phenotype more effectively (Laagland *et al.*, 2022). Outer wells were left void of constructs but hydrated with phosphate buffered saline (PBS; Gibco, UK). IPSC-MEPCs cultured in alginate, PEG/dNCM and NPgel were cultured in a physiological disc environment of 5% v/v O_2, with 5% v/v CO_2 at 37°C using a hypoxia glove box (Coy Laboratory Products, USA). Complete media was replaced three times a week during the culture period.

LIVE CELL VIABILITY STAINING WITH CALCEIN-AM AND PROPIDIUM IODIDE

To assess initial cell viability of iPSC-MEPCs & Albugel after culturing for 5 days and iPSC-MEPC cultured in Albugel, NPgel and NPgel/dNCM after culturing for 24 hours at 5% v/v O_2, with 5% v/v CO_2 at 37^{o}C. Constructs following culture were firstly washed in PBS w/o Ca^{2+} / Mg^{2+}, next, constructs were stained with 2µM Calcein-AM (Invitrogen™, UK; C1430) and 10mg/mL Propidium Iodide (PI; P4864, Sigma, Dorset, UK) diluted in N2B27 media and incubated at 5% v/v O_2, with 5% v/v CO_2 at 37^{o}C for 30 minutes. For iPSC-MEPC cultured in Albugel for 5-days, the constructs were washed three times with PBS w/o Ca^{2+} / Mg^{2+}, and N2B27 media was re-added. For the 24-hour culture of iPSC-MEPCs cultured in alginate, Albugel, NPgel and NPgel/dNCM, A small piece of the construct was taken and constrained between a microscope slide and coverslip and visualised on an Olympus BX60 Microscope using fluorescein isothiocyanate (FITC) and Texas red filter for visualising Calcein-AM and Propidium Iodide (PI) stains, respectively.

LIVE CELL VIABILITY STAINING WITH CALCEIN-AM AND HOECHST

To assess PKH26 labelled iPSC-MEPC viability seeded into alginate, Albugel, NPgel and NPgel/dNCM after culturing for 24 hours. IPSC-MEPCs were labelled with red cell dye tracker PKH26 as described above and seeded into biomaterials for 24 hours at 5% v/v O_2, with 5% v/v CO_2 at 37^{o}C. The constructs were then stained with Calcein-AM and Hoechst 33342 to assess viability. Non- labelled iPSC-MEPCs & Albugel and NPgel cultured for 5 days at 5% v/v O_2, with 5% v/v CO_2 at 37^{o}C, were assessed for viability within the constructs using Calcein-AM and Hoechst staining. For live cell viability staining with Calcein and Hoechst, constructs were firstly washed in PBS w/o Ca^{2+} / Mg^{2+}, next, constructs were stained with 2µM Calcein-AM (Invitrogen™, UK; C1430) for 30 minutes at 5% v/v O_2, with 5% v/v CO_2 at 37°C, washed three times with PBS w/o Ca^{2+} / Mg^{2+}, followed by 5pg/mL of Hoechst 33342 (H1399; Invitrogen™, UK) for 15 minutes at 37°C. After staining culture media was re-applied, and a small piece of the construct was taken and constrained between a microscope slide and

coverslip and visualised on an Olympus BX60 Microscope using fluorescein isothiocyanate (FITC) and 4',6-Diamidino-2-Phenylindole (DAPI) filter for visualising Calcein-AM and Hoechst stains, respectively.

HISTOLOGY ANALYSIS

MEPC phenotype and matrix deposition was investigated in acellular controls and cellular constructs following Phase I: 24 hours and 5 days in preliminary testing, Phase II: 2-week and Phase III: 1-week, 2-week, and 4-weeks in culture. IPSC-MEPC cultured in Albugel, NPgel (Phase I and II) and NPgel/dNCM (Phase II) of 300µL constructs were removed from culture and fixed in 10% w/v neutral buffered formalin for 20 minutes. With the smaller 50µL constructs, iPSC-MEPC cultured in alginate, PEG/dNCM and NPgel (Phase III), were fixed with 5% v/w formalin 200mM $CaCl_2$ for 1 hour prior to embedding the constructs in 2% v/v agarose in dH_2O. All constructs were then processed to wax overnight using the TP1020 tissue processor (Leica Microsystems, Newcastle, UK). Following fixing and embedding, 6µm sections were cut and mounted to X-tra® adhesive positively charged slides (Leica Microsystems, Newcastle, UK). For paraffin wax embedded samples, sections were dewaxed in Sub X (Leica Microsystems, Newcastle, UK) three times for 7 minutes and rehydrated in industrial methylated spirit (IMS; Fisher, Loughborough, UK) for three times for 7 minutes and running tap water for 5 minutes prior to histological staining. Sections were assessed using histological stains. H&E; Alcian Blue (pH 2.5); Masson's Trichrome (Atom Scientific Ltd, Hyde, UK); Safranin O/ Fast green; as described in Chapter 3 (Histological Analysis). All slides were examined with an Olympus BX51 microscope and images captured by digital camera and Capture Pro OEM v8.0 software (Media Cybernetics, UK). Histological sections were analysed, and representative images captured to document their histological appearance and cellular staining patterns.

IMMUNOHISTOCHEMISTRY ANALYSIS

Immunohistochemistry (IHC) was performed on iPSC-MEPCs cultured in biomaterials using methodology described previously in Chapter 3 (Immunohistochemistry and immunofluorescence analysis) and previously reported in Binch *et al.,* (2020). Specific antibodies were used to target antigens in relation to iPSC, MEPC, NC and NP phenotype along with NP matrix markers (Table 4.3). Primary antibody diluted in Dulbecco's Phosphate Buffered Saline (DPBS) w/o Ca^{2+} / Mg^{2+} (Lonza, Manchester, UK) with 5% w/v BSA (Sigma, Dorset, UK) was applied according to Table 4.3 alongside equivalent concentration IgG controls.

Table 4.3. Immunohistochemical and immunofluorescence procedures utilised for phenotypic characterisation of notochordal cells. *Primary antibody target, clonality, dilutions optimised and antigen retrieval. Including the secondary antibodies and dilutions, which were used for immunohistochemical and immunofluorescence staining.*

Primary Antibody	Target	Clonality	Optimal dilution	Antigen retrieval	Technique	Secondary Antibody	Optimal dilution
Aggrecan (AB3778, Abcam)	NP matrix	Mouse monoclonal	1:100	Heat	IHC	Rabbit Anti-Mouse (Ab6727, Abcam)	1:500
Brachyury (AF2085, Bio-techne)	NC/NP marker	Goat polyclonal	1:500	None	IHC	Donkey Anti-Goat (Ab208000, Abcam)	1:500
					IF	Donkey Anti-Goat (Alex Flour™ 488; A-11055, Life technologies)	1:500
Caspase 3 (AB4051, Abcam)	Apoptosis Marker	Rabbit polyclonal	1:400	None	IHC	Goat Anti-Rabbit (Ab6720, Abcam)	1:500
					IF	Donkey Anti-Rabbit (Alex Flour™ 594; A-21207, Life technologies	1:500
Collagen Type II (MAB1330, Sigma)	NP matrix	Mouse monoclonal	1:200	Enzyme	IHC	Rabbit Anti-Mouse (Ab6727, Abcam)	1:500
Cytokeratin 8, 18 & 19 (AB41825, Abcam)	NC/NP marker	Mouse monoclonal	1:400	Enzyme	IHC	Rabbit Anti-Mouse (Ab6727, Abcam)	1:500
					IF	Goat anti-mouse (Alex Flour™ 488, ab150113, Abcam)	1:500
FOXA2 (D56D6, Cell signalling)	NLC marker	Rabbit monoclonal	1:400	Heat	IHC	Goat Anti-Rabbit (Ab6720, Abcam)	1:500
Ki67 (ab15580,	Proliferation Marker	Rabbit polyclonal	1:250	Enzyme	IHC	Goat Anti-Rabbit (Ab6720, Abcam)	1:500
SOX9 (AB5535, Abcam)	NLC and NP marker	Rabbit polyclonal	1:1000	None	IHC	Goat Anti-Rabbit (Ab6720, Abcam)	1:500

IMMUNOFLUORESCENCE ANALYSIS

For immunofluorescence (IF) samples embedded in paraffin wax were dewaxed in Sub X for 7 minutes three times and rehydrated in IMS for 7 minutes three times. Following washes in TBS, sections were subjected to antigen retrieval methods as detailed in Table 4.3. Following antigen retrieval methods, sections were washed in TBS and blocked for 2 hours with normal serum derived from the animal in which the secondary antibody was raised; 5% w/v BSA (Sigma, Dorset, UK) in 75% TBS and 25% v/v normal serum. Primary antibody was applied overnight at 4^{o}C according to Table 4.3. On the second day, the sections were washed in TBS followed by fluorescent secondary antibody for 30 minutes. On samples with Phalloidin staining, 0.01% v/v Phalloidin-iFluor 594 (ab176757, Abcam, Cambridge, UK) diluted in 1mL DPBS w/o Ca^{2+} / Mg^{2+} (Lonza, Manchester, UK) with 1% BSA (Sigma, Dorset, UK) was added. To determine nuclear localisation sections were counterstained with DAPI using Vectashield® DAPI mountant (Sigma, Dorset, UK).

QUANTIFYING HISTOLOGICAL AND IMMUNOHISTOCHEMICAL STAINED SLIDES

Histological and immunohistochemical stained slides were digitally scanned using a Panoramic 250 Flash III (3DHistech, Budapest, HU) and quantified using QuPath v0.3.2 (Github). For cell counting within a tissue area, the region of tissue was measured through tissue detection by visual thresholding, to ensure the whole area of tissue was selected and cells were manually counted in the software. For quantification of immunopositive cells over a whole slide, positive cell detection was implemented to attain a set a visual threshold for each stain and biomaterial, and the generated script was run for the remaining repeats to generate percentage immunopositive cells (Bankhead *et al.*, 2017).

DIMETHYLMETHYLENE BLUE ASSAY

Media samples were collected after 24 hours in culture of the iPSC-MEPCs in biomaterial constructs and stored at -80^{o}C. Dimethyl methylene Blue (DMMB) reagent was generated and preformed as previously described in Chapter 3 (Dimethylmethylene Blue Assay).

STATISTICAL ANALYSIS

Statistics were performed in Graphpad prism 9.5.1. The normality of the data was assessed using the Shapiro-Wilk test. For the analysis of iPSC-MEPCs recovery after thawing, the data was found to be normally distributed, and therefore a t-test was performed comparing the post thawing and post laminin-521 cell count of the iPSC-MEPCs groups. In the Phase II tests, the iPSC-MEPC count in biomaterials Albugel, NPgel and NPgel/dNCM was not normally distributed therefore analysed with Kruskal-Wallis test, followed by Dunn's multiple comparisons test between the median values of biomaterial groups. Comparing the percentage of immunopositive iPSC-MEPC cultured in Albugel, NPgel and NPgel/dNCM and stained for FOXA2, Brachyury and SOX9, Kruskal-Wallis test was performed, followed by Dunn's multiple comparisons for each biomaterial group. In the Phase III tests; the iPSC-MEPC count in biomaterials alginate, PEG/dNCM and NPgel was normally distributed and therefore a one-way ANOVA was performed, followed by Tukey's multiple comparisons test. The percentage of fragmented nuclear cells in the two biomaterials PEG/dNCM and NPgel was performed by with a Mann-Whitney test for each time point. For the percentage of immunopositive iPSC- MEPCs for each antibody, an Man-Whitney test was performed for each time point of the two biomaterial groups PEG/dNCM and NPgel, as no data was collected for the alginate group. The glycosaminoglycan production of iPSC-MEPC seeded in alginate, PEG/dNCM and NPgel and media taken throughout the 4-week cultured was reported using DMMB analysis was assessed as being normally distributed therefore the difference of GAG production over the 4-week period was analysed with one-way ANOVA test followed by the recommended Turkey's multiple comparisons test. Statistical significance was accepted at $p \leq 0.05$.

RESULTS

ANALYSIS OF MESENDODERM PROGENITOR CELLS RECOVERY

The collaborators cryopreserved $2x10^6$ cells per vial of iPSC-MEPCs derived from MiPs-iPSC, PBMC-iPSC and TF-iPSC following differentiation to MEPCs. Analysing the recovery rate of iPSC-MEPCs after thawing and after seeding onto laminin-521 for 24 hours, showed good viability, with >75% viability post thawing and post laminin-521 culture (Fig. 4.4a). Live cell images following 24-hour culture on laminin-521 displayed appropriate morphology of MEPCs, with the appearance of adherent spindle shaped IPSC-MEPCs and suspended cells (Fig. 4.4a). The brightfield images also demonstrated IPSC-MEPCs confluency of around 60% in MiPs-iPSC-MEPCs, 50% PBMC-iPSC-MEPCs and 40% in the TF-iPSC-MEPCs. With a high population of IPSC-MEPCs that remained free floating and failed to attach after the 24-hour period of culture on laminin-521. There was a significant decline in cell count of IPSC-MEPC derived from PBMC-iPSC ($p \leq 0.01$) and TF-iPSC ($p \leq 0.01$) between first thawing to after 24 hours cultured on laminin-521 (Fig. 4.4b). Overall, from the initial 2 million cells that were cryopreserved and thawed, an average of 1.41×10^6 of MiPs-iPSC-MEPCs, 6.60×10^5 of PBMC-iPSC-MEPCs and 6.48×10^5 of TF-iPSC-MEPCs were recovered in total (Fig. 4.4), corresponding with image confluency.

Following recovery samples were taken to assess the MEPC phenotype. IPSC-MEPCs derived from iPSCs-PBMC were dual stained with Caspase 3 / Cytokeratin 8, 18 and 19, and dual stained with Phalloidin / Brachyury (Fig. 4.5). The iPSC-MEPC displayed staining of Brachyury, and cytokeratin 8, 18 and 19. Some iPSC-MEPCs had appearance of fragmented nuclei, which was associated with positive staining for caspase 3 and negative for Brachyury (Fig. 4.5).

A

Cells	Ship date	Thaw date	Post thawing viability	Post thawing cell count	Post 24hr laminin viability	Post 24hr laminin cell count	Brightfield representative image
MEPC (MiPs-iPSC) 2021.03.12	06/07/2021	28/07/2021	84%	$1.64x10^6$	83%	$1.19x10^6$	
MEPC (MiPs-iPSC) 2021.03.12	22/06/2021	19/07/2021	76%	$1.05x10^6$	86%	$1.75x10^6$	
MEPC (PBMC-iPSC) 2021.03.23	06/07/2021	17/05/2022	86%	$1.74x10^6$	77%	$1.02x10^6$	
MEPC (PBMC-iPSC) 2021.03.23	06/07/2021	02/12/2021	84%	$1.32x10^6$	86%	$3.82x10^5$	
MEPC (TF-iPSC) 2021.04.02	06/07/2021	25/11/2021	87%	$1.79x10^6$	77%	$8.52x10^5$	
MEPC (TF-iPSC) 2021.04.02	06/07/2021	02/12/2021	86%	$2.08x10^6$	76%	$4.43x10^5$	

B

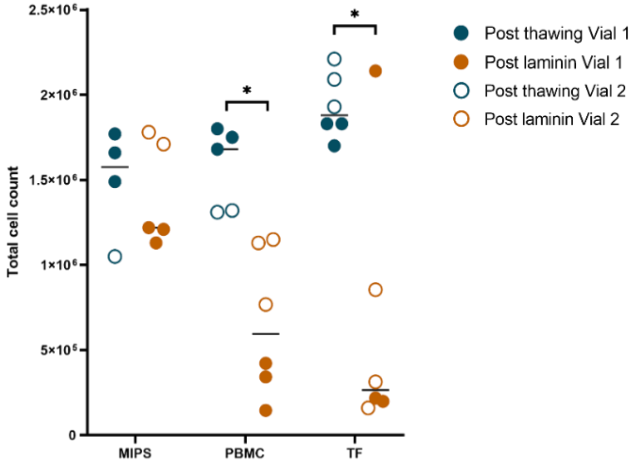

Figure 4.4. Recovery of Mesendoderm Progenitor Cell derived from either induced Pluripotent Stem Cells (iPSCs) MiPS, peripheral blood mononuclear cells (PBMC) or Thermofisher (TF) cell line. (A) *Table showing shipment batch, date MEPCs were thawed, the viability cell count post thawing and post 24-hours on culture on laminin-521, with brightfield images captured after 24-hours on laminin-521. Scale bar 200µm.* ***(B)*** *Graph, demonstrating the cell count recovery of MEPCs between derived groups. (n=2 technical repeats). Statistics performed with in GraphPad prism v9.5.1, t-test *p≤0.05.*

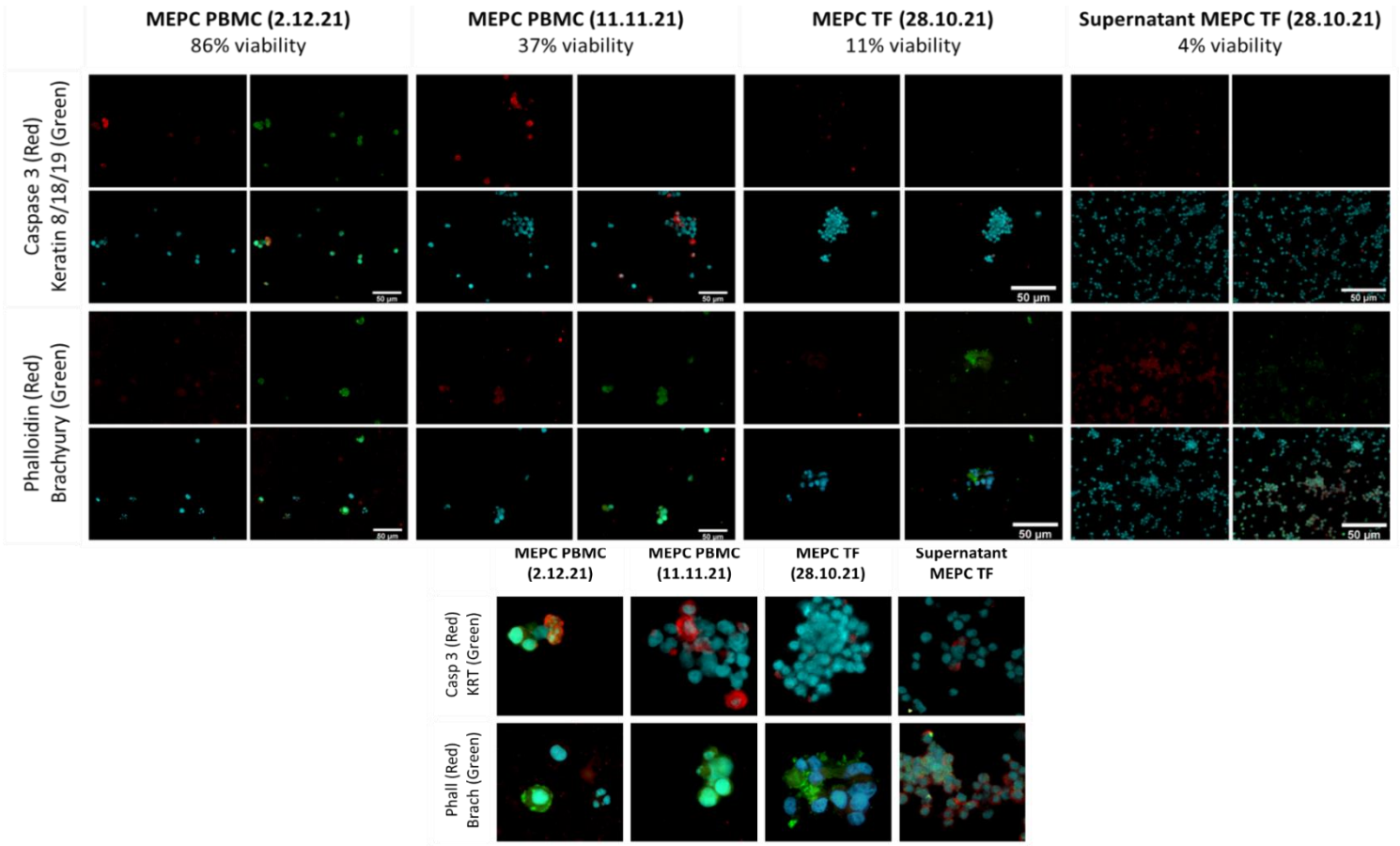

***Figure 4.5*. Mesendoderm progenitor cells (MEPCs) viability and phenotype after recovery from thawing.** *Immunofluorescence images of MEPCs derived from induced pluripotent stem cells (iPSCs) derived from peripheral blood mononuclear cells (PBMC) and Thermofisher (TF) cell line were analysed for phenotype after recovering post thawing and replating on laminin-521 for 24 hours (n=3 technical repeats). The MEPC groups were obtained from different vials representing differing viability, the supernatant was taken from the suspension which contained MEPCS that didn't adhere after the recovery process. MEPCs were dual stained with Caspase 3 (Casp 3; 594; red) and cytokeratin 8,18,19 (Kertain/KRT; 488; green) and the other dual stain of Phalloidin (Phall; 594; red) and Brachyury (Brach; 488; green).*

MESENDODERM PROGENTITOR CELL SEEDING DENISTY AND SURVIVAL IN BIOMATERIALS

A pilot study was implemented using recovered iPSC-MEPCs seeded into biomaterials to assess iPSC-MEPCs overall survival in 3D culture. Firstly, labelling and tracking iPSC-MEPCs during 3D culture was investigated with the use of cell dye PKH26 on the iPSC-MEPCs prior to seeding into biomaterials. Viability and cell count were investigated for iPSC-MEPCs before and after PKH26 labelling; the results showed the usual decline in viability after iPSC-MEPC recovery after thawing, however the cell count showed a further reduction in viable cells after iPSC-MEPCs were stained with PKH26 (Fig. 4.6). The fluorescence images also demonstrate limited viable iPSC-MEPCs in all biomaterials (Fig. 4.7). As the PKH26 may have affect iPSC-MEPC viability, no cell tracker was used in future studies.

	MEPC cells recovered			MEPC Post red dye		
NucleoCounter® image of All cells (green) Dead cells (blue)				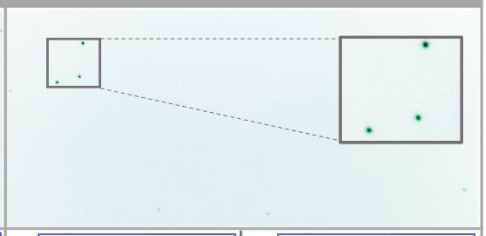		
NucleoCounter® report of All cells (AO) Dead cells (DAPI)	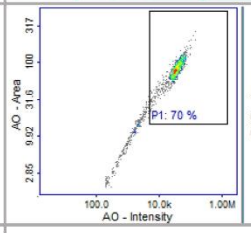	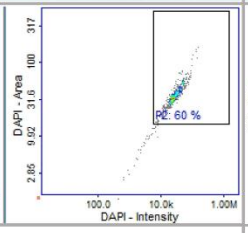		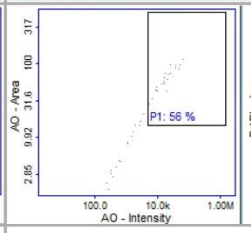	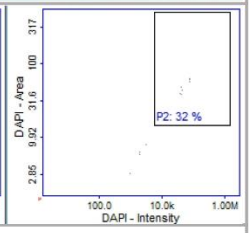	
Viability	44%	40%	40%	62%	86%	68%
Live cells (cells/mL)	$1.81x10^5$	$1.89x10^5$	$1.93x10^5$	$5.53x10^3$	$2.03x10^4$	$1.02x10^4$
Dead cells (cells/mL)	$2.32x10^5$	$2.83x10^5$	$2.9x10^5$	$3.46x10^3$	$3.39x10^3$	$4.74x10^3$
Total cells (cells/mL)	$4.13x10^5$	$4.72x10^5$	$4.83x10^5$	$8.99x10^3$	$2.37x10^4$	$1.49x10^4$

Figure 4.6. Mesendoderm Progenitor Cells (MEPCs) origin MiPs viability and count post recovery (MEPC cells recovered) and post staining with red cell dye PKH26 (MEPC Post red dye). *Using NucleoCounter® for triplicate technical repeated count analysing viability, live cell count, dead cell count (DAPI positive) and total cell count (AO positive), prior to seeded into alginate, Albugel, NPgel and NPgel/dNCM for 24 hours (n=3 technical repeats). Black box indicated zoomed images.*

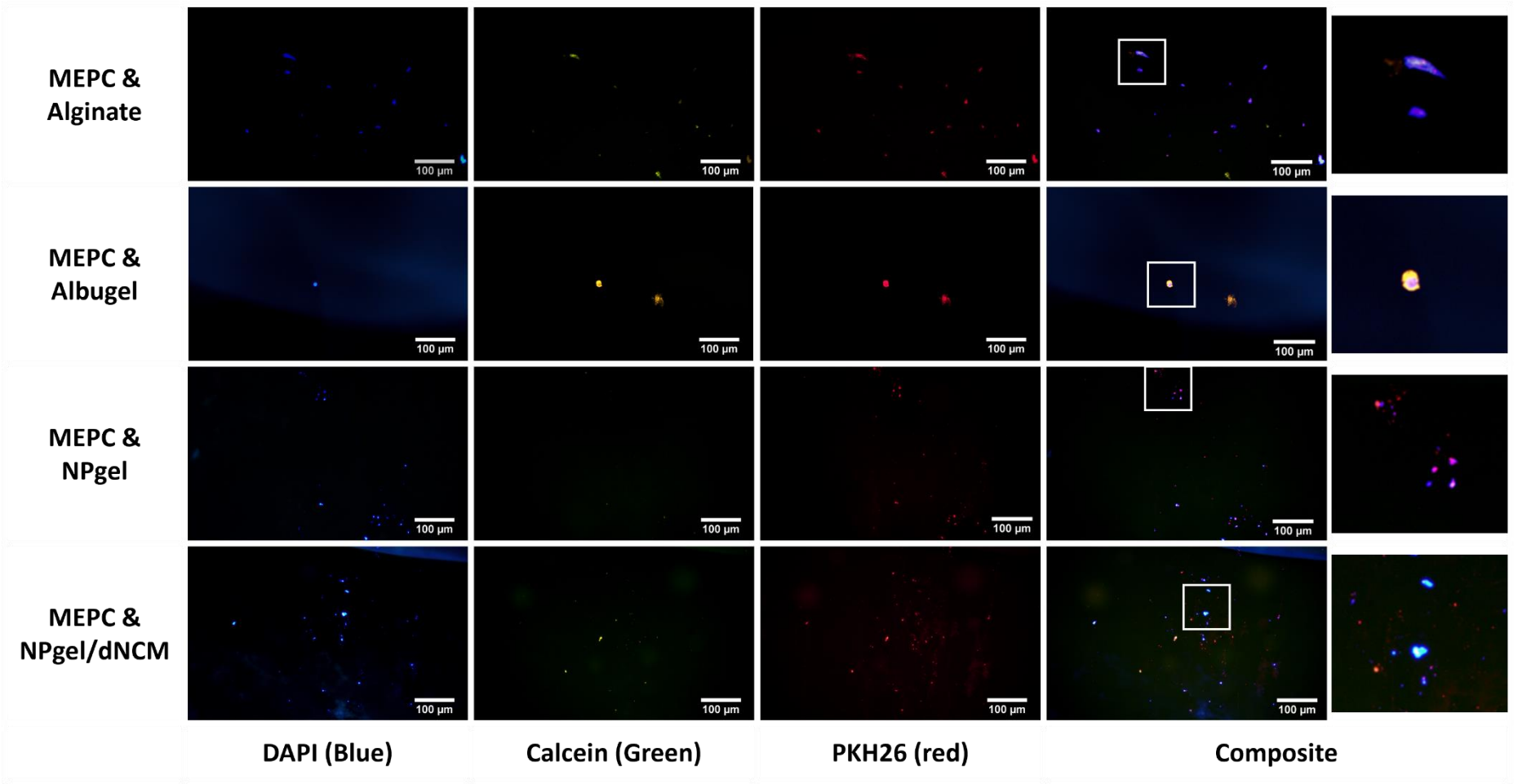

Figure 4.7. Live fluorescence images captured of Mesendoderm Progenitor Cells (MEPCs) origin MiPs labelled with red cell dye PKH26 seeded into alginate (MEPC & Alginate), Albugel (MEPC & Albugel), NPgel (MEPC & NPgel) and NPgel/dNCM (MEPC & NPgel/dNCM) for 24 hours*, followed by viability staining with Calcein-AM (green), Hoechst (blue) (n=3 technical repeats). White box indicated zoomed in composite image. Scale bar 100µm*

Viability was assessed depending on cell-seeding density of iPSC-MEPC in Albugel. Calcein-AM and PI stain was used to label viable iPSC-MEPC after 5-day culture in Albugel, the total cell viability between the cell-densities was not significantly different, with an observation of 46% of iPSC-MEPC were viable at cell density 0.4x10^{6}cells/mL, 32% viable cells at 4x10^{6}cells/mL and 47% viable cells at 1x10^{7}cells/mL after the 5-day culture period (Fig. 4.8).

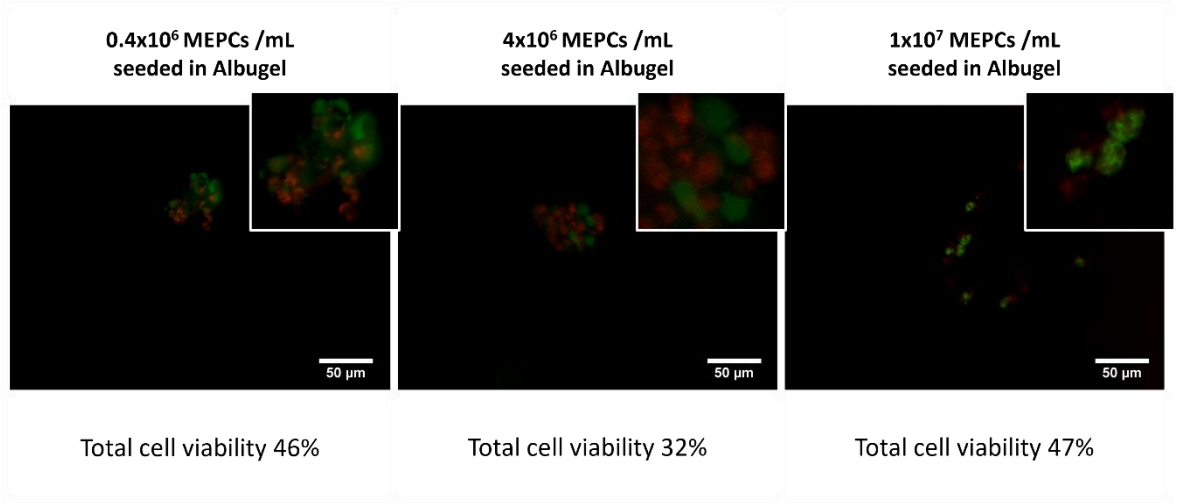

Figure 4.8. Mesendoderm Progenitor Cells (MEPCs) origin thermofisher seeded into Albugel at different cell density; *0.4x10^6 cells/mL, 4x10^{6}cells/mL, and 1x10^{7}cells/mL. Constructs were cultured for 5 days at 5% v/v oxygen at 37^{o}C before being stained with Calcein-AM (green) and PI (red) for manual viability count (n=3 technical repeats). White boxes indicate zoomed in images. Scale bar 50µm.*

PHASE I: MESENDODERM PROGENTITOR CELL SURVIAL AND MORPHOLOGY WITHIN NOVEL BIOMATERIALS

Following establishment of a seeding method for iPSC-MEPCs into biomaterials, further viability assessment was investigated with culturing iPSC-MEPC at $4x10^6$ cells/mL in Albugel and NPgel for 5 days, prior to being stained with Calcein-AM and Hoechst. The cell seeding density was selected as it was comparable to the NP cell density and from previous studies in Chapter 2 and 3. A 5-day culture period was also selected firstly because iPSC-MEPCs remained viable for up to 5 days in Albugel (Fig. 4.9). IPSC-MEPCs were Calcein-AM positive in MEPC cultured in Albugel and MEPC cultured in NPgel (Fig. 4.9). IPSC-MEPCs seeded at $4x10^6$ cells/mL and cultured for 5 days in Albugel and NPgel were stained histologically, and immunohistochemistry was used to assess the morphology and phenotype after this short culture period (Fig. 4.9).

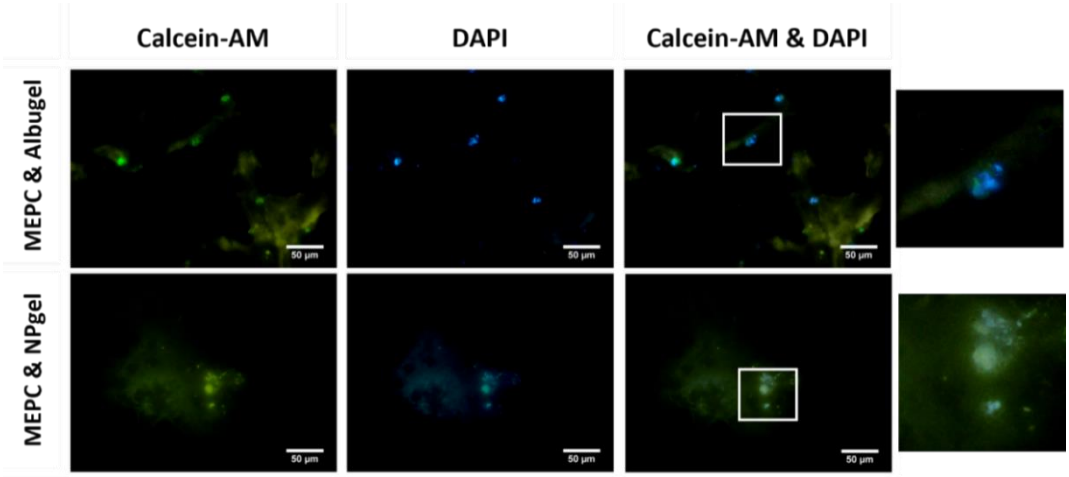

Figure 4.9. Mesendoderm Progenitor Cells (MEPCs) origin MiPs viability when seeded into Albugel (MEPC & Albugel) and NPgel (MEPC & NPgel). *Live MEPCs were stained with Calcein-AM (green) and DAPI (Blue) after 5 days of culture 5% v/v oxygen at 37°C (n=3 technical repeats). White box indicates zoomed in images. Scale bar 50µm.*

iPSC-MEPCs seeded into Albugel and NPgel, cellular structures were shown clearly in both biomaterials (Fig. 4.10). When comparing the morphology of the iPSC-MEPCs seeded in the Albugel and NPgel, fragmented nuclei appeared in iPSC-MEPCs cultured in Albugel constructs (Fig. 4.10; indicated with black arrows), whereas the iPSC-MEPCs cultured in NPgel displayed clear mononuclear morphology. Some indication of matrix staining was observed with the Masson's Trichrome stain in iPSC-MEPC cultured in NPgel, and Alcian Blue in iPSC-MEPC cultured in Albugel (Fig. 4.10), which was translated in positive Collagen type II and Aggrecan in iPSC-MEPCs seeded in both biomaterials (Fig. 4.11; indicated by white arrows). After 5 days in culture, iPSC-MEPCs displayed Cytokeratin 8, 18 and 19 positivity in both Albugel and NPgel, however there were limited Brachyury positive cells (Fig. 4.11).

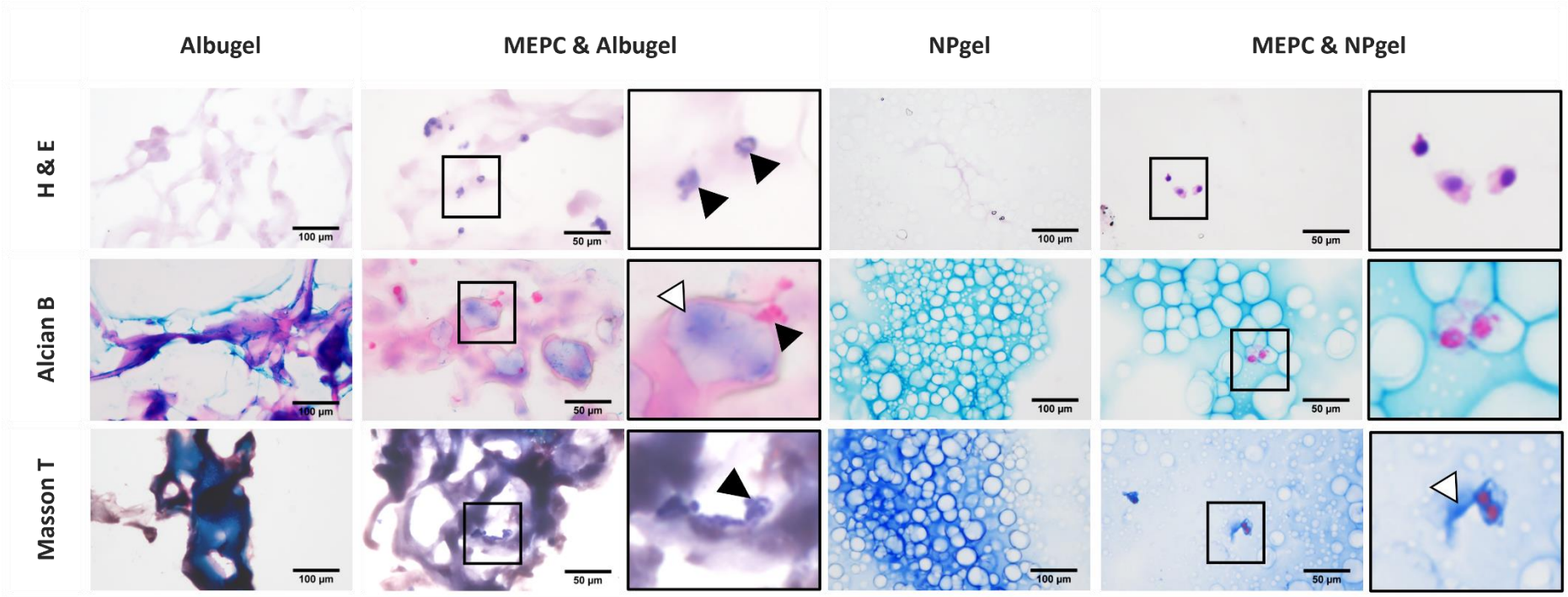

Figure 4.10. Mesendoderm progenitor cells morphology when cultured in biomaterials. *Histological images captured of Mesendoderm progenitor cells (MEPCs) origin of MiPs, thawed and recovered for 24 hours on laminin 521. Then seeded into biomaterials Albugel and NPgel for a 5-day pilot study at 5% v/v oxygen, 37^{o}C (n=3 technical repeats). Stained with Haematoxylin and eosin (H&E), Alcian Blue (Alcian B) and Masson's Trichrome (Masson's T)The acellular constructs (Albugel, NPgel) were captured at scale 100µm and MEPC seeded constructs (MEPC & Albugel, MEPC & NPgel) were captured at scale 50µm, with zoomed images highlighted with black box. Black arrows indicate MEPCs with fragmented nuclei, white arrows indicate extracellular matrix staining.*

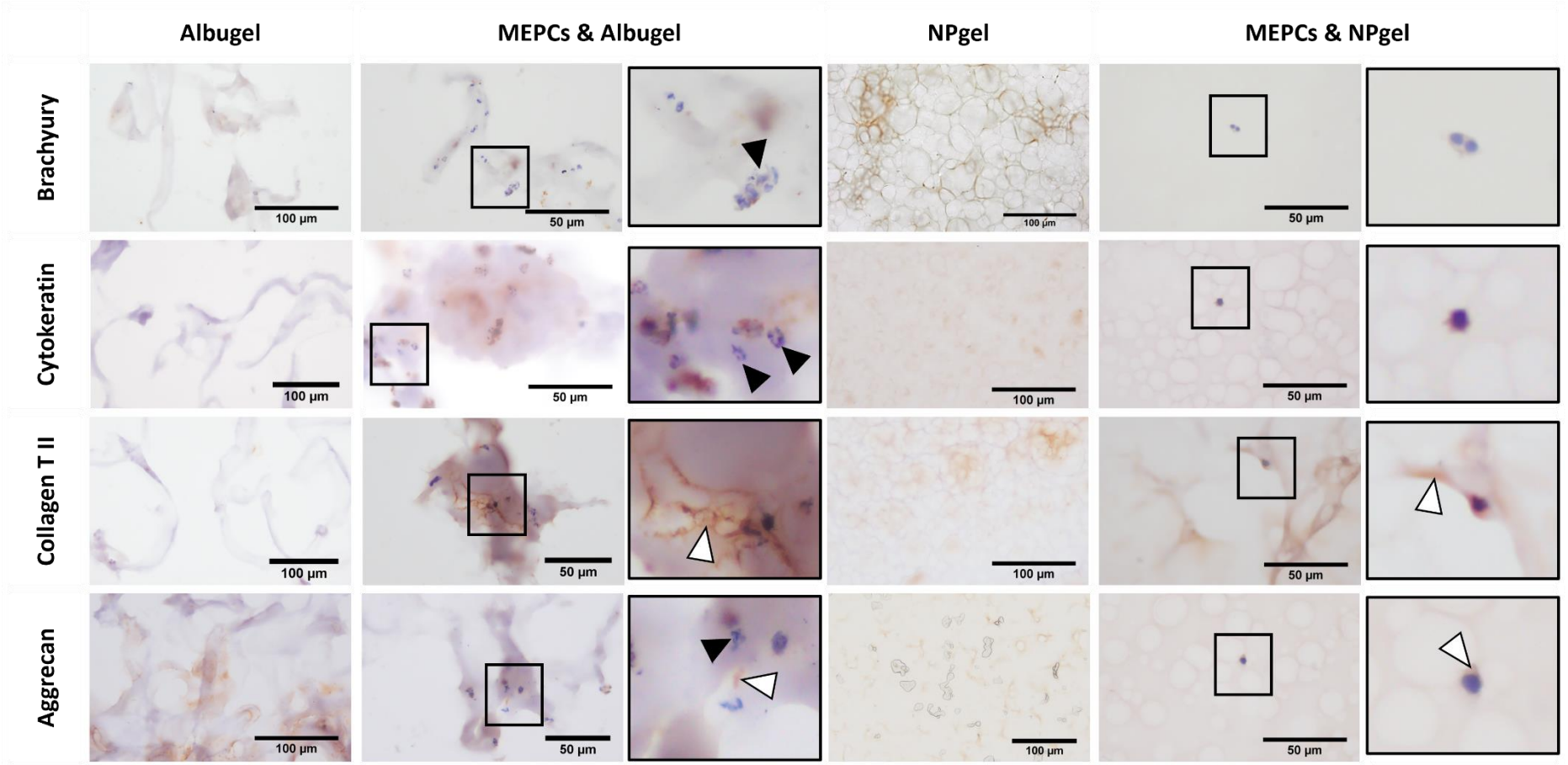

Figure 4.11. Mesendoderm progenitor cells phenotype when cultured in biomaterials. *Immunohistochemical images captured of Mesendoderm Progenitor Cells (MEPCs) origin of MiPs, thawed and recovered for 24 hours on laminin 521. Then seeded into biomaterials Albugel and NPgel for a 5-day pilot study at 5% v/v oxygen, 37^{o}C (n=3 technical repeats). Stained with Brachyury, Cytokeratin 8,18 & 19 (cytokeratin), Collagen Type II (Collagen T II) and Aggrecan. The acellular constructs (Albugel, NPgel) were captured at scale 100µm and MEPC seeded constructs (MEPC & Albugel, MEPC & NPgel) were captured at scale 50µm, with zoomed images highlighted with black box. Black arrows indicate MEPCs with fragmented nuclei, white arrows indicate extracellular matrix staining.*

PHASE II: MESENDODERM PROGENTITOR CELL CHARACTERISATION AND PHENOTYPIC ANALYSIS WITHIN BIOMATERIALS (ALBUGEL, NPGEL AND NPGEL/DNCM)

MORPHOLOGICAL ANALYSIS OF MESENDODERM PROGENTITOR CELL IN ALBUGEL, NPGEL AND NPGEL/DNCM

Following iPSC-MEPCs seeded into Albugel and NPgel for 5 days; the culture period was extended to 2 weeks and iPSC-MEPCs were seeded into Albugel, NPgel and NPgel/dNCM. The iPSC-MEPCs were shown to also survive after 2 weeks in all three biomaterials (Fig. 4.12), with a median value of $2.0x10^6$ cells/cm^3, $7.8x10^5$ cells/cm^3 and $5.8x10^5$ cells/cm^3 observed in Albugel, NPgel and NPgel/dNCM respectively (Fig. 4.12b). Interestingly, the iPSC-MEPCs in the Albugel presented as multi-nuclei (Fig. 4.12a; indicated with black arrows), which was also observed at 5 days (Fig. 4.10 and 4.11).

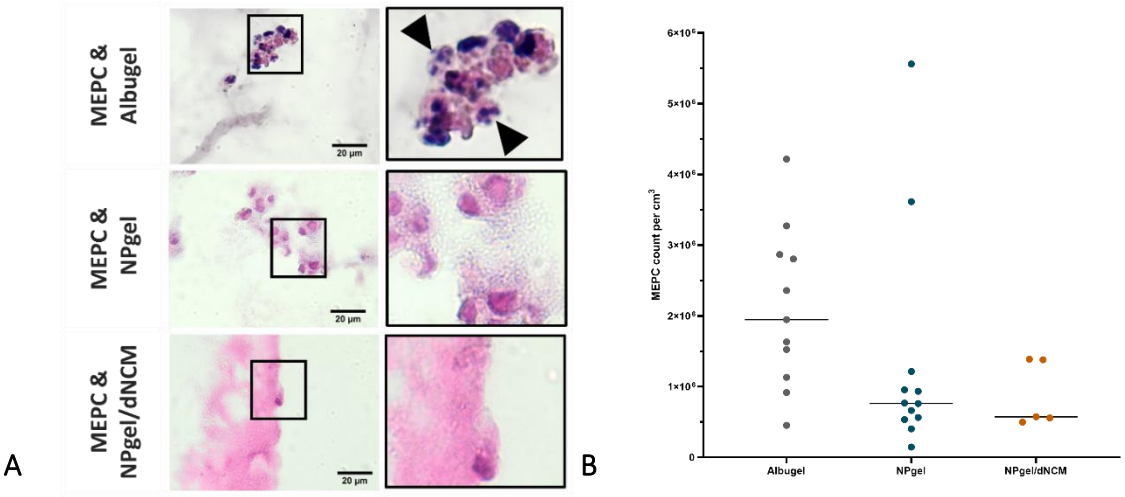

Figure 4.12. Mesendoderm progenitor cells morphology and survival when cultured in biomaterials: Albugel, NPgel and NPgel/dNCM. (A) *Histological images captured of Mesendoderm Progenitor Cells (MEPCs) origin of Thermofisher, thawed and recovered for 24 hours on laminin 521. Then seeded into biomaterials Albugel, NPgel and NPgel/dNCM for 2 weeks in N2B27 media at 5% v/v oxygen, 37°C (n=3 technical repeats). Stained with Haematoxylin and eosin (H&E). Black box indicated zoomed images. Black arrows indicate multi-fragmented nuclei. Images were captured at scale 20µm.* ***(B)*** *Graph quantifies the number of MEPCS observed in biomaterials after 2-week culture (n=3 technical repeats). Dots represent cells in a representative cm^3 area. Statistics performed with in GraphPad prism v9.5.1, Kruskal-Wallis test, followed by the Dunn's multiple comparisons test*

EXTRACELLULAR MATRIX PRODUCTION ANALYSIS OF MESENDODERM PROGENTITOR CELLS IN ALBUGEL, NPGEL AND NPGEL/DNCM.

Extracellular matrix production was also indicated with the positive cytoplasmic staining of Safranin O in iPSC-MEPC in all three biomaterials and Alcian Blue in iPSC-MEPC cultured in NPgel and iPSC-MEPC cultured in NPgel/dNCM (Fig. 4.13a; indicated with white arrows); this was also translated to extracellular positive extracellular staining of Aggrecan in iPSC-MEPC in all three biomaterials, yet collagen type II was only observed in iPSC-MEPC cultured in Albugel and NPgel (Fig. 4.13b).

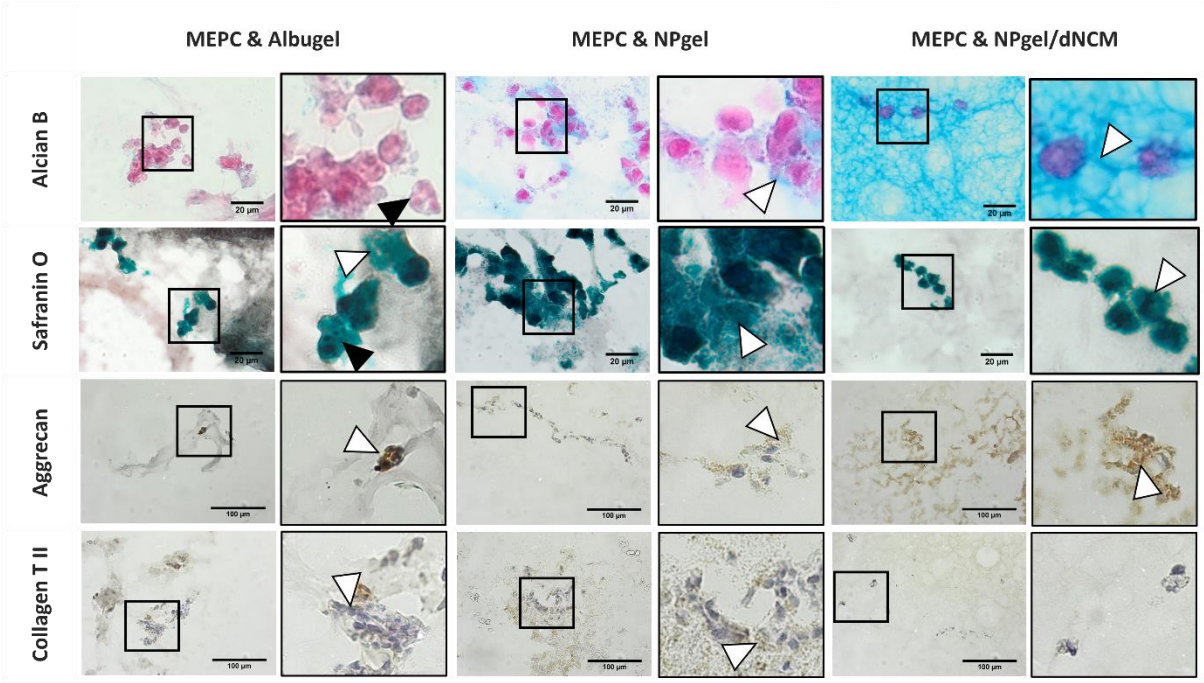

Figure 4.13. Mesendoderm progenitor cells extracellular matrix expression when cultured in biomaterials: Albugel, NPgel and NPgel/dNCM. *Histological and Immunohistochemical images captured of Mesendoderm Progenitor Cells (MEPCs) origin of Thermofisher, thawed and recovered for 24 hours on laminin 521. Then seeded into biomaterials Albugel, NPgel and NPgel/dNCM for 2 weeks in N2B27 media at 5% v/v oxygen at 37^{o}C (n=3 technical repeats). Stained with Alcian Blue (Alcian B), Safranin Orange (Safranin O), Aggrecan and Collagen Type II (Collagen T II). Alcian Blue and Safranin O images were captured at scale 20µm, Aggrecan and Collagen Type II. Black box indicated zoomed images. Black arrows indicate multi-fragmented nuclei, white arrows indicate matrix staining.*

PHENOTYPICAL ANALYSIS OF MESENDODERM PROGENTITOR CELLS IN ALBUGEL, NPGEL AND NPGEL/DNCM.

Markers utilised for phenotyping MEPCs were Cytokeratin 8, 18 and 19, FOXA2, Brachyury and SOX9. Positive immunopositive staining for Cytokeratin 8, 18 and 19 in iPSC-MEPCs cultured in NPgel/dNCM with little expression seen when cultured in Albugel or NPgel (Fig. 4.14a). Brachyury was highly expressed within the cytoplasm within iPSC-MEPCs cultured in Albugel and NPgel (Fig. 4.14a). Whereas the FOXA2 and SOX9, showed similar expression of <40% in all three biomaterials (Fig. 4.14). With the multi-fragmented nuclei appearance observed in

iPSC-MEPC cultured in Albugel and the significantly lower cell number survival in combination with lower Brachyury positive iPSC-MEPC observed in iPSC-MEPC cultured in NPgel/dNCM, NPgel was taken forward for Phase III testing.

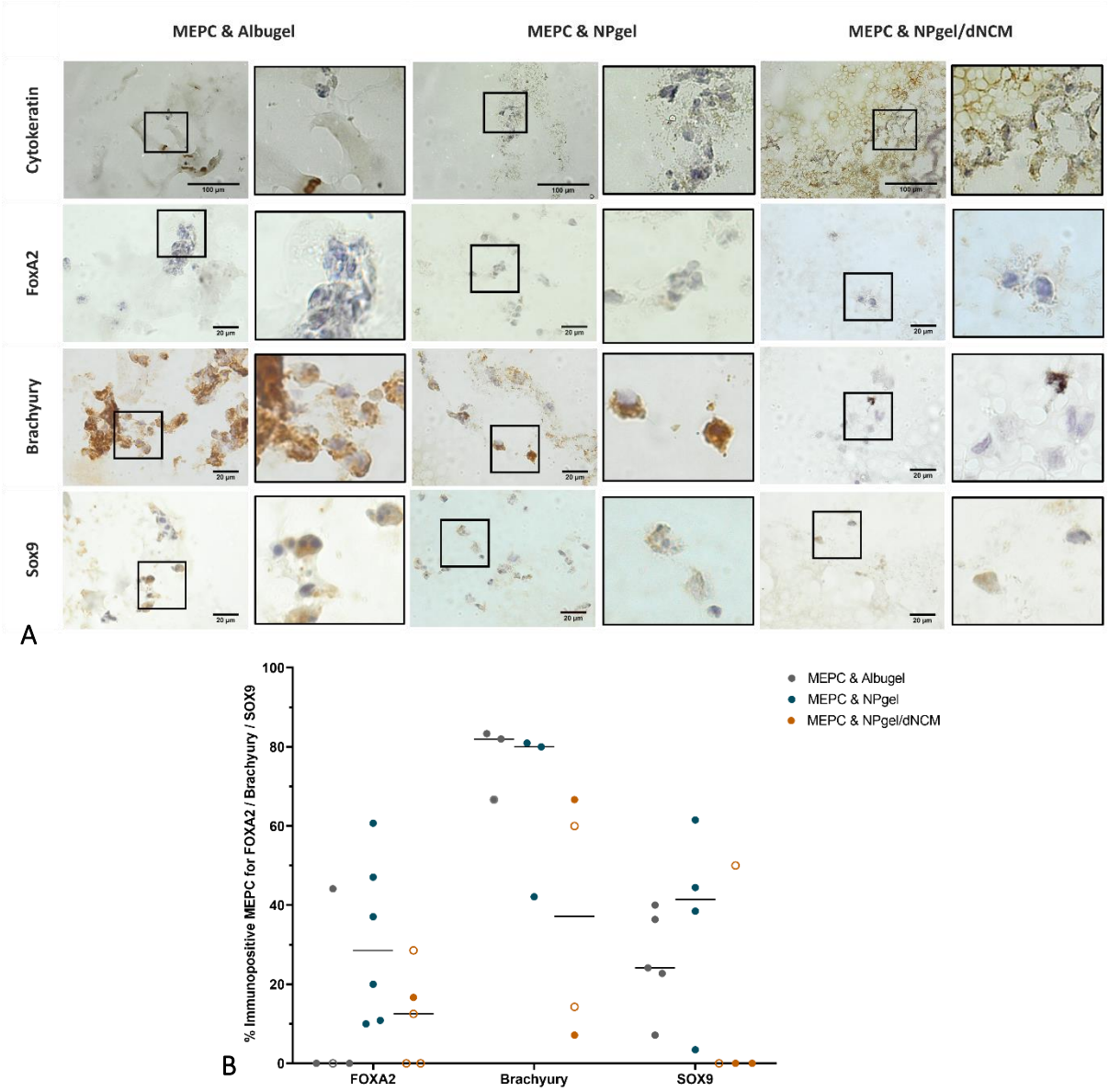

Figure 4.14. Mesendoderm progenitor cell phenotype when cultured in biomaterials: Albugel, NPgel and NPgel/dNCM. (A) *Immunohistochemistry images captured of Mesendoderm Progenitor Cells (MEPCs) origin of Thermofisher, seeded into biomaterials Albugel (MEPC & Albugel), NPgel (MEPC & NPgel) and NPgel/dNCM (MEPC & NPgel/dNCM) for 2 weeks in N2B27 media at 5% v/v oxygen at 37°C. Stained with Cytokeratin 8, 18 & 19 (cytokeratin), FOXA2, Brachyury, and SOX9. Black box indicated zoomed images. Scale bar 100µm for Cytokeratin images and scale bar 50µm for FOXA2/Brachyury/SOX9 images.* ***(B)*** *MEPCs counted and quantified for percentage of immunopositive cells in Albugel (MEPC & Albugel), NPgel (MEPC & NPgel) and NPgel/dNCM (MEPC & NPgel/dNCM) after 2-week culture (n=3 technical repeats). Each dot represent percentage of immunopositive cells observed in a sample, ○ indicated <10 cells were counted. Statistics performed with in GraphPad prism v9.5.1, Kruskal-Wallis test, followed by the Dunn's multiple comparisons test.*

PHASE III: MESENDODERM PROGENTITOR CELL CHARACTERISATION AND PHENOTYPIC ANALYSIS WITHIN BIOMATERIALS (ALGINATE, PEG/DNCM AND NPGEL)

MORPHOLOGICAL ANALYSIS OF MESENDODERM PROGENTITOR CELLS IN ALGINATE, PEG/DNCM AND NPGEL

For Phase III testing of iPSC-MEPCs culture and differentiation in novel biomaterials: iPSC-MEPCs were seeded into NPgel alongside alginate and another potentially clinical applicable biomaterial - PEG/dNCM, which had undergone parallel biomaterial screening and selection at the University of Galway. The iPSC-MEPCs and biomaterial constructs were then cultured for up to 4 weeks: harvesting constructs following 1-week, 2-week and 4-week timepoint. Within this phase of testing culture medium also was changed to DMEM with supplements to mimic more closely the culture media recommended for IVD cells (Cisewski *et al.*, 2018; Schubert *et al.*, 2018; Basatvat *et al.*, 2023). Morphologically, following 1-week of culture iPSC-MEPCs in alginate culture were large with a lack of distinct nuclei (Fig. 4.15a), whilst iPSC-MEPCs cultured in PEG/dNCM displayed cells with a large nucleus and the iPSC-MEPCs cultured in NPgel resembled cells with a distinct smaller nucleus (Fig. 4.15a). At later 4-week time point it was apparent that iPSC-MEPCs were no longer visible within the alginate cultures (Fig. 4.15a), with no iPSC-MEPCs counted in the triplicate technical repeats (Fig. 4.15b). The iPSC-MEPCs cultured in PEG/dNCM showed no morphological change (Fig. 4. 15a). The iPSC-MEPCs cultured in NPgel constructs were more populated with fragmented nuclear cells (Fig. 4.15a; indicated with black arrow; Fig. 4.15c). The number of iPSC-MEPC counted in biomaterials after 4-weeks was significantly different; the count of iPSC-MEPC cultured in NPgel was greater than when compared to iPSC-MEPC count when cultured in Albugel ($p \leq 0.001$) and when cultured in PEG/dNCM ($p \leq 0.01$). With double the average amount of iPSC-MEPC observed in NPgel than when cultured in PEG/dNCM at $7.0x10^5$ cells/cm^3 area compared to $2.5x10^5$ cells/cm^3 area respectively (Fig. 4.15b), although the count did include the multi-nuclei cells. Alginate cultures were omitted from quantification analysis as limited cells were present at any time point within the study.

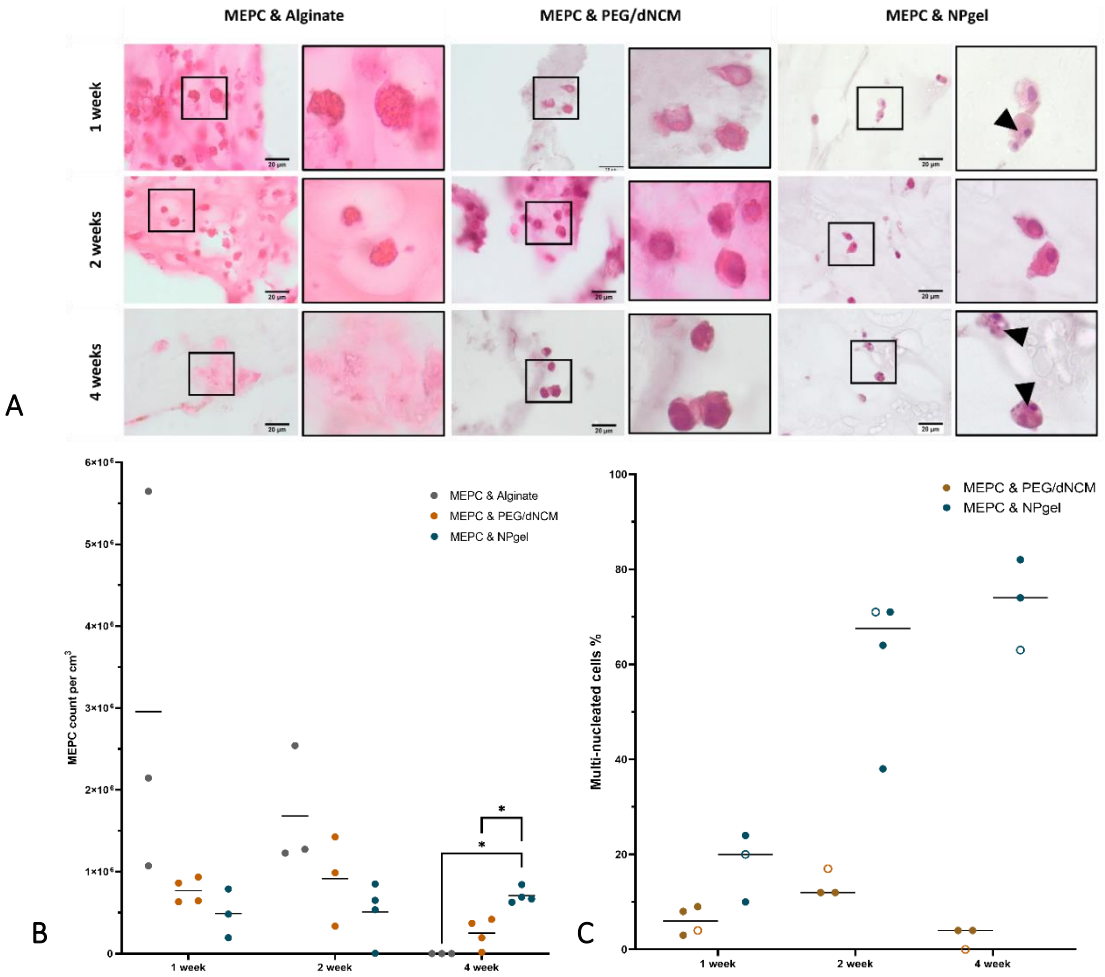

Figure 4.15. Mesendoderm progenitor cells morphology and survival when cultured in biomaterials: alginate, PEG/dNCM and NPgel. ***(A)*** *Histological images captured of Mesendoderm Progenitor Cells (MEPCs) origin of patient derived monoclonal, seeded into biomaterials alginate, PEG/dNCM and NPgel for 1,2 and 4-weeks and cultured with DMEM media at 5% v/v oxygen, 37°C (n=3 technical repeats). Stained with Haematoxylin and eosin. Black box indicated zoomed images. Black arrows indicate multi-fragmented nuclei. Scale bar 20µm.* ***(B)*** *MEPCs were counted per cm^3 area of biomaterial (each dot represents a technical repeat). Statistics performed with in GraphPad prism v9.5.1, one-way ANOVA test, followed by the Tukey's multiple comparisons test *p≤0.05.* ***(C)*** *percentage of MEPC that appeared to contain multi-nuclei. Each dot represents a technical repeat, ○ indicated < 10 cells were counted. Statistics performed with in GraphPad prism v9.5.1, Mann-Whitney test *p≤0.05.*

CELL SURVIVAL ANALYSIS OF MESENDODERM PROGENTITOR CELLS IN ALGINATE, PEG/DNCM AND NPGEL

The analysis of cell death and proliferation was highlighted with the use of caspase 3 and Ki67 expression (Fig. 4.16). Quantitatively, iPSC-MEPC cultured in PEG/dNCM displayed 25% at 1-week, 50% at 2-week and 26% at 4-week of caspase 3 positive cells (Fig. 4.16b) whereas iPSC-MEPC cultured in NPgel results show a range of 51% caspase 3 positive cells at 1-week, 49% at 2-week and 31% at 4-week (Fig. 4.16b). Proliferation marker Ki67 was positive in 63% of iPSC-MEPC cultured in PEG/dNCM at 1-week, 75% at 2-week and 73% at 4-week (Fig. 4.16d).

Similarly, in iPSC-MEPCs cultured in NPgel constructs, iPSC-MEPCs were Ki67 immunopositive in 32% of cells at 1 week, 31% at 2 weeks and 24% at 4 weeks (Fig. 4.16d).

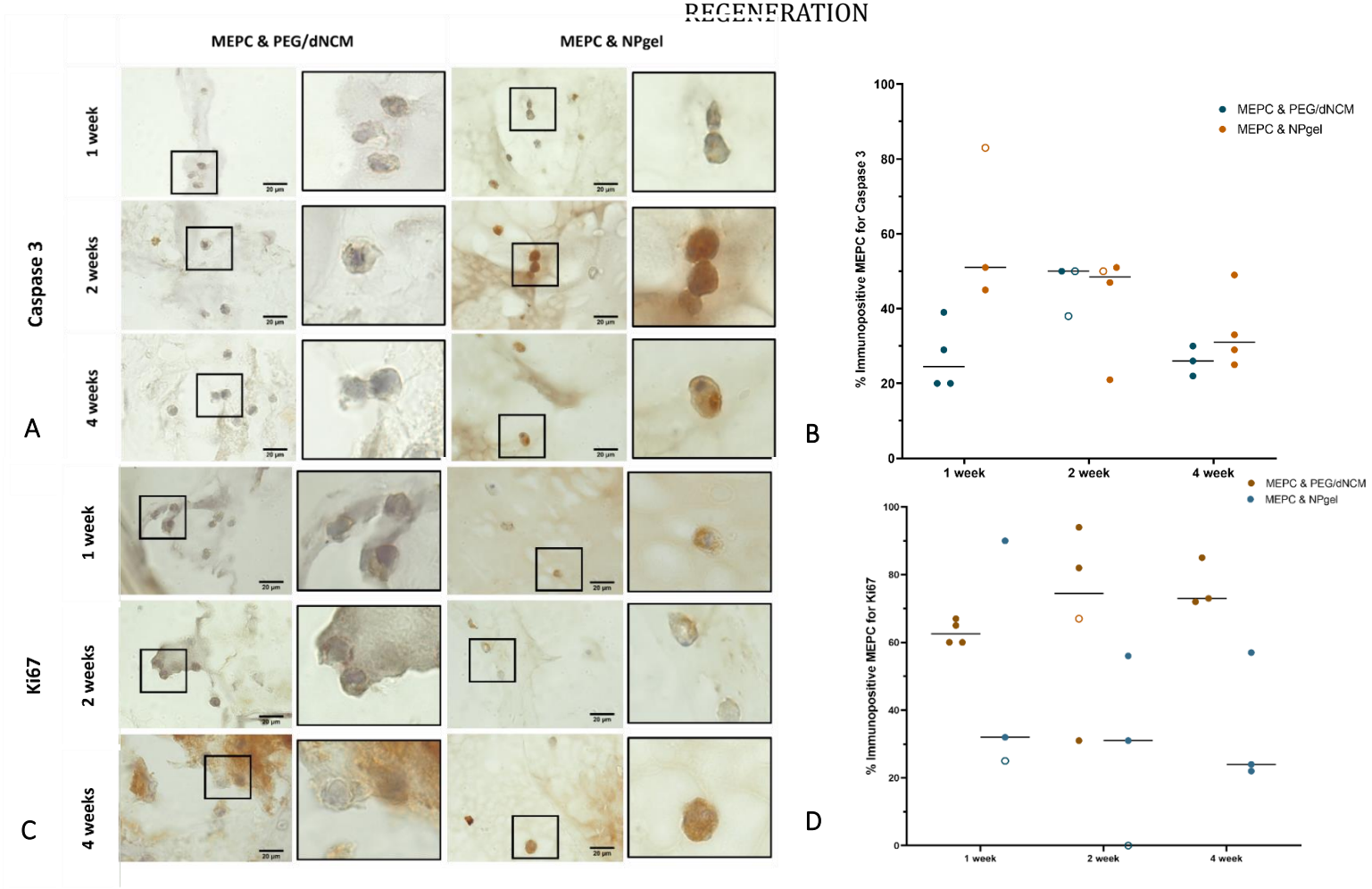

Figure 4.16. Mesendoderm progenitor cells viability when cultured in biomaterials: PEG/dNCM and NPgel. *Mesendoderm Progenitor Cells (MEPCs) origin of patient derived monoclonal, seeded into biomaterials PEG/dNCM and NPgel for 1,2 and 4-weeks with DMEM media at 5% v/v oxygen, 37°C (n=3 technical repeats). Immunohistochemical images of MEPCs cultured in PEG/dNCM and NPgel constructs when stained with* ***(A)*** *caspase 3 and* ***(C)*** *Ki67. Black box indicated zoomed in images. Scale bar 20µm. Immunopositive MEPC were also quantified and* ***(B)*** *percentage of MEPC cultured in PEG/dNCM and NPgel that were immunopositive for Caspase 3. Each dot represents a technical repeat, ○ indicated < 10 cells were counted in each repeat.* ***(D)*** *Percentage of MEPC cultured in PEG/dNCM and NPgel that were immunopositive for Ki67. Each dot represents a technical repeat, ○ indicated < 10 cells were counted in each repeat. Statistics performed with in GraphPad prism v9.5.1, Mann-Whitney test, not significant.*

PHENOTYPICAL ANALYSIS OF MESENDODERM PROGENTITOR CELLS IN ALGINATE, PEG/DNCM AND NPGEL

IPSC-MEPCs and biomaterial constructs were stained with a panel of selected MEPC and NP/NC markers. IPSC-MEPC cultured in NPgel showed no expression of FOXA2 marker, a NC-like cell marker, however iPSC-MEPC cultured in PEG/dNCM showed immunopositive FOXA2 stain at 2 weeks (Fig. 4.17a; indicated by black arrows). Expression of SOX9, a NP and NC-like cell marker, was observed in iPSC-MEPC cultured in NPgel at 4 weeks (Fig. 4.17b; indicated by black arrow). IPSC-MEPCs in both biomaterials, iPSC-MEPCs cultured in PEG/dNCM and iPSC-MEPC cultured in NPgel displayed positive cytoplasmic staining for Brachyury and Cytokeratin 8, 18 and 19 (Fig. 4.18). Brachyury immunopositive iPSC-MEPCs increased during the culture period, with the most immunopositive expressed iPSC-MEPCs at 4-week time point, with a median value of 91% and 66% in iPSC-MEPC cultured in PEG/dNCM and iPSC-MEPC cultured in NPgel respectively (Fig. 4.18a, b). IPSC-MEPC displayed consistent expression of Cytokeratin 8, 18 and 19 throughout the 4-week culture period when cultured in either PEG/dNCM or NPgel (Fig. 4.18c, d).

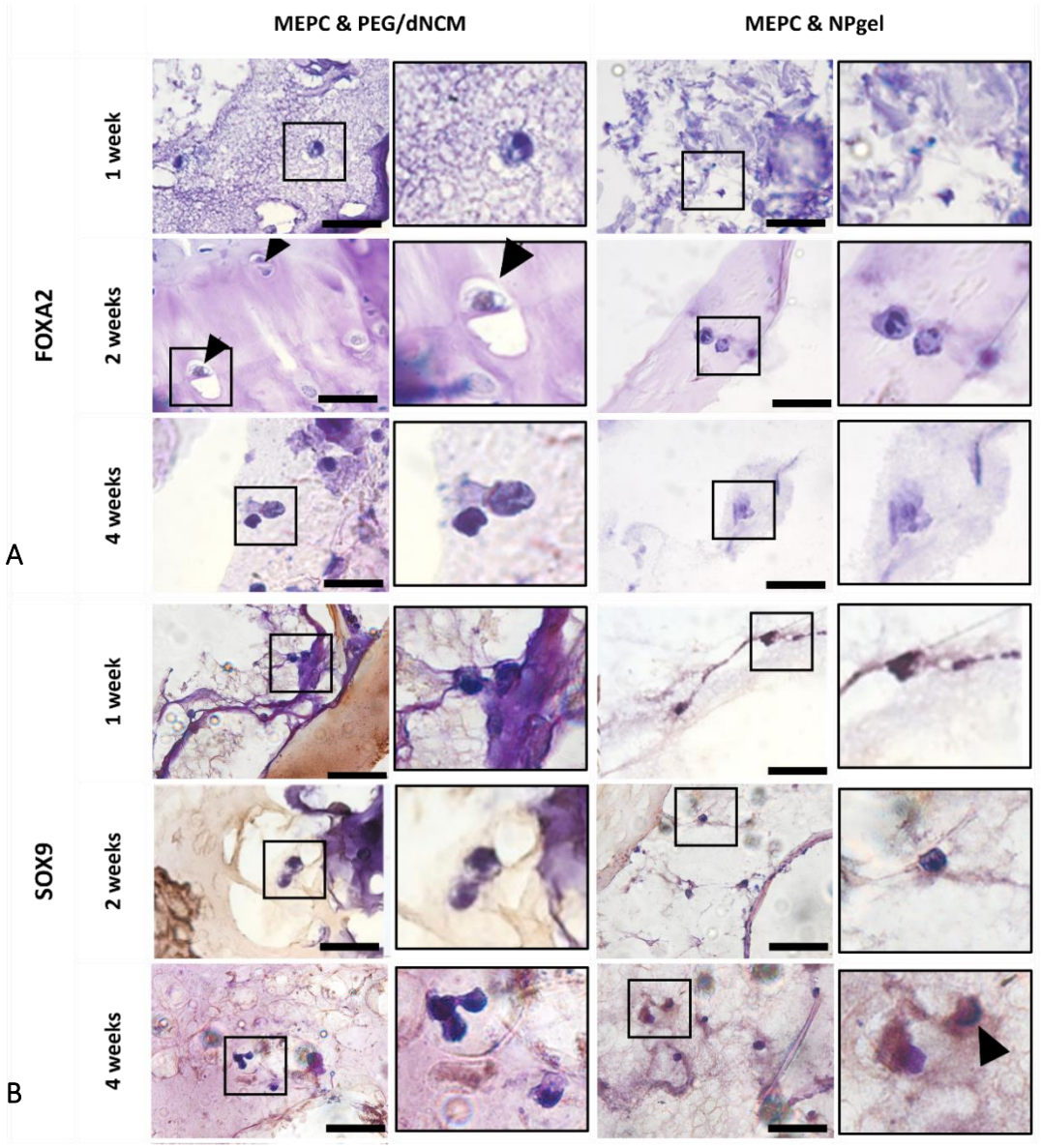

Figure 4.17. Mesendoderm progenitor cells phenotype when cultured in biomaterials: PEG/dNCM and NPgel. *Mesendoderm Progenitor Cells (MEPCs) origin of patient derived monoclonal, seeded into biomaterials PEG/dNCM and NPgel for 1,2 and 4-weeks in DMEM media at 5% v/v oxygen, 37°C (n=3 technical repeats). Immunohistochemical images of MEPC & PEG/dNCM and MEPC & NPgel constructs when stained with* ***(A)*** FOXA2 *and* ***(B)*** *SOX9. Black box indicated zoomed images. Black arrows indicate immunopositive MEPC. Scale bar 50µm. Cell count was limited and therefore unable to quantify.*

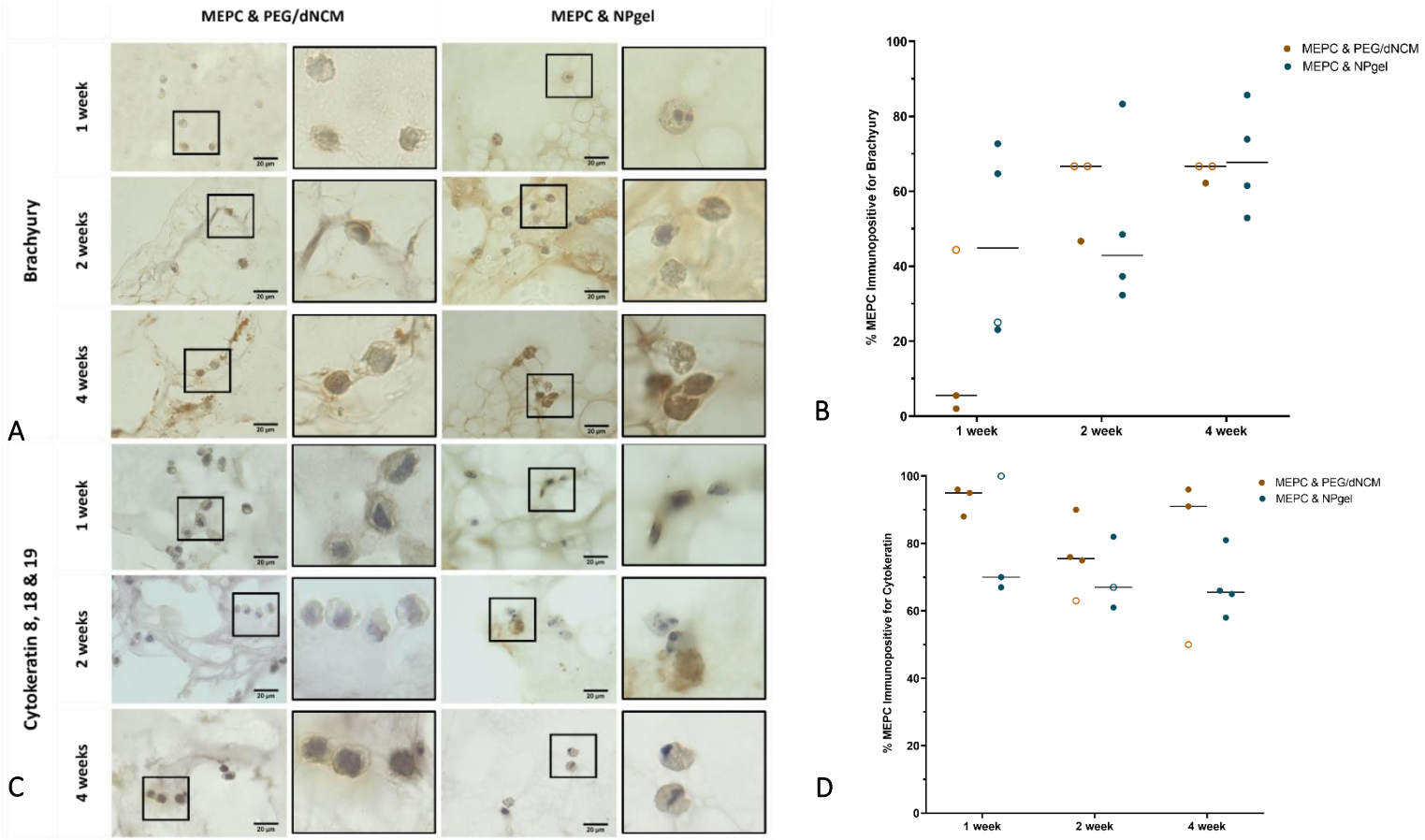

Figure 4.18. Mesendoderm progenitor cells phenotype when cultured in biomaterials: PEG/dNCM and NPgel. *Mesendoderm Progenitor Cells (MEPCs) origin of patient derived monoclonal, seeded into biomaterials PEG/dNCM and NPgel for 1,2 and 4-weeks in DMEM media at 5% v/v oxygen, 37°C (n=3 technical repeats). Immunohistochemical images of MEPC & PEG/dNCM and MEPC & NPgel constructs when stained with* ***(A)*** *Brachyury and* ***(C)*** *Cytokeratin 8, 18 and 19. Black box indicated zoomed images. Scale bar 20µm. Immunopositive MEPC were also counted and* ***(B)*** *Percentage of MEPC in MEPC & PEG/dNCM and MEPC & NPgel that were immunopositive for Brachyury. Each dot represents a technical repeat, ○ indicates <10 cells counted in each repeat.* ***(D)*** *Percentage of MEPC in MEPC & PEG/dNCM and MEPC & NPgel that were immunopositive for Cytokeratin 8, 18 ad 19. Each dot represents a technical repeat, ○ indicates <10 cells counted in each repeat. Statistics performed with in GraphPad prism v9.5.1, Mann-Whitney test, not significant.*

EXTRACELLULAR MATRIX PRODUCTION ANALYSIS OF MESENDODERM PROGENTITOR CELLS IN ALGINATE, PEG/DNCM AND NPGEL

iPSC-MEPC cultured in PEG/dNCM displays extracellular matrix staining indicated by the dark blue in Alcian Blue stain (Fig. 4.19a; indicated by white arrows), in the 4-week time point in the Masson's Trichrome stain (Fig. 4.19b; indicated by white arrows) and strong extracellular staining when stained with collagen type II (Fig. 4.20a; indicated by white arrows). Extracellular matrix staining was also identified in the iPSC-MEPC cultured in NPgel constructs with darker bluing around the iPSC-MEPCs with Masson's Trichrome staining (Fig. 4.20b; indicated by white arrows), teal green colour in the Safranin O stains (Fig. 4.19c; indicated by white arrows) and immunopositive staining for collagen type II and aggrecan (Fig. 4.20a, b). During the 4-week culture of iPSC-MEPCs cultured in alginate, PEG/dNCM and NPgel, media was also collected and analysed for glycosaminoglycan content (Fig. 4.20c). In iPSC-MEPC cultured in PEG/dNCM constructs, media collected at the beginning of the culture period: 1-day ($p \leq 0.05$), 1-week ($p \leq 0.01$) and 2-week ($p \leq 0.001$) contained significantly higher GAG that media collected at 4-week (Fig. 4.20c). Additionally, iPSC-MEPC cultured in PEG/dNCM at 2-week time point contained significantly higher levels of GAGs in the media, than following 3 weeks ($p \leq 0.01$). The iPSC-MEPCs cultured in NPgel constructs displayed constant GAG detection throughout the culture period (Fig. 4.20c).

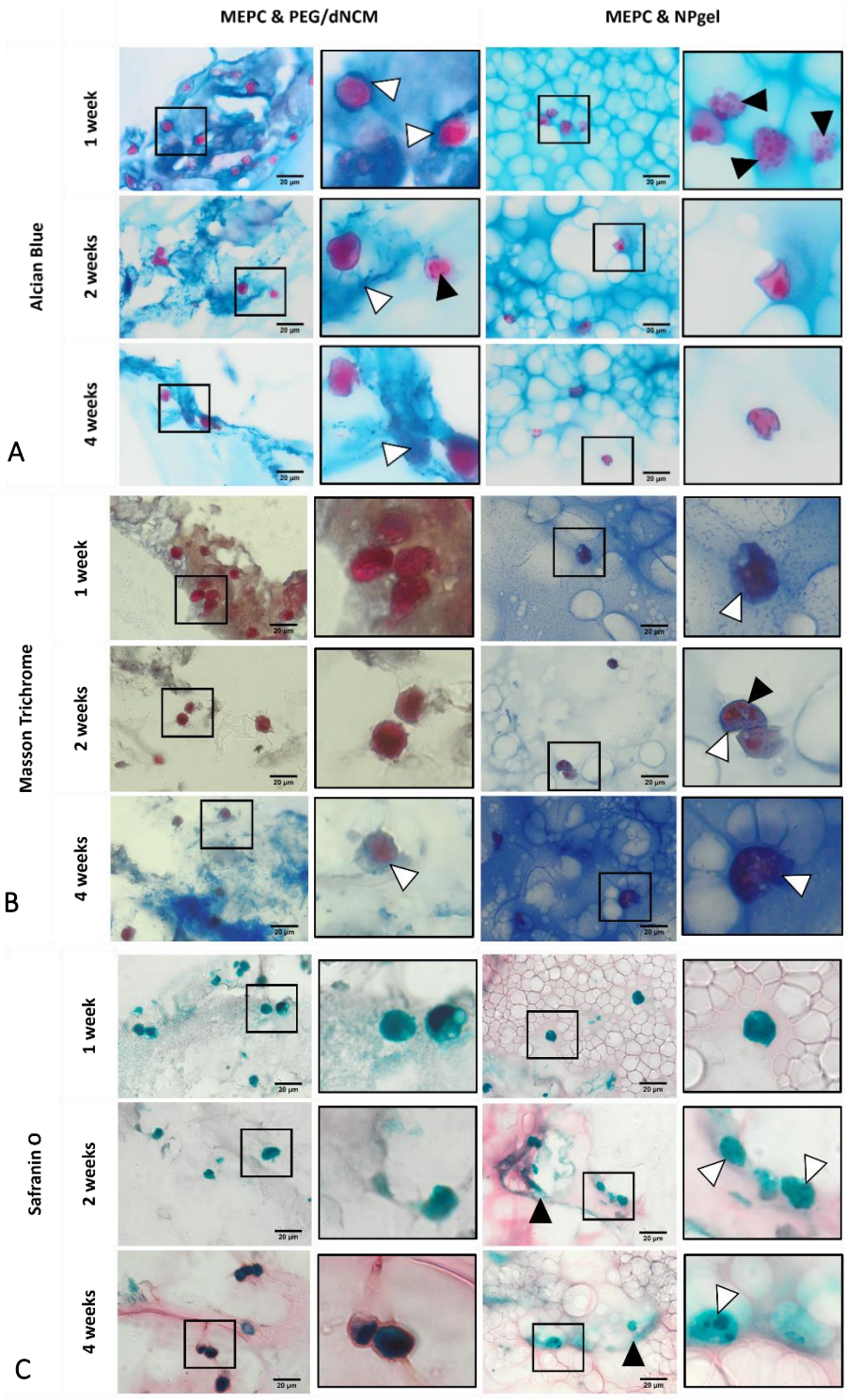

Figure 4.19. Mesendoderm progenitor cells morphology when cultured in biomaterials: PEG/dNCM and NPgel. *Histological images captured of Mesendoderm Progenitor Cells (MEPCs) origin of patient derived monoclonal, seeded into biomaterials alginate, PEG/dNCM and NPgel for 1,2 and 4-weeks in DMEM media at 5% v/v oxygen, 37^{o}C (n=3 technical repeats). Stained with* ***(A)*** *Alcian Blue,* ***(B)*** *Masson's Trichrome and* ***(C)*** *Safranin Orange (Safranin O). Black box indicated zoomed images. Black arrows indicate multi-fragmented nuclei. White arrows indicate matrix staining. Scale bar 20µm.*

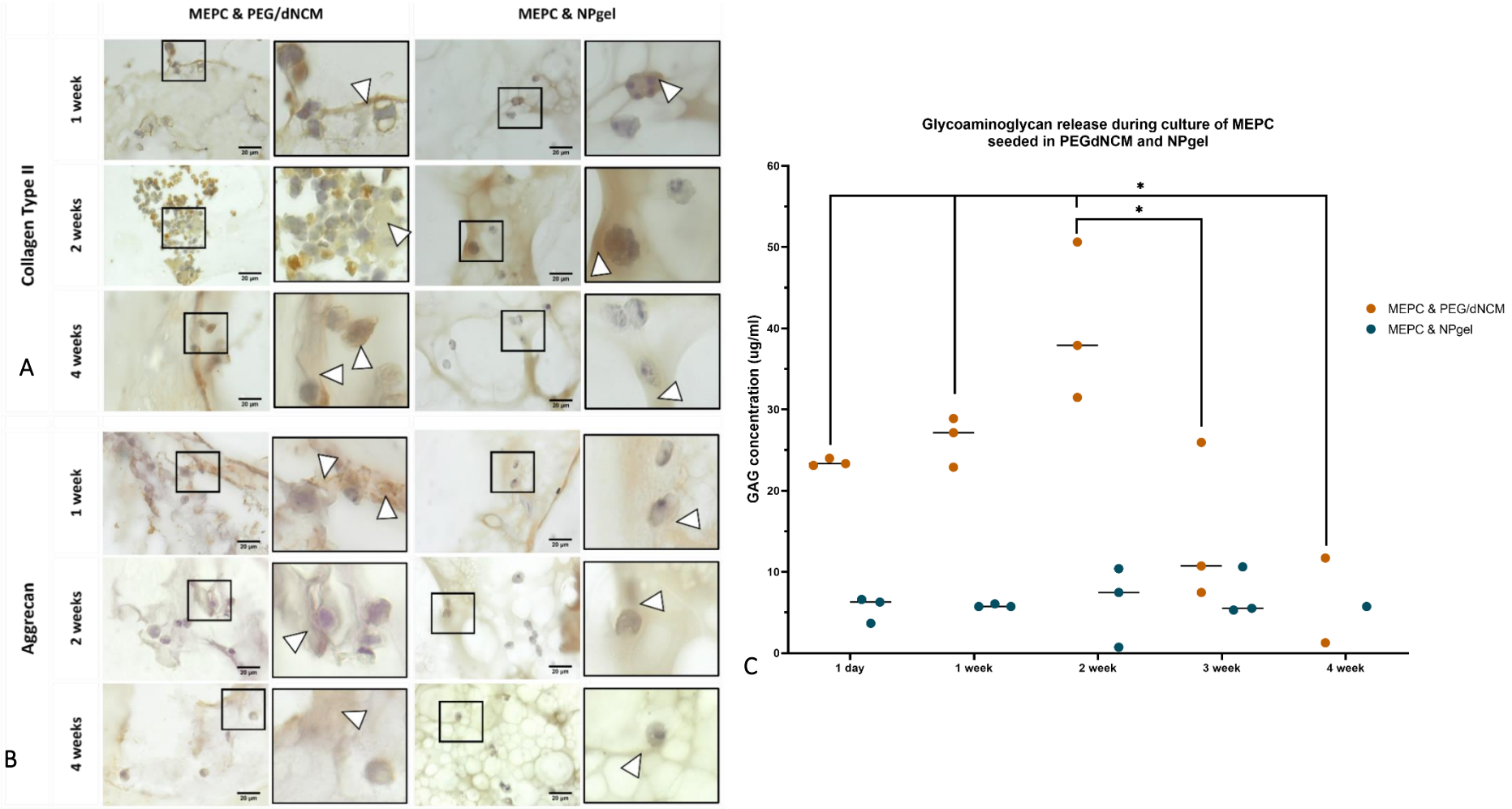

Figure 4.20. Mesendoderm progenitor cells extracellular matrix expression and release when cultured in biomaterials: PEG/dNCM and NPgel*. Immunohistochemistry images captured of Mesendoderm Progenitor Cells (MEPCs) origin of patient derived monoclonal, seeded into biomaterials alginate, PEG/dNCM and NPgel for 1,2 and 4-weeks in DMEM media at 5% v/v oxygen, 37^{o}C (n=3 technical repeats). Stained with **(A)** Collagen Type II and **(B)** Aggrecan. Black box indicated zoomed images. Black arrows indicate multi-fragmented nuclei. White arrows indicate matrix staining. Scale bar 20µm. Analysis of **(C)** Glycosaminoglycan (GAG) release using 1,9-Dimethylene blue (DMMB) assay in media collected over 4 weeks culture period of MEPC cultured in PEG/dNCM (MEPC & PEG/dNCM) and NPgel (MEPC & NPgel) at 5% v/v oxygen at 37^{o}C (n=3 technical repeats). Statistics performed with in GraphPad prism v9.5.1, one-way ANOVA test followed by the Tukey's multiple comparisons test *p≤0.05.*

DISCUSSION

Generating NC-like cells derived from induced pluripotent stem cells offers an alternative approach as a cellular therapy and provides a potential mechanism to deliver NC-like cells to the disc to initiate a regenerative response. For clinical use, NC-like cells would be generated through a cell bank which offers validated technical specification for cell culture-expansion, biobanking and extensive testing to ensure consistency and safety of cells for therapeutic use (Laurent *et al.,* 2020). Our ambition is to then deliver NC-like cells into the disc, with the use of a biomaterial carrier. Therefore, this study aimed to generate NC-like cells via seeding iPSC-MEPCs into biomaterials to investigate their differentiation within the biomaterials.

The immediate issue of the cryopreserved iPSC-MEPCs shipped to the UK from our collaborators was whether these iPSC-MEPCs could be recovered and healthy following thawing, and after 24-hour culture on laminin-521. Recovered iPSC-MEPCs after the 24 hours on Laminin-521, adhered to the laminin coated plates and displayed the correct morphology. However, many cells remained in suspension, whilst others showed elongated morphology, which indicated cells spreading prior to becoming more compact and uniform (Akhmanova *et al.*, 2015; Rivera *et al.*, 2020). The cryopreserved cells were also attained from different iPSC origins, including those commercially available from a Thermofisher line, and two from lab developed lines from our collaborators: MiPs and PBMC differentiated with four factor procedure. MEPCs from MiPs-iPSCs showed a recovery of ~50% whereas the other origins showed 25% of recovered iPSC-MEPCs after laminin-521, unfortunately MiPs were also not available for routine use due to limited supply. Obtaining cells from working cell banks offers an abundance of safe cells for therapeutic use, as biobanking includes validated technical specification for cell culture-expansion and extensive testing to ensure consistency (Laurent et al., 2020). Once a cell bank is established cells are cryopreserved in vials, stored in liquid nitrogen, and shipped to laboratories that will commence recovery procedure. However, an observation of low viability and low cell numbers after iPSC-MEPC recovery from cryopreservation highlights key difficulties particularly associated with cryopreservation and restoration. Suggesting, that using iPSC-MEPC via this method was inefficient and ineffective for translational potential. An abundance of problems can occur with cryopreservation that affect cell viability. When cells are exposed to fluctuating temperatures, such as during the shipment process on dry ice and are not kept in liquid nitrogen; this instability can lead to ice re-crystallization, resulting in the progressive loss of cell viability (Yuan *et al.*, 2016). Cryoprotectant solution can aid and prevent this loss due to temperature fluctuation however, cell aggregates could also be problematic due to a lack of cryoprotectant penetrating into cell clumps (Yuan *et al.*, 2016). IPSC also are susceptible to osmotic shock, which is caused during thawing by a sudden change in extracellular osmolality, also effecting cell viability (Uhrig *et al.,* 2022). Other studies have also discovered iPSC recovery to be difficult, with efficiency of plating to be particularly low (Reubinoff *et al.*, 2001; Fujioka *et al.*, 2004; Richards *et al.*, 2004). To combat this issue of cell damage occurring during cryopreservation of cells, reviews have researched into improving cell recovery through optimising freeze thawing techniques (Uhrig

et al., 2022), particularly through utilising novel molecules and compounds as cryoprotectants (Stubbs *et al.*, 2020). An alternative method avoiding cryopreservation has been studied in literature by utilising a semipermeable alginate hydrogel, which encapsulates cells and has been shown to successfully store hMSC for 5 days in a sealed cryovial. Concluding that a simple application of alginate hydrogel encapsulation may offer a robust alternative to cryopreservation for the transport and storage of stem cells (Chen *et al.*, 2013).

MESENDODERM PROGENITOR CELL VIABILITY ONCE SEEDED INTO A BIOMATERIAL

To our knowledge there has been no research conducted with iPSC-MEPCs in biomaterials, accordingly, a pilot test was implemented with the aim to determine if MEPCs could be seeded into biomaterials and remained viable after a short 24-hour period. Starting with 2 million cells per vial, the recovery rate after thawing iPSC-MEPC was 40 to 44% viability; iPSC-MEPCs were labelled with PKH26 cell tracker which resulted in a final viable cell count of ~$1.20x10^4$ cells/mL, losing more than 99% of cells during the process of iPSC-MEPC recovery and cell labelling. Suggesting that iPSC-MEPCs are difficult to handle; that the iPSC-MEPCs have not properly recovered prior to cell labelling, or that the iPSC-MEPCs may have been over-labelled with PKH26 which resulted in a loss of membrane integrity and reduced cell recovery (Regan, 2022). It has been noted that the lipophilic fluorescent dyes PKH26 can interfere with cell-cell or matrix interactions and has been shown to affect migration of stem cells (Kelp *et al.*, 2017), nevertheless studies have clearly shown PKH26 labelling does not affect cell viability in human mesenchymal stromal cells (Shao-Fang *et al.*, 2011; Kelp *et al.*, 2017). Thus, raising the question if the iPSC-MEPCs are fully recovered from the thawing process; thus, a study comparing freshly prepared, non-cryopreserved iPSC-MEPCs, against those which were cryopreserved would be essential to investigate.

CELL SEEDING DENSITY EFFECT ON MESENDODERM PROGENITOR CELL LINEAGE

During the first seeding of iPSC-MEPC into biomaterials, iPSC-MEPC viability was not affected by cell seeding densities, when iPSC-MEPC were seeded at $0.4x10^6$ MEPC/mL, $4x10^6$ MEPC/mL or $10x10^7$ MEPC/mL for 5 days. Although, higher cell number has been shown to promote differentiation effectiveness of stem cells to ectoderm lineage in 3D culture (Tchieu *et al.*, 2017; Farzaneh *et al.*, 2018; Chen *et al.*, 2019; Bogacheva *et al.*, 2021), with the downregulation of Brachyury being observed in increasing cell density (Tchieu *et al.*, 2017), mimicking the process of mesodermal condensation. Additionally, the use of $10x10^6$cells/mL would not be feasible as transporting cells were limited to vials containing $2.0x10^6$cells/mL. Therefore, iPSC-MEPCs were seeded at $4x10^6$ MEPC/mL in further constructs, which also mimics the native cell density of the NP and matched the cell density utilised for pNC seeded biomaterial testing (Chapter 3). Whilst also preventing induction of ectoderm differentiation. However, a study by Dia-Hernandez et al., (2020) seeded $25x10^6$ cells/mL in a micromass to enhance differentiation of human embryonic stem cells into NCs (Diaz-Hernandez *et al.*, 2020). This resulted in 3D high density micromass culture significantly improved notochordal differentiation when compared to monolayer culture.

COMPARING MESENDODERM PROGENITOR CELLS CULTURED IN PHASE II BIOMATERIALS VERSUS PHASE III BIOMATERIALS

The study divides the analysis of iPSC-MEPCs in biomaterials into three phases, Phase I and II highlights iPSC-MEPCs of commercial origin (Thermofisher, TF) seeded into biomaterials that have been previously selected and undergone analysis with porcine NCs (Chapter 3). These studies used N2B27 complete media developed to support iPSC-MEPCs in monolayer culture. Whilst Phase III investigated the forerunning biomaterial from Phase II testing alongside a biomaterial selected in parallel testing by partners in Galway. Within these studies the iPSC cell line selected from the consortia to demonstrate highest potential for NC differentiation within parallel studies (iPSC-MEPCs derived from PBMCs from patient 190). These studies were performed using culture media which mimics more closely the disc environment with low glucose DMEM in a FCS free media as described recently for NP cell 3D culture (Basatvat *et al.*, 2023). However, within Phase III testing, the iPSC-MEPC cell count per 40mm^2 of biomaterial was decreased. Taking NPgel as the common variable, in Phase II iPSC-MEPC cultured in NPgel 3.3x10^2 MEPC/cm^3 were observed in comparison to Phase III iPSC-MEPC cultured in NPgel were around 2.5x10^1 MEPC/cm^3 were counted in 1-week, 2-week and 4-week cultures. The differing variables of the Phase II and Phase III tests were the media (N2B27 vs DMEM), size of the construct (300µL vs 50µL), and iPSC-MEPC origin (TF vs PBMC). Thus, the specific reason for this decrease is not clear and therefore discussed further below.

BASAL MEDIA DIFFERENCE

An analysis of the difference in basal media used between the two phases. In Phase II, N2B27 media (composed of DMEM/F-12 (3.1g/mL glucose) supplemented with GlutaMAX™) media was supplemented with CHIR, a Wnt agonist, which activates the core mesendodermal regulators Brachyury and FOXA2 (Kubo *et al.*, 2004). N2B27 media is widely used in stem cell culture, differentiating stem cells to alternative lineages with added supplements such as, Wnt3a or CHIR for mesendodermal linage (Thomson *et al.*, 2011; Kreuser *et al.*, 2020); and Noggin (Gerrard *et al.*, 2005), retinoic acid (Thomson *et al.*, 2011) or FGF (Thomson *et al.*, 2011) for neural differentiation. The media used in Phase II was low glucose DMEM, which represents more closely the glucose concentration in the disc and recommended for 3D culture of disc cells (Humphreys *et al.*, 2018; Basatvat *et al.*, 2023), as literature demonstrates that glucose concentration can be highly influential upon cell viability. With low glucose DMEM having a lower glucose composition of 1g/L (5.5mM) compared to DMEM/F-12 supplemented with GlutaMAX™ of 3g/L (17.5mM), media with high glucose level 4.5g/L (25mM) in studies has been shown to enhance osteogenic capacity (Wang *et al.*, 2019) and suppresses ectodermal differentiation (Chen *et al.*, 2018). However, for NCs high glucose composition induces senescence and apoptosis (Park and Jong Beom Park, 2013; Park *et al.*, 2015), while low-glucose is linked to NC viability and retention of NC morphology and phenotype (Park and Jong Beon Park, 2013; Humphreys *et al.*, 2018). Therefore, low glucose

may be beneficial for differentiation into NC-like cells, with the recommendation of using osmolality 400mOsm/kg for NC culture (Chapter 2).

SIZE OF CONSTRUCTS

The size of the construct may have played a part of limited iPSC-MEPC observed in the constructs in Phase II study. There is an abundance of research into spheroid size in relation to differentiation, with smaller spheroids differentiating more effectively than larger ones (Farzaneh *et al.*, 2018; Bogacheva *et al.*, 2021), as smaller the constructs have greater access to media and nutrients (Anton *et al.*, 2015). However, in the current study it was the smaller constructs which showed lower cell density. This could also be due to increased migration out of the materials in a smaller volume. Alternatively, in larger constructs the inter-construct environment is less effected by external environment and creates a stable niche.

MESENDODERM PROGENITOR CELLS MORPHOLOGICAL DIFFERENCE WITHIN BIOMATERIALS

The appearance of fragmented nuclear cells was observed in iPSC-MEPC cultured in Albugel from the Phase II and iPSC-MEPC cultured in NPgel from Phase III, interestingly iPSC-MEPCs cultured in NPgel Phase II did not display this feature. Delving into cytology, fragmented nuclear cells could suggest proliferating cells undergoing mitotic prophase displaying a nuclei of irregular shape, however, many other cellular morphological features, such as: apoptotic bodies, darkly stained nuclei, dying or crushed cells can be mistaken for mitotic figures (Ibrahim *et al.*, 2022). The iPSC-MEPCs cultured in NPgel in Phase II were predominantly mono-nuclear cells. However, in Phase II iPSC-MEPC cultured in Albugel and Phase III iPSC-MEPC cultured in NPgel were predominately cells with fragmented nuclei. Ki67 cell proliferation marker was lower in fragmented nuclei iPSC-MEPCs in Phase III iPSC-MEPC cultured in NPgel than in the corresponding biomaterial Phase III iPSC-MEPC cultured in PEG/dNCM, in which the morphology didn't resemble fragmented cells. Initially suggesting that the fragmented nuclear morphology is linked to increased cell death and lower proliferation. However, their fragmented nuclei were not associated with cell death, as there was no difference in Caspase 3 expression between the Phase III, iPSC-MEPCs cultured in NPgel or PEG/dNCM. Nevertheless, apoptotic cells are smaller in size, with a dense, eosinophilic cytoplasm. Whereas the fragmented nuclear iPSC-MEPC appear to have clumped chromatin, with an associated slightly eosinophilic cytoplasm and the absence of nuclear membranes - as seen in mitosis (Ibrahim et al., 2022; Toledo & Oliva, 2008). Additionally, the iPSC-MEPC cell count in NPgel Phase III is consistent throughout the culture period and there is a lack of visible Karyorrhectic cells (a feature of a dead or dying cell, showing dissolved nuclear material), which would demonstrate the later stages of apoptosis, in comparison to iPSC-MEPC cultured in alginate where we see a gradual reduction in cell count and no visible cells at 4-week time point. Giving inconclusive evidence of what the fragmented nuclear cells are.

The observed disappearance and suggested apoptosis of iPSC-MEPC cultured in alginate (Phase III) was an interesting result, as alginate was included as a 'control' biomaterial, due to its common use in *in vitro* 3D culture and has been shown to support growth of stem cells (Zhang *et al.*, 2013; Capeling *et al.*, 2019; Fannon *et al.*, 2021) and disc cells (Le Maitre *et al.*, 2005; Erwin *et al.*, 2011; Gantenbein *et al.*, 2014; Humphreys *et al.*, 2018; Basatvat *et al.*, 2023). Alginate is identified as a soft minimally supportive growth matrix with very limited inherent cell adhesion and cellular interaction (Andersen *et al.*, 2015; Huang *et al.*, 2018; Zhao *et al.*, 2022). The observed decreased iPSC-MEPC cell count and cell death in alginate may be due to lack of adhesive cues as similarly described in Capeling et al., (2019); despite the theory that using a biomaterial that exerts no adhesion and metabolic effect allows the seeded cell to create newly synthesized extracellular components, as chondrocytes and nucleus pulposus cells do in agarose and alginate (Buschmann *et al.*, 1992; Bonaventure *et al.*, 1994). Alternatively, the synthetic biomaterials, PEG/dNCM and NPgel shows more biocompatibility with iPSC-MEPC. Biomaterial properties of stiffness and adhesive ligand presentation can affect stem cell differentiation and proliferating cells (Rowlands *et al.*, 2008; Evans *et al.*, 2009). Adding ECM has been shown to promote differentiation as Liu *et al.,* (2014) cultured iPSC onto NP matrix directly promoted iPSC to successfully differentiate into NC-like cells (Liu *et al.*, 2014; Liu *et al.*, 2015) and stiffer biomaterials support cell-extracellular matrix attachment, cell migration and promotes Mesendoderm differentiation (Evans *et al.*, 2009). Laminin-521 matrix is used in iPSC-MEPC single-cell culture, as laminin-521 interacts strongly with integrins of cells, leading to good adherence and spreading, resulting in cell survival (Rodin, Antonsson, Hovatta, *et al.*, 2014; Rodin, Antonsson, Niaudet, *et al.*, 2014). Alternative matrices, such as Matrigel to which iPSC-MEPC do not attach and survive on, are often supplemented with ROCKi to improve cell attachment (Rodin, Antonsson, Niaudet, *et al.*, 2014; Uhrig *et al.*, 2022). The application of ROCKi to iPSCs can selectively differentiate iPSC towards the mesendodermal lineage (Kurosawa, 2012; Maldonado *et al.*, 2016). As such, it is possible that N2B27 media supplemented with ROCKi resulted in the difference between cell count in Phase II and Phase III, which was also highlighted in spheroid culture; as cell viability was improved with the constant presence of the ROCKi in the differentiation media (Bogacheva *et al.*, 2021). Thus, this study highlights that for iPSC-MEPC survival in constructs *in vitro*, the biomaterial must have adequate stiffness and adherent properties, which is possibly differing qualities that NCs need to synthesis extracellular matrix. This study involved multiple variables, such as different media, construct size, cell origin and biomaterials, which may have influenced the viability of iPSC-MEPC once seeded within a biomaterial system. Further work to directly compare media within one cell and biomaterial system, keeping to one cell origin would be highly advantageous.

The iPSC-MEPCs observed in biomaterials didn't show signs of morphotypical-NCs, as vacuoles and cell clusters were not observed. However, the expression of NC- like phenotypic markers suggested initial differentiation towards this and similar lineages, with higher expression of Brachyury than FOXA2 and SOX9, with extracellular matrix staining demonstrated in the Phase

II study and high expression of Brachyury and Cytokeratin 8, 18 and 19, with extracellular matrix staining in Phase III. These findings are inconsistent with the finding of Sheyn et al., (2019), where iPSC-NC-like cells in an *in vivo* model expressed Cytokeratin 18/19, Brachyury and NOTO but didn't display the typical morphology of an NC. Additionally, there have been studies that injected rat IVD with hydrogels seeded with human iPSCs which observed that the coculture with rat NP cells resulted in the iPSC successfully differentiating into a chondrogenic linage (Hu *et al.*, 2020). This suggests that the environment does have an influence on the differentiation potential of iPSCs.

TRANSLATIONAL POTENTIAL OF MEPCS CULTURED IN BIOMATERIALS

The translational potential of these constructs was also considered. During the Phase III 4-week culture, degradation of some biomaterials constructs was observed. Macroscopically the iPSC-MEPCs cultured in PEG/dNCM constructs began to disintegrate during the culture period; this was also observed in the DMMB analysis, where high amounts of GAGs were detected in the media. Similarly, dNCM was seen to release GAGs into the media in Chapter 3 within NPgel/dNCM constructs following 4-weeks in culture, although in this case the integrity was retained (Chapter 3). Which indicates dNCM leaching out of the hydrogels and into the media; suggests that the biomaterial may require some additional crosslinking to extend the longevity of the PEG/dNCM gels; PEG hydrogels are often used as biodegradable vehicles for therapeutic cell delivery, due to their degradation properties (Martin et al., 2020). This study was conducted *in vitro* setting, to test the translation potential of iPSC-MEPC cultured within biomaterials, these constructs will need to be tested in a more physiological environment to mimic the harsh environment of the degenerative IVD.

CONCLUSION

As limited research has been conducted with iPSC-MEPC in biomaterials, this study screens biomaterials that would respond best for iPSC-MEPCs differentiation to NC-like cells and highlighting different variables which have influence on the viability of iPSC-MEPCs once seeded within a biomaterial system. It was concluded that biomaterials enabled initial iPSC-MEPC encapsulation and facilitated iPSC-MEPC survival. The PEG/dNCM and NPgel biomaterial analysed could have potential to be utilised in the injection of iPSC-NC-like cells into the disc, where they may continue to differentiate into NC-like cells.

ACKNOWLEDGMENTS

This work was supported by the funding received from the European Union's Horizon 2020 research and innovation programme [grant agreement No 825925]. MAT is financially supported by the Dutch Arthritis Society (LLP22). iPSC-MEPCs were generated at INSERM, University of Nantes, France.

CONFLICT OF INTEREST

CLM and CS are named inventors on the patent for NPgel, KB is named inventor on the patent for the albumin/ hyaluronan hydrogel.

CHAPTER 5
CULTIVATING INDUCED PLURIPOTENT STEM CELL DERIVED MESENDODERM PROGENITOR CELLS AS A CELL SOURCE FOR REGENERATING THE NUCLEUS PULPOSUS

CONTEXT OF RESEARCH

As highlighted in Chapter 4, the use of iPSC-MEPC resulted in low viability and low cell numbers after recovery from cryopreservation. Therefore, an investigation into generating iPSC-MEPCs *in situ* was performed, with a focus on refining and optimising the methods of differentiating MEPCs from iPSC, to produce a more efficient cell source. The contribution of research involved demonstrating the limitations associated with the use of iPSC, highlighting issues around viability, cell handling, with emphasis on the implications of inter-laboratory comparisons, and the limitations of distributing cryopreserved cells. All which are highly important factors to take into consideration for clinically translating and upscaling iPSC-MEPC manufacturing.

AUTHORS

Rebecca J. Williams[1,2], Julie Warin[3], Lisanne Laagland[4], Ronak Janani[5], Chris Sammon[5], Anne Camus[3], Mariana A. Tryfonidou[4], Joseph W. Snuggs[1,2], Christine Le Maitre[1,2]

AFFILIATIONS

[1] Department of Oncology and Metabolism, University of Sheffield, UK. [2] Biomolecular Sciences Research Centre, Sheffield Hallam University, UK. [3] Regenerative Medicine and Skeleton, University of Nantes, Nantes, France. [4] Department of Clinical Sciences, Faculty of Veterinary Medicine, Utrecht University, The Netherlands. [5] Materials Engineering research Institute, Sheffield Hallam University, UK.

AUTHOR CONTRIBUTIONS

RJW, CLM and JWS contributed to conception and design of the study; JW, LL and AC generated original iPSC-MEPC differentiation method; RJ, CS, JWS contributed to biomaterial synthesis; RJW contributed to acquisition of laboratory data; RJW performed most of the data analysis; RJW, CLM, JWS contributed to interpretation of the data; RJW, CLM and JWS drafted the manuscript.

DETAILED CONTRIBUTIONS MADE

I conducted experiments: recovery, culturing and maintaining iPSC working cell bank (Fig. 5.5, 5.6 and 5.7), I optimised differentiation methods of differentiating iPSC into MEPCs and imaged daily (Fig. 5.8) alongside performing an cell descriptive analysis of iPSC-MEPCs (Fig. 5.9), I analysed the gene expression of iPSC and differentiated iPSC-MEPCs, with quantitative polymerase chain reaction (Fig. 5.10) and flow cytometry (Fig. 5.11), I compared the fresh and cryopreserved iPSC-MEPC cultured in NPgel for 2 weeks and performed histological (Fig. 5.12) and immunohistochemical analysis (Fig. 5.13). I preformed all data analysis and statistical analysis relating to these experiments and drafted the entire manuscript.

(IN PREPARATION) Cultivating Induced Pluripotent Stem Cell Derived Mesendoderm Progenitor Cells as a Cell Source for Regenerating the Nucleus Pulposus. Rebecca J. Williams, Julie Warin, Lisanne Laagland, Ronak Janani, Chris Sammon, Anne Camus, Mariana A. Tryfonidou, Joseph W. Snuggs, Christine Le Maitre.

ABSTRACT

Lower back pain is common in society and often results in disability and chronic pain. Cellular treatment is becoming a realistic possibility for targeting the regeneration of the intervertebral disc, which has been linked as one of the root causes of lower back pain. Differentiating induced pluripotent stem cells (iPSC) is a powerful, innovative tool in the world of regenerative medicine; allowing the means to generate an abundance of quintessential cells, in our case, notochordal cells (NC) that have the capability of regenerating the intervertebral disc and can be utilised for clinically treatment. However, in the literature the generation of pure populations of NC-like cells has been problematic *in vitro*, as such the utilisation of NC precursors. Therefore, this study demonstrates the cultivation of NC precursors - mesendodermal progenitor cell (MEPC) from iPSCs. A comparison of supplementary factors, involved in the Wnt/ FGF / BMP and NODAL signalling pathways were used in modified methodologies to understand the effects on MEPC culture and differentiation into NC-like cells. The effects of cryopreservation on cells were also investigated and directly compared to uninterrupted culture of MEPCs. Discussion of the translational potential of iPSC derived MEPC and the inter-laboratory comparisons involved. Methodologies excluding cryopreservation produced a higher yield of cells with more differentiation potential. Concluding the challenges involved in iPSC differentiation especially into MEPC require further refinement. However, the iPSC-MEPCs generated from this study, demonstrated positive markers for MEPC differentiation when cultured within the biomaterial systems.

INTRODUCTION

LOWER BACK PAIN AND INTERVERTEBRAL DISC DEGENERTAION

Lower back pain is a common condition that will affect the majority of the population at some point in their lifetime, of which some cases will develop into chronic lower back pain (Andersson, 1999). Individuals that suffer with chronic lower back pain, are left with crippling recurring disability, that has an enormous impact on lifestyles and livelihoods; creating a major socioeconomic burden on healthcare systems and economies (Andersson, 1999; Maetzel and Li, 2002; Hartvigsen *et al.*, 2018). The treatment of lower back pain involves therapeutic pain relief (Bogduk, 2004), which has resulted in contributing to an epidemic of opioid use (Martell *et al.*, 2007; Manchikanti *et al.*, 2012; Deyo *et al.,* 2015; Häuser *et al.,* 2017; Wilson *et al.*, 2020). In literature, there is a lack of evidence of efficacy for opioid use (Deyo *et al.,* 2015), highlighting there is an unmet clinical need for an alternative treatment targeting the pathophysiology of IVD degeneration. Research has deduced that disc degeneration is an associated cause for lower back pain (Luoma *et al.*, 2000) and efforts have been made to understand the underlying causes of disc degeneration. The biological repair of the central part of the IVD, the nucleus pulposus (NP) is now targeted as an approach to regenerate the degenerative disc (Kalson *et al.,* 2008); predominantly focusing on cell-based approaches to restore biomechanical tissue function (Binch *et al.*, 2021; Williams *et al.*, 2021).

CELL-BASED THERAPIES

Using cell-based therapies involving the delivery of viable cells to the disc aims to repopulate and regenerate the tissue which has already experienced a reduction in the functional cell population through apoptosis and senescence during disc degeneration (Le Maitre *et al.,* 2004; Roberts *et al.*, 2006; Le Maitre *et al.,* 2007). Ideally, this approach aims to repopulate and repair the damaged disc by restoring cellular-generated extracellular matrix (Binch *et al.*, 2021; Zhang *et al.*, 2022), as extracellular matrix degradation is one of the main pathological characteristics of disc degeneration (Antoniou *et al.*, 1996). In recent publications, notochordal cells (NC), which are the pre-existing cells in the NP region of the human IVD prior to adulthood, are described as a prime cell choice for synthesizing a proteoglycan-rich matrix and play a protective role in a catabolic environment (Gantenbein *et al.*, 2014; Potier and Ito, 2014; Spillekom *et al.*, 2014; Williams *et al.*, 2021; Bach *et al.*, 2022). To date, NC harvested from porcine origin have been utilised *in vitro* within a set of novel biomaterials (Chapter 3) demonstrating their capabilities of maintaining their phenotype and indicating regenerative potential as an injectable treatment. However, the use of cross-species cells as a potential treatment for clinical disc degeneration has its own limitations. Xenotransplantation of porcine tissue into humans has the effect of hyperacute rejection, where natural human antibodies are directed against and bind to pig antigens. This response from the hosts innate-immune cells recognises differences in the porcine major histocompatibility complex glycosylation patterns, leading to haemorrhage, coagulation, and thrombosis in the human host (Platt *et al.*, 1991; Sachs, 1994; Fishman and Patience, 2004). Another potential obstacle

of the use of porcine cells is the risk of transmitting infectious agents, especially porcine endogenous retroviruses (Mueller and Fishman, 2004). Therefore, an alternative cell source for the generation of NC-like cells needs to be established to enable production of unlimited, ethically sourced, and safe cells.

UTILISING INDUCED PLURIPOTENT STEM CELLS

Generating an alternative source of NC can be implemented by harnessing the utility of induced pluripotent stem cells (iPSCs) (Takahashi *et al.*, 2007). Working cell banks are often generated to offer high amounts of safe cells for therapeutic use, by validating technical specification for cell culture-expansion, biobanking and extensive testing to ensure consistency (Laurent *et al.*, 2020). Once a cell bank is established cells are cryopreserved in vials, stored in liquid nitrogen, and shipped to laboratories that will commence recovery procedure. Our ambition is to utilise a cell bank of allogenic and autogenic NC-like cells that can then be recovered and cultured within biomaterials *in situ*, as an injectable treatment for disc regeneration. Up to now NC-like cells have proven difficult to generate with high cell yield and in pure populations required for regulatory approval. Thus, Mesendoderm progenitor cells derived from iPSC are currently being investigated to be cultured in biomaterials, which will hopefully augment further differentiation into NC -like cells. Previous studies have shown iPSC differentiated into Mesendoderm progenitor cells can survive in biomaterials up to 4 weeks at 5% O_2, 5% CO^2 at 37^{o}C (Chapter 4). However, the main issue raised was the lack of cells observed after the 4-week culture in biomaterials. This was demonstrated to be due to cells being lost during each step of the process: the main decrease was seen during initial cell recovery from cryopreservation, starting with $2x10^6$ cells/mL in a vial to low cell viability after recovery, to ~$5.0x10^5$ cells/cm^3 following seeding at $4x10^6$ cells/mL being observed once seeded into biomaterials (Chapter 4). Usually, working cell banks are characterized by a viability of ~98% after recovery, with successful up-scaling and transport highly important for translational research to be effective (Laurent *et al.*, 2020). Cryopreserving cells have many favourable aspects, from being able to store cells for decades, maximining efficiency and reducing industrial costs (Abbasalizadeh *et al.*, 2017). However, cryopreservation is a crucial step that can affect cell quality (Liu and Chen, 2014).

Within this study, an analysis of factors needed for iPSC differentiation to MEPCs, together with influence of recovery from cryopreservation, was investigated to refine the process for clinical development of MEPC, which can then be used for further studies investigating injectable treatments for disc regeneration. Here, the step-by-step cultivation of MEPCs derived from iPSC (iPSC-MEPC) was investigated, followed by seeding into biomaterials to compare iPSC-MEPCs that haven't been subjected to freezing, thaw recovery process and to iPSC-MEPCs that were subject to recovery (which mimics the method iPSC-MEPCs were subject to in Chapter 4). IPSC-MEPCs were analysed during culture for visual morphology and for phenotypic marker expression. The iPSC-MEPCs and biomaterial constructs were analysed for cell phenotype, NC characteristics and the expression of extracellular matrix markers using

histological and immunohistochemical staining. This study analyses the cultivation and fine tuning of iPSC-MEPCs for the proposal of using this cell source for potentially regenerating the IVD.

METHODS

EXPERIMENTAL DESIGN

Commercial iPSCs were recovered and grown *in situ*, with analysis of morphology and phenotypic expression. Next, the method of differentiating iPSC into MEPCs were critically analysed, investigating the use of factors at influence of time course of treatments, and to highlight the effect of replating and cryopreserving cells. After iPSC-MEPCs were generated, these cells were also analysed morphologically and phenotypically. Next, these *in situ* iPSC-MEPCs were cultured within NPgel (n=2, used in Chapter 3 and 4), alongside cryopreserved and recovered iPSC-MEPC cultured in NPgel (n=2) for 2 weeks within physioxic conditions in relation to the IVD physiological conditions (Fig. 5.2). This study was implemented to investigate the effects of cryopreservation and recovery on the final regenerative potential of iPSC-MEPC when cultured in biomaterials for the use in IVD regeneration.

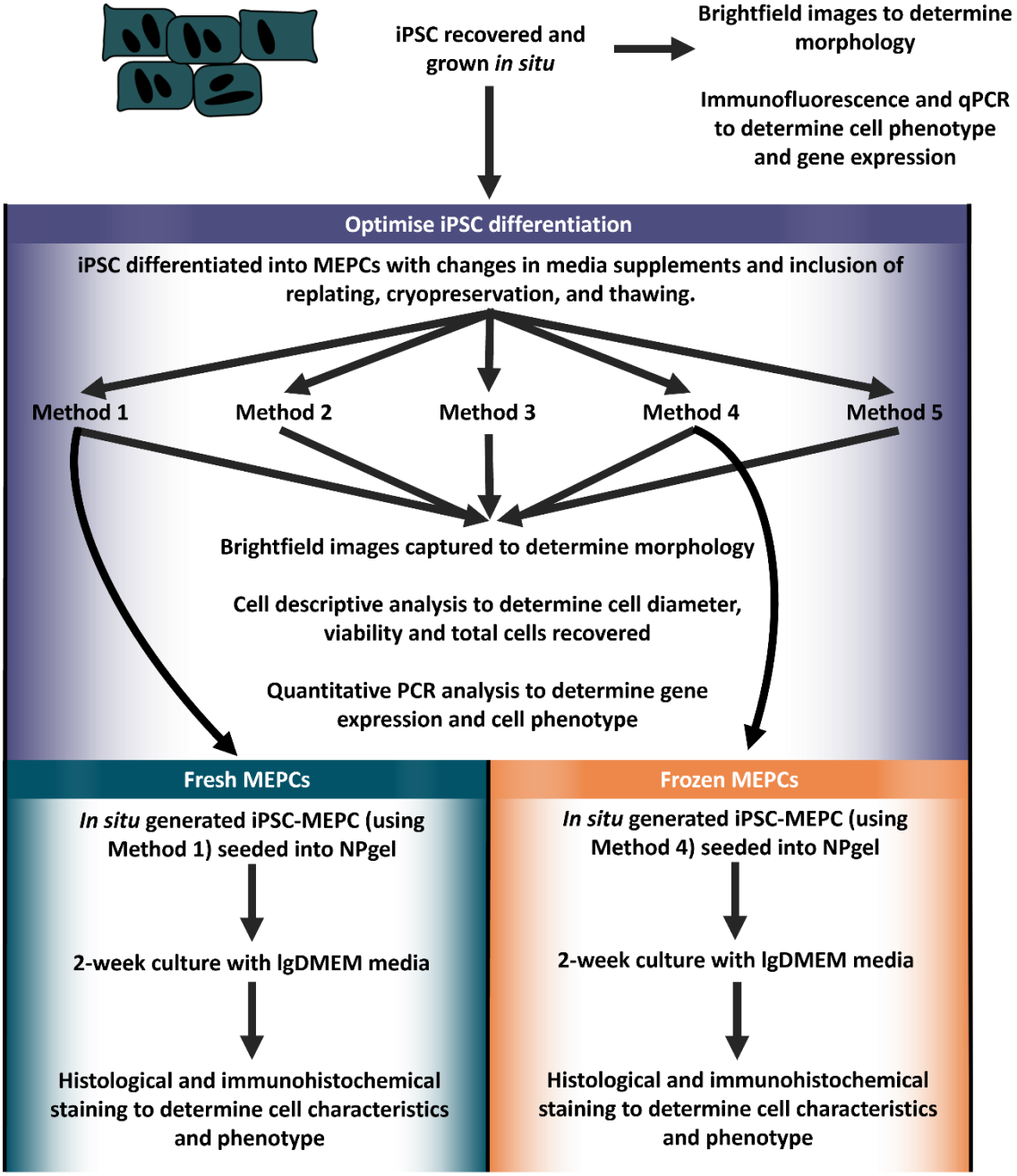

Figure 5.1. Illustration representing the experimental design. *Gibco® Human Episomal induced pluripotent stem cells (iPSC) line (2329323, Life technologies, Madison, USA) were recovered and growth in situ, prior to being differentiated into Mesendoderm progenitor cells (MEPCs) via 5 different methods (Method 1, Method 2, Method 3, Method 4, and Method 5). Generated iPSC derived MEPCs from Method 1 (fresh MEPCs) and Method 4 (Frozen/cryopreserved MEPCs) were seeded into NPgel and cultured for 2 weeks with lgDMEM (DMEM, low glucose, glutaMAX™ (life technologies, Paisley, UK) containing P/S 50U/mL (Life Technologies UK), amphotericin B 2.5ug/mL (Sigma, Dorset, UK), L-ascorbic acid 25ug/mL (Sigma, Dorset, UK), 1% Insulin-transferrin-Selenium v/v (ITS-X), 1% L-glutamine v/v (life technologies, UK), L-proline 40ug/mL (Life technologies, UK) and Albumax 1.25mg/mL (Life technologies, UK)) at 5% v/v oxygen, 37°C. illustration also shows the downstream analysis and staining performed during the study.*

THAWING INDUCED PLURIPOTENT STEM CELLS

Gibco® Human Episomal iPSC line (2329323, Life technologies, Madison, USA) was thawed rapidly using a sterile 37^{o}C water bath and gently resuspended in 1mL of mTeSR™ Plus Medium (comprised of 100mL mTeSR™ Plus 5X supplement (Stemcell technologies, Cambrigde, UK) to 400mL of mTeSR™ Plus Basal Medium (Stemcell technologies, Cambridge, UK) supplemented with 10µM ROCK inhibitor Y-27632 (ROCKi; StemCell technologies, Cambridge, UK), so that a single piece of ice remains, before transferring to a 15mL falcon and gently add 5mL of mTeSR™ Plus Medium w/o ROCKi. The iPSC suspension was then centrifuged at 200*g* for 5 minutes at room temperature and gently resuspend in 1mL of mTeSR™ Plus Medium with 10µM ROCKi. IPSC suspension was plated at 6.87x10^{4}cells/cm^{2} or 1.37x10^{5} cells/cm^{2} (or 330µL and 660µL of the 1mL iPSC suspension per well) onto a precoated Falcon® 6 well plate (Corning, Flintshire, UK) with diluted 1% Geltrex™ LDEV-Free, hESC-Qualified, Reduced Growth Factor Basement Membrane Matrix (Life technologies, NY, USA) in DMEM-F12 (ThermoFisher, Massachusetts, USA). Plates were rocked prior to placing into the 37^{o}C incubator to get an even distribution of cells and incubated at 37^{o}C, 21% O_2, plates were left undisturbed for 24 hours to allow for the iPSCs to adhere.

INDUCED PLURIPOTENT STEM CELL MAINTENANCE, PASSAGING AND CRYOPRESERVATION

IPSCs were visualised daily for the assessment of the size and density of the plated cell aggregates. IPSCs were fed every other day, with 2mL per well of a 6 well plate with mTeSR™ Plus Medium (comprised of 100mL mTeSR™ Plus 5X supplement (Stemcell technologies, Cambrigde, UK) and 400mL of mTeSR™ Plus Basal Medium (Stemcell technologies, Cambridge, UK). IPSCs were passaged when most colonies were large, compact, and showed dense centres, which appeared bright (Fig. 5.2 And Fig. 5.3a), which was subject to plating at high density, typically iPSCs were passaged every 4-5 days (Fig. 5.2; iPSC ready to passage indicated by *). When appropriate to passage, media was aspirated and iPSC were washed twice with Dulbecco's Phosphate Buffered Saline (1X) without Calcium and Magnesium (DPBS w/o Ca^{2+} / Mg^{2+}; Lonza, Manchester, UK) and 1mL of ReLeSR™ (Stemcell Technologies, Cambridge, UK) was added to each well for <1 minute before aspirating. Next, the plate was incubated at 37°C for 5-6 minutes and visualised to check when bright gaps appeared between cells, before 1mL of mTeSR™ Plus Medium was added. Colonies were further dissociated into clumps of approximately 50-200µm (Fig. 5.3b) in size by tapping for approximately 30 seconds and pipetted with a 5mL pipette to break up cell aggregates. The concentration of cell aggregates was both manually and automatically counted (Fig. 5.3). For manual aggregated count, 5µL suspension was combined with trypan blue and placed within a haemocytometer for counting the number of clumps in a field of view under a microscope (for example 200 clumps, 400 clumps and 800 clumps (Fig. 5.2)). Alternatively, automated cell count was performed with 10µL of iPSC suspension diluted with 990µL mTeSR™ Plus Medium and loaded into the Via1-Cassette™ (Chemometec, Allerod, DK) and read with the NucleoCounter® NC-200™ (Chemometec, Allerod, DK) to provide a viability and cell count. Cells were replated at 200,

400 or 800 aggregates or $6.87x10^4$ cells/cm^2 onto precoated Falcon® 6 well plate (353046, Corning, Flintshire, UK) with diluted 1% Geltrex™ LDEV-Free, hESC-Qualified, Reduced Growth Factor Basement Membrane Matrix (Life technologies, NY, USA) in DMEM-F12 (ThermoFisher, Massachusetts, USA). The plates were rocked prior to placing into the 37°C incubator to get an even distribution of cells and incubated at 37°C, 21% O_2. For cryopreservation of iPSC cells, iPSCs were passaged as described above and iPSC suspension was centrifuged at 200*g* for 5 minutes at room temperature. The supernatant was then aspirated, and the cell pellets were resuspended in 1mL of CryoStor® CS10 (Stemcell technologies, Cambridge, UK) at a cell density of $2.0x10^6$ cells/mL and transferred to cryovials. Cryovials were then frozen at -80°C for 24 hours within a MrFrosty™ freezing container, followed by long term storage in at -135°C (liquid nitrogen).

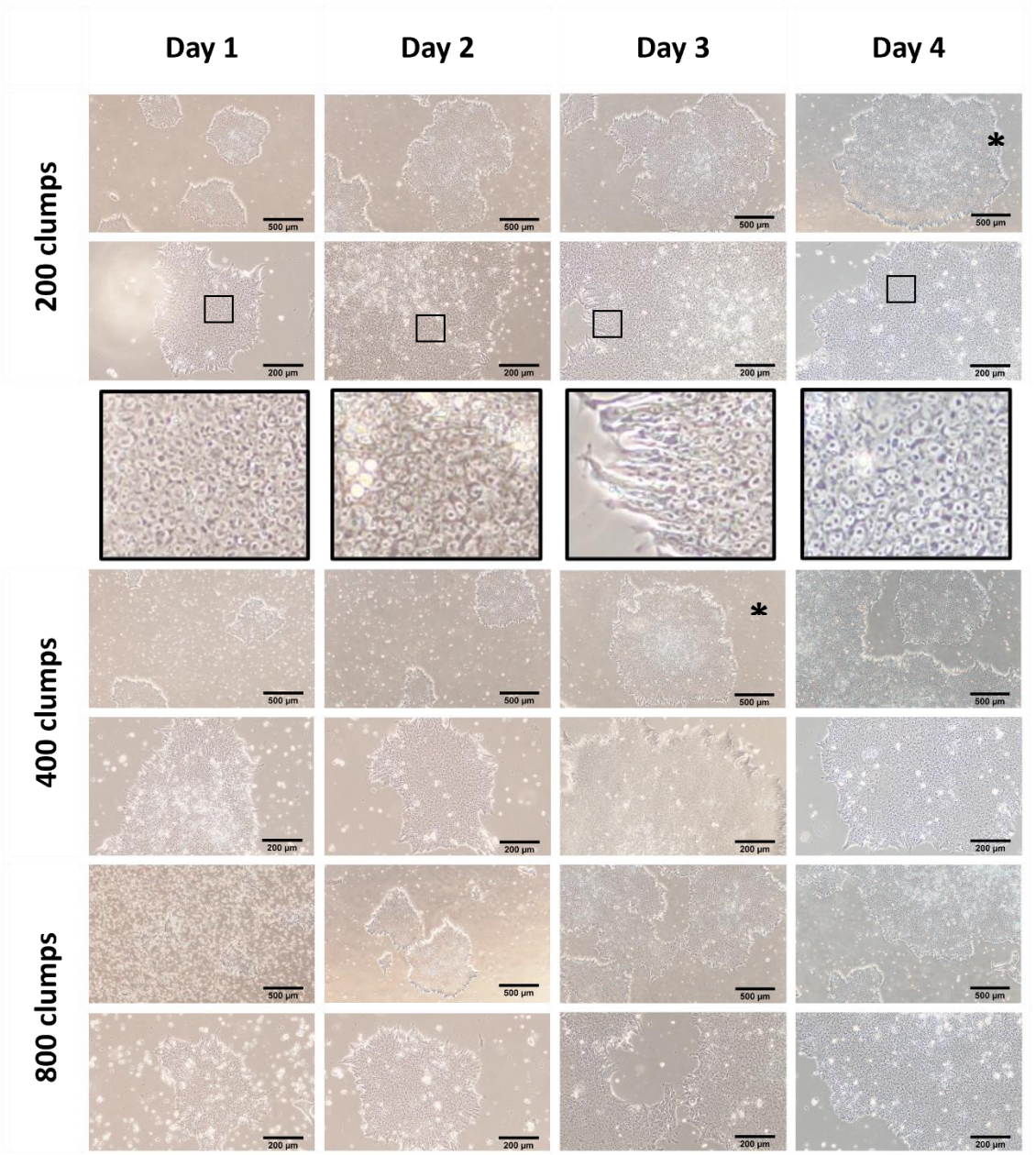

Figure 5.2. Brightfield live images of Gibco ® Human Episomal induced pluripotent stem cell (IPSC) line *(2329323, Life Technologies, Madison, USA) cultured in mTeSR™ Plus Medium (Stemcell technologies, Cambrigde, UK) at 21% v/v oxygen, 37°C and imaged daily after passaging; IPSCs were passaged by number of cell aggregates (200, 400 and 800 clumps), which is correlated to the colony density observed at the next passage. IPSC were ready to passage when the majority of colonies were large, compact and have centres that are dense and appear bright (as seen in images with *). Black box indicated zoomed images. Scale bar 500µm and 200µm.*

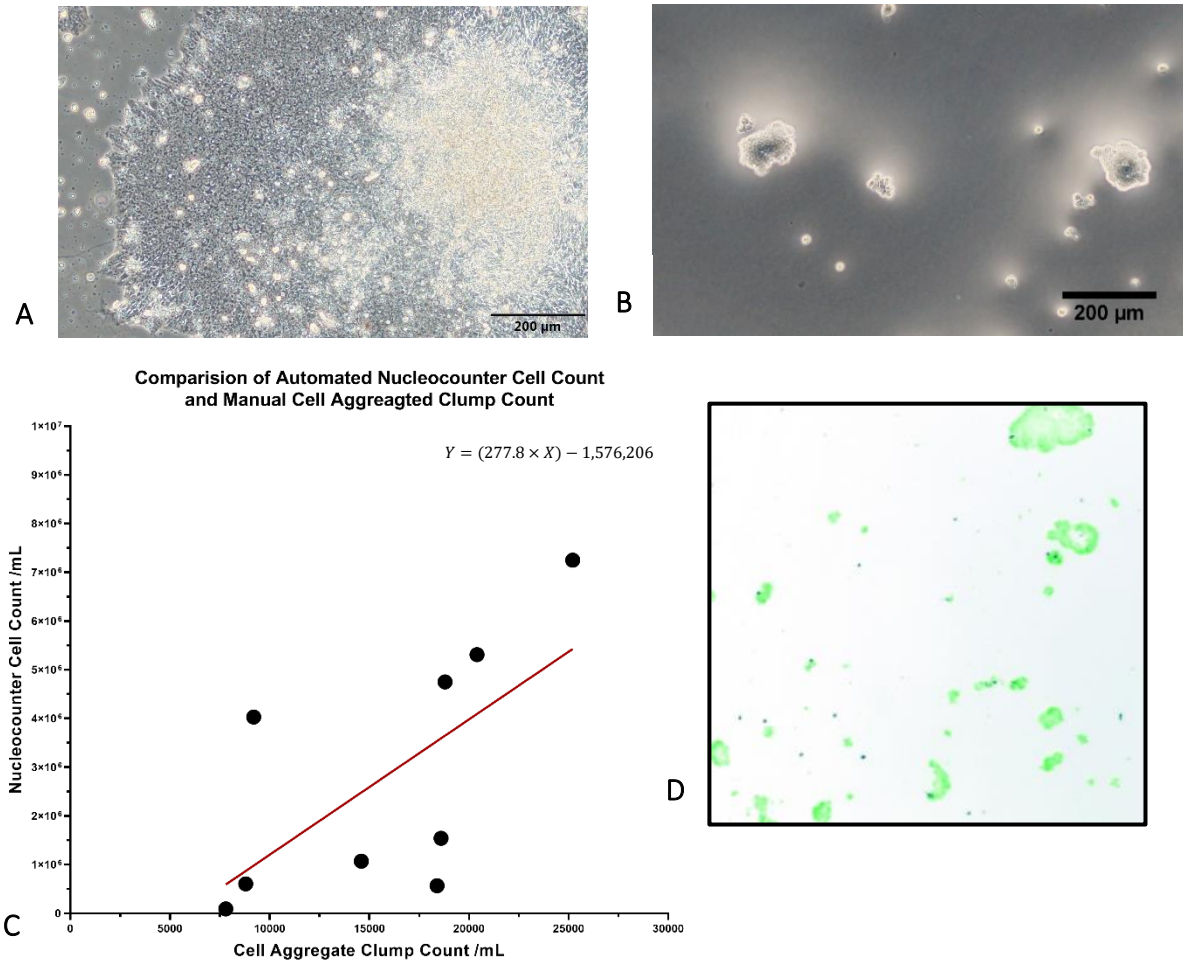

Figure 5.3. Method of counting Induced pluripotent stem cells*. Brightfield live images of Gibco ® Human Episomal induced pluripotent stem cell (iPSC) line (2329323, Life Technologies, Madison, USA)* ***(A)*** *demonstrating optimal morphology for passaging and* ***(B)*** *demonstrating optimal aggregate size after passaging with ReLeSR™ (Stemcell Technologies, Cambridge, UK), aggregate size should be around 50-200µm in size.* ***(C)*** *Comparing the method of counting aggregated iPSC during passaging. X axis represents the manual cell count of iPSC clumps /mL against the y axis of manual cell count using a NucleoCounter® NC-200™ (Chemometec, Allerod, DK).* ***(D)*** *image generated from Nucleocounter® NC-200™, AO highlights all cells and DAPI stains dead cells. Scale bar 200µm.*

INDUCED PLURIPOTENT STEM CELL DIFFERENTIATION

To differentiate iPSC into MEPCs, iPSCs were passaged as described above and were seeded at 2.0x10^4 cells/cm^2 onto precoated Falcon® 6 well plate (Corning, Flintshire, UK) with 5µg/mL Laminin-521 (Corning, Flintshire, UK) diluted in PBS Ca^{2+} / Mg^{2+} (Sigma, Dorset, UK), for the analysis of five different differentiation methods (Fig. 5.4). Method 1, which resembled the method carried out by our collaborators (Chapter 4) which included two phase transition; firstly, exposing the iPSCs to a different matrix, laminin-521 (Corning, Flintshire, UK) for 48 hours, then treating the iPSCs to different media N2B27 media (Chapter 4; Table 4.1) supplemented with CHIR99021 (3µM; Miltenyi, Surrey, UK), for an additional 48 hours. Method 2 used N2B27 media supplemented with CHIR99021 (3µM; Miltenyi, Surrey, UK) and Noggin (100ng/mL; Miltenyi, Surrey, UK) at day 3 and 4 to resemble the media used in iPSC-

MEPC recovery after thawing. For Method 3, iPSC were replated and had an extra 24 hours (day 5) of culture with N2B27 media supplemented with CHIR99021 (3µM; Miltenyi, Surrey, UK), Noggin (100ng/mL; Miltenyi, Surrey, UK) and ROCKi (10µM; StemCell technologies, Cambridge, UK), to resemble the method of iPSC-MEPC differentiation, and recovery period used post cryopreservation used from our collaborators to our lab (Chapter 4), but without subjecting the cells through cryopreservation/thawing process. For Method 4, at day 5, cells were cryopreserved and thawed prior to being recovered for 24 hours with N2B27 media supplemented with CHIR99021 (3µM; Miltenyi, Surrey, UK), Noggin (100ng/mL; Miltenyi, Surrey, UK) and ROCKi (10µM; StemCell technologies, Cambridge, UK) to mimic the process performed within Chapter 4. For Method 5, N2B27 media supplemented with CHIR99021 (3µM; Miltenyi, Surrey, UK), Noggin (100ng/mL; Miltenyi, Surrey, UK) and ROCKi (10µM; StemCell technologies, Cambridge, UK) was immediately added for 48 hours, to investigate whether the cells required the phased transition on laminin-521.

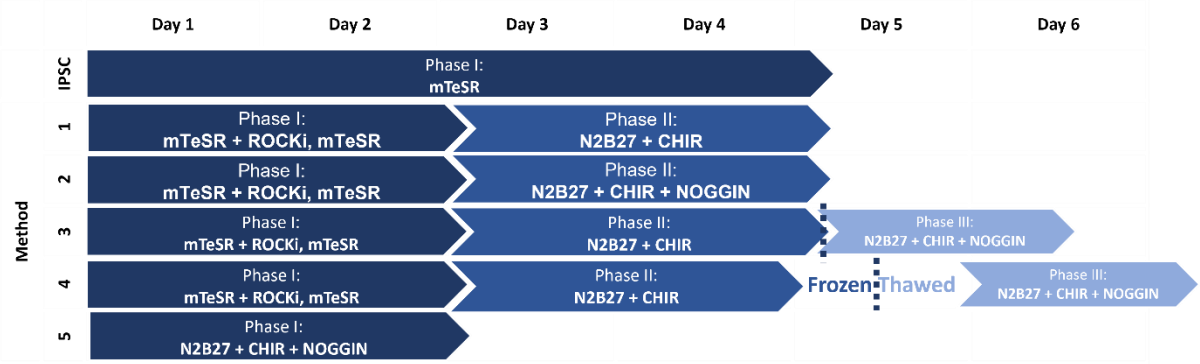

Figure 5.4. Illustration displaying the optimisation of differentiation method used to differentiate iPSC into MEPCs: *involving culturing IPSC for up to 6 days at 21% v/v oxygen, 37°C with differing media and supplements. Dashed line indicates where cells were replated.*

QUANTITATIVE POLYMERASE CHAIN REACTION

During passaging, cells were also taken for quantitative reverse transcription polymerase chain reaction (qRT-PCR), following media aspiration and PBS washing, 1x10^{6}cells/mL were lysed in Trizol (Life technologies, Paisley, UK) for 10 minutes at room temperature. To extract RNA, chloroform (Sigma, Dorset, UK) was added, and the cell samples were then vortexed and left to stand for 10 minutes at room temperature before centrifugation at 12,000*g* for 15 minutes at 4°C. From the separated mixture, the transparent, aqueous ribonucleic acid (RNA) layer was collected and 500µL of isopropanol (Sigma, Dorset, UK) was added to precipitate RNA. Samples were stored in isopropanol for ≥ 1 hour at -80°C, prior to centrifugation at 12,000*g* for 15 minutes at 4°C. Supernatant was removed and the pellet was then washed with molecular grade ethanol (Sigma, Dorset, UK) and centrifuged for 5 minutes at 7,500*g*. Supernatant was removed, and the pellet was air-dried for 5 minutes. Finally, RNA was resuspended in 14µL RNase-free water and incubated at 60°C for 5 minutes and subsequently converted to cDNA. Thirty-six microlitres of reverse transcriptase master mix (100U BioScript™ reverse transcriptase, 13.9% [v/v] BioScript™ 5× reaction buffer, 1.7 mM dNTPs [Bioline],

1.4µM random hexamers [Thermo] in RNase-free water) was added per 14µL of RNA sample. Samples were incubated in a PCR thermocycler programmed to hold samples at 42^{o}C for 2 hours to synthesize cDNA, followed by 10 minutes at 80^{o}C to denature the BioScript™ reverse transcriptase enzyme and stored on ice at 4°C prior to RT-PCR analysis. To each well of a 96-well FAST PCR plates (Life technologies, Paisley, UK) 2µL of DNA sample was added in combination with 0.5µL Taqman™ predesigned Primers (Table 5.1; Life technologies, Paisley, UK), 5µL 2xTaqman™ fast master mix (Life technologies, Paisley, UK) and 2.5µL sterile deionised H_20. The plate was sealed with MicroAmp™ optical adhesive film (Life technologies, Paisley, UK), and read in an Applied Biosystems QuantStudio™ 3 real time PCR machine (Life technologies, Paisley, UK) to determine the expression of target genes in samples. Gene expression was normalized to the mean of housekeeping genes GAPDH and 18S levels and data was analysed according to the $2^{-\Delta Ct}$ method (Basatvat *et al.,* 2023).

Table 5.1. TaqMan™ gene expression assays (Life technologies, Paisley, UK) used in quantitative polymerase chain reaction for the assessment of induced pluripotent stem cells and Mesendoderm progenitor cells, *and the target for gene expression.*

TaqMan™ Primers	Assay ID	Target
T (Brachyury)	Hs00610080_m1	Mesendoderm, mesoderm lineage and notochordal marker
LEF1	Hs01547250_m1	Definitive endoderm marker
NODAL	Hs00415443_m1	Mesoderm marker
LEFTY1	Hs00764128_s1	Definitive endoderm marker
FOXA2	Hs05036278_s1	Mesendoderm and endoderm lineage marker
SOX9	Hs00165814_m1	Mesoderm marker
SHH	Hs00179843_m1	Mesoderm marker
NOGGIN	Hs00271352_s1	Endoderm marker
GAPDH	Hs99999905_m1	Housekeeping genes
18S	HS99999901_s1	Housekeeping genes

FLOW CYTOMETERY

During passaging, cells were also fixed for flow cytometry, 2x10^{5} cells per stain were fixed with 1mL of 4% paraformaldehyde for 10 minutes at room temperature. Cells were then washed twice with DPBS w/o Ca^{2+} / Mg^{2+} (Lonza, Manchester, UK) and centrifuged at 200*g* for 10 minutes at room temperature. Cells were then permeabilized for 10 minutes with 0.1% v/v

Triton™ X-100 (Sigma, Dorset, UK) diluted in DPBS w/o Ca^{2+} / Mg^{2+} (Lonza, Manchester, UK) with 10% v/v normal serum depended on the secondary antibody species: normal donkey serum (ab7475, Abcam, Cambridge, UK) and normal Rabbit Serum (ab7487, Abcam, Cambridge, UK). The cells were then centrifuged again at 200*g* for 10 minutes, before a primary antibody was applied (Table 5.2; diluted in DPBS w/o Ca^{2+} / Mg^{2+} (Lonza, Manchester, UK) with 0.1% w/v bovine serum albumin (BSA; Sigma, Dorset, UK) and incubated for 1 hour at 4^{o}C. Next, cells were washed twice in staining buffer, consisting of DPBS w/o Ca^{2+} / Mg^{2+} (Lonza, Manchester, UK) with 5% v/v normal serum depended on the secondary antibody species and 0.1% v/v Tween®20 (Sigma, Dorset, UK). Followed by incubation with secondary antibodies ((Donkey anti-goat Alex Flour® 488 (Life technologies, Paisley, UK) Donkey anti-rabbit Alex Flour® 594 (Life technologies, Paisley, UK) and Goat anti-mouse Alex Flour® 488 (ab150113, Abcam, Cambridge, UK)) diluted in staining buffer for 2 hours at 4^{o}C. The cells were then washed twice in staining buffer for 5 minutes, prior to being resuspended in 500µL of staining buffer and analysed using a CytoFLEX LX flow cytometer (Beckman Coulter, IN, USA) and FlowJo™ v10.8.1 software (BD life Science, OR, USA).

THAWING MESENDODERM PROGENITOR CELLS

A cryo-vial of 2 million iPSC-MEPCs (generated as described above) was thawed as described in detail in Chapter 4 (Thawing Mesendoderm progenitor cells).

MESENDODERM PROGENITOR CELL DISSOCIATION AND CELL COUNT

Twenty-four hours after thawing, iPSC-MEPCs are visualised using Olympus IX81 Motorized Inverted System Microscope (Olympus Europa GMBH, Germany) and dissociated following the protocol as described in Chapter 4 (Mesendoderm progenitor cell dissociation and cell count). Cell count was performed with a sample of iPSC-MEPCs suspension using a NucleoCounter® NC-200™ (Chemometec, Allerod, DK), as described in Chapter 2 (Calculating cell number).

SEEDING MESENDODERM PROGENITOR CELLS INTO NPGEL

For seeding, suspended iPSC-MEPCs were centrifuged, and media was aspirated, but a little remained to resuspend the cell pellet prior to the addition of biomaterial NPgel. NPgel was prepared as previously described by Thorpe *et al.,* (2016) and in Chapter 3 (NPgel preparation). IPSC-MEPCs were seeded at 4x10^{6} cells/mL into the NPgel, as described in Chapter 4 (Seeding Mesendoderm progenitor cells into Phase I biomaterials). Three hundred microlitres of the cell and biomaterial constructs were extruded through a 27-gauge needle to mimic injection into the disc into 48 well culture plate. Duplicate technical repeats were generated of cryopreserved and fresh iPSC-MEPCs cultured in NPgel for 2-week at 5% O_2, 5% CO_2 at 37^{o}C, with 500µL of lgDMEM media (as described in Chapter 4; Seeding Mesendoderm Progenitor Cells Into Phase III Biomaterials).

HISTOLOGY ANALYSIS

MEPC phenotype and matrix deposition was investigated in fresh and cryopreserved iPSC-MEPCs in NPgel following 2 weeks in culture. After culture samples were fixed, embedded into wax, and sectioned as described in Chapter 3 (Histological analysis). Sections were dewaxed, rehydrated, and assessed using histological stains. H&E: Alcian Blue (pH 2.5): Masson's Trichrome (Atom Scientific Ltd, Hyde, UK): Safranin O/ Fast green (described in detail in Chapter 3; Histological analysis). After specific histological staining, sections were dehydrated three times for 10-minute washes in IMS, cleared in Sub-X three times for 10-minute and mounted in Pertex (Leica Microsystems, Newcastle, UK). All slides were examined with an Olympus BX51 microscope and images captured by digital camera and Capture Pro OEM v8.0 software (Media Cybernetics, UK). Histological sections were analysed, and representative images captured to document their histological appearance and cellular staining patterns.

IMMUNOHISTOCHEMISTRY ANALYSIS

Immunohistochemistry (IHC) as previously reported (Binch et al., 2020) and as described in Chapter 3 (Immunohistochemistry and immunofluorescence analysis), was also performed on iPSC-MEPCs cultured in biomaterials. Specific antibodies were used to target antigens in relation to iPSC, MEPC and NC phenotype along with NP matrix markers (Table 5.2).

IMMUNOFLUORESCENCE ANALYSIS

Immunofluorescence (IF) staining of samples was performed as described in Chapter 3 (Immunohistochemistry and immunofluorescence analysis) using antigen retrieval methods as detailed in Table 5.2. On samples with Phalloidin staining, 0.01% v/v Phalloidin-iFluor 594 (ab176757, Abcam, Cambridge, UK) diluted in 1mL DPBS w/o Ca^{2+} / Mg^{2+} (Lonza, Manchester, UK) with 1% BSA (Sigma, Dorset, UK) was added. To determine nuclear localisation sections were counterstained with DAPI using Vectashield® DAPI mountant (Sigma, Dorset, UK).

Table 5.2. Immunohistochemical, immunofluorescence and flow cytometry procedures utilised for phenotypic characterisation of porcine notochordal cells. *Primary antibody target, clonality, dilutions optimised and antigen retrieval. Including the secondary antibodies and dilutions, which were used for immunohistochemical, immunofluorescence staining and flow cytometry.*

Primary Antibody	Target	Clonality	Optimal dilution	Antigen retrieval	Technique	Secondary Antibody	Optimal dilution
Aggrecan (AB3778, Abcam)	NP matrix	Mouse monoclonal	1:100	Heat	IHC	Rabbit Anti-Mouse (Ab6727, Abcam)	1:500
Brachyury (AF2085, Bio-techne)	NC/NP marker	Goat polyclonal	1:500	None	IHC	Donkey Anti-Goat (Ab208000, Abcam)	1:500
					Flow, IF	Donkey Anti-Goat (Alex Flour™ 488; A-11055, Life technologies)	1:500
Caspase 3 (AB4051, Abcam)	Apoptosis Marker	Rabbit polyclonal	1:400	None	Flow, IF	Donkey Anti-Rabbit (Alex Flour™ 594; A-21207, Life technologies	1:500
Collagen Type II (MAB1330, Sigma)	NP matrix	Mouse monoclonal	1:200	Enzyme	IHC	Rabbit Anti-Mouse (Ab6727, Abcam)	1:500
Cytokeratin 8 + 18 + 19 (AB41825, Abcam)	NC/NP marker	Mouse monoclonal	1:400	Enzyme	IHC	Rabbit Anti-Mouse (Ab6727, Abcam)	1:500
					Flow, IF	Goat anti-mouse (Alex Flour™ 488, ab150113, Abcam)	1:500
FOXA2 (D56D6, Cell signalling)	NLC marker	Rabbit monoclonal	1:400	Heat	IHC	Goat Anti-Rabbit (Ab6720, Abcam)	1:500
					Flow	Donkey Anti-Rabbit (Alex Flour™ 594; A-21207, Life technologies	1:500
SOX9 (AB5535, Abcam)	NLC and NP marker	Rabbit polyclonal	1:1000	None	IHC	Goat Anti-Rabbit (Ab6720, Abcam)	1:500
					Flow	Donkey Anti-Rabbit (Alex Flour™ 594; A-21207, Life technologies	1:500

QUANTIFYING HISTOLOGICAL AND IMMUNOHISTOCHEMICAL STAINED SLIDES

Histological and immunohistochemical stained slides where quantified as described in Chapter 4 (Quantifying histological and immunohistochemical stained slides).

DIMETHYLMETHYLENE BLUE ASSAY

Media samples were collected during every media change during the culture of the iPSC-MEPCs in biomaterial constructs and stored at -80^{o}C. Dimethyl methylene Blue (DMMB) reagent was generated and preformed as previously described in Chapter 3 (Dimethylmethylene Blue Assay).

STATISTICAL ANALYSIS

Statistics were performed in Graphpad prism 9.5.1. The normality of the data was assessed using the Shapiro-Wilk test. Differentiated iPSC-MEPCs descriptive analysis data and gene expression data of differentiated iPSC into MEPCs optimisation experiment was assess as normally distributed and therefore analysed by one-way ANOVA test followed by turkey's multiple comparison test, comparing between each differentiation method. The Flow

cytometry data demonstrating the percentage of positive cells for specific antibodies was assessed with Mann-Whitney test on iPSC and MEPC group. The GAG production of fresh or cryopreserved iPSC-MEPCs seeding in NPgel and then cultured for 2 weeks was normally distributed and analysed using t test to compare the difference between fresh and cryopreserved iPSC-MEPCs cultured in NPgel. Statistical significance was accepted at $p \leq 0.05$.

RESULTS

CULTURE AND MAINTENANCE OF INDUCED PLURIPOTENT STEM CELLS

The progression of cell morphology from the first day of thawing to day 4, changed from spindle shaped cells at day 1 to cobble shaped cells by day 3 (Fig. 5.5). By day 4 the iPSC cells resembled undifferentiated cells, that were tightly packed and exhibited a typical morphology of high-nuclear-to cytoplasm ratio, with a prominent nucleolus (Fig. 5.5). IPSCs plated at a density of $1.37x10^5$ cells/cm^2 showed more suspended cells, when compared to the lower plated density of $6.87x10^4$ cells/cm^2. Whilst non-adherent cells which remained in suspension had an average viability of 9.3% and did not reattach upon replating (Fig. 5.6).

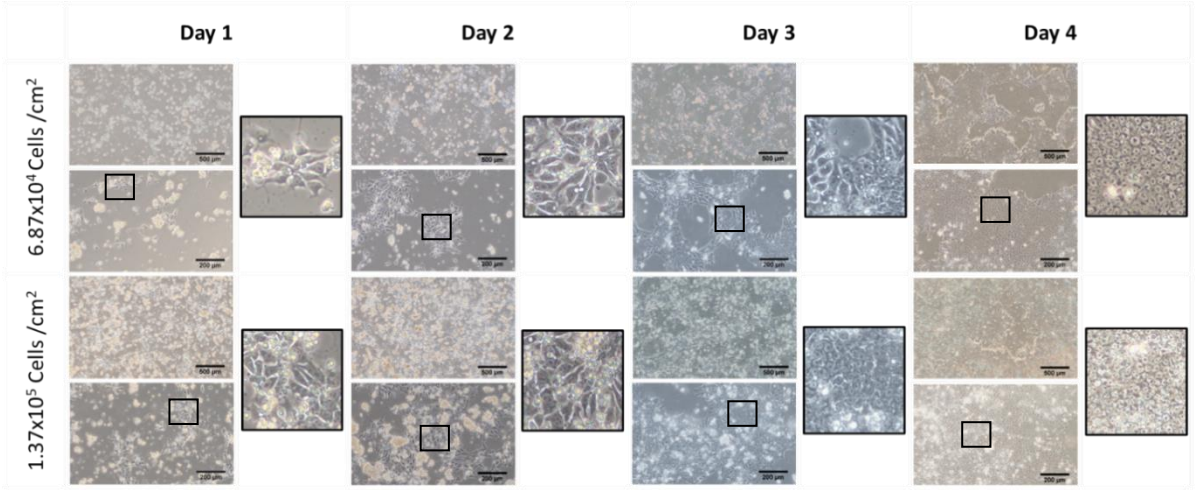

Figure 5.5 Brightfield live images of Gibco ® Human Episomal induced pluripotent stem cell (iPSC) line (2329323, Life Technologies, Madison, USA) imaged daily*, after thawing with mTeSR Plus (Stemcell technologies, Cambridge, UK) supplemented with ROCK inhibitor Y-27632 (Stemcell technologies, Cambridge, UK) at 21% v/v oxygen, 37^{o}C. Cells were plated at densities of $6.87x10^4$ Cells/cm^2 and $1.37x10^5$ cells/cm^2. Scale bar at 500µm and 200µm.*

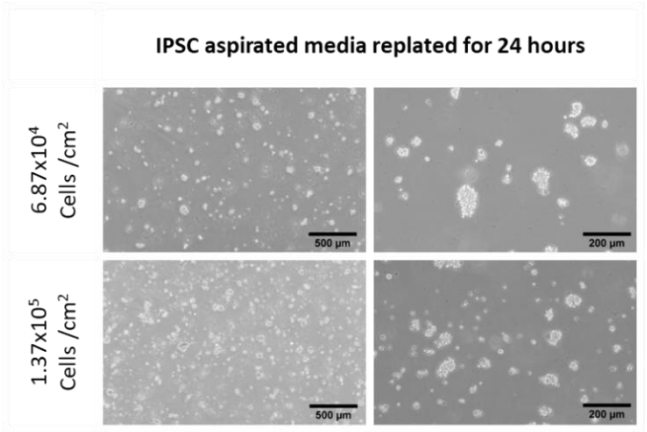

Cell viability and Count Assay

	1	2	3	4	Average
Total cell/ml	$8.81x10^4$	$1.08x10^5$	$9.49x10^4$	$7.61x10^4$	$9.18x10^4$
Viability %	15.4	12.5	0	9.1	9.3%

Figure 5.6. Brightfield live images of media aspirated from culture plate of Gibco ® Human Episomal induced pluripotent stem cell (iPSC) line *(2329323, Life Technologies, Madison, USA) (which were plated at densities of $6.87x10^4$ cells/cm^2 and $1.37x10^5$ cells/cm^2) (n=4 technical repeats). The aspirated media was replated and cultured for 24 hours with mTeSR Plus (Stemcell technologies, Cambridge, UK) supplemented with ROCK inhibitor Y-27632 (Stemcell technologies, Cambridge, UK) at 21% v/v oxygen, 37^{o}C. Scale bar at 500µm and 200µm.*

Undifferentiated iPSCs expressed FOXA2, NOGGIN and LEFTY1, with limited expression of Lymphoid Enhancer Binding Factor 1 (LEF1), SOX9, SHH, NODAL and Brachyury (Fig. 5.7a). The expression of these markers was also sustained throughout the passages (Fig. 5.7b). Strong immunofluorescence staining for FOXA2 was observed in comparison to Brachyury and caspase 3 (Fig. 5.7c).

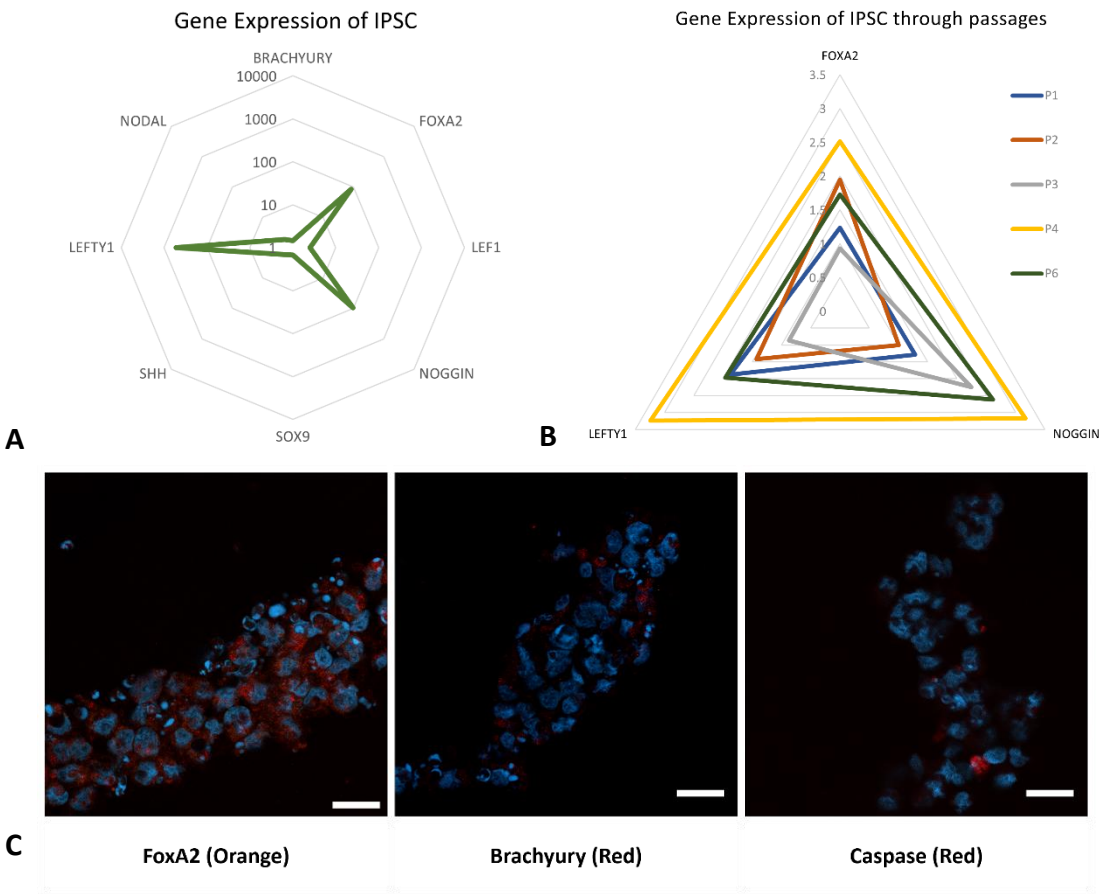

Figure 5.7. Gene expression of Gibco ® Human Episomal induced pluripotent stem cell (iPSC) line (2329323, Life Technologies, Madison, USA) (A) *with an in-depth analysis of gene expression for Brachyury, FoxA2, LEF1, Noggin, SOX9, SHH, LEFTY1 and Nodal at passage 6 (n=3 technical repeats).* ***(B)*** *in relation to FOXA2, LEFTY1, NOGGIN throughout multiple passages* ***(C)*** *immunofluorescence images of iPSC and stained for FOXA2, Brachyury and Caspase 3.*

MORPHOLOGICAL AND DISCRIPTIVE ANALYSIS MESENDODERM PROGENITOR CELLS SUBJECT TO DIFFERING DIFFERENTIATION METHODS

At passage 6, when iPSCs were stable, iPSC differentiation was investigated. Here, different methods of differentiating iPSC to MEPCs with changes in media supplements and inclusion of replating, cryopreservation, and thawing (Fig. 5.8a). The morphology of the cells did not change depending on methodology (Fig. 5.8). However, the replating (Fig. 5.8; Method 3, dotted line) and cryofreeze/ thawing (Fig. 5.8; Method 4) generated spindle shaped cells, which resembled the iPSCs at day 1 of methods 1,2,3 and 4 (Fig. 5.8a and b); whilst in Method 5, no spindle shaped cells were observed at day 1 (Fig. 5.8a). Following culture iPSC-MEPCs were harvested and assessed for cell diameter, viability and total cells. The total number of cells harvested were significantly lower in Method 4 (Method 4 v iPSC, $p \leq 0.001$; Method 4 v Method 1, $p \leq 0.01$; Method 4 v Method 2, $p \leq 0.001$) and Method 5 (Method 5 v

undifferentiated iPSC, p≤0.0001; Method 5 v Method 1, p≤0.01; Method 5 v Method 2, p≤0.001) (Fig. 5.9a). Of the cells that were harvested from Method 1, 2, 3 and 4, similar diameter of between 12.1µm to 13.9µm was observed, whereas significant larger cell diameter ranging from 15.1µm to 16.2µm were observed in undifferentiated iPSC (iPSC v Method 1, p≤0.0001; iPSC v Method 2, p≤0.0001; iPSC v Method 3, p≤0.0001; iPSC v Method 4, p≤0.001) and Method 5 MEPCs (Method 5 v Method 1, p≤0.0001; Method 5 v Method 2, p≤0.001; Method 5 v Method 3, p≤0.0001; Method 5 v Method 4, p≤0.001; Fig. 5.9b). The viability of MEPCs that were harvested were significantly higher in methods that didn't involve freeze/thawing and replating, when compared to the other methods (Method 3 v iPSC, p≤0.0001; Method 3 v Method 1, p≤0.0001; Method 3 v Method 2, p≤0.001; Method 3 v Method 5, p≤0.001; Method 4 v iPSC, p≤0.0001, Method 4 v Method 1, p≤0.0001; Method 4 v Method 2, p≤0.0001; Method 4 v Method 3, p≤0.05; Method 4 v Method 5, p≤0.0001; Fig. 5.9c).

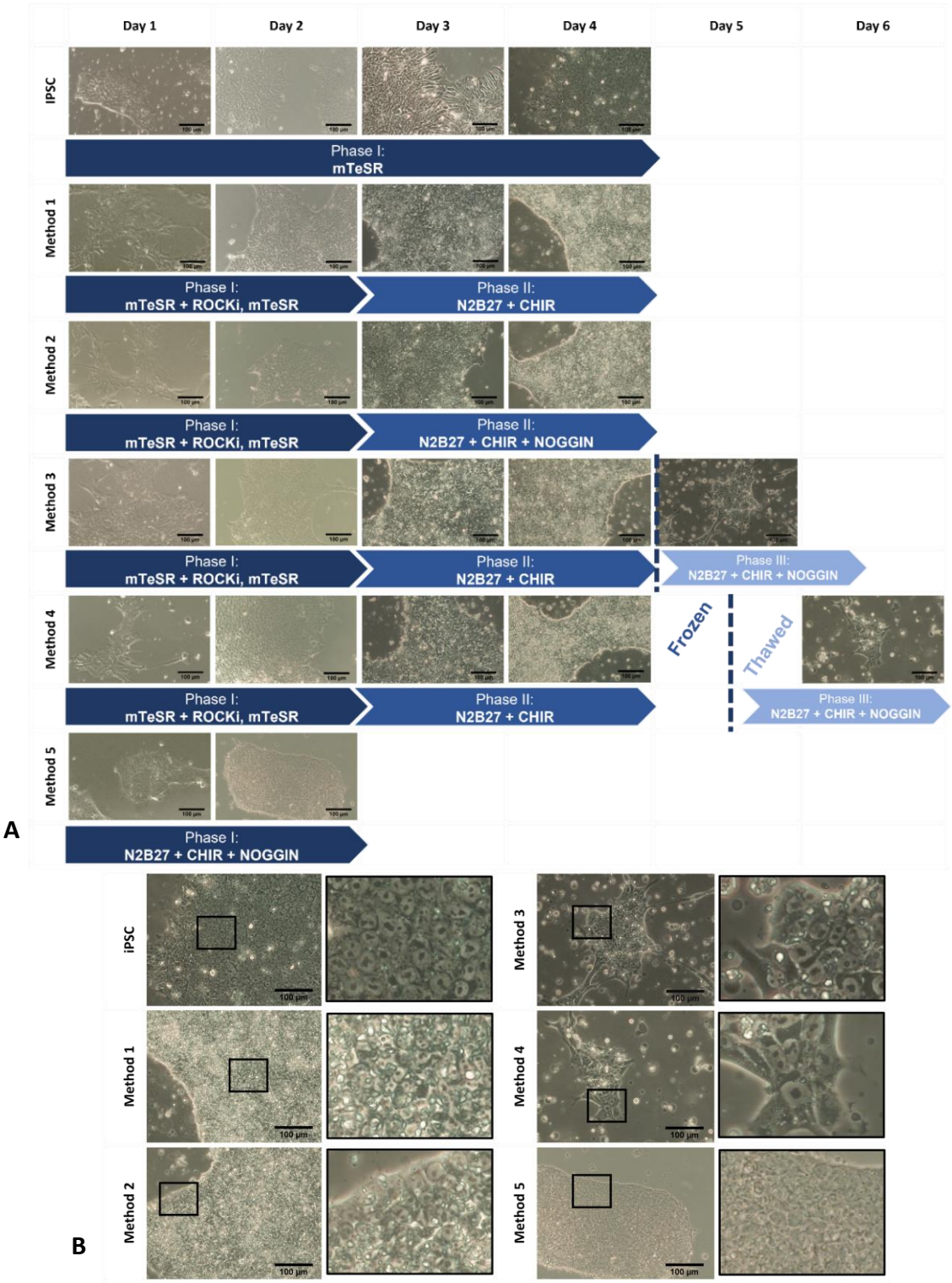

Figure 5.8. Live visualisation of differentiating induced pluripotent stem cells (iPSC) to Mesendoderm progenitor cells (MEPCs). (A) *Brightfield images captured of Gibco ® Human Episomal iPSC line (2329323, Life Technologies, Madison, USA) when subject to differing iPSC to MEPC differentiation protocols cultured at 21% v/v oxygen, 37°C (n=3 technical repeats). Method 1 resembles the protocol carried out by our collaborators. Method 4, at day 5, cells were cryopreserved and thawed prior to being recovered for 24 hours, which resembles cells subject to freeze thaw recovery.* ***(B)*** *with zoomed in images at the end of each differentiation method. Scale bar 100µm.*

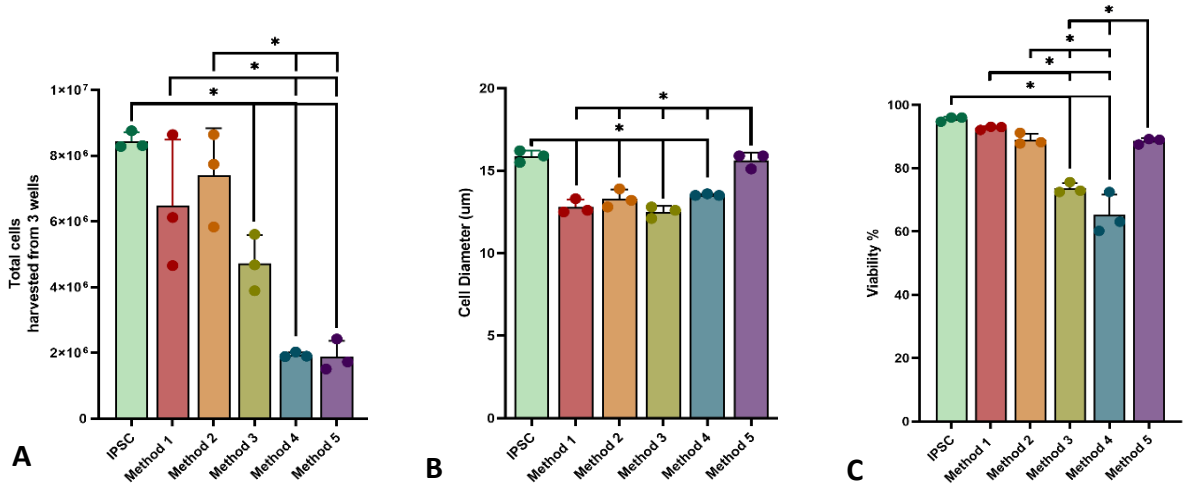

Figure 5.9. Downstream cell descriptive analysis of Gibco ® Human Episomal induced pluripotent stem cell (iPSC) line (2329323, Life Technologies, Madison, USA) when subject to differing iPSC to Mesendoderm progenitor cell (MEPC) differentiation protocols*, in relation to* ***(A)*** *total cells harvested,* ***(B)*** *cell diameter and* ***(C)*** *viability of cells after passaging (n=3 technical repeats). Statistics performed with in GraphPad prism v9.5.1, one-way ANOVA test, followed by the Tukey's multiple comparisons test *p≤0.05.*

PHENOTYPIC ANALYSIS MESENDODERM PROGENITOR CELLS SUBJECT TO DIFFERING DIFFERENTIATION METHODS

These cells were further assessed for gene expression of iPSC and MEPCs markers: Brachyury, FOXA2, LEF1, Noggin, SOX9, SHH, Lefty1 and Nodal (Fig. 5.10). From the differentiation methods the two cell populations that differed the most, were from Method 1 and Method 5. IPSC-MEPC in Method 1 showed a significant increase in FOXA2 (when compared to iPSC, p≤0.001; Method 2, p≤0.001; Method 3, p≤0.001; Method 4, p≤0.001 and Method 5, p≤0.001), with a visible but not significant increase in Noggin and Lefty1 and not significant decrease in Brachyury (Fig. 5.10). Whereas the iPSC-MEPCs generated from Method 5 displayed a significant increase in expression of SOX9 (when compared to iPSC, p≤0.0001; Method 1, p≤0.0001; Method 2, p≤0.0001; Method 3, p≤0.0001 and Method 4, p≤0.0001) and SHH (when compared to iPSC, p≤0.0001; Method 1, p≤0.0001; Method 2, p≤0.0001; Method 3, p≤0.0001 and Method 4, p≤0.0001), with a visible decrease in expression of noggin when compared to the other iPSC-MEPCS from the differentiation methods (Fig. 5.10). Flow cytometry was utilised to investigate marker expression within iPSC-MEPCs differentiated by Method 1, showing a distinct difference of cell population from the iPSC to MEPC, with the iPSC-MEPC population increasing cell staining for Brachyury and cytokeratin (Fig. 5.11).

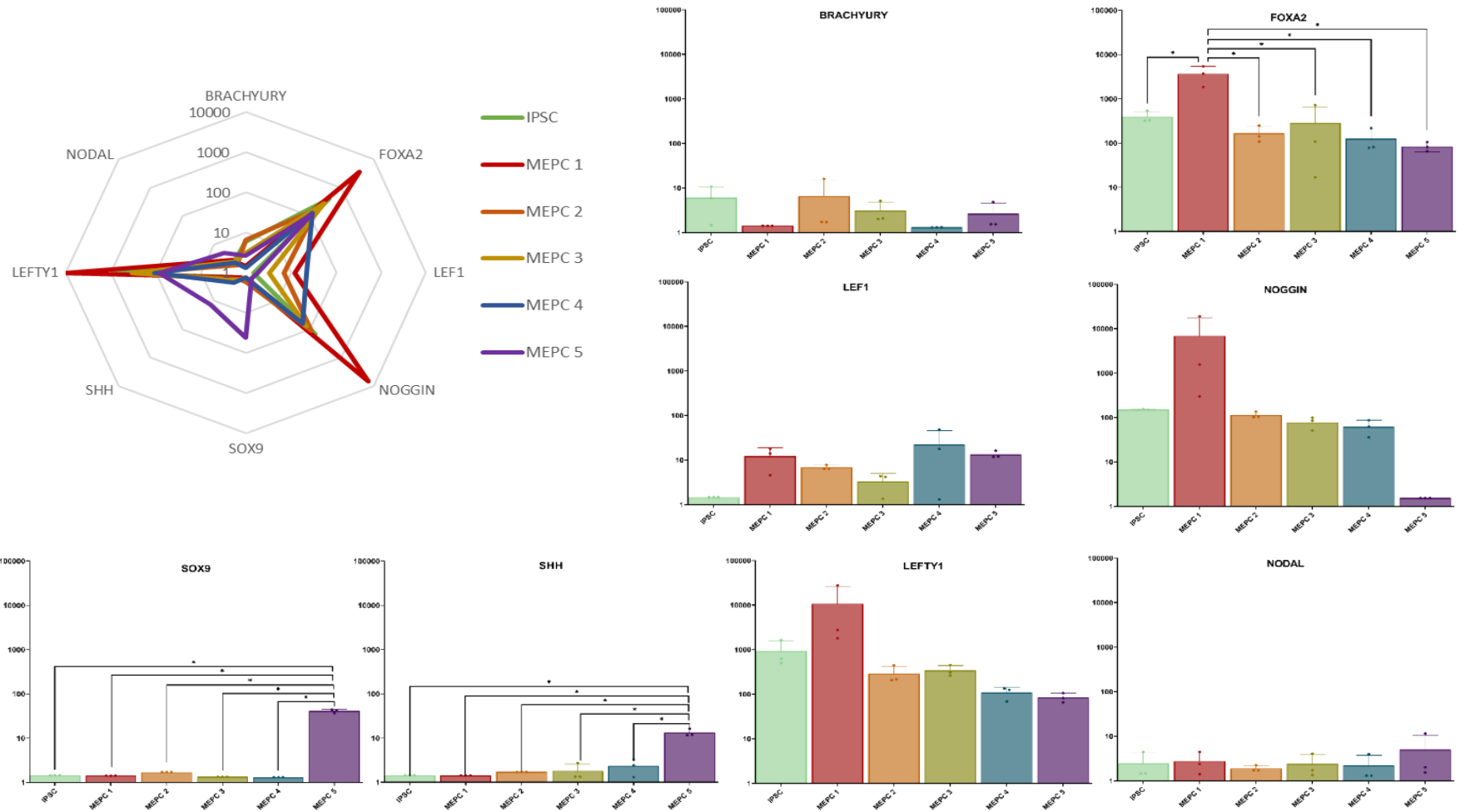

Figure 5.10. Gene expression of Gibco ® Human Episomal induced pluripotent stem cell (iPSC) line (Life Technologies, Madison, USA) when subject to differing iPSC to MEPC differentiation protocols. *Quantitative polymerase chain reaction analysis was performed on cells taken from different methods of differentiating iPSC into MEPC (iPSC; MEPC 1; MEPC 2; MEPC 3; MEPC 4; MEPC 5), analysing gene expression of Brachyury, FoxA2, LEF1, Noggin, SOX9, SHH, LEFTY1 and Nodal from the MEPC (n=3 technical repeats). Statistics performed with in GraphPad prism v9.5.1, one-way ANOVA test, followed by the Tukey's multiple comparisons test *p≤0.05.*

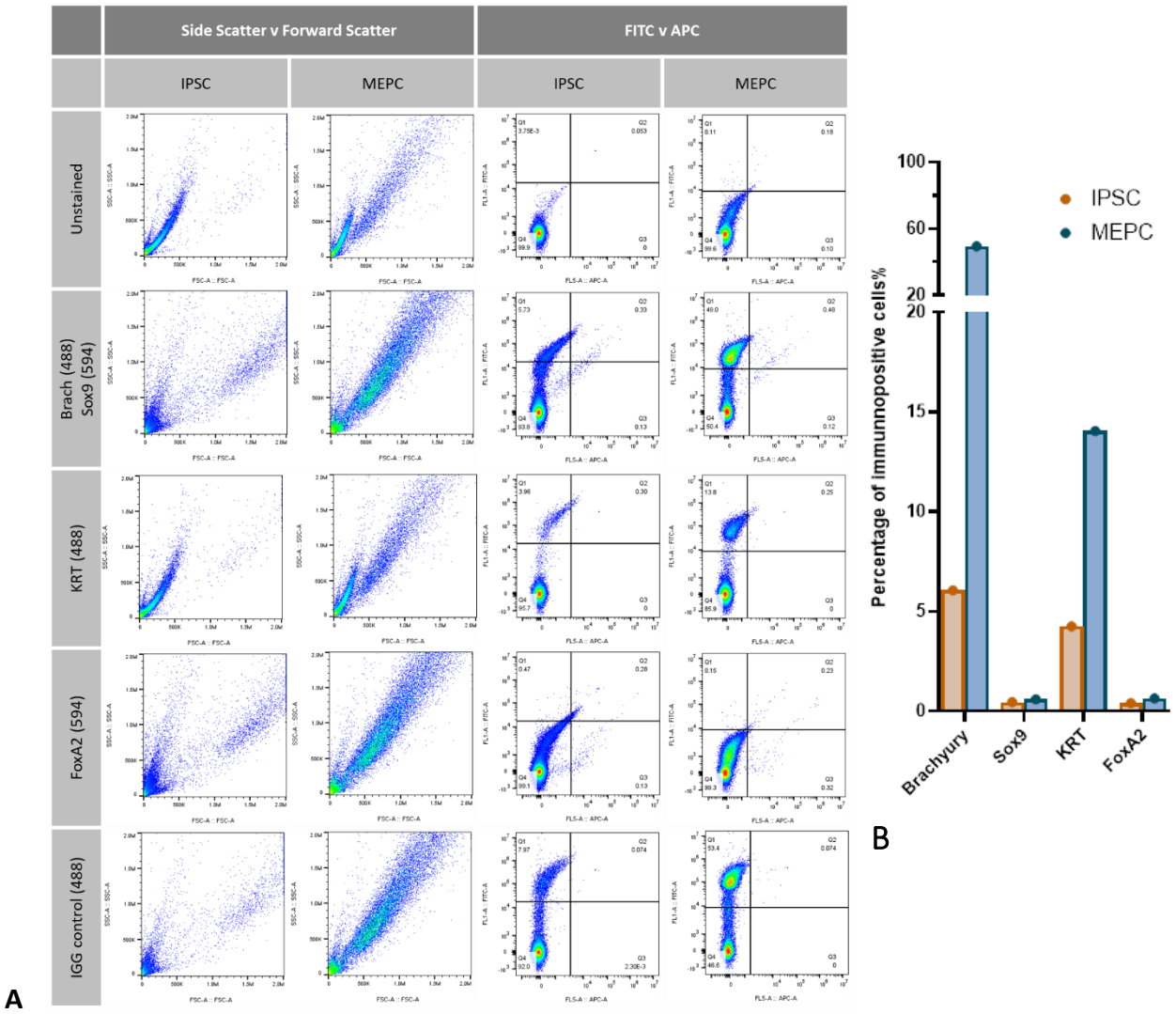

Figure 5.11. Fresh and cryopreserved induced pluripotent stem cells and Mesendoderm progenitor cells phenotype. (A) *Flow cytometry graphs displaying the different cell population when Gibco ® Human Episomal induced pluripotent stem cell (IPSC) line (2329323, Life Technologies, Madison, USA), when differentiated into Mesendoderm progenitor cells using Method 1 (N2B27 + CHIR media for 48h) and labelled with Brachyury (Brach), SOX9, Cytokeratin (KRT), FOXA2.* ***(B)*** *Illustrates the percentage of IPSC (orange) and MEPC (Blue) expressing Brachyury, SOX9, Cytokeratin (KRT) and FOXA2 (n=3 technical repeats). Statistics performed with in GraphPad prism v9.5.1, Mann-Whitney test.*

A COMPARISION OF FRESH AND FROZEN MEPCS IN NPGEL

Using the same method (Method 1) of differentiating iPSC into MEPCs, fresh iPSC-MEPCs were generated and seeded into NPgel for 2 weeks alongside iPSC-MEPCs that were cryopreserved following Method 4. Allowing the analysis of freeze, thaw and recovery process on the viability and regenerative potential of iPSC-MEPCs. Histological and immunohistochemical images were taken of the iPSC-MEPCs constructs. From analysing the morphology of the iPSC-MEPCs in NPgel constructs, H+E and Alcian Blue stains iPSC-MEPC appear with smaller nuclei in the cryopreserved iPSC-MEPCs when compared to the fresh iPSC-MEPCs (Fig. 5.12a). This feature can also be observed in the IHC staining, especially in the immunopositivity for cytokeratin (Fig. 5.13a). Generally, cytoplasmic staining appeared more spread out and denser in the fresh

iPSC-MEPCs cultured in NPgel than the cryopreserved iPSC-MEPCs culture in NPgel (Fig. 5.12a; indicated with black arrows). The number of iPSC-MEPC survival in the biomaterial was also counted, resulting in no difference between iPSC-MEPCs seen in NPgel biomaterial after 2 weeks in culture, although a greater range was observed in fresh cultures (Fig. 5.12b).

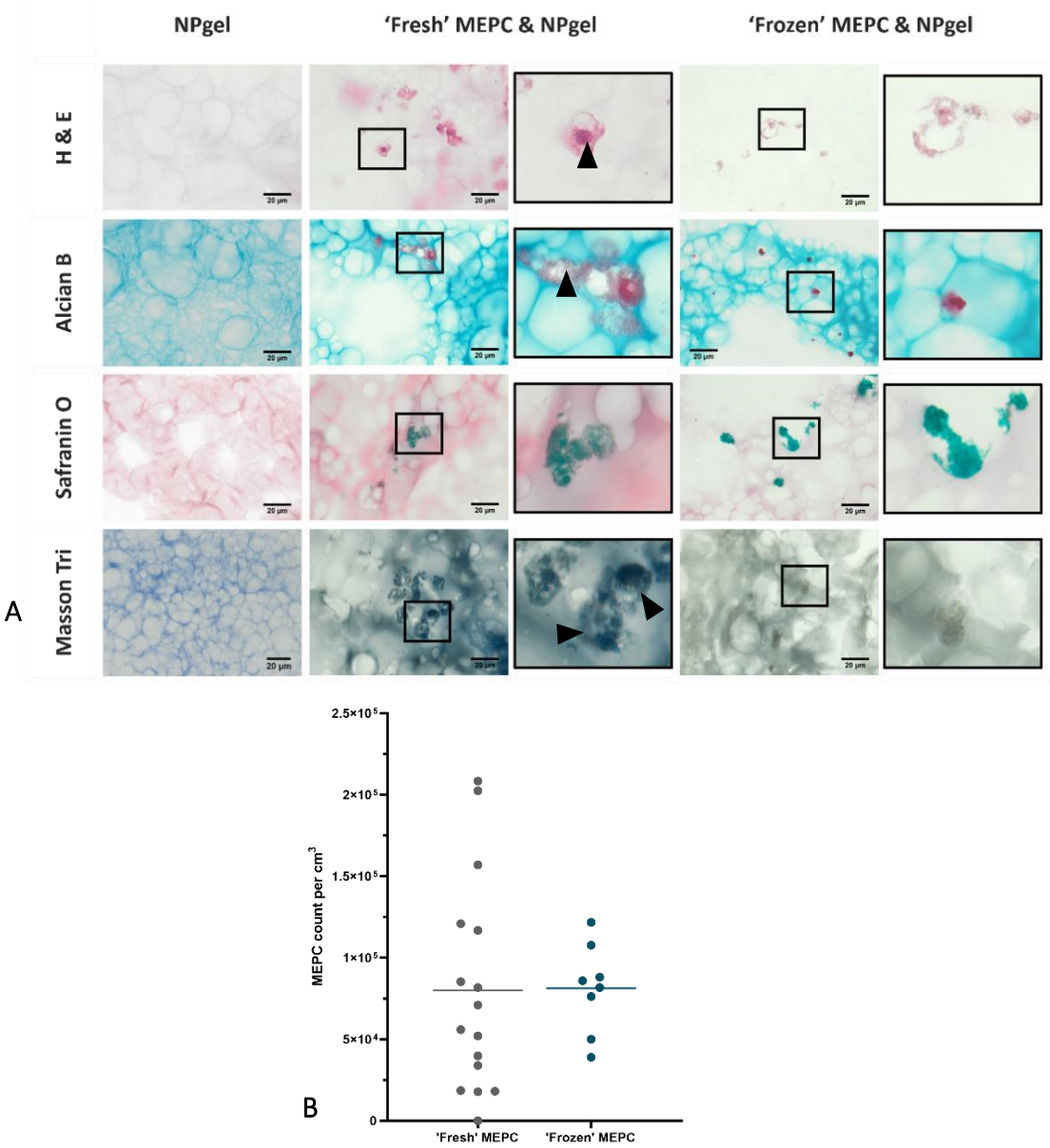

Figure 5.12. Fresh and cryopreserved Mesendoderm progenitor cells morphology and survival when seeded in NPgel. (A) *Histological images captured of Immunohistochemical images captured of 'Fresh' Mesendoderm progenitor cells (MEPCs; differentiated from Gibco ® Human Episomal induced pluripotent stem cell (IPSC) line (2329323, Life Technologies, Madison, USA) and the same MEPC undergone cryopreservation and recovery ('Frozen' MEPCs). Prior to being seeded into NPgel for 2 weeks in DMEM standard media at 5% v/v oxygen, 37°C. Stained with Haematoxylin and Eosin (H+E), Alcian Blue (Alcian B), Safranin Orange (Safranin O) and Masson's Trichrome (Masson's Tri). Black boxes indicate zoomed in images. Black arrows indicate cytoplasmic staining. Scale bar 20µm.* ***(B)*** *Cell count of MEPC observed within cm^3 of biomaterial (n=3 technical repeats). Statistics performed with in GraphPad prism v9.5.1, t test, not significant.*

Weak immunopositivity for SOX9 was observed around the cell nuclei in fresh iPSC-MEPC cultured in NPgel construct (Fig. 5.13a) and both fresh and cryopreserved iPSC-MEPC displayed some matrix accumulation surrounding the cell with immunopositive staining for aggrecan and collagen type II (Fig. 5.13a). Unfortunately, there were not enough cells found in the constructs to quantify the immunopositive expression of SOX9, FOXA2, Brachyury and Cytokeratin 8, 18 and 19. The release of GAG into the culture media was also assessed with DMMB assay, fresh iPSC-MEPC released significantly more GAGs into the culture medium than cryopreserved iPSC-MEPCs cultured in NPgel at 24 hours ($p \leq 0.01$), 1 week ($p \leq 0.05$) and 2 weeks ($p \leq 0.05$) in culture (Fig. 5.13b).

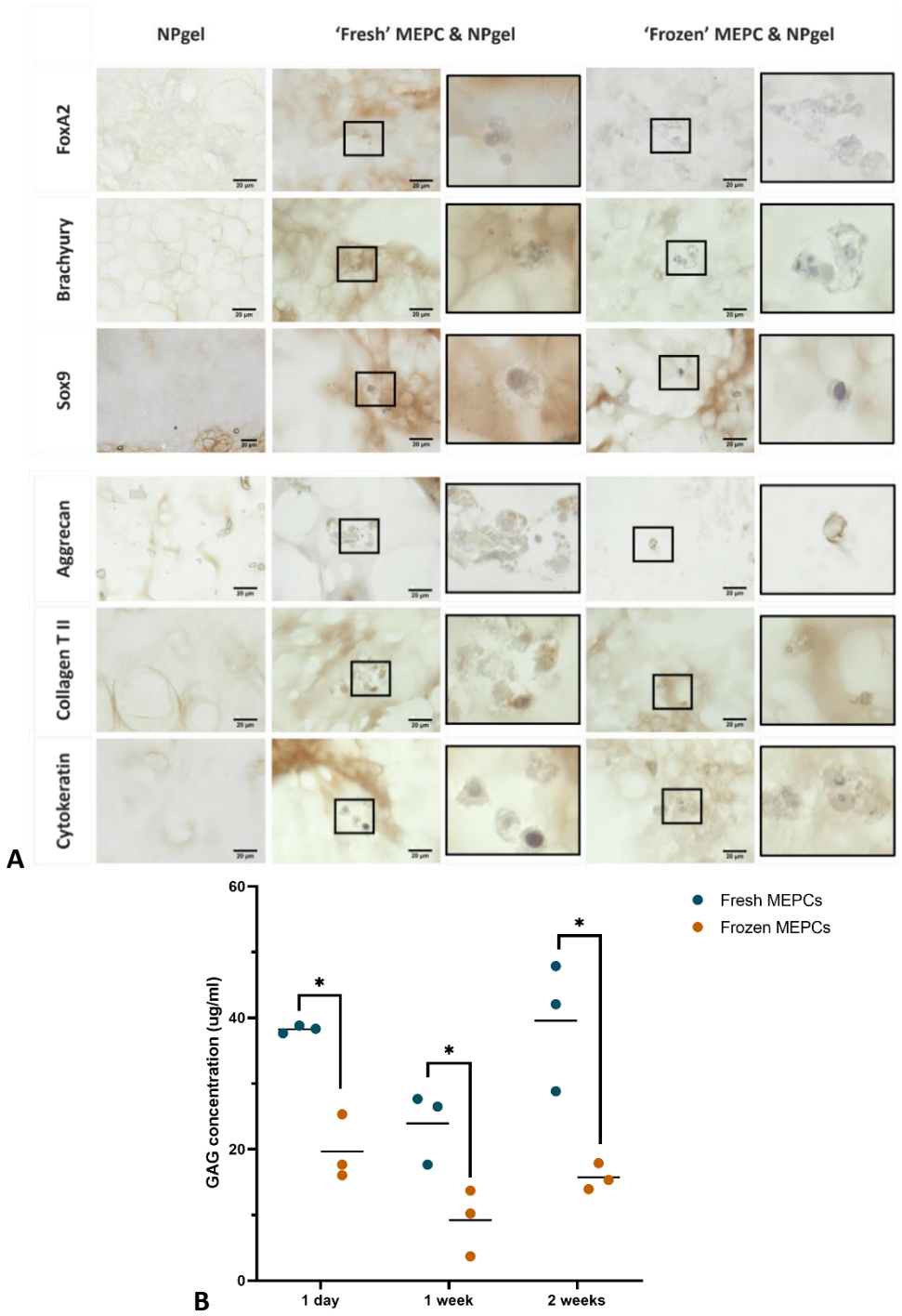

Figure 5.13. Fresh and cryopreserved Mesendoderm progenitor cells phenotype, extracellular matrix expression and release when cultured in NPgel. (A) *Immunohistochemical images captured of 'Fresh' Mesendoderm progenitor cells (MEPCs; differentiated from Gibco ® Human Episomal induced pluripotent stem cell (iPSC) line (2329323, Life Technologies, Madison, USA) and the same MEPC undergone cryopreservation and recovery ('Frozen' MEPCs). Prior to being seeded into NPgel for 2 weeks in DMEM standard media at 5% v/v oxygen, 37°C. Stained with FOXA2, Brachyury, SOX9, Aggrecan, Collagen Type II (Collagen T II) and Cytokeratin 8, 18 and 19 (Cytokeratin), Aggrecan and Collagen type II. Scale bar 20µm.* ***(B)*** *Glycosaminoglycan (GAG) release using 1,9-Dimethylene blue (DMMB) assay in media collected over 2 weeks of Fresh and cryopreserved MEPCs in NPgel constructs (n=3 technical repeats). Statistics performed with in GraphPad prism v9.5.1, t test, *p<0.05.*

DISCUSSION

IPSCs are an innovative, alternative to generating primary cell types for use in cell-based therapy. Differentiating iPSCs into NC-like cells has been employed previously using numerous strategies involving series of growth factors and cytokines (Chen *et al.*, 2013; Chon *et al.*, 2013; Liu *et al.,* 2014; Liu *et al.*, 2015; Tang *et al.*, 2018). However, challenges remain in the culture and differentiation, as successfully producing NC-like cells comes at the cost of low cell yield and heterogeneous cell population therefore, in this study the precursor cells, iPSC-MEPCs were cultivated and assessed for further differentiation towards NC-like cells and their compatibility in biomaterial carrier assessed. Successful up scaling and industrial transportation of these cells is of high importance to allow for clinical use of these cells.

MAINTAINING AN INDUCED PLURIPOTENT STEM CELL BANK

Generating a bank of iPSC was successfully implemented, which was evaluated based on continued maintenance of morphological profile of iPSC throughout passages. The method of monitoring iPSC by morphological character alone was adopted as cells were subject a limited number of passages; the technique is a non-invasive and manual microscopic observation can clearly assess the homogeneity and undifferentiated signature of iPSC in culture, which has also been successfully used as quality control during iPSC cell culture (Adewumi *et al.*, 2007; Scherf *et al.*, 2012; Suga *et al.*, 2015). Alternatively, for long-term culture and expansion of iPSC, alongside morphological assessment, pluripotency can be analysed through gene expression, ability to generate embryoid bodies, karyotyping and genetic integrity which are recommended every 10-20 passages (Buzzard *et al.*, 2004; Mitalipova *et al.*, 2005; Shafa *et al.*, 2012). Gene expression of iPSC demonstrated the expression of LEFTY1, NOGGIN and FOXA2, whilst they were negative for Brachyury, LEF1, SOX9, SHH and NODAL. In literature NOGGIN supports the maintenance of undifferentiated stem cells and acts as a BMP inhibitor (McMahon *et al.*, 1998; Chaturvedi *et al.*, 2009). FOXA2 is expressed early in the posterior epiblast through active signalling of nodal and is involved in definitive endoderm and mesoderm signalling (Burtscher and Lickert, 2009). LFFTY1 is also produced via Nodal signalling, as a negative feedback due to its function as an extracellular nodal pathway antagonist (Arnold and Robertson, 2009). Demonstrating that these markers are expressed in the epiblast during tissue regionalization. Ideally, true pluripotency should have been analysed with Oct4, SOX2 and NANOG (Takahashi and Yamanaka, 2006; Yu *et al.*, 2007).

DIFFERENTIATION OF INDUCED PLURIPOTENT STEM CELLS INTO MESENDODERM PROGENITOR CELLS

Differentiation of iPSC into Mesendoderm progenitor cells was assessed using differing techniques, focusing on temporal alteration of the media and supplements. For Method 1, 2, 3 and 4, Day 1 consisted of replating the cells on laminin-521, with continued cultured in iPSC media supplemented with ROCKi. This allowed the iPSC to adjust to the passage prior to altering the media. For Method 5, this recovery period was discarded, and the iPSC cells were

immediately exposed and treated with differentiation media. Despite not having a 'recovery' period and absence of ROCKi, viability was unaltered and cells were observed in sizable colonies; as ROCKi reduces apoptosis which is usually seen as a result of dissociating iPSC and supports cell aggregate formation (Watanabe *et al.*, 2007). Perhaps since iPSC were dissociated and passaged in clumps and no single cells, ROCKi is not essential and also noted as optional supplement in the passaging protocol of hPSC colonies (Liu and Chen, 2014). Total cells recovered over the culture period was significantly lower in the methods that harvested for 1 to 2 days after passage (Method 3, 4 and 5), suggesting that 2 days of culture was insufficient to enable iPSC time to proliferate. Interestingly, the cells recovered from iPSC and Method 5, retained significantly larger cell diameter than any other method, suggesting that differentiation reduced the cell size. Complementary to the noted cell diameter of iPSC in literature as ~15µm in size, was similar to that seen in the current study, and where iPSC are noted smaller than fibroblasts at ~30µm (Hammerick *et al.*, 2011).

The standard differentiation media utilised was N2B27 media supplemented with CHIR. In research the use of Glycogen Synthase Kinase 3β (GSK3β) inhibitor, CHIR, is widely applied in 24 to 48 hour pulses to mimic Wnt signalling (Kumar *et al.*, 2015; Kreuser *et al.*, 2020). Canonical Wnt is specifically required for primitive streak formation (Arnold *et al.*, 2000; Jager *et al.*, 2016), activating the mesendodermal population and regulators Brachyury and FOXA2 (Arnold *et al.*, 2000; Lindsley *et al.*, 2006); mature mesodermal lineages fail to develop *in vitro* in the absence of Wnt activity (Gadue *et al.*, 2006). Accordingly, inhibitors of GSK3β activates the cues involved in Wnt signalling and in theory mediates the mesodermal lineage. Therefore, an expression of Brachyury comparable to the expression of FOXA2 should have been observed. Suggesting that the iPSC-MEPCs were demonstrating a MEPCs phenotype. Noggin was introduced to media in Method 2, which didn't seem to have an effect morphologically, however phenotypically, the absence of Noggin in Method 1 resulted in an increase in FOXA2. Noggin functions by blocking the other signalling pathways active in the primitive streak - BMP and nodal signalling, thus inhibiting the neuroectoderm lineage. However, there is evidence that noggin can also mediate the suppression of endodermal and mesodermal lineage, functioning as an efficient uniform neural conversion of pluripotent cells (Chambers *et al.*, 2009). Therefore, isn't necessarily needed for differentiation of mesendoderm into notochordal lineage. Other studies have also added factors that inhibit the pan retinoic signalling, with retinoic acid being important in patterning and differentiation of the notochord (Draut *et al.,* 2019; Diaz-Hernandez *et al.*, 2020). The most differing gene expression from the 'MEPC' were from cells that were cultured in N2B27 media supplemented with CHIR and Noggin for 48 hours, without 48-hour recovery period with iPSC media and on laminin-521 (Method 5). SOX9 and SHH were upregulated; SHH is exclusive to late gastrulation in the mesoderm (Echelard *et al.*, 1993), whereas SOX9 can be expressed in all three germ lineages, but not at affective as Brachyury for inducing mesoderm cells (Yamamizu *et al.,* 2014). Suggesting these cells are also potential for mesoderm lineage.

THE EFFECT OF FREEZE-THAW PROCESS FOR RECOVERING MESENDODERM PROGENITOR CELLS

In the different methodologies, subjecting the cells to freeze-thaw and replating also had significant effect on the total cells harvested and viability. Cryopreservation of cells was included to resemble the clinical application of mass-producing MEPs, prior to recovering the cells and seeding them in biomaterials for clinical use. This was further investigated by comparing directly passaged and differentiated iPSC-MEPCs fresh and thawing cryopreserved cells were implemented and cultured in biomaterials. The immediate issue of the cryopreserved iPSC-MEPCs shipped to the UK from our collaborators were the discrepancy if these iPSC-MEPCs were fully recovered and healthy after the 24-hours in laminin-521 (Chapter 4). Live images of recovered iPSC-MEPCs after the 24 hours on Laminin-521, demonstrated adherent iPSC-MEPCs with the correct morphology, but many cells remained in suspension or displayed an elongated shape. Which indicates the cells were spreading and attaching prior to becoming more compact and uniform (Akhmanova *et al.*, 2015; Rivera *et al.*, 2020). Suggesting that 24 hours is not enough time for cells to become confluent and are likely not fully recovered from thawing. The after-culture analysis showed both fresh and cryopreserved iPSC-MEPC survival in biomaterials and presented as single cells. Fresh iPSC-MEPC displayed larger nuclei and released greater glycosaminoglycan into culture medium than cryopreserved iPSC-MEPCs. An abundance of problems can occur with cryopreservation that affect cell viability. Liu and Chen (2014) identified that cell survival increased when passaged <4 days before cryopreservation occurs, who recommended to avoid static culturing of cells before cryopreservation is due (Liu and Chen, 2014). When cells are exposed to fluctuating temperatures, such as during the shipment process on dry ice and are not kept in liquid nitrogen; this instability can lead to ice re-crystallization, resulting in the progressive loss of cell viability (Yuan *et al.*, 2016). Cryoprotectant solution can aid and prevent this loss due to temperature fluctuation however, cell aggregates could also be problematic due to a lack of cryoprotectant penetrating into cell clumps (Yuan *et al.*, 2016). IPSC also are susceptible to osmotic shock, which is caused during thawing by a sudden change in extracellular osmolality, also effecting cell viability (Uhrig *et al.,* 2022). Difficulty in recovering iPSC successfully was not limited to this study, others have also found efficiency of plating to be typically low (Reubinoff *et al.*, 2001; Fujioka *et al.*, 2004; Richards *et al.*, 2004) and reviews have been written to improve cell recovery through optimising freeze thawing techniques (Uhrig *et al.,* 2022). There has also been a resurgence in discovering molecule and compounds as cryoprotectants to resolve this issue of cell damage occurring during cryopreservation of cells (Stubbs *et al.*, 2020).

Reports demonstrating successful differentiation of iPSC into NC-like cells suffer from several limitations such as low yield of NCs, inferior ability to produce native NCs, longer duration of differentiation protocol, use of many expensive differentiation factors, lack of detailed characterization of NCs and poor regenerative capacity of generated notochord cells (Chen *et al.*, 2013b; Chon *et al.*, 2013; Liu and Chen, 2014; Tang *et al.*, 2018). Kreuser *et al.,* (2020) also

postulated that iPSC differentiation *in vitro* is overly laborious, expensive and inefficient (Kreuser *et al.*, 2020). For iPSCs to be used clinically, refining iPSC differentiation into NC-like cells is needed.

CONCLUSION

As part of a collaborative study for the regeneration of IVD other laboratories have generated a cell bank of iPSC- derived MEPCs; these iPSC-MEPCs were cryopreserved and shipped to our laboratory to then be thawed and recovered prior for seeding into biomaterials (Chapter 4). However, after recovery low viability and low cell numbers were encountered, suggesting that this method was inefficient and ineffective for the aim of seeding $4x10^6$ cells/mL of recovered iPSC-MEPCs into biomaterials, to observe if the cells would display disc regenerative properties. The aim of this study was to compare *in situ* generated iPSC-MEPCs and iPSC-MEPCs subjected to the freeze and thaw process that mimicked the methodology of recovering iPSC-MEPCs from Chapter 4. In this study, we recapitulated the cultivation of iPSC-MEPCs with simple supplementary factors, to gain an understanding of which factors enable the iPSC differentiation towards the mesendodermal lineage. The study demonstrated the limitations involved with the use of iPSC, including viability, cell handling, the effects of freeze-thawing and the use of ROCKi. Interestingly, by comparing fresh iPSC-MEPCs to cryopreserved iPSC-MEPCs, this report highlights the implications of inter-laboratory comparisons, and the limitations of distributing cryopreserved cells, which are correlated to issues that occur during clinically translating and upscaling iPSC-MEPC manufacturing. Many challenges remain in this relatively new field of utilising iPSC-NC-like cell therapy ranging from, refining culture differentiation, comparing tailored biomaterial carriers for these iPSC-MEPCs, which would be involved in clinical administration of cells into the intervertebral disc, and developing a further understanding of how these cells will behave in the native environment of the disc.

ACKNOWLEDGMENTS

This work was supported by the funding received from the European Union's Horizon 2020 research and innovation programme [grant agreement No 825925]. MAT is financially supported by the Dutch Arthritis Society (LLP22).

CONFLICT OF INTEREST

CLM and CS are named inventors on the patent for NPgel.

CHAPTER 6
THE EFFECTS OF EXTERNAL DISC ENVIRONMENT ON CELL-SEEDED BIOMATERIALS FOR DISC REGENERATION

CONTEXT OF RESEARCH

Up until this Chapter, cell-seeded biomaterial constructs have been cultured within standard culture media which whilst the physiological oxygen concentration was investigated, other environmental conditions of the disc were not considered. Here, pNC were cultured in NPgel and iPSC-MEPCs cultured in NPgel and subjected to a microenvironment that mimics the hostile degenerative IVD environment. The contribution to research is the novel culturing of pNC and iPSC-MEPCs in NPgel *in vitro* for up to 4 weeks in degenerative disc-like media that contained altered pH, osmolality, and inclusion of catabolic cytokines within a hypoxic environment.

AUTHORS

Rebecca J. Williams[1,2], Shaghayegh Basatvat[1,2], Ronak Janani[4], Chris Sammon[4], Mariana A. Tryfonidou[5], Joseph W. Snuggs[1,2], Christine Le Maitre[1,2]

AFFILIATIONS

[1] Department of Oncology and Metabolism, University of Sheffield, UK. [2] Biomolecular Sciences Research Centre, Sheffield Hallam University, UK. [3] Eindhoven University of Technology, The Netherlands. [4] Materials Engineering research Institute, Sheffield Hallam University, UK. [5] Department of Clinical Sciences, Faculty of Veterinary Medicine, Utrecht University, The Netherlands.

AUTHOR CONTRIBUTIONS

RJW, CLM and JWS contributed to conception and design of the study; RJ, CS, JWS contributed to biomaterial synthesis; RJW contributed to acquisition of laboratory data; RJW performed

most of the data analysis; RJW, CLM, JWS contributed to interpretation of the data; RJW, CLM and JWS drafted the manuscript.

DETAILED CONTRIBUTIONS MADE

I conducted experiments: investigated the effect of healthy and degenerate media on pNCs cultured in NPgel, with histological staining (Fig. 6.1) and immunohistochemical expression (Fig. 6.2, 6.3 and 6.4); I investigated the effect of healthy and degenerate media on iPSC-MEPCs cultured in NPgel, with histological staining (Fig. 6.5) and immunohistochemical expression (Fig. 6.6, 6.7 and 6.8). SB developed the healthy and degenerated media composition. I preformed all data analysis and statistical analysis relating to these experiments and drafted the entire manuscript.

(IN PREPARATION) The Effects of External Disc Environment on Cell-Seeded Biomaterials for Disc Regeneration. Rebecca J. Williams, Shaghayegh Basatvat, Ronak Janani, Chris Sammon, Mariana A. Tryfonidou, Joseph W. Snuggs, Christine Le Maitre.

CHAPTER 6: THE EFFECTS OF EXTERNAL DISC ENVIRONMENT ON CELL-SEEDED BIOMATERIALS FOR DISC REGENERATION

ABSTRACT

Lower back pain affects much of the population and can often lead to the onset of debilitating, chronic pain. Despite this prevalence, current treatments target symptoms related to lower back pain rather than the underlining cause, which in around 40 percent of cases is linked to intervertebral disc degeneration. Cell-based treatments are perceived to be a viable option to attempt to regenerate discs. Previous work has defined cells of notochordal origin as favourable for their regenerative properties, and efforts have been made to screen potential biomaterials to function as biomechanically supportive carriers and as a delivery system to inject notochordal like cells into the degenerate disc. To date, the harmonisation of a biomaterial and notochordal-like cells has been established *in vitro*, therefore this study focused on the effect of external factors, associated with a degenerative disc, has on the cell-seeded biomaterials *in vitro.* Previously investigated Notochordal cells (pNC) of porcine origin and Mesendoderm progenitor cells (MEPC), derived from induced pluripotent stem cells from human origin, were investigated here within a biomaterial carrier (NPgel) and exposed to media designed to mimic a healthy and degenerate disc for up to 4 weeks culture under 5% oxygen. Theses cell types were selected as we have previously demonstrated these cells remain viable and present regenerative potential once cultured within NPgel, however we have yet to subject the cell-seeded biomaterial constructs to harsh degenerate disc-like environments. The constructs were investigated through histological, immunohistochemical and glycosaminoglycans analysis to investigate cell viability, phenotype, and extracellular matrix synthesis. The results demonstrated that cultivating either pNC or MEPC seeded in NPgel within a degenerative disc media environment had no real impact on the morphology and phenotype of the cells. Leading to the conclusion that these cell-seeded biomaterial constructs could retain these same characteristics and regenerative properties with additional resistance to the degenerative disc *in vivo.*

INTRODUCTION

LOWER BACK PAIN AND INTERVERTEBRAL DISC DEGENERATION

Lower back pain (LBP) is the leading cause of disability worldwide (Hartvigsen *et al.*, 2018), and still remains a significant global concern due to the resultant effects to the economic and costly relapse healthcare treatments (Maetzel and Li, 2002). But most importantly patients' lives are severely impacted with pronounced effects on a patients livelihood, and reported 1 in 4 patients with chronic LBP experience psychological co-morbidity (Fullen *et al.*, 2022). The usual guidelines for lower back pain involves a sequence of therapy targeting the management of symptoms, which involves exercise, nonsteroidal anti-inflammatory drugs, and invasive surgery (Nice, 2018). Emphasis has been placed on developing better treatments as an alternative to the unsustainable long-term opioid medication prescribed to manage chronic lower back pain (Qaseem *et al.*, 2017) and spinal fusion, which also lacks evidence as being more beneficial than intensive rehabilitation for patients with chronic LBP (Fritzell *et al.*, 2001; Brox *et al.*, 2010). Highlighting that there is still an unmet clinical need, as current treatments do not address the underlining cause of lower back pain. It is still difficult to identify a clear causation to LBP, however, it is estimated that 40% of cases of LBP are associated with degeneration of the intervertebral disc (IVD) (Luoma *et al.*, 2000; Sakai and Andersson, 2015). Thus, targeting the regeneration of the IVD is now the forefront of lower back pain research and cell-based therapy has become a topic of interest (Binch *et al.*, 2021).

REGENERATING THE INTERVERTEBRAL DISC WITH CELL-BIOMATERIAL TREATMENTS

The theory of cell-based treatment for disc degeneration involves the delivery of viable cells to the inner disc region, the nucleus pulposus, in attempts to repopulate and repair the damaged disc (Binch *et al.*, 2021; Williams *et al.*, 2021). Cells of greatest potential are nucleus pulposus cells, notochordal cells (NC), chondrocytes and stem cells; based on the ability of the cells to survive in an IVD environment, and their regenerative potential through extracellular matrix composition (Arkesteijn *et al.,* 2017; Binch *et al.*, 2021; Williams *et al.*, 2021). During disc degeneration there is an homeostatic imbalance of extracellular matrix synthesis and matrix-degrading molecules including matrix metalloproteinase (MMPs) and aggrecanases, targeting the unfavourable breakdown of aggrecan and collagen type II (Le Maitre *et al.*, 2007a ; 2007b). This impacts the ability of the IVD to retain water, and to resist and redistribute compressive loads (McNally and Adams, 1992; Adams and Roughly, 2006). Highlighting that cells, extracellular matrix and biomechanics are very much interlinked, and the reintroduction of extracellular matrix-producing cells into a degenerate disc could reinstate the biomechanical properties of the IVD (Vergroesen *et al.*, 2015). Previous work has screened potential cells together with potential biomaterials and has focused on the harmonisation of these two elements. In Chapter 3, porcine NC (pNC) remained viable in NPgel biomaterial for up to 4 weeks in a physiological disc environment of 5% v/v O_2, with 5% v/v CO_2 at 37°C, in αMEM containing Penicillin streptomycin (P/S), amphotericin B, L-ascorbic acid, Insulin-transferrin-Selenium (ITS), L-glutamine, L-proline and Albumax (Basatvat *et al.*, 2023), with

the results indicating seeded pNCs retained their NC phenotype and expression of healthy extracellular matrix. In literature it has been shown that to enable culturing of NC in alginate the following parameters are essential to maintain NC phenotype: hypoxia (Erwin *et al.*, 2009), pH ≥ 7.2 (Guehring *et al.*, 2009), using αMEM as basal culture medium (Guehring *et al.*, 2009; Spillekom *et al.*, 2014), and additional supplementation such as ascorbic acid and ITS. Furthermore, in Chapter 4, Mesendoderm progenitor cells (MEPCs) derived from human induced pluripotent stem cells also remained viable after 4 weeks in NPgel, when cultured at 5% v/v O_2, with 5% v/v CO_2 at 37°C, in low glucose DMEM media containing: glutaMAX™, P/S, amphotericin B, L-ascorbic acid, ITS, L-glutamine, L-proline and Albumax (Basatvat *et al.*, 2023). There was also evidence of healthy extracellular matrix expression which is indicative of cellular differentiation into an NC-like phenotype. However, if these cell-seeded biomaterials were to become clinically translated as an injectable treatment for disc regeneration, then the next phase of testing would be to determine whether the cells could be maintained within a degenerative disc micro-environment, going beyond simply investigating physioxia, as previously investigated.

DEGENERATIVE DISC ENVIRONMENT

The nucleus pulposus is naturally a hostile environment, due to the avasculature and limited nutrient supply (Kauppila, 1995; Roberts *et al.*, 1995). The degenerate disc environment has been reported to comprise of potent pro-inflammatory cytokines such as interleukin-1β (IL-1β) and TNF (Le Maitre *et al.,* 2005; Hoyland *et al.,* 2008; Purmessur *et al.*, 2013; Phillips *et al.*, 2015), the upregulation of matrix degrading enzymes directly resulting in a decreased content of glycosaminoglycans (GAG) (Le Maitre *et al.*, 2007; Thorpe *et al.*, 2018), which also facilitating the ingrowth of neural and vascular structures (Roberts *et al.*, 1995). The decreased GAG content also causes a reduction in tissue osmolality due to decreased water and ion content within the nucleus pulposus (Ishihara *et al.*, 1997; Thorpe *et al.*, 2018). IL-1β production has been shown to influence human disc cells, responding by increasing production of other cytokines as well as itself, creating a positive feedback loop. Philips et al., (2015), demonstrated that IL-1β was a key player in modulating inflammatory cytokine production and catabolic regulation in the IVD, as treatment with IL-1β was shown to induce cytokines and chemokines as well as extracellular remodelling in human NP cells; all characteristics that are observed in a degenerate disc (Phillips *et al.*, 2015). Other features of the IVD are low pH and low glucose, as during disc degeneration there is a further lack of nutrient supply, resulting in disc cells consuming and limiting oxygen and glucose levels further, and adding to the acidity of the pH by producing lactic acid (Mokhbi Soukane *et al.,* 2009).

Therefore, in this study media was composed to mimic the healthy and degenerate disc environment (developed within the iPSPINE consortia – manuscript in preparation), altering the osmolality, pH, and key pleiotropic cytokine, IL-1, within low glucose DMEM basal media, and their effects on the cell-seeded biomaterial constructs. To pose the hypothesis that the

alteration of environmental media to resemble a degenerative disc has no effect on the viability and regenerative potential of the proposed pNC and iPSC-MEPC seeded in biomaterials. Investigating cellular response and if there was an indication of biomaterials protection from to degenerative environment. The cellular and biomaterial constructs were analysed for cell phenotype, characteristics and the expression of extracellular matrix markers using histological and immunohistochemical staining.

METHODOLOGY

EXPERIMENTAL DESIGN

The focus of this study was to expose the cell-seeded biomaterial constructs to media that resembled a healthy and degenerate IVD microenvironment. Previously tested and handled pNC (Chapter 3) and *in situ* fresh iPSC-MEPCs (Chapter 5) were seeded into NPgel; generating pNC seeded into NPgel (pNC & NPgel in n=3) and iPSC-MEPC seeded into NPgel (MEPC & NPgel in n=3) that were cultured in 'healthy', 'degenerate' and standard media for 2-week and 4-week time points *in vitro* at 5% oxygen, with acellular constructs in parallel.

NOTOCHORDAL CELL EXTRACTION

Porcine NC were obtained from lumbar IVDs harvested from young pigs (<15 weeks old) (Marr Grange Butchers, UK). Following the protocol described in Chapter 2 (Recommendations for digestion of Nucleus pulposus tissue and Notochordal cell extraction). Porcine NC clusters were counted post harvesting using a NucleoCounter® NC-200™ (Chemometec, Allerod, DK), as described in Chapter 2 (Calculating cell number).

GENERATING MESENDODERM PROGENITOR CELLS DERIVED FROM INDUCED PLURIPOTENT STEM CELLS

Gibco® Human Episomal iPSC line (2329323, Life technologies, Madison, USA) was previously thawed and maintained as described in Chapter 5 (Thawing induced pluripotent stem cells; Induced pluripotent stem cell maintenance, passaging and cryopreservation), and differentiated into MEPCs using the method described in Chapter 5 (Method 1; Induced pluripotent stem cell differentiation).

MESENDODERM PROGENITOR CELL DISSOCIATION AND CELL COUNT

After the differentiation process, iPSC-MEPCs were dissociated following the protocol as described in Chapter 4 (Mesendoderm progenitor cell dissociation and cell count). Cell count was performed with a sample of iPSC-MEPCs suspension using a NucleoCounter® NC-200™ (Chemometec, Allerod, DK), as described in Chapter 2 (Calculating cell number).

NPGEL PREPARATION

NPgel was prepared as described by Thorpe *et al.,* (2016) and in Chapter 3 (NPgel preparation).

INCORPORATION OF CELLS INTO BIOMATERIALS

For seeding pNC into NPgel, harvested pNC were centrifuged at 200*g* for 5 minutes, the supernatant was removed, and the NC pellet was resuspended in 10% v/v extraction media. Cell density of $4x10^6$ cells/mL of pNC was seeded into NPgel. In addition, parallel acellular biomaterial controls were established. Each 300µL pNC and biomaterial constructs were extruded through a 27-gauge needle to mimic injection into the disc into 48 well culture plate, left to gel at 37^{o}C for <5 minutes. For seeding MEPC into NPgel, suspended iPSC-MEPCs were centrifuged at 200*g* for 5 minutes, the supernatant was aspirated, and the MEPC pellet was resuspended in 10% mTeSR™ Plus Medium supplemented with 10µM ROCKi v/v. IPSC-MEPCs were seeded at $4x10^6$ cells/mL into the NPgel, creating 300µL constructs, which were extruded through a 27-gauge needle to mimic injection into the disc into 48 well culture plate, and left to gel at 37^{o}C for ~5 minutes.

CULTURE MEDIA HEALTHY, DEGENERATE AND STANDARD FOR PNC AND MEPCS

Five hundred microliters of media were added to each well of cultured pNC seeded in NPgel or iPSC-MEPC seeded in NPgel. Cell-seeded biomaterial constructs were cultured in standard, healthy or degenerate media (Table 6.1). Standard media used for pNC seeded in NPgel contained αMEM (life technologies, Paisley, UK) containing P/S 50U/mL (Life Technologies UK), amphotericin B 2.5ug/mL (Sigma, Dorset, UK), L-ascorbic acid 25ug/mL (Sigma, Dorset, UK), 1% Insulin-transferrin-Selenium v/v (ITS-X), 1% L-glutamine v/v (life technologies, UK), L-proline 40ug/mL (Life technologies, UK) and Albumax 1.25mg/mL (Life technologies, UK) (Basatvat *et al.*, 2023). For the standard media use in iPSC-MEPC seeded in NPgel, comprised of N2B27 media (DMEM F-12 (Life Technologies, Paisley, UK) containing 1% MEM non-essential amino acid v/v (Life Technologies, Paisley, UK), 1% Glutamax v/v (Life Technologies, Paisley, UK), 0.16% Beta-mercaptoethanol v/v (Life Technologies, Paisley, UK), 0.5% N2 supplement v/v (Life Technologies, Paisley, UK), 1% B27 supplement v/v (Life Technologies, Paisley, UK) and 0.05% bovine albumin w/v (Sigma, Dorset, UK). In both pNC and iPSC-MEPC seeded in NPgel, the same healthy and degenerate media was used; the healthy media comprises of DMEM (1g/L Glucose + Pyruvate), sodium Bicarbonate 0.85g/L (pH 7.1 at 5% v/v CO_2), N-Methyl-D-glutamine HCL 92.5mM (NaCl homologue) to adjust to 450 mOsm/kg, P/S 50U/mL (Life Technologies, Paisley, UK), amphoterionin B 2.5ug/mL (Sigma, Dorset, UK), 1% ITS-X v/v (Life Technologies, Paisley, UK), 1% L-glutamine v/v (Life Technologies, Paisley, UK), L-Proline 40ug/mL (Life Technologies, Paisley, UK), Albumax 1.25mg/mL (Life Technologies, Paisley, UK); the degenerate media comprised of DMEM (1g/L Glucose + Pyruvate), sodium Bicarbonate 0.426g/L (pH 6.8 at 5% v/v CO_2), N-Methyl-D-glutamine HCL 47.5 mM (NaCl homologue) to adjust to 350 mOsm/kg, P/S 50U/mL (Life Technologies, Paisley, UK), amphoterionin B 2.5ug/mL (Sigma, Dorset, UK), 1% ITS-X v/v (Life Technologies, Paisley, UK), 1% L-glutamine v/v (Life Technologies, Paisley, UK), L-Proline 40ug/mL (Life Technologies, Paisley, UK), Albumax 1.25mg/mL (Life Technologies, Paisley, UK), IL-1β 100pg/mL. Leaving the outer wells void of constructs but hydrated with phosphate buffered saline (PBS; Gibco, UK).

Triplicate technical repeats of pNC and iPSC-MEPC seeded in NPgel and acellular controls were cultured for up to 4 weeks in a physiological disc environment of 5% v/v O_2, with 5% v/v CO_2 at 37°C using a hypoxia glove box (Coy Laboratory Products, USA). Media was replaced three times a week during the culture period. Cell phenotype and matrix deposition was investigated in pNC and iPSC-MEPC seeded in NPgel constructs following 2 and 4 weeks in culture.

Table 6.1. The parameters difference in media used in culture for pNC seeded in NPgel (Standard (pNC); Healthy; Degenerate), used in culture for MEPC seeded in NPgel (Standard (MEPC); Healthy; Degenerate). *Reviewing the Osmolality, pH, cytokines, and Basal media of the medias.*

	Standard (pNC)	Standard (MEPC)	Healthy (pNC or MEPC)	Degenerate (pNC or MEPC)
Osmolality	300 mOsm/kg	310 mOsm/kg	450 mOsm/kg	350 mOsm/kg
pH	7.4	7.2	7.1	6.8
Cytokines	-	-	-	100pg/mL IL-1β
Basal media	Low Glucose αMEM	High Glucose DMEM/F-12	Low Glucose DMEM	Low Glucose DMEM

HISTOLOGICAL ANALYSIS

After 2 and 4 weeks in culture pNC and iPSC-MEPC seeded in NPgel constructs were fixed, embedded into wax, and sectioned as described in Chapter 3 (Histological analysis). Sections were dewaxed, rehydrated, and assessed using histological stains. H&E: Alcian Blue (pH 2.5): Masson's Trichrome (Atom Scientific Ltd, Hyde, UK): Safranin O/ Fast green (described in detail in Chapter 3; Histological analysis). After specific histological staining, sections were dehydrated three times for 10-minute washes in IMS, cleared in Sub-X three times for 10-minute and mounted in Pertex (Leica Microsystems, Newcastle, UK). All slides were examined with an Olympus BX51 microscope and images captured by digital camera and Capture Pro OEM v8.0 software (Media Cybernetics, UK). Histological sections were analysed, and representative images captured to document their histological appearance and cellular staining patterns.

IMMUNOHISTOCHEMISTRY ANALYSIS

Immunohistochemistry (IHC) as previously reported (Binch et al., 2020) and as described in Chapter 3 (Immunohistochemistry and immunofluorescence analysis), was also performed on pNCs and iPSC-MEPCs seeded in biomaterials. Specific antibodies were used to target antigens in relation to extracellular matrix markers, and MEPC and NC phenotypic markers (Table 6.2).

Table 6.2. Immunohistochemical procedures utilised for phenotypic characterisation of porcine notochordal cells. *Primary antibody target, clonality, dilutions optimised and antigen retrieval. Along with the Secondary antibodies and dilutions, which were used for immunohistochemical staining the staining methods.*

Primary Antibody	Target	pNC & NPgel or MEPC & NPgel	Clonality	Optimal dilution	Antigen retrieval	Secondary Antibody	Optimal dilution
Aggrecan (AB3778, Abcam)	NP matrix	pNC & NPgel MEPC & NPgel	Mouse monoclonal	1:100	Heat	Rabbit Anti-Mouse (Ab6727, Abcam)	1:500
Brachyury (AF2085, Bio-techne)	NC/NP marker	pNC & NPgel MEPC & NPgel	Goat polyclonal	1:500	None	Donkey Anti-Goat (Ab208000, Abcam)	1:500
Caspase 3 (AB4051, Abcam)	Apoptosis Marker	pNC & NPgel MEPC & NPgel	Rabbit polyclonal	1:400	None	Goat Anti-Rabbit (Ab6720, Abcam)	1:500
Collagen Type II (MAB1330, Sigma)	NP matrix	pNC & NPgel MEPC & NPgel	Mouse monoclonal	1:200	Enzyme	Rabbit Anti-Mouse (Ab6727, Abcam)	1:500
Cytokeratin 8 + 18 + 19 (AB41825, Abcam)	NC/NP marker	pNC & NPgel MEPC & NPgel	Mouse monoclonal	1:400	Enzyme	Rabbit Anti-Mouse (Ab6727, Abcam)	1:500
FoxA2 (D56D6, Cell signalling)	MEPC marker	MEPC & NPgel	Rabbit monoclonal	1:400	Heat	Goat Anti-Rabbit (Ab6720, Abcam)	1:500
Sox9 (AB5535, Abcam)	MEPC marker	MEPC & NPgel	Rabbit polyclonal	1:1000	None	Goat Anti-Rabbit (Ab6720, Abcam)	1:500

DIMETHYLMETHYLENE BLUE ASSAY

Media samples were collected during every media change during the culture of the pNC and iPSC-MEPCs in biomaterial constructs and stored at -80^{o}C. Dimethyl methylene Blue (DMMB) reagent was generated and preformed as previously described in Chapter 3 (Dimethylmethylene Blue Assay).

ENZYME-LINKED IMMUNOSORBENT ASSAY

Media samples collected during every media change were also analysed using the DuoSet® Enzyme-Linked Immunosorbent Assay (ELISA) Development Kit for sandwich ELISA to measure levels of natural and recombinant human active and pro-matrix metalloproteinase 3 (MMP-3; R&D Systems). The Duoset® Ancillary Reagent Pack, containing: 96 well microplates, plate sealers, substrate solution, stop solutions, plate coating buffer, wash buffer and reagent dilutant (R&D Systems), was used in combination with the Human total MMP-3 Duoset® ELISA containing: Human MMP-3 Capture antibody, Human MMP-3 Detection antibody, Human MMP-3 standard and streptavidin-HRP (R&D Systems) according to the manufactures protocol.

STATISTICAL ANALYSIS

Statistics were performed in GraphPad prism v9.5.1. The normality of the data was assessed using the Shapiro-Wilk test. The cell distribution of pNC when cultured with standard αMEM,

healthy and degenerate media was not normally distributed and therefore analysed with a Kruskal-Wallis test, followed by Dunn's multiple comparisons test for comparing between the media groups. For the statistical analysis of GAG production and detection of matrix metalloproteinase 3 in pNC & NPgel and MEPC & NPgel when cultured with standard, healthy and degenerate media, data was shown to follow a normal distribution, thus, one-way ANOVA was performed, followed by the recommended Turkeys multiple comparisons test to compare each media group. The number of iPSC-MEPC observed in NPgel when cultured with standard, healthy and degenerate media was assessed as normally distributed and analysed with one-way ANOVA, followed by Turkey's multiple comparisons test. The amount of glycosaminoglycan released into media during the culturing of construct was measured with DMMB assay, the data was normalised to corresponding media and assessed to be normally distributed. Therefore, a one-way ANOVA, followed by Turkey's multiple comparisons test was performed on between the different media groups. Data from the ELISA test showed normal distribution; therefore, a one-way ANOVA was carried out followed by the recommended Turkeys multiple comparison test to compare media groups. Statistical significance was accepted at $p \leq 0.05$.

RESULTS

HEALTHY AND DEGENERATIVE ENVIRONMENT ON PORCINE NOTOCHORDAL CELLS SEEDED INTO NPGEL

Porcine NC and NPgel constructs were cultured in standard αMEM, 'healthy' or 'degenerate' media for up to 4 weeks, with inclusion of a 2-week and 4-week time point. At 2 weeks, the pNC seeded in NPgel constructs cultured in standard αMEM and degenerate media displayed large clusters with morphotypic vacuolated notochordal cells (Fig. 6.1a; indicated with black arrows). The pNC seeded in NPgel construct cultured in healthy media for 2 weeks differed morphologically, along with demonstrating a significant reduction in cell numbers in clusters when compared to pNC seeded in NPgel and cultured in standard αMEM ($p \leq 0.001$); as the median of 3 pNCs per cluster were observed in constructs cultured in healthy media, compared to the 12 and 5 pNC per cluster observed in the standard αMEM (standard) and degenerate group retrospectively (Fig. 6.1b). The was no significant difference between the number of clusters observed in pNC seeded in NPgel and cultured in standard αMEM and the degenerate group (Fig. 6.1b). Constructs that were cultured further for 4 weeks displayed pNCs that lost their vacuoles and morphotopic characteristic in all media groups (Fig. 6.1c). Similar to the 2-week time point, histological staining demonstrated pNC seeded in NPgel constructs cultured in standard αMEM and degenerate displayed resembling morphology and sustained clusters (Fig. 6.1c). Whereas pNC seeded in NPgel constructs cultured in healthy media recurrently displayed significantly less pNC per cluster ($p \leq 0.05$) at a median of 4 pNCs per cluster, compared to 7 and 7 pNC per clusters observed in standard αMEM and degenerate retrospectively (Fig. 6.1d). Generally, pNC seeded in NPgel and cultured in standard αMEM

displayed the largest cluster size of 59 cell cluster at 2-week and 46 cells per cluster at 4 weeks, this characteristic of retaining large clusters was reduced when cultured in either healthy (at 4 weeks there was a maximum of 7 cells per clusters in healthy group and maximum 22 cells per cluster in degenerate group).

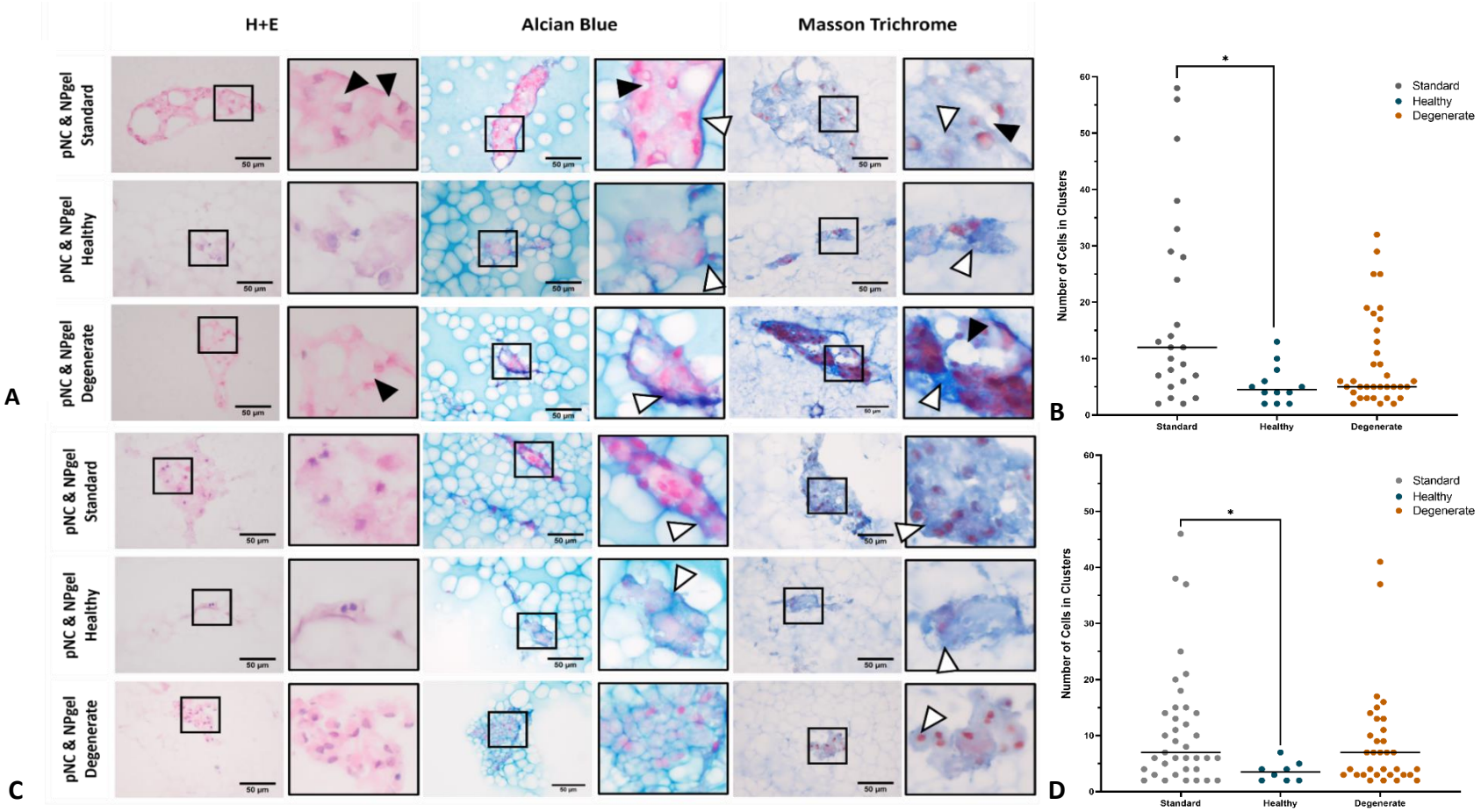

Figure 6.1. Porcine notochordal cells (pNC) morphology and cell survival when seeded in NPgel and cultured in healthy and degenerate media. *Histological staining of pNC seeded in NPgel (pNC & NPgel) and cultured in standard αMEM (pNC & NPgel Standard), Healthy (pNC & NPgel Healthy) and degenerate media (pNC & NPgel Degenerate) for up to* ***(A)*** *2 weeks and* ***(C)*** *4 weeks at 5% v/v oxygen, 37°C (n=3 technical repeats). Haematoxylin and Eosin (H+E), Alcian Blue and Masson's Trichrome. Black boxed indicate zoomed in images. Black arrows highlight vacuole features of a pNC. White arrows indicate extracellular matrix deposition. Scale bar 50µm.With corresponding pNC cluster size within NPgel when cultured in standard αMEM, Healthy, and degenerate media for* ***(B)*** *2 weeks and* ***(D)*** *4 weeks. A single dot represents a cluster of pNCs. Statistics performed with in GraphPad prism v9.5.1, Kruskal-Wallis test, followed by the Dunn's multiple comparisons test *p≤0.05.*

Constructs were then stained with immunohistochemistry to assess viability and phenotype of pNC after 4 weeks culture. Cell death was analysed through the expression of caspase 3, pNC seeded in NPgel constructs at 2-week displayed more staining of caspase 3, especially in standard αMEM and degenerate groups. The staining was then reduced in the 4-week cultured pNC seeded in NPgel constructs (Fig. 6.2).

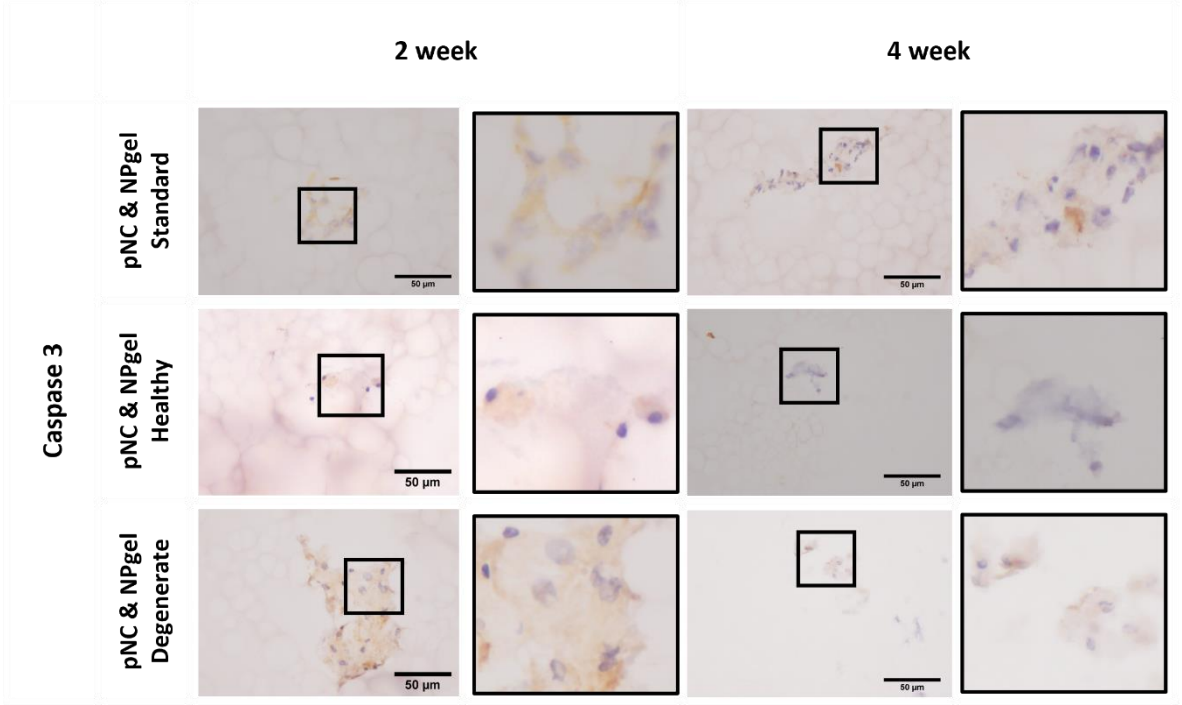

Figure 6.2. Porcine notochordal cells expression of caspase 3 when seeded in NPgel and cultured in healthy and degenerate media. (A) *Immunohistochemistry staining of porcine notochordal cells (pNC) seeded in biomaterial NPgel (pNC & NPgel) and cultured in standard αMEM (pNC & NPgel Standard), Healthy (pNC & NPgel Healthy) and degenerate media (pNC & NPgel Degenerate) for up to 4 weeks at 5% v/v oxygen, 37^{o}C (n=3 technical repeats). Two and 4-week images stained with Caspase 3. Black boxed images represent zoomed in images. Scale bar 20µm. Not enough cells were observed to generate a quantifiable data on the immunopositive cells in samples.*

Brachyury was expressed in pNC seeded in NPgel constructs cultures in standard αMEM and degenerate media, whereas in the healthy group there was no evidence of Brachyury expression (Fig. 6.3). Equally, cytokeratin 8, 18 and 19 were expressed more in pNC seeded in NPgel constructs cultured with standard αMEM, than when cultured in degenerate and even less in healthy media group (Fig. 6.3).

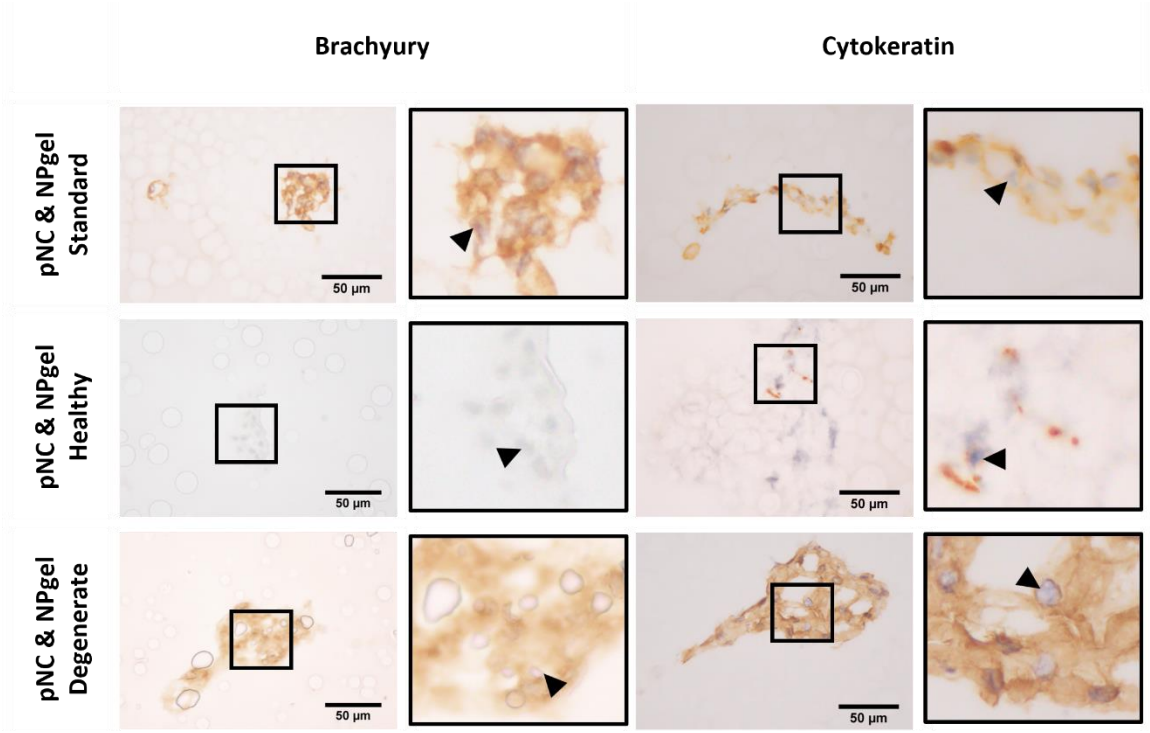

Figure 6.3. Porcine notochordal cells phenotype when seeded in NPgel and cultured in healthy and degenerate media. *Immunohistochemistry staining of porcine notochordal cells (pNC) seeded in NPgel (pNC & NPgel) and cultured in standard αMEM (pNC & NPgel Standard), Healthy (pNC & NPgel Healthy) and degenerate media (pNC & NPgel Degenerate) for up to 4 weeks at 5% v/v oxygen, 37^{o}C (n=3 technical repeats). Stained with Brachyury and Cytokeratin 8, 18 and 19. Black boxed images represent zoomed in images. Black arrows highlight examples of pNC. Scale bar 50µm. Not enough cells were observed to generate a quantifiable data on the immunopositive cells in samples.*

Extracellular matrix expression was also analysed through immunohistochemical staining of Aggrecan and Collagen type II at 4-weeks. Some collagen type II expression was observed in all media groups (Fig. 6.4a), which also translated to the bluing observed in the Alcian Blue histological images (Fig. 6.1c; indicated by white arrows). However, Aggrecan staining was observed in pNC seeded in NPgel with standard αMEM (Fig. 6.4a; indicated by white arrows), with little expression in the other media groups. The regulation of extracellular matrix was investigated by conducting DMMB and ELISA assay with culture media harvested throughout the culture period. GAG released into media at 3-weeks and 4-weeks in culture was observed to be significantly greater in pNC seeded in NPgel constructs exposed to degenerative media than standard αMEM media ($p \leq 0.05$) (Fig. 6.4b). With this, the level of matrix degrading enzyme MMP-3 was also shown to be significantly higher in degenerate media then in the standard αMEM ($p \leq 0.001$) or healthy groups ($p \leq 0.0001$) at 3- weeks (Fig. 6.4c). In the pNC seeded in NPgel and cultured in healthy media were observed to be significantly lower than standard αMEM group at 3-weeks ($p \leq 0.001$; Fig. 6.4c). At 4-weeks again pNC seeded in NPgel

and cultured in degenerate media expressed significantly more MMP-3 in the media than when compared to standard αMEM (p≤0.0001) or healthy media groups (p≤0.0001; Fig. 6.4c).

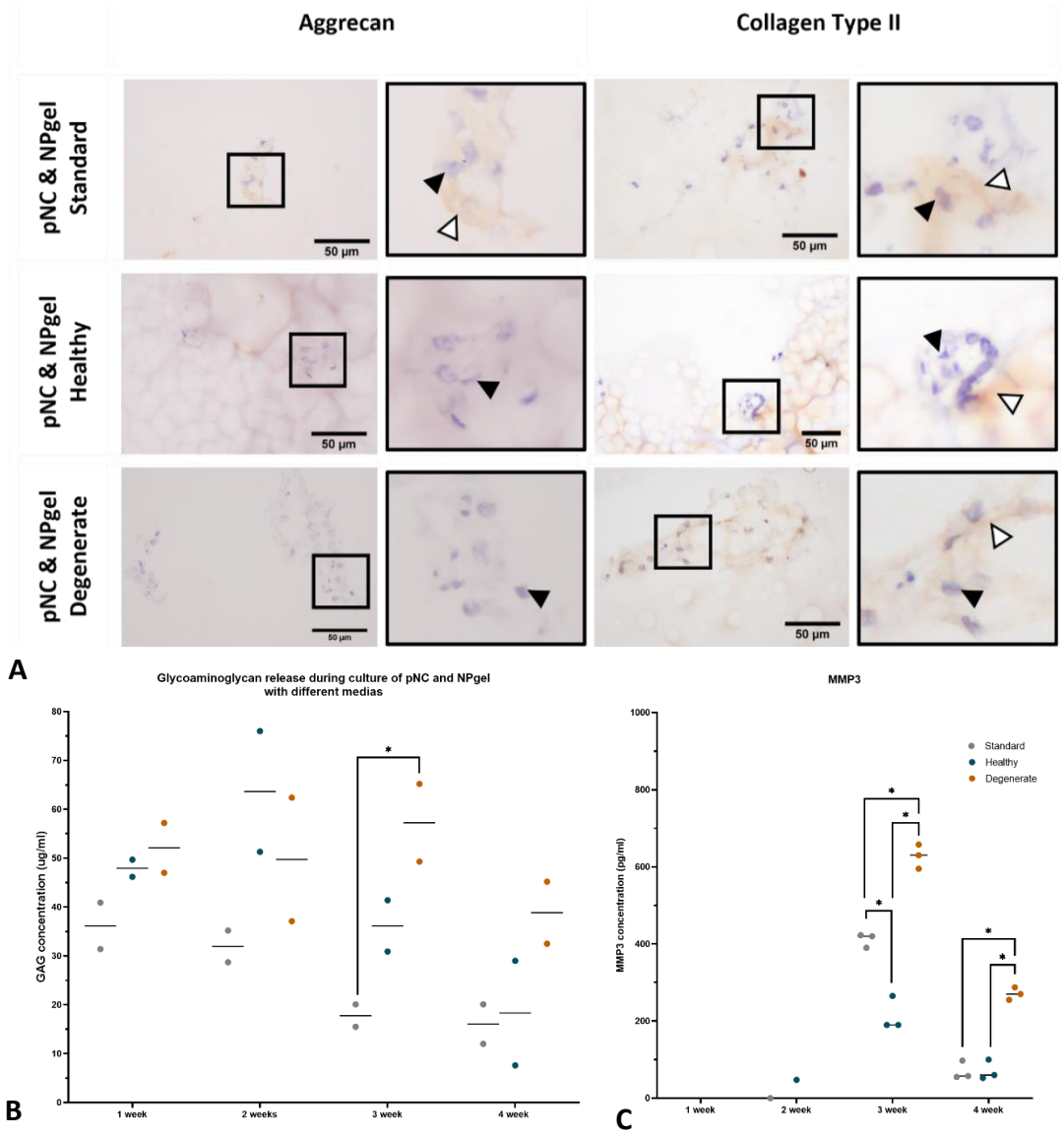

Figure 6.4. Porcine notochordal cells extracellular matrix expression, release and breakdown when seeded in NPgel and cultured in healthy and degenerate media. (A) *Immunohistochemistry staining of porcine notochordal cells (pNC) seeded in NPgel (pNC & NPgel) and cultured in αMEM (pNC NPgel αMEM), Healthy (pNC NPgel Healthy) and degenerate media (pNC NPgel Degenerate) for up to 4 weeks at 5% v/v oxygen, 37°C (n=3 technical repeats), including acellular controls (Acellular NPgel) and porcine disc. Stained with Aggrecan and Collagen type II. Black boxed images represent zoomed in images. Black arrows highlight examples of pNC. White arrows highlight matrix staining. Scale bar 50µm. Including downstream analysis with collected media over the 4-week culture, demonstrating **(B)** glycosaminoglycan (GAG) release using 1,9-Dimethylene blue (DMMB) assay and **(C)** the detection of matrix metalloproteinase 3 (MMP-3) using an Enzyme-linked immunosorbent assay (ELISA). Statistics performed with in GraphPad prism v9.5.1, one-way ANOVA followed by Turkey's multiple comparisons test *p≤0.05.*

HEALTHY AND DEGENERATIVE ENVIRONMENT ON MESENDODERM PROGENITOR CELLS SEEDED INTO NPGEL

IPSCs directly differentiated into MEPCs using 48 hours of CHIR stimulation were seeded into NPgel and exposed to healthy and degenerate media. Histological analysis displayed iPSC-MEPC morphology with large nuclei in iPSC-MEPCs seeded in NPgel cultured in standard and degenerate groups at 2-week and 4-week (Fig. 6.5a, b). After 4-week in culture the number of iPSC-MEPC observed in NPgel were significantly greater in degenerate media than standard and healthy group (Fig. 6.5c). The median number of cells that expressed caspase 3 was higher in 2-week time point for iPSC-MEPC seeded in NPgel cultured in degenerate media, then decreased following 4-weeks in culture (Fig. 6.6), although this did not reach statistical significance ($p \leq 0.05$).

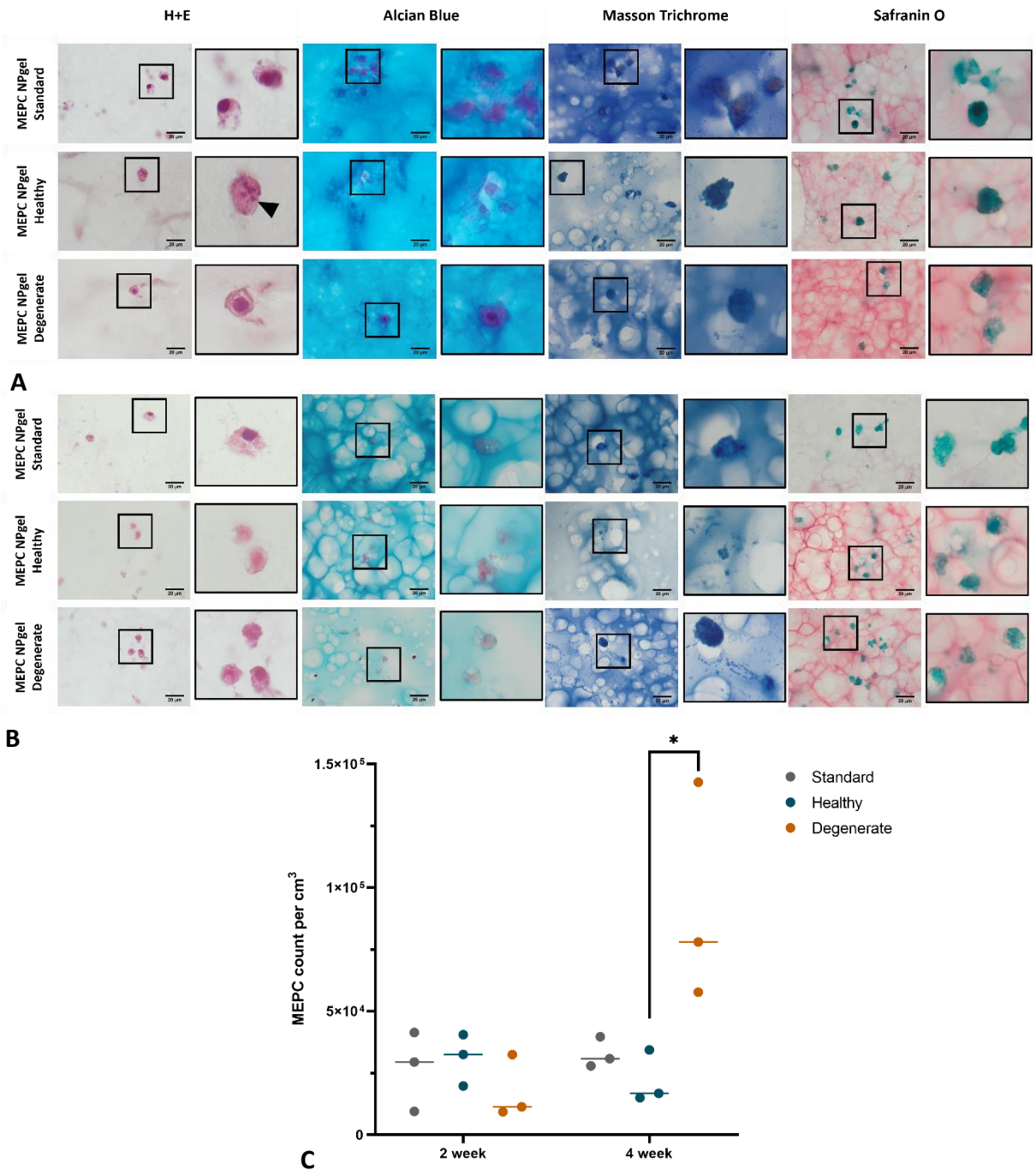

Figure 6.5. Mesendoderm progenitor cells morphology and cell survival when seeded in NPgel and cultured in healthy and degenerate media. *Histological staining of Mesendoderm progenitor cells seeded in NPgel (MEPC NPgel), and cultured in standard (MEPC NPgel standard), Healthy (MEPC NPgel Healthy) and degenerate media (MEPC NPgel Degenerate) for up to* ***(A)*** *2 weeks and* ***(B)*** *4 weeks in a hypoxia unit of at 5% v/v oxygen, 37°C (n=3 technical repeats). Haematoxylin and Eosin (H+E), Alcian Blue, Masson's Trichrome and Safranin Orange (Safranin O). Images with black outline are high magnification regions of constructs. Black arrows highlight multi-fragmented nuclei. Scale bar 20µm.* ***(C)*** *Cell count of MEPC observed within cm^3 of NPgel biomaterial. Statistics performed with in GraphPad prism v9.5.1, one-way ANOVA test, followed by the Tukey's multiple comparisons test *p<0.05.*

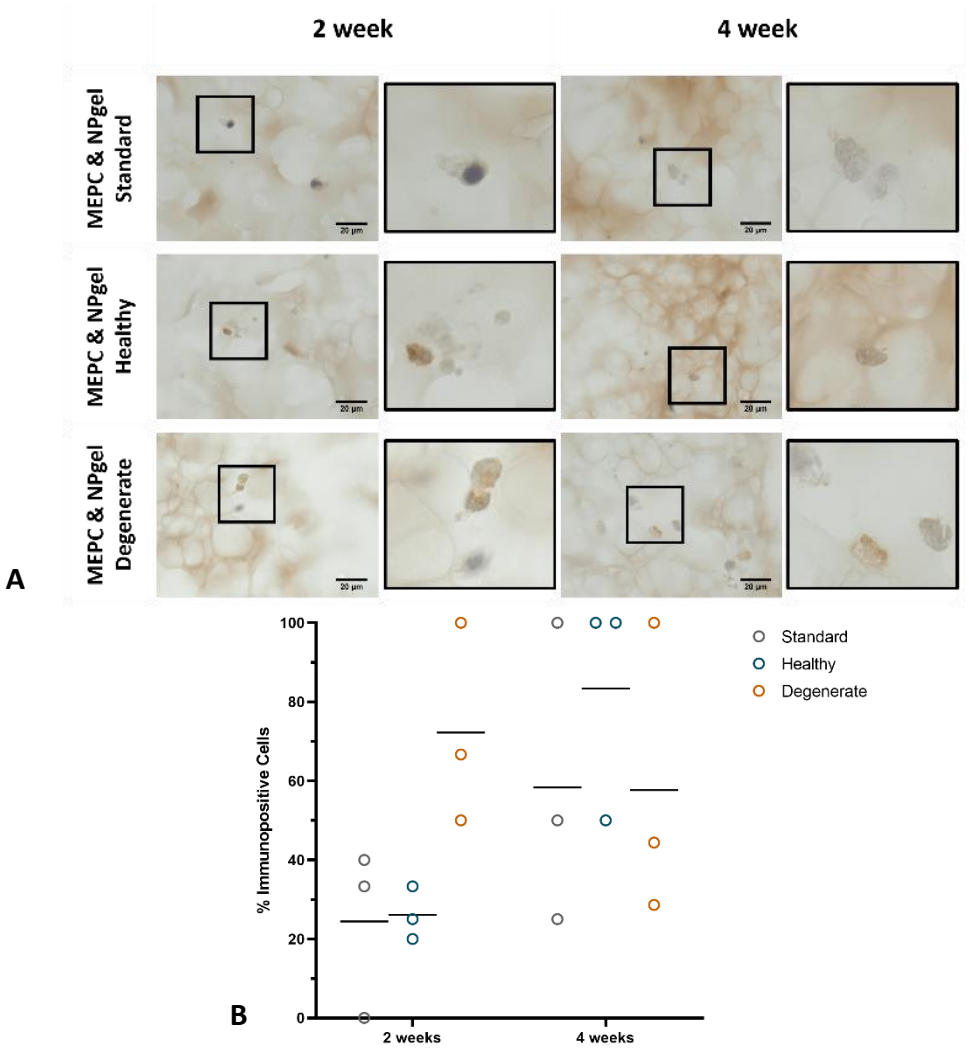

Figure 6.6. Mesendoderm progenitor cells expression of caspase 3 when seeded in NPgel and cultured in healthy and degenerate media. (A) *Immunohistochemistry staining of Mesendoderm progenitor cells (MEPC) seeded in biomaterial NPgel (MEPC & NPgel) and cultured in standard (MEPC & NPgel Standard), Healthy (MEPC & NPgel Healthy) and degenerate media (MEPC & NPgel Degenerate) for up to 4 weeks at 5% v/v oxygen, 37°C (n=3 technical repeats). Two and four-week cultures stained with Caspase 3. Black boxed images represent zoomed in images. Scale bar 20µm.* ***(B)*** *Percentage of MEPC seeded in NPgel and cultured in standard, healthy and degenerate that were immunopositive for Caspase 3. Each dot represents a technical repeat, ○ indicates <10 cells counted in each repeat. Statistics performed with in GraphPad prism v9.5.1, Kruskal-Wallis test, followed by the Dunn's multiple comparisons test, not significant.*

After 4-weeks the iPSC-MEPC seeded in NPgel constructs were analysed for markers related to MEPC and NC phenotype. The iPSC-MEPCs seeded in NPgel cultured in standard media for 4 weeks displayed positive expression of FoxA2, Brachyury and cytokeratin 8, 18 and 19 (Fig. 6.7). Whereas iPSC-MEPC seeded in NPgel cultured in healthy media exhibited predominately Sox9 and Brachyury positive staining. Whilst iPSC-MEPC seeded in NPgel cultured in degenerate media showed little positive staining for Sox9, FoxA2, Brachyury or Cytokeratin 8, 18 and 19 (Fig. 6.7; Not enough cells were observed to generate a quantifiable data on the immunopositive cells in these samples).

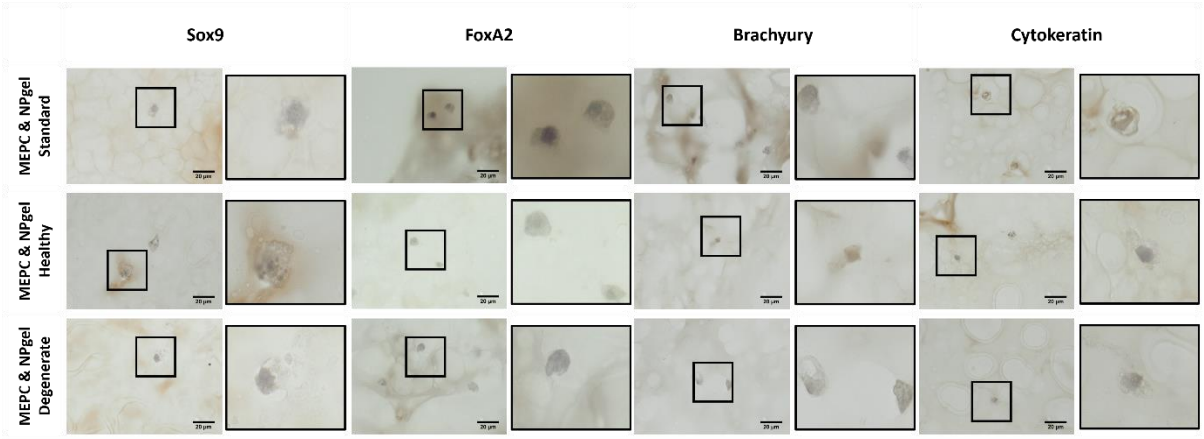

Figure 6.7. Mesendoderm progenitor cells phenotype when seeded in NPgel and cultured in healthy and degenerate media. *Immunohistochemistry staining of Mesendoderm progenitor cells (MEPC) seeded in biomaterial NPgel (MEPC & NPgel) and cultured in standard (MEPC & NPgel Standard), Healthy (MEPC & NPgel Healthy) and Degenerate media (MEPC & NPgel Degenerate) for 4 weeks at 5% v/v oxygen, 37^{o}C (n=3 technical repeats). 4-week images stained with Sox9, FoxA2, Brachyury and Cytokeratin 8, 18 and 19 (cytokeratin). Black boxed images represent zoomed in images. Scale bar 20µm.*

Extracellular matrix expression was analysed using immunohistochemical staining for aggrecan and collagen type II. IPSC-MEPC seeded in NPgel constructs in all culture media displayed positive extracellular matrix staining for collagen type II (Fig. 6.8a; indicated with white arrows). Aggrecan showed less positive staining for matrix in the iPSC-MEPC seeded in NPgel constructs (Fig. 6.8). The detection of GAG through harvested culture media throughout the culture period, demonstrated a gradual increase of GAG release from 1-week to 4-week in standard and degenerate groups (Fig. 6.8b). With significantly higher GAG release observed in standard ($p \leq 0.05$) and degenerate groups ($p \leq 0.01$) when compared to iPSC-MEPC seeded in NPgel cultured in healthy media at the 2-week time point (Fig. 6.8b). The detection of MMP-3 showed no real trend throughout the cultures (Fig. 6.8c).

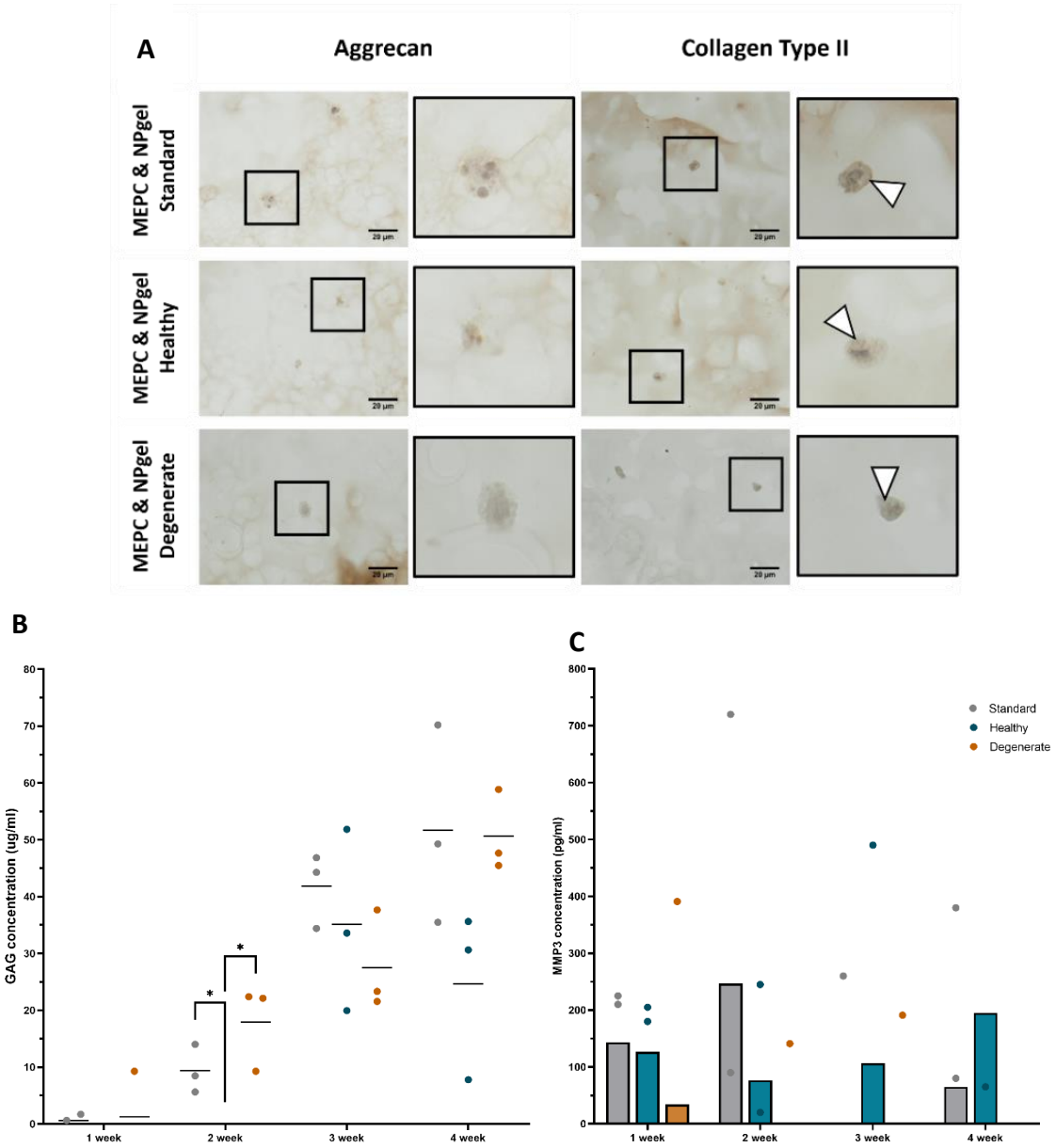

Figure 6.8. Mesendoderm progenitor cells extracellular matrix expression and release when seeded in NPgel and cultured in healthy and degenerate media. (A) *Immunohistochemistry staining of Mesendoderm progenitor cells (MEPC) seeded in biomaterial NPgel (MEPC & NPgel) and cultured in standard (MEPC & NPgel Standard), Healthy (MEPC & NPgel Healthy) and Degenerate media (MEPC & NPgel Degenerate) for 4 weeks at 5% v/v oxygen, 37^{o}C (n=3 technical repeats). Stained with Aggrecan and Collagen Type II porcine notochordal cells (pNC) seeded in NPgel (pNC & NPgel) and cultured in αMEM (pNC NPgel αMEM), Healthy (pNC NPgel Healthy) and degenerate media (pNC NPgel Degenerate) for up to 4 weeks at 5% v/v oxygen, 37^{o}C. Stained with Aggrecan and Collagen type II. Black boxed images represent zoomed in images. White arrows highlight matrix staining. Scale bar 20µm. Including downstream analysis with collected media over the 4-week culture, demonstrating* ***(B)*** *glycosaminoglycan (GAG) release using 1,9-Dimethylene blue (DMMB) assay, and* ***(C)*** *the detection of matrix metalloproteinase 3 (MMP-3) using an Enzyme-linked immunosorbent assay (ELISA) (n=3 technical repeats). Statistics performed with in GraphPad prism v9.5.1, one-way ANOVA test, followed by the Tukey's multiple comparisons test, *p<0.05.*

DISCUSSION

The clinical application of cell-seeded biomaterials for the treatment of disc degeneration is restricted by the hostile environment that is associated with the IVD. The IVD conditions can affect the survival of transplanted cells and would limit the constructs' ability to repair and regenerate. Therefore, this study tested the hypothesis that two constructs: pNC seeded in NPgel and MEPC seeded in NPgel, can survive, and retain their regenerative properties *in vitro*, when exposed to the healthy and degenerate disc environments, with an emphasis on altering the glucose concentration, osmolality, pH and cytokines with all cultures performed under physioxia. The study demonstrated that the potential injectable cell-seeded biomaterials showed limited effects by degenerative media, although an increase of MMP-3 was seen in NC cells cultured in degenerate media.

CELL-SEEDED BIOMATERIALS MORPHOLOGICAL AND PHENOTYPIC DIFFERENCE IN THE HEALTHY AND DEGENERATE MEDIA

Porcine NC seeded within NPgel was the first construct to be assessed with healthy and degenerate media for up to 4 weeks, taking a 2-week and 4-week time point. Morphologically at 2-weeks the pNC seeded in NPgel cultured with standard αMEM presented with vacuoles that disappeared at 4-weeks. The disappearance of vacuoles was also observed in Chapter 3, and in other publication were NCs are cultured in long-term 3D alginate beads and when injected into *in vivo* setting (Arkesteijn *et al.*, 2015; Arkesteijn *et al.,* 2017). The typical characteristic of pNC presented in clusters was demonstrated in the standard media control group and was also sustained in the degenerate media group. Likewise, the typical NC phenotypic expression of positive staining of Brachyury and cytokeratin 8, 18 and 19 was demonstrated in the standard and degenerate media. Interestingly, the pNC seeded in NPgel construct cultured in healthy media displayed no vacuoles at 2-weeks, a smaller number of pNC in clusters and no immunopositive staining for Brachyury and cytokeratin 8, 18 and 19.

The second construct MEPC seeded in NPgel was next assessed in the healthy and degenerate media. Morphologically the iPSC-MEPC remained visible in all media groups, however the iPSC-MEPC seeded in NPgel constructs in the healthy group lacked definitive nuclei staining. Interestingly iPSC-MEPC count increased significantly at 4-week culture in degenerate media when compared to standard and healthy groups, suggesting the iPSC-MEPCs proliferated. Cell proliferation was improved in a study comparing Mesendoderm progenitor cells culture in a 3D biodegradable gelatin microcryogels and 2D culture, the study observed the 3D culture promoted iPSC-MEPC proliferation (Zhang *et al.*, 2017). Based on this observation of improved iPSC-MEPC cell number and sustained morphology in the degenerate culture group, the iPSC-MEPC seeded in NPgel constructs also favoured the degenerate environment, as did pNC seeded in NPgel.

With both constructs demonstrating a resistance to the degenerative media, but also displayed a negative impact of the healthy media. A deeper look of the effect of pH and IL-1β was investigated in similar studies.

THE EFFECT OF OSMOLALITY ON CELL-SEEDED BIOMATERIALS

A preliminary study comparing only the effect of osmolality at 300 mOsm/kg compared to 400 mOsm/kg on pNC & NPgel constructs, indicated that osmolality did not visibly affect the morphology and phenotype of pNCs (data not shown). Different osmolality media have been previously examined in NP cells, where in these studies human degenerate NP cells and canine NP cells were exposed to hyperosmolality of 400 mOsm/kg and 500 mOsm/kg. The exposure of high osmolality during expansion of NP cells was shown to exert beneficial effects of improved NP cell phenotype and more GAG expression during culture in hydrogel (Krouwels *et al.*, 2018; Laagland *et al.*, 2022). However, varying osmolality had no effect during culture of human degenerate NP cell once in hydrogel culture (Krouwels *et al.*, 2018; Krouwels *et al.*, 2018). In canine NC seeded into alginate beads, increase osmolality was shown to influence favourable phenotype of high expression of Brachyury, cytokeratin 18, and aggrecan, GAG production (Spillekom *et al.*, 2014). The NPgel biomaterial could have protective properties of osmolality, as NPgel has ion binding, and therefore produce its own internal osmolality. Subjecting the pNCs to a consistent osmotic gradient regardless of the external media (Boyes *et al.*, 2021).

THE EFFECT OF PH VARIATION ON CELL-SEEDED BIOMATERIALS

Our study results of pNC seeded in NPgel being unaffected when cultured in degenerative media are conflicting. As in previous studies, the effect of pH on pNC when seeded into alginate beads, resulted in cell count remaining the same when cultured in DMEM with at pH 7.2, but reduced to <50% of initial cell when pH was modified to 6.8. however, Guehring *et al.,* (2009) study used NC clusters that sustained additionally digested to produce individual cells prior to cell seeding, suggesting that cells in clusters could have a protective effect on external conditions (Guehring *et al.*, 2009). Another study also observed that seeding human chondrocytes in alginate bead culture exposed to differing pH 7.2 and 6.2 and oxygen (<1%, 2%, 5%, and 21%) revealed that when chondrocytes were incubated at pH 6.2 significantly reduced the cell viability at <1%, 2% and 21% O_2. Interestingly when the cells were cultured at 5% O_2, 5% CO_2 cell viability was resistant to pH variability (Collins *et al.*, 2013), which may also explain the lack of response to lower pH seen in the current study. The effect of pH was shown to be dependent on cell type; from a study utilising iPSC -derived NC injected into a *in vivo* degenerate disc, the main finding was that inclusion of iPSC-NC were shown to change the intradiscal pH comparable to a healthy IVD. Whereas the injected MSC group showed no significant difference to degenerate disc model (Sheyn *et al.*, 2019). Another study highlights that pH has negative effect on proliferation and viability of MSC, with significant loss of cellularity and decreased biosynthesis rates found at pH 6.5 with pH of 7.1 also affecting the

cell proliferation (Wuertz *et al.*, 2009), on the other hand they contradictory demonstrated that no changes was observed in caspase 3 expression (Wuertz *et al.*, 2009).

It is apparent that there is link between extracellular matrix and pH, as one study concluded that NC and iPSC-NCs may play a protective role by preventing the matrix degradation that is correlated with low pH levels in the degenerated disc (Sheyn *et al.*, 2019), and others reported the severe effects on aggrecan gene expression at acidic pH (Wuertz *et al.*, 2009). However, pH and extracellular matrix would rationally be indirectly linked if acidic pH reduced the metabolic activity and therefore extracellular production of NCs. In this study, pNC seeded in NPgel demonstrated significant increase in GAG released into media at 3-week and 4-week cultured in degenerative media, however this accompanied a significant increase in matrix digestion enzymes (MMP-3) also observed at 3-week and 4-week in the degenerate group. In the iPSC-MEPC seeded in NPgel construct there was a gradual increase in GAG release in media throughout the culture period in the degenerate group, but no clear trend in MMP-3 detection. The association of GAG release and MMP-3 could suggest that the extracellular matrix is being broken down, MMP-3 would degrade the collagens and to some extent the proteoglycans in the constructs, thus releasing GAGs to the surrounding media. If the cells aren't producing extracellular matrix, then the trend would be an initial high detection peak early in the culture period (from harvesting and digestion from tissues or biomaterials) which then declines throughout the remaining time, which is what is observed in pNC seeded in NPgel cultured in healthy media. Functional proteoglycan synthesis by NPCs is highest between pH 7.1 and 6.9 (Ohshima and Urban, 1992), and is oxygen sensitive, with optimal matrix synthesis occurred between 1% and 5% O_2 (Yang *et al.*, 2017; Jaworski *et al.*, 2019). MMP-3 expression was only significantly increased within the 5% oxygen tension group (Jaworski *et al.*, 2019). MMP-3 also targets collagen II preferentially and is natively expressed within the disc (Cui et al., 2010; Tallant et al., 2010; Baillet et al., 2013).

It is understood that NC are more metabolic active at pH 7.2 than at pH 6.8 (Guehring *et al.*, 2009), consequent to high consumption of oxygen and glucose and lactate production. To which extra lactate will amplify the acidic environment. Interestingly one study hypothesized that stem cells utilised supplemented sodium lactate as an energy source and adapting to the change in environment, which has also been shown in other cells such as hESC (Chen *et al.*, 2010) and germ cells (Mita and Hall, 1982; Erkkilä *et al.*, 2002). With the addition that lactate concentration and pH can influence differentiation of stem cells, reporting that exogenous lactic acid induces chondrogenic differentiation (Guehring *et al.*, 2009). In this study, it would have been beneficial to have assessed metabolic activity of these cellular constructs further, with either measuring mitochondrial membrane potential, nitric oxide, intracellular ATP and ROS levels.

THE EFFECT OF IL-1B ON CELL-SEEDED BIOMAETERIALS

In a degenerate IVD the IL-1β level is significantly increased and IL-1β participates in multiple pathological processed of disc degeneration (Le Maitre *et al.*, 2005; Le Maitre *et al.*, 2007). In

the IVD, IL-1β has been shown to be secreted by IVD cells (Le Maitre *et al.,* 2005; 2007), with the active suppression of IL-1β has been reported as a potential therapy for prevention of disc degeneration (Le Maitre *et al.,* 2007). However, low levels of IL-1β are found within non-degenerative disc cells (Le Maitre *et al.*, 2007), and the loss of IL-1 inhibitor in null mice lead to IVD degeneration (Phillips *et al.*, 2013), suggesting that IL-1 participates in the degeneration of IVD tissue (Le Maitre *et al.*, 2007). Reviewing previous studies investigating the effect of IL-1β, the presence of IL-1β overall had an effect on GAG content in NP cells (De Vries *et al.*, 2019), with a presence of IL-1β led to a 4–5 fold increase in GAG release from human chondrocytes after 24 hours in all oxygen tensions (Collins *et al.*, 2013). Further investigation observed that IL-1β did not affect further alteration in intracellular pH (Collins *et al.*, 2013). Therefore the causation between IL-1β and GAG content has been linked to IL-1β inducing MMP-3 gene expression; which was observed in NP cells (Le Maitre *et al.*, 2005), bone marrow MSC (Carrero *et al.*, 2012), annulus fibrosus cells (Le Maitre *et al.*, 2005; Gruber *et al.*, 2010) and chondrocytes (Collins *et al.*, 2013), with the addition of enhance cell migration observed in MSC (Sullivan *et al.*, 2014; Chang *et al.*, 2021). As the degradation of matrix allows for cell migration. At present there is a lack of studies on the effects of IL-1β on iPSC-MEPCs culture.

As the seeded cells were not adversely affected by the degenerate parameters of the degenerate media suggests that the biomaterial served as a protective environment during cell culture, as shown previously with MSC (Vickers *et al.*, 2019), or that the cells have adapted and thrive in degenerate media in comparison to the healthy media. This also leads to a theory suggesting that another parameter, other than those investigated in this study, could be involved with the change in NC to NP cells that is observed in natural degenerative discs. In the future, the influence of mechanical loading should also be investigated to study the response under physiological loading and nutrient perfusion, as this would be more indicative of the *in vivo* environment mechanical cues, which play an important role in balancing cellular metabolism and phenotype (Adams and Roughly, 2006; Guehring *et al.*, 2010; Neidlinger-Wilke *et al.*, 2012; Purmessur *et al.*, 2013).

CONCLUSION

Cell-seeded biomaterials in the form of pNC seeded in NPgel and iPSC-MEPC seeded in NPgel were subjected to the IVD hostile environment, which is known to limit the ability of cells to repair and regenerate, which included nutrient deprivation and biochemical alterations. The results determined that there is initial evidence that both constructs were not defective by media that mimicked the degenerate disc microenvironment. Demonstrating that pNC seeded in NPgel and iPSC-MEPC seeded in NPgel construct could potentially survive *in vivo* following transplantation into a degenerate disc. Therefore, these cell-seeded biomaterials have the potential to be utilised for regenerating a degenerate IVD.

ACKNOWLEDGMENTS

This work was supported by the funding received from the European Union's Horizon 2020 research and innovation programme [grant agreement No 825925]. MAT is financially supported by the Dutch Arthritis Society (LLP22).

CONFLICT OF INTEREST

CLM and CS are named inventors on the patent for NPgel.

CHAPTER 7
GENERAL DISCUSSION AND FUTURE DIRECTIONS

SUMMARY OF RESULTS

This thesis aimed to investigate novel cell-based treatments that target the pathways which could lead to regeneration of the NP within the IVD. The first chapter of the thesis provided a literature review and discussion of potential cell sources proposed for NP tissue regeneration. Assessing each cell-source on parameters that were identified necessary for adequate translational potential and regenerative characteristics. The conclusion was that iPSC derived NC-like cells could have the potential for regenerating the NP in degenerate discs and thus required further study to assess their regenerative ability and safety. However, in research there has been a limited use of NC *in vitro* and therefore recommended, methodologies and standard operation procedures are severely lacking for facilitating the use of this cell source. Chapter 2 provided key recommendations for the extraction of NCs from multiple species from mice to humans, and extensive characterisation of NC was conducted through a phenotypic panel approach, involving several groups worldwide who utilise NCs. Once an understanding of NC characterisation *in vivo* and *in vitro* was established, in Chapter 3 accessible porcine NCs were used to facilitate the screening of novel injectable biomaterials intended to be used as cell delivery systems whilst also providing mechanical support and restoration. The results demonstrated that pNC can retain viability and maintain NC markers in an array of natural to synthetic biomaterials, Albugel, NPgel and NPgel/dNCM for up to 4 weeks *in vitro* in physiological 5% v/v oxygen. With the promising biomaterials showing cytocompatibility with NCs of porcine origin, next the principal cell source was investigated in these biomaterials. Unfortunately, iPSC derived NCs were unattainable through our consortia due to issues with poor purity during differentiation, and progenitor cells MEPCs were utilised instead. Chapter 4 analysed which biomaterials maintained iPSC-MEPCs viability and the potential to additionally drive iPSC-MEPCs differentiation to NC-like cells. The biomaterials used in this chapter included the original Albugel, NPgel and NPgel/dNCM from Chapter 3, with a screening of additional biomaterials: alginate and PEG/dNCM (a leading biomaterial from a collaborating University). It was concluded the PEG/dNCM and NPgel biomaterial showed most potential due the observation of iPSC-MEPC survival and the demonstration of regenerative properties through positive extracellular matrix staining and iPSC-MEPCs expressing NC- like phenotype up to 4 weeks *in vitro* in physiological 5% v/v oxygen. However, handling of iPSC-MEPC during this Chapter demonstrated key difficulties particularly associated with cryopreservation and restoration, resulting in low viability and low cell

numbers after iPSC-MEPC recovery from cryopreservation. Suggesting, that using iPSC-MEPC via this method was inefficient and ineffective for translational potential. Thus, Chapter 5 went on to compare *in situ* generated iPSC derived MEPCs and iPSC-MEPCs subject to cryopreservation and recovery process, which mimicked the iPSC-MEPCs used in Chapter 4. Additionally, demonstrating the limitations involved with the use of iPSC, highlighting issues around viability, cell handling, the effects of cryopreservation and the use of ROCKi. In conclusion, Chapter 5 highlighted the implications of inter-laboratory comparisons, and the limitations of distributing cryopreserved cells, which can be correlated to issues that clinically translating and upscaling iPSC-MEPC manufacturing. Following this non cryopreserved iPSC-MEPCs were combined with NPgel biomaterial and was used in further testing in Chapter 6. Porcine NC were also included in this chapter as iPSC-MEPC showed they had limited translational potential and accordingly limited data supporting whether iPSC-MEPCs are the best cell choice clinically. Therefore, in Chapter 6 the effect of the IVD hostile environment upon pNC seeded in NPgel and iPSC-MEPC seeded in NPgel were investigated. The results demonstrated evidence that pNC seeded in NPgel and iPSC-MEPC seeded in NPgel construct were morphological unaffected by degenerative mimicking media that contained cytokines. However, there were the observation of increased extracellular matrix breakdown in the media, and some changed phenotypic marker expression within iPSC-MEPCs.

FUTURE DIRECTIONS

As the last chapter began to expose the cell-seeded biomaterial constructs to the micro-environment of the disc. Future directions would also include the addition of mechanical loading exerted upon the cell-seeded biomaterial constructs. A pilot study was conducted targeting the effect of mechanical compression upon pNC seeded in NPgel constructs by subjecting the constructs to a basic loading regime after 2 weeks in culture at 5% v/v oxygen. To test the hypothesis that compressive loading would not affect the viability of cells when seeded in biomaterials. The experimental design including culturing pNC seeded in NPgel for 2 weeks as per methods described in Chapter 3, using standard αMEM media and culturing at 5% O_2, 5% CO_2 and at 37^{o}C. After 2-weeks the construct was biopsy punched, placed within a Perspex ring to provide a semi constrained culture, and positioned onto the loading simulator (Electro force 5200). The whole loading simulator and construct was cultured within standard αMEM media, and the loading regime was set to sine wave of 1Hz of 7%-11% displacement for 20 hours to stimulate 'walking'. From the initial 20 hours of sustained confined compression there was no change to cell morphology (Fig. 7.1) and NC extracellular matrix degradation (Fig. 7.2). Future testing should involve the utilisation of more physiological loading regimes (e.g. simulated daily loading), and using culture medium resembling healthy, degenerate disc environments as described in Chapter 6. An example of this type of regime would be described as dynamic loading in a human physiological range of between 0.2 – 1Mpa disc pressure at 1Hz (Korecki *et al.,* 2008; Korecki *et al.*, 2010; Chan *et al.,* 2011). As it has been

shown that pressure in the L4-L5 disc range from 0.1Mpa when lying down to 0.95Mpa during physical activity to the an extreme of 2.3Mpa when performing weight bearing exercises (Wilke *et al.*, 1999) and may involve a complex loading regime similar to that reported in Le Maitre *et al.,* (2009) where daily activities were simulated.

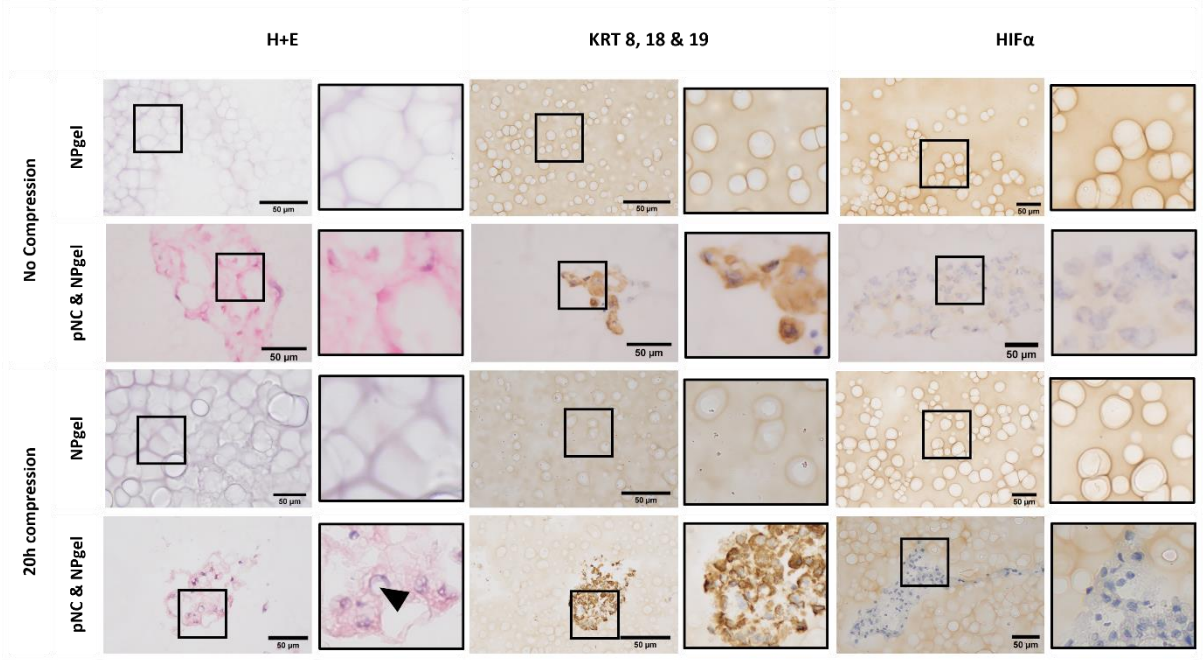

Figure 7.1. Porcine notochordal cell morphology and phenotype when seeded in NPgel when subject to compression. *Histological and Immunohistochemical staining of porcine Notochordal cells cultured in NPgel (pNC & NPgel) with acellular controls (NPgel) for 2 weeks prior to subject to 7%-11% displacement for 20 hours (20h) at 5% v/v oxygen, 37^{o}C (n=3 technical repeats). Stained with Haematoxylin and Eosin (H&E), pan cytokeratin (KRT 8/18/19) and HIFα. Black boxed images indicate zoomed in area. Black arrow indicate cells with vacuole like structures.*

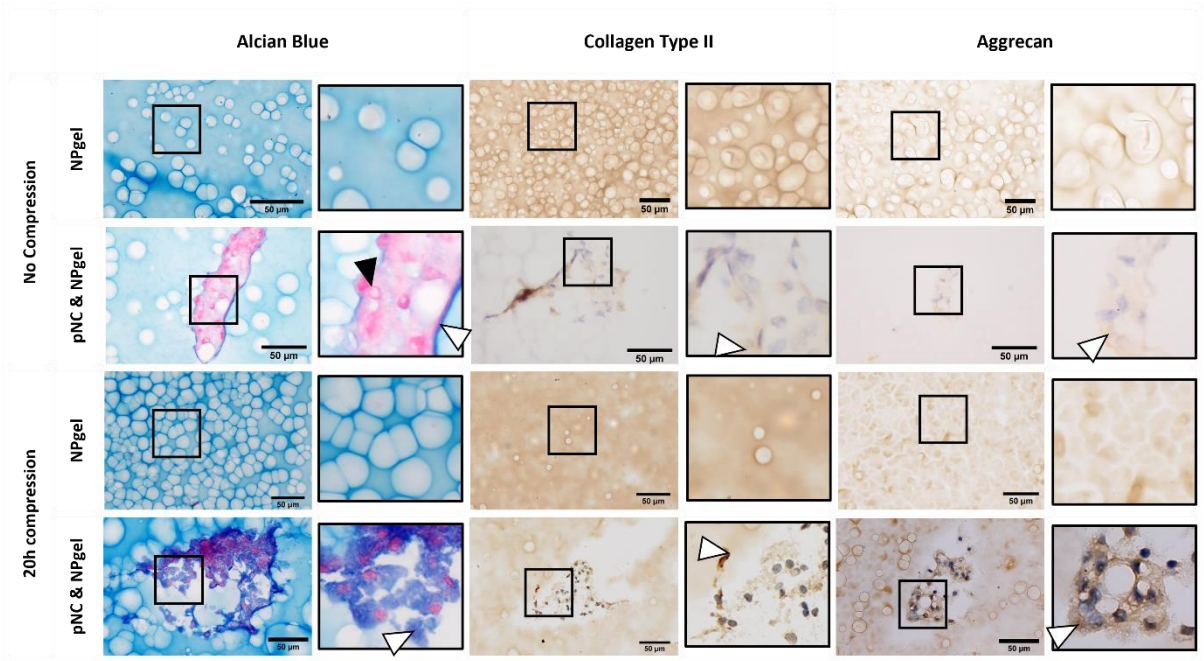

Figure 7.2. Porcine notochordal cell extracellular expression when seeded in NPgel and subject to compression. *Histological and Immunohistochemical staining of porcine Notochordal cells cultured in NPgel (pNC & NPgel) with acellular controls (NPgel) for 2 weeks prior to subject to 7%-11% displacement for 20 hours (20h) at 5% v/v oxygen, 37°C (n=3 technical repeats). Stained with Alcian Blue, Collagen Type II and Aggrecan. Black boxed images indicate zoomed in area. Black arrows indicate cells with vacuole like structures. White arrows indicate extracellular matrix staining.*

Abnormal or prolonged loading and intradiscal pressure has been theorised to accelerate the process of disc degeneration, therefore it is important to perform an investigation of loading effects on cell-seeded biomaterials. A study of exerting a cyclic compressive loading of 50 to 300N at 1Hz for a period of only 2 hours demonstrated that MRI parameters are sensitive to changes in the NP water content induced during loading (Périé *et al.*, 2006). A thought to consider is during progressive disc degeneration the loading can change; for instance, as the disc height decreases in disc degeneration, the force is transmitted to the facet joints which will then take up the compensatory load (Dunlop *et al.,* 1984). In severe cases of disc space narrowing up to 70% of axial load can be borne by the facet joints (Adams and Hutton, 1983; Park *et al.,* 2013), which translates to intradiscal pressure measured at 0.53MPa in healthy discs, <0.4MPa in mild and <0.2MPa in moderate to <0MPa in severe degenerative discs (Park *et al.,* 2013). The effect of loading upon NC has been investigated in rabbit IVD *in vivo*; with the result of physiological, dynamic hydrostatic pressure for 2 hours/ day induced NC differentiation (Guehring *et al.*, 2010). Additionally, an interesting hypothesis that mechanical loadings effect on biomechanical signalling of the cells and the vacuoles that are a prevalent characteristic of NC, that are lost during culture. No research has yet been conducted of the presence of primary cilia on NC. Primary cilia are a non-motile ancient organelle that protrudes from the cell surface of most mammalian cell type, and acts as a sensory structure and facilitates the cell response to exterior environmental cues (Pazour and Witman, 2003). The primary cilia are not exclusively flow sensors, but also responds to compressive and

osmotic loading conditions (Spasic and Jacobs, 2017). Here, a preliminary study was performed to investigate the presence of primary cilia on pNCs. Demonstrating that structures resembling the primary cilia in pNC cultured in alginate beads for 7 days presented with that are positive for immunofluorescence for α-tubulin (Fig. 7.3). In literature, a longer cilia is observed on a endothelial cells resulting in the cells producing significantly more nitric oxide, also suggesting enhanced mechanosensitivity (Kathem et al., 2014). Interestingly, in endothelial cells, removal of cilia increased inflammatory gene expression *in vivo.* For disc cells the primary cilia on NP cells alter their lengths in response to changes in extracellular osmolarity (Choi *et al.*, 2019), with a shorter cilia length or lost in degenerate discs (Li *et al.*, 2020; Snuggs *et al.*, 2021). Other studies utilising mechanical loading, found that loading disrupted the cilia elongation, which was induced by IL-1β, and resulted in the suppression of nitric oxide and prevented cartilage degradation (Fu et al., 2019, 2021). The primary cilia structure is docked by caveolin-1 and caveolae are conserved plasma membrane structures in notochord vacuolated cells, the loss of caveolin -1 (Cav1) causes NCs to collapse and is linked to a reduced NCs in the NP (Bach et al., 2016; Garcia et al., 2017; Smolders et al., 2013). Therefore, the relationship between these primary cilia, vacuoles and mechanical compression would be a very interesting subject matter to understand more about why the NC differentiate or disappear.

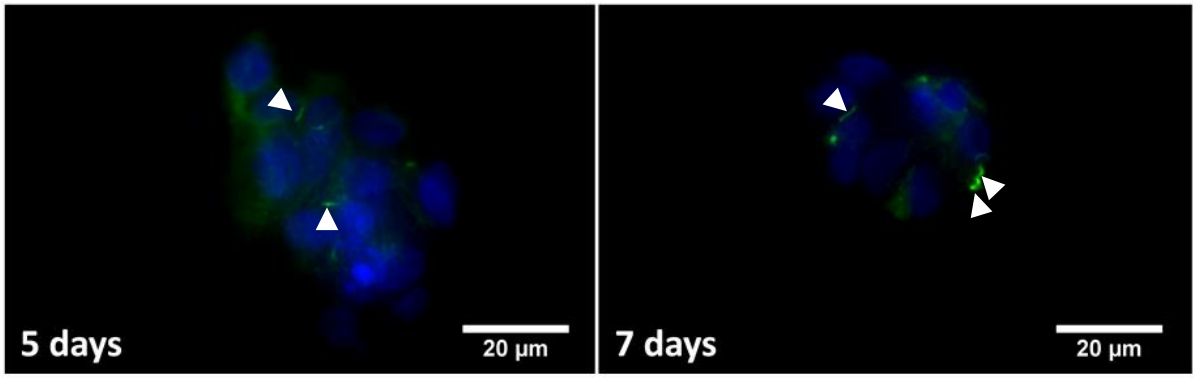

Figure 7.3. Porcine notochordal cell primary cilia staining in alginate culture. *Porcine Notochordal Cells cultured in alginate beads for 5 days and 7 days in standard αMEM media at 5% v/v oxygen, 37^{o}C (n=3 technical repeats). Stained with αtubulin (green) and Hoechst 33342 (DAPI; Invitrogen™, UK). White arrows indicate cilia.*

Disc Research has undertaken significant advances of understanding the disc microenvironment and their effects on the potential of cellular regeneration (Buckley *et al.*, 2018). The *in vitro* manipulation of oxygen, glucose, pH, inflammatory cytokines, biophysical loading, and osmolality is limited to adding external factor and lacks the interconnection displayed across the whole-body systems. As a result, the next direction would to intradiscally inject the cell-seeded biomaterials into *ex vivo* organ culture models or better yet, *in vivo* animal models. With a true test of subjecting the cell-seeded biomaterial constructs to the disc microenvironment with the involvement of immune system, loading and other external factors. With emphasis to find how the disc will respond to the biomaterials and the cells, as we have no real understanding of how the reintroduction of NC-like cells will have on NP of

the disc. Questions that should be addressed during further *ex vivo* and *in vivo* investigations include understanding and identifying: (1) if the transplanted cells can refrain from differentiating into mature NP cells, or disappear as they do *in vivo*; (2) would introducing more cells negatively add to the disease state, adding to the metabolism and nutrient demand to the already avascular, acidic degenerated disc (Horner and Urban, 2001). Investigating the permeability state of the CEP, to provide nutrient supply to the injected cell therapy (Wong *et al.*, 2019); (3) if the injected cell-seeded biomaterial constructs simply generate extracellular matrix and replace the disease like tissue; (4) would the cell-seeded biomaterials provide signals to facilitate and stimulate an effective repair response and allow host cells to migrate, integrate and regenerate; (5) will the production of new matrix translate into symptomatic pain relief for the patient (Buckley *et al.*, 2018; Binch *et al.*, 2021). The disc field has not yet fully understood the cause of disc degeneration that facilitates the disappearance of NC in adulthood. Therefore, it is important to investigate these constructs in a living organ to understand more if this concept can really have potential for NP regeneration.

LIMITATIONS

Throughout this thesis limited number of porcine NCs and iPSC-MEPCs were available to generate biomaterial constructs. Which affected the number of repeats and time points which could be investigated. If an unlimited number of cells were available, for every investigation, complete time course studies including day 0, 1-week, 2-week, 3-week and 4-week time point would have been completed with the minimum of three repeats per timepoint. An attempted of multiple timepoints were generated in the iPSC-MEPC in Phase III testing in Chapter 5, which lead to compromising the size of the cell-biomaterial constructs to 50µl from our standard 300µl. This resulted in the complete disappearance of iPSC-MEPC seeded in alginate biomaterial samples after 3 weeks in culture.

Another limitation in this thesis was the downstream analysis when working with biomaterials. The inability of cellular component to be extracted from the biomaterial once seeded lead to the only downstream analysis of imaging stains and media analysis. With dependence of characterising of cells based of the morphological NC seeded in biomaterials that display bubbles like features. Completely clear staining was never accomplished when performing IHC staining on these biomaterials, the properties of the biomaterials resulted in non-specific staining of DAB and fluorescent molecules, leading to autofluorescence and some background staining of biomaterials. Throughout the thesis, a DMMB biochemical analysis was performed on the media, this analysis could have too been performed on the constructs themselves. In other studies, this involved digesting the constructs overnight with enzymes (such as papain) and would involve sacrificing a construct to this analysis (Martyniak *et al.*, 2022). This would result in quantitative data for the amount of GAGs contained in the constructs through the culture period. Furthermore the extraction of GAGs from some of the biomaterials such as NPgel is not possible due to the synthetic polymer forming steric entanglement with any matrix components as has been reported previously (Thorpe *et al.*,

2016). An alternative method of staining for extracellular matrix produced directly from cells was further investigated. Here, we began to optimise a direct staining or labelling of GAG produced directly by the cells themselves; using N-azidoacetylgalactosamine-tetraacylated (Ac4GalNAz) (CLK-1086; Jena Bioscience, Germany) supplemented to culture media throughout the period of culturing cell-seeded biomaterials. Human disc explants and human NP cells (hNP) seeded in NPgel were cultured for 2 week with either standard dMEM media (as described in Basatvat *et al.,* (2019); low glucose dMEM (1g/L glucose + pyruvate (Gibco, UK), 50µg/mL l-Ascorbic acid 2-phosphate sesquimagnesium salt hydrate (Sigma, UK), 1% v/v L-glutamine (Gibco, UK), 1% v/v ITS-X (Gibco, UK), 40µg/mL L-proline (Sigma, UK), 1.25mg/mL Albumax (Gibco, UK)), or standard dMEM culture media supplemented with the Ac4GalNAz (GAG media; Fig. 7.4). Samples were fixed as described previously at 2 weeks, sectioned into 6µm and washed in PBS for 5 minutes prior to staining for 1 hour at room temperature with a solution containing 1µM sulfo-cy5-alkyne (CLK-Ta116; Jena Bioscience, Germany), 100µg/mL DAPI, 4mg/mL Sodium L-ascorbate (Sigma, UK), 0.5mg/mL copper sulphate pentahydrate (Scientific laboratory suppliers, UK). Samples were washed again three times with PBS for 5 minutes prior to being visualised on an Olympus BX60 Microscope using Texas red filter and DAPI filter for visualising Ac4GalNAz sulfo-Cy5-Alkyne and Hoechst stains, respectively. From the initial investigation of GAG labelling, after 2-week in culture visible staining of Ac4GalNAz was highlighted in the human disc explant sample, whereas this was not observed in the hNP cells seeded in NPgel group. Suggesting that either the biomaterial prevents staining and labelling or GAGs or that the isolated hNP cells were not producing GAGs. This is a question that needs to be addressed. Further investigation into the quality of the extracellular matrix produced should also be researched, as the balance between synthesis, breakdown and accumulation of matrix macromolecules determines the integrity of the matrix, and thus directly linking to efficiency of regenerating the mechanical behaviour of the disc itself (Urban and Roberts, 2003).

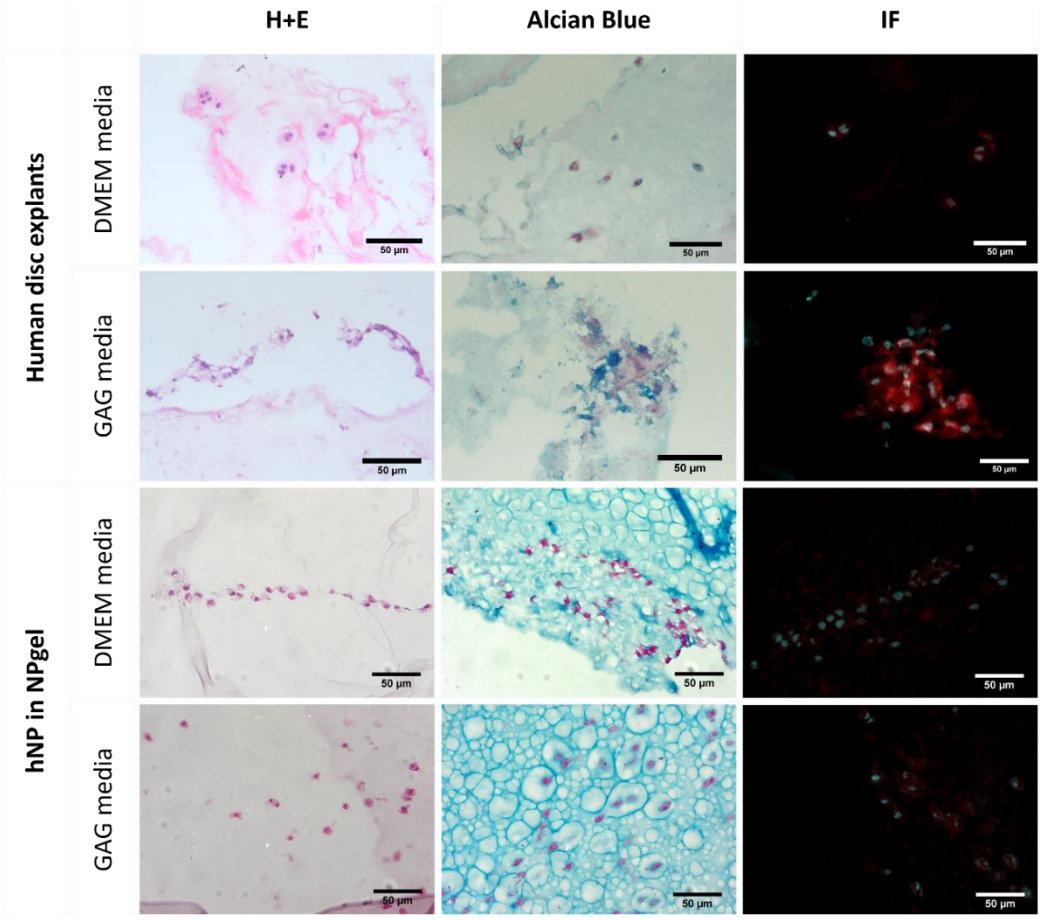

Figure 7.4. Glycosaminoglycan tracking in Human disc explants and human nucleus pulposus cells cultured in NPgel. *Human disc explants and human Nucleus pulposus cells (hNP) seeded into NPgel biomaterial, cultured in standard DMEM or standard DMEM supplemented with N-azidoacetylgalactosamine-tetraacylated (Ac4GalNAz) to label glycosaminoglycans (GAGs) production of the cells at 21% v/v oxygen, 37^{o}C (n=3 technical repeats). Stained with Haematoxylin and eosin (H+E), Alcian Blue and Immunofluorescence (IF) images; Ac4GalNAz (red) used to highlight GAGs, Hoechst (Cyan) to highlight the nucleus. Scale bar 50µm.*

TRANSLATIONAL POTENTIAL

The eventual usage of these cell-seeded biomaterials was intentionally for novel injectable therapy for disc regeneration. If further *in vitro* and *in vivo* testing results in these constructs are successful for sufficient concept purposes, the cell-seeded biomaterial would be described clinically as an advanced medicinal product (ATMP) or if to be used as biomaterial alone as a medical device product (the Medical Device Regulation; EU2017/745 (The European Parliament And The Council Of The European Union, 2017)). From a regulatory perspective, biomaterials can be considered medical devices if the therapeutic effect primarily comes from their intrinsic structure, as a means for facilitating the physical and mechanical replacement and modification of the IVD. Whereas, the cell-seeded biomaterial or the biomaterial containing dNCM will be classed and regulated under ATMP regulations; as the principle mode of action is pharmacological, metabolic or immunological benefits (EUROPEAN COMISSION, 2001). The biggest hurdle with medical devices products is acquiring Food and Drug

Administration (FDA, Unites States of America) or Notified Body (NB, European Union) approval. These regulatory affairs and governing body approvals are time-consuming processes, which involve products meeting essential general safety and performance requirements with clinical evidence (Melvin and Torre, 2019). For example for the biomaterial only, the ISO 10,993-1 and ISO 10,993-9 provides guidelines for evaluating biocompatibility and biological evaluation of medical devices; ISO 18,192-2 provides guidelines of recommended mechanical testing for NP prostheses (Williams, 2017; Schmitz *et al.*, 2020). Schmitz et al., (2020) has written an excellent report, providing guideline of necessary parameters to evaluate biomaterials intended for clinical translation as a IVD product, referring to standards ASTM-E111–17 (Young's modulus), ASTM-F2346–18 (Artificial Discs), ASTM-F2423–11 (Total Disc Prostheses), ASTM-D2990–17 (Mechanical Testing of Plastics), ASTM-F2789–10 (Mechanical and Functional Characterization of Nucleus Devices) and the ISO 10,993-9 (Schmitz *et al.*, 2020). It has become more favourable to produce a product that classifies as a medical device; as the translational pathway involves less restrictions, resulting in products being more affordable, reaching clinic earlier and being accessible to patients quicker (Øvrebø *et al.*, 2022). Suggesting that more regulatory efforts will have to be conducted with the selected biomaterials that contain dNCM, than with other biomaterials such as NPgel with this thesis.

THE UP-SCALING OF A PRODUCT TO CLINIC INVOLVES ATTAINING PREDICTABLE ROBUSTNESS, BATCH-TO-BATCH VARIABILITY, SAFETY PROFILING, REPRODUCIBILITY, AND PROFICIENCY. UP-SCALING THE CELL-SEEDED BIOMATERIALS INVESTIGATED IN THIS THESIS WOULD INVOLVE GENERATING A WORKING CELL BANK AND THE INVOLVEMENT OF ALLOGENEIC CELLS IS A FAR BETTER 'OFF-THE-SHELF' BUSINESS MODEL THAN THE USE OF AUTOLOGOUS CELLS, AS USING PATIENTS OWN CELLS CREATES MANUFACTURING CHALLENGE AS EXTRA CELL QUALITY AND SAFETY TEST ADDS TO THE COMPLEXITY FOR LARGE SCALE PRODUCTION AND COST EFFECTIVENESS (MASON AND DUNNILL, 2009; HEATHMAN *ET AL.*, 2015). FROM CHAPTER 4, WE ESTABLISHED THAT THE IPSC-MEPCS CELL BANK FROM OUR PARTNERS PROVED TO BE PROBLEMATIC WITH RECOVERY RATE OF SUB-OPTIMAL CELL NUMBER FOR SEEDING INTO VOLUMES LARGER THAN 300ML BIOMATERIAL, LEADING TO THE GENERATION OF OUR OWN IPSC-MEPCS IN CHAPTER 5. HOWEVER, THIS METHOD WOULD NOT BE SUSTAINABLE FOR UP-SCALING, AS IT INVOLVED INTER-LAB VARIABILITY, INCREASED PATHWAY COMPLEXITY, COST TO DEVELOPMENT AND CLINICAL REGULATION NEEDED TO BE APPROVED (HEATHMAN *ET AL.*, 2015; MOUNT *ET AL.*, 2015). IN A SUCCESSFUL METHOD ESTABLISHED FROM THE SWISS FETAL TRANSPLANTATION PROGRAM (LAURENT *ET AL.*, 2021), PARENTAL CELL BANK WAS ESTABLISHED AND SENT TO A SPECIALIST LABORATORY THAT IS GOOD MANUFACTURING PRACTICE (GMP)-CERTIFIED PRODUCTION AND STORAGE FACILITY (BIORELIANCE; MERK GROUP, GLASGOW, UK), TO GENERATE MASTER CELL BANKS AND WORKING CELL BANKS THAT ARE SAFETY TESTED CONTINUOUSLY THROUGHOUT THE BIOPROCESSING AND MANUFACTURING WORKFLOW (LAURENT *ET AL.*, 2020). OUTSOURCING CELLS FROM A GMP-CERTIFIED LABORATORY WILL PROVIDE CONFIDENCE IN SAFETY, MAXIMISED EFFICIENCY AND OPTIMISES COST FOR TRANSLATION. ALTERNATIVELY, THE USED OF PRIMARY XENOGRAPHIC CELLS IS ALSO GROWING IN CLINIC, AS SAFETY IS IMPROVING WITH THE USE OF CROSS-SPECIES CELLS (SACHS, 1994; SHAFER ET AL., 2004). BASED ON THE SUCCESSFUL USE OF PORCINE ISLETS CELLS TRANSPLANTATION IN A PRIMATE DIABETES MODEL IN CLINICAL TRIALS, WHICH IS ACCOMPLISHED BY KNOCKING DOWN THE GENE FOR ALPHA-1,3-GALACTOSYLTRANSFERASE LACKING ALPHA 1,3-GAL SUGARS ON THE PORCINE CELL SURFACES, THAT REACTS TO THE INNATE IMMUNE SYSTEM (LAI *ET AL.*, 2002; KUWAKI *ET AL.*, 2004; THOMPSON *ET AL.*, 2011; SHIN *ET AL.*, 2015). FROM THE RESEARCH CONDUCTED THROUGHOUT THIS THESIS AND UPON REFLECTION OF THE PROJECTS AIMS, THE APPLICATION OF CELLS INCORPORATED WITHIN A BIOMATERIAL LIMITS THE TRANSLATIONAL DEVELOPMENT OF AN INJECTABLE TREATMENT. THIS DATA IS A GREAT EXAMPLE OF THE CYTOCOMPATIBILITY OF THE BIOMATERIALS SCREENED AND GIVES AN INSIGHT ON HOW THE BIOMATERIALS WILL PERFORM IN A DEGENERATIVE DISC ENVIRONMENT. HOWEVER, THE CELLS USED IN THIS STUDY ARE NOT READY FOR TRANSLATION AND CLINICAL TREATMENT. AS HIGHLIGHTED THROUGHOUT, NOT ENOUGH CELLS ARE GENERATED AND THE SAFETY OF IPSC-MEPCS ARE YET TO BE CONFIRMED. THE ADDITION OF CELLS OFTEN RESULTS IN ADDITIONAL COST TO MANUFACTURE AND CAN ADD TO THE INCONSISTENCY OF A TREATMENT. THE BIOMATERIALS ON THE OTHER HAND CAN OFFER IMPROVED DISC HEIGHT AND STRUCTURE STABILISATION, WITH SOME ARE ALREADY

IN CLINICAL TRIALS AND PROVED TO BE CLINICALLY SAFE. IF THE UTILITY OF CELLS WAS AIMED TO ENHANCE THE MATRIX PRODUCTION AND REHYDRATION OF A DEGENERATE DISC, AND THIS CAN BE ESTABLISHED WITH THE USE OF BIOMATERIALS ALONE, THEN THE QUESTION IS, IS THERE A NEED FOR CELLS? MOVING FORWARD, MORE RESEARCH NEEDS TO BE CONDUCTED ON ESTABLISHING A WORKING CELL BANK FOR NC-LIKE CELLS FOR GREATER CELL SEEDING DENSITY INTO THE BIOMATERIALS FOR FURTHER *IN VITRO* OR *EX VIVO* TESTING. IN THE MEANTIME, BIOMATERIALS ALONE COULD BE APPLIED TO FURTHER *EX VIVO* OR *IN VIVO* STUDIES, TO TRULY TEST ITS RESPONSE TO A DEGENERATIVE DISC IN A WHOLE ORGAN SYSTEM. PATIENT PROFILING

As the cell-seeded biomaterial is intended for the regeneration of the nucleus pulposus, the target patient of this therapeutic product would be those diagnosed with mild-moderate disc degeneration, with conservative AFs; or as a treatment for adjacent segment disease. This is due to the gel like characterisation of the biomaterials; while the biomaterials can fill small AF fissures, the biomaterials would protrude out from severe AF fissures. Therefore, for the target of complete disc rupture an additional AF repair is needed or spinal decompression (for sciatica patients; (NICE, 2018)) or discectomy followed by fusion is recommended (for chronic low back pain patients; (NICE, 2017)). To select for mild-moderate discs, the gold standard to date has been the Pfirrmann disc degeneration grading system based on signal intensity from T2-weighted MRI to estimate water content with morphological parameters (Pfirrmann *et al.*, 2001). However, is it ethical to subject patients to biomaterial injection into non-symptomatic discs with intact AF based of the MRI diagnosis alone, functioning as a preventative rather than symptomatic treatment? Thus demonstrating the need for improved imaging modalities to be applied clinically enabling patient stratification.

CONCLUSION STATEMENT

The contribution to knowledge demonstrated in this thesis included the pioneering research on notochordal cells, establishing *in vitro* characterisation and phenotyping for these cells that will enable the acceleration of future research with NCs and iPSCs use. The combination of pNC and iPSC-MEPC seeded into biomaterials was a key novel aspect, with the exciting prospect that cell survival was attained, and the cells even displayed NC characteristics which can lead to regenerative properties after 4-week *in vitro* culture. For the biomaterial interest within this thesis, it has been established the fantastic novel biomaterials that have been generated in mind for nucleus pulposus replacement and regeneration. The innovative research involving cell incorporation into the biomaterials have demonstrated the cytocompatibility of the biomaterials with progenitor disc cells.

REFERENCES

Abbasalizadeh, S. *et al.* (2017) 'Allogeneic cell therapy manufacturing: process development technologies and facility design options', *Expert opinion on biological therapy*, 17(10), pp. 1201–1219. Available at: https://doi.org/10.1080/14712598.2017.1354982.

Ben Abdelkhalek, H. *et al.* (2004) 'The mouse homeobox gene Not is required for caudal notochord development and affected by the truncate mutation', *Genes & development*, 18(14), pp. 1725–1736. Available at: https://doi.org/10.1101/GAD.303504.

Adams, M. and Roughly, P. (2006) 'What is intervertebral disc degeneration, and what causes it?', *Spine*, 31(18), pp. 2151–2161. Available at: https://doi.org/10.1097/01.BRS.0000231761.73859.2C.

Adams, M.A. and Hutton, W.C. (1983) 'The mechanical function of the lumbar apophyseal joints', *Spine*, 8(3), pp. 327–330. Available at: https://doi.org/10.1097/00007632-198304000-00017.

Adewumi, O. *et al.* (2007) 'Characterization of human embryonic stem cell lines by the International Stem Cell Initiative', *Nature Biotechnology 2007 25:7*, 25(7), pp. 803–816. Available at: https://doi.org/10.1038/nbt1318.

Adler, J.H., Schoenbaum, M. and Silberberg, R. (1983) 'Early onset of disk degeneration and spondylosis in sand rats (Psammomys obesus)', *Veterinary pathology*, 20(1), pp. 13–22. Available at: https://doi.org/10.1177/030098588302000102.

Aguiar, D.J., Johnson, S.L. and Oegema, T.R. (1999) 'Notochordal cells interact with nucleus pulposus cells: Regulation of proteoglycan synthesis', *Experimental Cell Research*, 246(1), pp. 129–137. Available at: https://doi.org/10.1006/excr.1998.4287.

Akhmanova, M. *et al.* (2015) 'Physical, Spatial, and Molecular Aspects of Extracellular Matrix of In Vivo Niches and Artificial Scaffolds Relevant to Stem Cells Research', *Stem Cells International*, 2015. Available at: https://doi.org/10.1155/2015/167025.

van den Akker, G.G.H. *et al.* (2020) 'A Membranome-Centered Approach Defines Novel Biomarkers for Cellular Subtypes in the Intervertebral Disc', *Cartilage*, 11(2), pp. 203–220. Available at: https://doi.org/10.1177/1947603518764260.

Alini, M. *et al.* (2008) 'Are animal models useful for studying human disc disorders/degeneration?', *European Spine Journal*. Springer, pp. 2–19. Available at: https://doi.org/10.1007/s00586-007-0414-y.

Alini, M. *et al.* (2023) 'An update on animal models of intervertebral disc degeneration and low back pain: Exploring the potential of artificial intelligence to improve research analysis and development of prospective therapeutics', *JOR Spine*, 6(1), p. e1230. Available at: https://doi.org/10.1002/JSP2.1230.

Alkhatib, B. *et al.* (2018) 'IVD Development: Nucleus Pulposus Development and Sclerotome Specification', *Current Molecular Biology Reports*, 4(3), pp. 132–141. Available at: https://doi.org/10.1007/s40610-018-0100-3.

Amirdelfan, K. *et al.* (2021) 'Allogeneic mesenchymal precursor cells treatment for chronic low back pain associated with degenerative disc disease: a prospective randomized, placebo-controlled 36-month study of safety and efficacy', *The Spine Journal*, 21(2), pp. 212–230. Available at: https://doi.org/10.1016/J.SPINEE.2020.10.004.

Andersen, T., Auk-Emblem, P. and Dornish, M. (2015) '3D Cell Culture in Alginate Hydrogels', *Microarrays*, 4(2), p. 133. Available at: https://doi.org/10.3390/MICROARRAYS4020133.

Andersson, G.B.J. (1999) 'Epidemiological features of chronic low-back pain', *Lancet (London, England)*, 354(9178), pp. 581–585. Available at: https://doi.org/10.1016/S0140-6736(99)01312-4.

Anton, D. *et al.* (2015) 'Three-dimensional cell culture: a breakthrough in vivo', *International journal of molecular sciences*, 16(3), pp. 5517–5527. Available at: https://doi.org/10.3390/IJMS16035517.

Antoniou, J. *et al.* (1996) 'The human lumbar intervertebral disc: evidence for changes in the biosynthesis and denaturation of the extracellular matrix with growth, maturation, ageing, and degeneration', *The Journal of clinical investigation*, 98(4), pp. 996–1003. Available at: https://doi.org/10.1172/JCI118884.

Arkesteijn, I. *et al.* (2015) 'Effect of coculturing canine notochordal, nucleus pulposus and mesenchymal stromal cells for intervertebral disc regeneration', *Arthritis Research & Therapy*, 17(1), p. 60. Available at: https://doi.org/10.1186/s13075-015-0569-6.

Arkesteijn, I.T.M., Potier, E. and Ito, K. (2017) 'The Regenerative Potential of Notochordal Cells in a Nucleus Pulposus Explant', *Global Spine Journal*, 7(1), pp. 14–20. Available at: https://doi.org/10.1055/s-0036-1583174.

Arnold, S.J. *et al.* (2000) 'Brachyury is a target gene of the Wnt/beta-catenin signaling pathway', *Mechanisms of development*, 91(1–2), pp. 249–258. Available at: https://doi.org/10.1016/S0925-4773(99)00309-3.

Arnold, S.J. and Robertson, E.J. (2009) 'Making a commitment: cell lineage allocation and axis patterning in the early mouse embryo', *Nature reviews. Molecular cell biology*, 10(2), pp. 91–103. Available at: https://doi.org/10.1038/NRM2618.

Ashton, K. *et al.* (2009) 'Substance P in intervertebral discs: Binding sites on vascular endothelium of the human annulus fibrosus', *Acta Orthopaedica Scandinavica*, 65, pp. 635–639. Available at: https://doi.org/10.3109/17453679408994620.

Aulisa, L. *et al.* (1998) 'Immunohistochemical investigation on type III and VI collagen organization in human intervertebral discs in the neonatal period', *Child's nervous system : ChNS : official journal of the International Society for Pediatric Neurosurgery*, 14(3), pp. 104–108. Available at: https://doi.org/10.1007/S003810050188.

Bach, F. *et al.* (2015) 'The species-specific regenerative effects of notochordal cell-conditioned medium on chondrocyte-like cells derived from degenerated human intervertebral discs', *European Cells and Materials*, 30, pp. 132–147. Available at: https://doi.org/10.22203/ECM.V030A10.

Bach, F.C. *et al.* (2016) 'Increased caveolin-1 in intervertebral disc degeneration facilitates repair', *Arthritis Research and Therapy*, 18(1), p. 59. Available at: https://doi.org/10.1186/S13075-016-0960-Y.

Bach, F.C. *et al.* (2018) 'Biologic canine and human intervertebral disc repair by notochordal cell-derived matrix: From bench towards bedside', *Oncotarget*, 9(41), pp. 26507–26526. Available at: https://doi.org/10.18632/oncotarget.25476.

Bach, F.C. *et al.* (2019) 'Hedgehog proteins and parathyroid hormone-related protein are involved in intervertebral disc maturation, degeneration, and calcification', *JOR Spine*, 2(4). Available at: https://doi.org/10.1002/JSP2.1071.

Bach, F.C. *et al.* (2022) 'Notochordal Cell-Based Treatment Strategies and Their Potential in Intervertebral Disc Regeneration', *Frontiers in cell and developmental biology*, 9. Available at: https://doi.org/10.3389/FCELL.2021.780749.

Bae, W.C. *et al.* (2013) 'Morphology of the cartilaginous endplates in human intervertebral disks with

ultrashort echo time MR imaging', *Radiology*, 266(2), pp. 564–574. Available at: https://doi.org/10.1148/radiol.12121181.

Bagwell, J. *et al.* (2020) 'Notochord vacuoles absorb compressive bone growth during zebrafish spine formation', *eLife*, 9(51221). Available at: https://doi.org/10.7554/eLife.51221.

Bai, X.D. *et al.* (2017) 'Coculture with Partial Digestion Notochordal Cell-Rich Nucleus Pulposus Tissue Activates Degenerative Human Nucleus Pulposus Cells', *https://home.liebertpub.com/tea*, 23(15–16), pp. 837–846. Available at: https://doi.org/10.1089/TEN.TEA.2016.0428.

Balmer, S., Nowotschin, S. and Hadjantonakis, A.K. (2016) 'Notochord morphogenesis in mice: Current understanding & open questions', *Developmental Dynamics*, 245(5), pp. 547–557. Available at: https://doi.org/10.1002/DVDY.24392.

Bankhead, P. *et al.* (2017) 'QuPath: Open source software for digital pathology image analysis', *Scientific Reports 2017 7:1*, 7(1), pp. 1–7. Available at: https://doi.org/10.1038/s41598-017-17204-5.

Barrionuevo, F. *et al.* (2006) 'Sox9 is required for notochord maintenance in mice', *Developmental biology*, 295(1), pp. 128–140. Available at: https://doi.org/10.1016/J.YDBIO.2006.03.014.

Basatvat, S. *et al.* (2023) 'Harmonization and standardization of nucleus pulposus cell extraction and culture methods', *JOR Spine*, p. e1238. Available at: https://doi.org/10.1002/JSP2.1238.

Baskin, J.M. *et al.* (2007) 'Copper-free click chemistry for dynamic in vivo imaging'. Available at: www.pnas.org/cgi/content/full/ (Accessed: 3 December 2022).

Baumgartner, L. *et al.* (2021) 'Multiscale regulation of the intervertebral disc: Achievements in experimental, in silico, and regenerative research', *International Journal of Molecular Sciences*. MDPI AG, pp. 1–42. Available at: https://doi.org/10.3390/ijms22020703.

Beckers, A. *et al.* (2007) 'The mouse homeobox gene Noto regulates node morphogenesis, notochordal ciliogenesis, and left right patterning', *Proceedings of the National Academy of Sciences of the United States of America*, 104(40), pp. 15765–15770. Available at: https://doi.org/10.1073/PNAS.0704344104.

Beers, J. *et al.* (2012) 'Passaging and colony expansion of human pluripotent stem cells by enzyme-free dissociation in chemically defined culture conditions', *Nature Protocols*, 7(11), pp. 2029–2040. Available at: https://doi.org/10.1038/nprot.2012.130.

Benz, K. *et al.* (2012) 'Intervertebral disc cell- and hydrogel-supported and spontaneous intervertebral disc repair in nucleotomized sheep', *European Spine Journal*, 21(9), p. 1758. Available at: https://doi.org/10.1007/S00586-012-2443-4.

Benz, Karin *et al.* (2010) 'A Polyethylene Glycol-Crosslinked Serum Albumin/Hyaluronan Hydrogel for the Cultivation of Chondrogenic Cell Types', *Advanced Engineering Materials*, 12(9), pp. B539–B551. Available at: https://doi.org/10.1002/ADEM.201080028.

Berg, S. *et al.* (2009) 'Total disc replacement compared to lumbar fusion: A randomised controlled trial with 2-year follow-up', *European Spine Journal*, 18(10), pp. 1512–1519. Available at: https://doi.org/10.1007/s00586-009-1047-0.

Bergknut, N. *et al.* (2012) 'The dog as an animal model for intervertebral disc degeneration?', *Spine*, 37(5), pp. 351–358. Available at: https://doi.org/10.1097/BRS.0b013e31821e5665.

Bergknut, N. *et al.* (2013) 'Intervertebral disc degeneration in the dog. Part 1: Anatomy and physiology of the intervertebral disc and characteristics of intervertebral disc degeneration', *Veterinary Journal*, pp. 282–291. Available at: https://doi.org/10.1016/j.tvjl.2012.10.024.

Bergmann, W. *et al.* (2022) 'Intervertebral disc degeneration in warmblood horses: Histological and biochemical characterization', *Veterinary pathology*, 59(2), pp. 284–298. Available at: https://doi.org/10.1177/03009858211067463.

Bhunia, B.K., Kaplan, D.L. and Mandal, B.B. (2018) 'Silk-based multilayered angle-ply annulus fibrosus construct to recapitulate form and function of the intervertebral disc', *Proceedings of the National Academy of Sciences of the United States of America*, 115(3), pp. 477–482. Available at: https://doi.org/10.1073/pnas.1715912115.

Bibby, S.R.S. *et al.* (2005) 'Metabolism of the intervertebral disc: Effects of low levels of oxygen, glucose, and pH on rates of energy metabolism of bovine nucleus pulposus cells', *Spine*, 30(5), pp. 487–496. Available at: https://doi.org/10.1097/01.brs.0000154619.38122.47.

Binch, A., Snuggs, J. and Le Maitre, C.L. (2020) 'Immunohistochemical analysis of protein expression in formalin fixed paraffin embedded human intervertebral disc tissues', *JOR Spine*, 3(3). Available at: https://doi.org/10.1002/JSP2.1098.

Binch, A.L. *et al.* (2014) 'Expression and regulation of neurotrophic and angiogenic factors during human intervertebral disc degeneration', *Arthritis Research and Therapy*, 16(5), p. 416. Available at: https://doi.org/10.1186/s13075-014-0416-1.

Binch, A.L.A. *et al.* (2015) 'Nerves are more abundant than blood vessels in the degenerate human intervertebral disc', *Arthritis Research & Therapy*, 17(1), p. 370. Available at: https://doi.org/10.1186/s13075-015-0889-6.

Binch, A.L.A. *et al.* (2021) 'Cell-based strategies for IVD repair: clinical progress and translational obstacles', *Nature Reviews Rheumatology*. Nature Research, pp. 158–175. Available at: https://doi.org/10.1038/s41584-020-00568-w.

Blanco, J.F. *et al.* (2019) 'Autologous mesenchymal stromal cells embedded in tricalcium phosphate for posterolateral spinal fusion: Results of a prospective phase I/II clinical trial with long-term follow-up', *Stem Cell Research and Therapy*, 10(1), p. 63. Available at: https://doi.org/10.1186/s13287-019-1166-4.

Bogacheva, M.S. *et al.* (2021) 'Differentiation of Human Pluripotent Stem Cells Into Definitive Endoderm Cells in Various Flexible Three-Dimensional Cell Culture Systems: Possibilities and Limitations', *Frontiers in Cell and Developmental Biology*, 9, p. 2405. Available at: https://doi.org/10.3389/FCELL.2021.726499/BIBTEX.

Bogduk, N. (2004) 'Management of chronic low back pain', *Medical Journal of Australia*, 180(2), pp. 79–83. Available at: https://doi.org/10.5694/j.1326-5377.2004.tb05805.x.

Bonaventure, J. *et al.* (1994) 'Reexpression of cartilage-specific genes by dedifferentiated human articular chondrocytes cultured in alginate beads', *Experimental cell research*, 212(1), pp. 97–104. Available at: https://doi.org/10.1006/EXCR.1994.1123.

Boos, N. *et al.* (1994) 'Quantitative MR imaging of lumbar intervertebral disc and vertebral bodies: methodology, reproducibility, and preliminary results', *Magnetic resonance imaging*, 12(4), pp. 577–587. Available at: https://doi.org/10.1016/0730-725X(94)92452-X.

Bowles, R.D. and Setton, L.A. (2017) 'Biomaterials for intervertebral disc regeneration and repair', *Biomaterials*. Elsevier Ltd, pp. 54–67. Available at: https://doi.org/10.1016/j.biomaterials.2017.03.013.

Boyes, V.L. *et al.* (2021) 'One-pot precipitation polymerisation strategy for tuneable injectable Laponite®-pNIPAM hydrogels: Polymerisation, processability and beyond', *Polymer*, 233, p. 124201.

Available at: https://doi.org/10.1016/J.POLYMER.2021.124201.

De Bree, K., De Bakker, B.S. and Oostra, R.J. (2018) 'The development of the human notochord', *PLOS ONE*, 13(10), p. e0205752. Available at: https://doi.org/10.1371/JOURNAL.PONE.0205752.

Brinjikji, W. *et al.* (2015) 'MRI findings of disc degeneration are more prevalent in adults with low back pain than in asymptomatic controls: A systematic review and meta-analysis', *American Journal of Neuroradiology*, 36(12), pp. 2394–2399. Available at: https://doi.org/10.3174/ajnr.A4498.

Bron, J.L. *et al.* (2009) 'Rheological characterization of the nucleus pulposus and dense collagen scaffolds intended for functional replacement', *Journal of orthopaedic research : official publication of the Orthopaedic Research Society*, 27(5), pp. 620–626. Available at: https://doi.org/10.1002/JOR.20789.

Brown, S. *et al.* (2018) 'Cell Clusters Are Indicative of Stem Cell Activity in the Degenerate Intervertebral Disc: Can Their Properties Be Manipulated to Improve Intrinsic Repair of the Disc?', *https://home.liebertpub.com/scd*, 27(3), pp. 147–165. Available at: https://doi.org/10.1089/SCD.2017.0213.

Brox, J.I. *et al.* (2010) 'Four-year follow-up of surgical versus non-surgical therapy for chronic low back pain', *Annals of the rheumatic diseases*, 69(9), pp. 1643–1648. Available at: https://doi.org/10.1136/ARD.2009.108902.

Buckley, C.T. *et al.* (2018) 'Critical aspects and challenges for intervertebral disc repair and regeneration-Harnessing advances in tissue engineering', *JOR spine*, 1(3). Available at: https://doi.org/10.1002/JSP2.1029.

Burtscher, I. and Lickert, H. (2009) 'Foxa2 regulates polarity and epithelialization in the endoderm germ layer of the mouse embryo', *Development (Cambridge, England)*, 136(6), pp. 1029–1038. Available at: https://doi.org/10.1242/DEV.028415.

Buschmann, M.D. *et al.* (1992) 'Chondrocytes in agarose culture synthesize a mechanically functional extracellular matrix', *Journal of orthopaedic research : official publication of the Orthopaedic Research Society*, 10(6), pp. 745–758. Available at: https://doi.org/10.1002/JOR.1100100602.

Buzzard, J.J. *et al.* (2004) 'Karyotype of human ES cells during extended culture', *Nature Biotechnology 2004 22:4*, 22(4), pp. 381–382. Available at: https://doi.org/10.1038/nbt0404-381.

Camus, A. *et al.* (2000) 'The morphogenetic role of midline mesendoderm and ectoderm in the development of the forebrain and the midbrain of the mouse embryo', *Development (Cambridge, England)*, 127(9), pp. 1799–1813. Available at: https://doi.org/10.1242/DEV.127.9.1799.

Capeling, M.M. *et al.* (2019) 'Stem Cell Reports Resource Nonadhesive Alginate Hydrogels Support Growth of Pluripotent Stem Cell-Derived Intestinal Organoids'. Available at: https://doi.org/10.1016/j.stemcr.2018.12.001.

Cappello, R. *et al.* (2006) 'Notochordal cell produce and assemble extracellular matrix in a distinct manner, which may be responsible for the maintenance of healthy nucleus pulposus', *Spine*, 31(8), pp. 873–882. Available at: https://doi.org/10.1097/01.brs.0000209302.00820.fd.

Carrero, R. *et al.* (2012) 'IL1β induces mesenchymal stem cells migration and leucocyte chemotaxis through NF-κB', *Stem cell reviews and reports*, 8(3), pp. 905–916. Available at: https://doi.org/10.1007/S12015-012-9364-9.

Centeno, C. *et al.* (2017) 'Treatment of lumbar degenerative disc disease-associated radicular pain with culture-expanded autologous mesenchymal stem cells: A pilot study on safety and efficacy', *Journal of Translational Medicine*, 15(1), p. 197. Available at: https://doi.org/10.1186/s12967-017-

1300-y.

Chambers, S.M. *et al.* (2009) 'Highly efficient neural conversion of human ES and iPS cells by dual inhibition of SMAD signaling', *Nature biotechnology*, 27(3), p. 275. Available at: https://doi.org/10.1038/NBT.1529.

Chan, L.K.Y. *et al.* (2013) 'Decellularized bovine intervertebral disc as a natural scaffold for xenogenic cell studies', *Acta Biomaterialia*, 9(2), pp. 5262–5272. Available at: https://doi.org/10.1016/j.actbio.2012.09.005.

Chan, S.C.W., Ferguson, S.J. and Gantenbein-Ritter, B. (2011) 'The effects of dynamic loading on the intervertebral disc', *European Spine Journal*, 20(11), p. 1796. Available at: https://doi.org/10.1007/S00586-011-1827-1.

Chang, C.H. *et al.* (2021) 'Interleukin-1β-induced matrix metalloproteinase-3 via ERK1/2 pathway to promote mesenchymal stem cell migration', *PLoS ONE*, 16(5 May). Available at: https://doi.org/10.1371/JOURNAL.PONE.0252163.

Chaturvedi, G. *et al.* (2009) 'Noggin maintains pluripotency of human embryonic stem cells grown on Matrigel', *Cell Prolif*, 42, pp. 425–433. Available at: https://doi.org/10.1111/j.1365-2184.2009.00616.x.

Chee, A. *et al.* (2016) 'Cell Therapy with Human Dermal Fibroblasts Enhances Intervertebral Disk Repair and Decreases Inflammation in the Rabbit Model', *Global Spine Journal*, 6(8), pp. 771–779. Available at: https://doi.org/10.1055/s-0036-1582391.

Chen, B. *et al.* (2013) 'A novel alternative to cryopreservation for the short-term storage of stem cells for use in cell therapy using alginate encapsulation', *Tissue engineering. Part C, Methods*, 19(7), pp. 568–576. Available at: https://doi.org/10.1089/TEN.TEC.2012.0489.

Chen, C. *et al.* (2020) 'Autologous fibroblasts induce fibrosis of the nucleus pulposus to maintain the stability of degenerative intervertebral discs', *Bone Research*, 8(1), p. 7. Available at: https://doi.org/10.1038/s41413-019-0082-7.

Chen, J. *et al.* (2013) 'Differentiation of Mouse Induced Pluripotent Stem Cells (iPSCs) into Nucleus Pulposus-Like Cells In Vitro', *PLoS ONE*, 8(9). Available at: https://doi.org/10.1371/journal.pone.0075548.

Chen, J.W. *et al.* (2014) 'Significance of Hypoxia in the Physiological Function of Intervertebral Disc Cells', *Critical Reviews™ in Eukaryotic Gene Expression*, 24(3), pp. 193–204. Available at: https://doi.org/10.1615/CRITREVEUKARYOTGENEEXPR.2014010485.

Chen, S., Emery, S.E. and Pei, M. (2009) 'Coculture of synovium-derived stem cells and nucleus pulposus cells in serum-free defined medium with supplementation of transforming growth factor-β1: A potential application of tissue-specific stem cells in disc regeneration', *Spine*, 34(12), pp. 1272–1280. Available at: https://doi.org/10.1097/BRS.0b013e3181a2b347.

Chen, W.-H. *et al.* (2006) 'Tissue-engineered intervertebral disc and chondrogenesis using human nucleus pulposus regulated through TGF-β1 in platelet-rich plasma', *Journal of Cellular Physiology*, 209(3), pp. 744–754. Available at: https://doi.org/10.1002/jcp.20765.

Chen, X. *et al.* (2010) 'Investigations into the Metabolism of Two-Dimensional Colony and Suspended Microcarrier Cultures of Human Embryonic Stem Cells in Serum-Free Media', *https://home.liebertpub.com/scd*, 19(11), pp. 1781–1792. Available at: https://doi.org/10.1089/SCD.2010.0077.

Chen, X. *et al.* (2016) 'A comparison between nucleus pulposus-derived stem cell transplantation and

nucleus pulposus cell transplantation for the treatment of intervertebral disc degeneration in a rabbit model', *International Journal of Surgery*, 28, pp. 77–82. Available at: https://doi.org/10.1016/j.ijsu.2016.02.045.

Chen, X. *et al.* (2018) 'High Glucose Inhibits Neural Stem Cell Differentiation Through Oxidative Stress and Endoplasmic Reticulum Stress', *Stem Cells and Development*, 27(11), p. 745. Available at: https://doi.org/10.1089/SCD.2017.0203.

Chen, Y. *et al.* (2019) 'Chemically-Defined Neural Conversion of Human Pluripotent Stem Cells', *Methods in molecular biology (Clifton, N.J.)*, 1919, p. 59. Available at: https://doi.org/10.1007/978-1-4939-9007-8_5.

Choi, H. *et al.* (2019) 'Nucleus pulposus primary cilia alter their length in response to changes in extracellular osmolarity but do not control TonEBP-mediated osmoregulation', *Scientific Reports 2019 9:1*, 9(1), pp. 1–16. Available at: https://doi.org/10.1038/s41598-019-51939-7.

Choi, K.S., Cohn, M.J. and Harfe, B.D. (2008) 'Identification of nucleus pulposus precursor cells and notochordal remnants in the mouse: Implications for disk degeneration and chordoma formation', *Developmental Dynamics*, 237(12), pp. 3953–3958. Available at: https://doi.org/10.1002/DVDY.21805.

Choi, K.S. and Harfe, B.D. (2011) 'Hedgehog signaling is required for formation of the notochord sheath and patterning of nuclei pulposi within the intervertebral discs', *Proceedings of the National Academy of Sciences of the United States of America*, 108(23), pp. 9484–9489. Available at: https://doi.org/10.1073/pnas.1007566108.

Chon, B.H. *et al.* (2013) 'Human umbilical cord mesenchymal stromal cells exhibit immature nucleus pulposus cell phenotype in a laminin-rich pseudo-three-dimensional culture system', *Stem Cell Research and Therapy*, 4(5), p. 120. Available at: https://doi.org/10.1186/scrt331.

Cisewski, S.E. *et al.* (2018) 'Comparison of Oxygen Consumption Rates of Nondegenerate and Degenerate Human IVD Cells', *Spine*, 43(2), p. E60. Available at: https://doi.org/10.1097/BRS.0000000000002252.

Collins, J.A. *et al.* (2013) 'Oxygen and pH-sensitivity of human osteoarthritic chondrocytes in 3-D alginate bead culture system', *Osteoarthritis and Cartilage*, 21(11), p. 1790. Available at: https://doi.org/10.1016/J.JOCA.2013.06.028.

Colombier, P. *et al.* (2016) 'Generation of human nucleus pulposus cells from stem cells: First steps towards intervertebral disc regeneration.', *Osteoarthritis and Cartilage*, 24, pp. S11–S12. Available at: https://doi.org/10.1016/j.joca.2016.01.051.

Colombier, P. *et al.* (2020) 'NOTO Transcription Factor Directs Human Induced Pluripotent Stem Cell-Derived Mesendoderm Progenitors to a Notochordal Fate', *Cells*, 9(2), p. 509. Available at: https://doi.org/10.3390/cells9020509.

Colombini, A. *et al.* (2015) 'In Vitro Characterization and In Vivo Behavior of Human Nucleus Pulposus and Annulus Fibrosus Cells in Clinical-Grade Fibrin and Collagen-Enriched Fibrin Gels', 21, pp. 793–802. Available at: https://doi.org/10.1089/ten.tea.2014.0279.

Constant, C. *et al.* (2022) 'Comparison and optimization of sheep in vivo intervertebral disc injury model', *JOR Spine*, 5(2). Available at: https://doi.org/10.1002/JSP2.1198.

Copp, A.J., Greene, N.D.E. and Murdoch, J.N. (2003) 'The genetic basis of mammalian neurulation', *Nature Reviews Genetics*, pp. 784–793. Available at: https://doi.org/10.1038/nrg1181.

Corallo, D. *et al.* (2013) 'Emilin3 is required for notochord sheath integrity and interacts with Scube2

to regulate notochord-derived Hedgehog signals', *Development (Cambridge)*, 140(22), pp. 4594–4601. Available at: https://doi.org/10.1242/dev.094078.

Cornejo, M.C. *et al.* (2015) 'Soluble factors from the notochordal-rich intervertebral disc inhibit endothelial cell invasion and vessel formation in the presence and absence of pro-inflammatory cytokines', *Osteoarthritis and Cartilage*, 23(3), pp. 487–496. Available at: https://doi.org/10.1016/j.joca.2014.12.010.

Croft, A.S. *et al.* (2021) 'Effect of different cryopreservation media on human nucleus pulposus cells' viability and trilineage potential', *JOR Spine*, 4(1). Available at: https://doi.org/10.1002/JSP2.1140.

D'amour, K.A. *et al.* (2005) 'Efficient differentiation of human embryonic stem cells to definitive endoderm', *NATURE BIOTECHNOLOGY*, 23. Available at: https://doi.org/10.1038/nbt1163.

Dahia, C.L., Mahoney, E. and Wylie, C. (2012) 'Shh Signaling from the Nucleus Pulposus Is Required for the Postnatal Growth and Differentiation of the Mouse Intervertebral Disc', *PLoS ONE*, 7(4). Available at: https://doi.org/10.1371/JOURNAL.PONE.0035944.

Deyo, R.A., Von Korff, M. and Duhrkoop, D. (2015) 'Opioids for low back pain', *BMJ (Online)*. BMJ Publishing Group. Available at: https://doi.org/10.1136/bmj.g6380.

Diaz-Hernandez, M.E. *et al.* (2020) 'Derivation of notochordal cells from human embryonic stem cells reveals unique regulatory networks by single cell-transcriptomics', *Journal of Cellular Physiology*, 235(6), pp. 5241–5255. Available at: https://doi.org/10.1002/jcp.29411.

Dowell, D., Haegerich, T.M. and Chou, R. (2016) 'CDC guideline for prescribing opioids for chronic pain-United States, 2016', *JAMA - Journal of the American Medical Association*, 315(15), pp. 1624–1645. Available at: https://doi.org/10.1001/jama.2016.1464.

Draut, H., Liebenstein, T. and Begemann, G. (2019) 'New Insights into the Control of Cell Fate Choices and Differentiation by Retinoic Acid in Cranial, Axial and Caudal Structures', *Biomolecules*, 9(12). Available at: https://doi.org/10.3390/BIOM9120860.

Dunlop, R.B., Adams, M.A. and Hutton, W.C. (1984) 'Disc space narrowing and the lumbar facet joints', *The Journal of bone and joint surgery. British volume*, 66(5), pp. 706–710. Available at: https://doi.org/10.1302/0301-620X.66B5.6501365.

Echelard, Y. *et al.* (1993) 'Sonic hedgehog, a member of a family of putative signaling molecules, is implicated in the regulation of CNS polarity', *Cell*, 75(7), pp. 1417–1430. Available at: https://doi.org/10.1016/0092-8674(93)90627-3.

Elabd, C. *et al.* (2016) 'Intra-discal injection of autologous, hypoxic cultured bone marrow-derived mesenchymal stem cells in five patients with chronic lower back pain: A long-term safety and feasibility study', *Journal of Translational Medicine*, 14(1), p. 253. Available at: https://doi.org/10.1186/s12967-016-1015-5.

Ellerström, C. *et al.* (2007) 'Facilitated Expansion of Human Embryonic Stem Cells by Single-Cell Enzymatic Dissociation', *Stem Cells*, 25(7), pp. 1690–1696. Available at: https://doi.org/10.1634/stemcells.2006-0607.

Ellis, K., Bagwell, J. and Bagnat, M. (2013) 'Notochord vacuoles are lysosome-related organelles that function in axis and spine morphogenesis', *Journal of Cell Biology*, 200(5), pp. 667–679. Available at: https://doi.org/10.1083/jcb.201212095.

Endres, M. *et al.* (2010) 'Intervertebral disc regeneration after implantation of a cell-free bioresorbable implant in a rabbit disc degeneration model', *Biomaterials*, 31(22), pp. 5836–5841. Available at: https://doi.org/10.1016/j.biomaterials.2010.03.078.

Erkkilä, K. *et al.* (2002) 'Lactate inhibits germ cell apoptosis in the human testis', *Molecular Human Reproduction*, 8(2), pp. 109–117. Available at: https://doi.org/10.1093/MOLEHR/8.2.109.

Erwin, W.M. *et al.* (2009) 'The regenerative capacity of the notochordal cell: Tissue constructs generated in vitro under hypoxic conditions - Laboratory investigation', *Journal of Neurosurgery: Spine*, 10(6), pp. 513–521. Available at: https://doi.org/10.3171/2009.2.SPINE08578.

Erwin, W.M. *et al.* (2011) 'Notochordal cells protect nucleus pulposus cells from degradation and apoptosis: implications for the mechanisms of intervertebral disc degeneration', *Arthritis Research and Therapy*, 13(6), p. R215. Available at: https://doi.org/10.1186/ar3548.

Erwin, W.M. (2013) 'Biologically Based Therapy for the Intervertebral Disk: who is the Patient?', *Global Spine Journal*, 3(3), pp. 193–199. Available at: https://doi.org/10.1055/s-0033-1343074.

Erwin, W.M. *et al.* (2013) 'Intervertebral Disc-Derived Stem Cells', *Spine*, 38(3), pp. 211–216. Available at: https://doi.org/10.1097/BRS.0b013e318266a80d.

EUROPEAN COMISSION (2001) *MEDICAL DEVICE: Guidance document. GUIDELINES RELATING TO THE APPLICATION OF : THE COUNCIL DIRECTIVE 90/385/EEC ON ACTIVE IMPLANTABLE MEDICAL DEVICES THE COUNCIL DIRECTIVE 93/42/EEC ON MEDICAL DEVICES*. Available at: https://www.team-nb.org/wp-content/uploads/2015/05/documents2012andolders/2_1_3____07-2001.pdf (Accessed: 1 June 2023).

Evans, N.D. *et al.* (2009) 'Substrate stiffness affects early differentiation events in embryonic stem cells', *European cells & materials*, 18, pp. 1–13. Available at: https://doi.org/10.22203/ECM.V018A01.

F.D.A. Infection Control Devices Branch (2016) *Submission and Review of Sterility Information in Premarket Notification (510(k)) Submissions for Devices Labeled as Sterile Guidance for Industry and Food and Drug Administration Staff*, *US FDA*.

Fannon, O.M. *et al.* (2021) 'A Fiber Alginate Co-culture Platform for the Differentiation of mESC and Modeling of the Neural Tube', *Frontiers in Neuroscience*, 14, p. 1386. Available at: https://doi.org/10.3389/FNINS.2020.524346/BIBTEX.

Farzaneh, Z. *et al.* (2018) 'Developing a Cost-Effective and Scalable Production of Human Hepatic Competent Endoderm from Size-Controlled Pluripotent Stem Cell Aggregates', *Stem cells and development*, 27(4), pp. 262–274. Available at: https://doi.org/10.1089/SCD.2017.0074.

Fishman, J.A. and Patience, C. (2004) 'Xenotransplantation: infectious risk revisited', *American journal of transplantation : official journal of the American Society of Transplantation and the American Society of Transplant Surgeons*, 4(9), pp. 1383–1390. Available at: https://doi.org/10.1111/J.1600-6143.2004.00542.X.

Foster, N.E. *et al.* (2018) 'Prevention and treatment of low back pain: evidence, challenges, and promising directions', *The Lancet*. Lancet Publishing Group, pp. 2368–2383. Available at: https://doi.org/10.1016/S0140-6736(18)30489-6.

Frauchiger, D.A. *et al.* (2018) 'Differentiation of MSC and annulus fibrosus cells on genetically engineered silk fleece-membrane-composites enriched for GDF-6 or TGF-β3', *Journal of Orthopaedic Research®*, 36(5), pp. 1324–1333. Available at: https://doi.org/10.1002/jor.23778.

Freemont, A.J. *et al.* (1997) 'Nerve ingrowth into diseased intervertebral disc in chronic back pain', *Lancet*, 350(9072), pp. 178–181. Available at: https://doi.org/10.1016/S0140-6736(97)02135-1.

Fritzell, P. *et al.* (2001) '2001 Volvo Award Winner in Clinical Studies: Lumbar fusion versus nonsurgical treatment for chronic low back pain: a multicenter randomized controlled trial from the Swedish Lumbar Spine Study Group', *Spine*, 26(23), pp. 2521–2534. Available at:

https://doi.org/10.1097/00007632-200112010-00002.

Fu, S. *et al.* (2019) 'Mechanical loading inhibits cartilage inflammatory signalling via an HDAC6 and IFT-dependent mechanism regulating primary cilia elongation', *Osteoarthritis and Cartilage*, 27(7), pp. 1064–1074. Available at: https://doi.org/10.1016/j.joca.2019.03.003.

Fu, S. *et al.* (2021) 'Activation of TRPV4 by mechanical, osmotic or pharmaceutical stimulation is anti-inflammatory blocking IL-1β mediated articular cartilage matrix destruction', *Osteoarthritis and Cartilage*, 29(1), pp. 89–99. Available at: https://doi.org/10.1016/j.joca.2020.08.002.

Fujii, K. *et al.* (2019) 'Discogenic Back Pain: Literature Review of Definition, Diagnosis, and Treatment', *JBMR plus*, 3(5). Available at: https://doi.org/10.1002/JBM4.10180.

Fujioka, T. *et al.* (2004) 'A simple and efficient cryopreservation method for primate embryonic stem cells', *International Journal of Developmental Biology*, 48(10), pp. 1149–1154. Available at: https://doi.org/10.1387/IJDB.041852TF.

Fullen, B. *et al.* (2022) 'Management of chronic low back pain and the impact on patients' personal and professional lives: Results from an international patient survey', *Pain practice : the official journal of World Institute of Pain*, 22(4), pp. 463–477. Available at: https://doi.org/10.1111/PAPR.13103.

Fusaki, N. *et al.* (2009) 'Efficient induction of transgene-free human pluripotent stem cells using a vector based on Sendai virus, an RNA virus that does not integrate into the host genome', *Proceedings of the Japan Academy. Series B, Physical and biological sciences*, 85(8), pp. 348–362. Available at: https://doi.org/10.2183/PJAB.85.348.

Gadue, P. *et al.* (2006) 'Wnt and TGF-β signaling are required for the induction of an in vitro model of primitive streak formation using embryonic stem cells', *Proceedings of the National Academy of Sciences of the United States of America*, 103(45), p. 16806. Available at: https://doi.org/10.1073/PNAS.0603916103.

Gan, Y. *et al.* (2021) 'Spatially defined single-cell transcriptional profiling characterizes diverse chondrocyte subtypes and nucleus pulposus progenitors in human intervertebral discs', *Bone Research 2021 9:1*, 9(1), pp. 1–15. Available at: https://doi.org/10.1038/s41413-021-00163-z.

Ganey, T. *et al.* (2003) 'Disc Chondrocyte Transplantation in a Canine Model: A Treatment for Degenerated or Damaged Intervertebral Disc', *Spine*, 28(23), pp. 2609–2620. Available at: https://doi.org/10.1097/01.BRS.0000097891.63063.78.

Gansner, J.M. and Gitlin, A.J.D. (2008) 'Essential role for the alpha 1 chain of type VIII collagen in zebrafish notochord formation', *Developmental Dynamics*, 237(12), pp. 3715–3726. Available at: https://doi.org/10.1002/dvdy.21779.

Gantenbein-Ritter, B. and Chan, S.C.W. (2012) 'The evolutionary importance of cell ratio between notochordal and nucleus pulposus cells: an experimental 3-D co-culture study', *European Spine Journal*, 21(Suppl 6), p. 819. Available at: https://doi.org/10.1007/S00586-011-2026-9.

Gantenbein, B. *et al.* (2014) 'Activation of intervertebral disc cells by co-culture with notochordal cells, conditioned medium and hypoxia', *BMC Musculoskeletal Disorders*, 15(1), p. 422. Available at: https://doi.org/10.1186/1471-2474-15-422.

Gao, C. *et al.* (2018) 'Rapamycin prevents the intervertebral disc degeneration via inhibiting differentiation and senescence of annulus fibrosus cells', *Aging*, 10(1), pp. 131–143. Available at: https://doi.org/10.18632/aging.101364.

Garcia, J. *et al.* (2017) 'Sheath Cell Invasion and Trans-differentiation Repair Mechanical Damage Caused by Loss of Caveolae in the Zebrafish Notochord', *Current Biology*, 27(13), pp. 1982-1989.e3.

Available at: https://doi.org/10.1016/j.cub.2017.05.035.

Gay, M.H. *et al.* (2019) 'Nose to back: compatibility of nasal chondrocytes with environmental conditions mimicking a degenerated intervertebral disc', *European cells & materials*, 37, pp. 214–232. Available at: https://doi.org/10.22203/eCM.v037a13.

Gebhard, H. *et al.* (2010) *Total disc replacement using a tissue-engineered intervertebral disc in vivo: new animal model and initial results*, *Evidence-Based Spine-Care Journal*. Available at: https://doi.org/10.1055/s-0028-1100918.

Gerrard, L., Rodgers, L. and Cui, W. (2005) 'Differentiation of human embryonic stem cells to neural lineages in adherent culture by blocking bone morphogenetic protein signaling', *Stem cells (Dayton, Ohio)*, 23(9), pp. 1234–1241. Available at: https://doi.org/10.1634/STEMCELLS.2005-0110.

Gilchrist, C.L. *et al.* (2011) 'Extracellular Matrix Ligand and Stiffness Modulate Immature Nucleus Pulposus Cell-Cell Interactions', *PLOS ONE*, 6(11), p. e27170. Available at: https://doi.org/10.1371/JOURNAL.PONE.0027170.

Gomez-Ruiz, V. *et al.* (2023) 'Autologous mesenchymal stem cell transplantation for spinal fusion: 10 years follow-up of a phase I/II clinical trial', *Stem cell research & therapy*, 14(1), p. 78. Available at: https://doi.org/10.1186/S13287-023-03298-4.

Götz, W. *et al.* (1997) 'Detection and distribution of the carbohydrate binding protein galectin-3 in human notochord, intervertebral disc and chordoma', *Differentiation; research in biological diversity*, 62(3), pp. 149–157. Available at: https://doi.org/10.1046/J.1432-0436.1997.6230149.X.

Gruber, H.E. *et al.* (2005) 'The SOX9 transcription factor in the human disc: decreased immunolocalization with age and disc degeneration', *Spine*, 30(6), pp. 625–630. Available at: https://doi.org/10.1097/01.BRS.0000155420.01444.C6.

Gruber, H.E. *et al.* (2010) 'Micromass culture of human anulus cells: Morphology and extracellular matrix production', *Spine*, 35(10), pp. 1033–1038. Available at: https://doi.org/10.1097/BRS.0b013e3181bc3e04.

Guehring, T. *et al.* (2009) 'Notochordal intervertebral disc cells: Sensitivity to nutrient deprivation', *Arthritis and Rheumatism*, 60(4), pp. 1026–1034. Available at: https://doi.org/10.1002/art.24407.

Guehring, T. *et al.* (2010) 'Sensitivity of notochordal disc cells to mechanical loading: an experimental animal study', *European Spine Journal*, 19(1), p. 113. Available at: https://doi.org/10.1007/S00586-009-1217-0.

Hammerick, K.E. *et al.* (2011) 'Elastic Properties of Induced Pluripotent Stem Cells', *Tissue Engineering. Part A*, 17(3–4), p. 495. Available at: https://doi.org/10.1089/TEN.TEA.2010.0211.

Han, B. *et al.* (2014) 'Nucleus Pulposus Mesenchymal Stem Cells in Acidic Conditions Mimicking Degenerative Intervertebral Discs Give Better Performance than Adipose Tissue-Derived Mesenchymal Stem Cells', *Cells Tissues Organs*, 199(5–6), pp. 342–352. Available at: https://doi.org/10.1159/000369452.

Hang, D. *et al.* (2017) 'One-Stage Positron Emission Tomography and Magnetic Resonance Imaging to Assess Mesenchymal Stem Cell Survival in a Canine Model of Intervertebral Disc Degeneration', *Stem Cells and Development*, 26(18), pp. 1334–1343. Available at: https://doi.org/10.1089/scd.2017.0103.

Hansen, H.J. (1951) 'A pathologic-anatomical interpretation of disc degeneration in dogs', *Acta orthopaedica Scandinavica*, 20(4), pp. 280–293. Available at: https://doi.org/10.3109/17453675108991175.

Harmon, M.D. *et al.* (2020) 'Growing a backbone-functional biomaterials and structures for intervertebral disc (IVD) repair and regeneration: Challenges, innovations, and future directions', *Biomaterials Science*. Royal Society of Chemistry, pp. 1216–1239. Available at: https://doi.org/10.1039/c9bm01288e.

Hartvigsen, J. *et al.* (2018) 'What low back pain is and why we need to pay attention', *The Lancet*. Lancet Publishing Group, pp. 2356–2367. Available at: https://doi.org/10.1016/S0140-6736(18)30480-X.

Haufe, S.M.W. and Mork, A.R. (2006) 'Intradiscal injection of hematopoietic stem cells in an attempt to rejuvenate the intervertebral discs', *Stem Cells and Development*, 15(1), pp. 136–137. Available at: https://doi.org/10.1089/scd.2006.15.136.

Häuser, W., Schug, S. and Furlan, A.D. (2017) 'The opioid epidemic and national guidelines for opioid therapy for chronic noncancer pain: A perspective from different continents', in *Pain Reports*. Lippincott Williams and Wilkins, p. 599. Available at: https://doi.org/10.1097/PR9.0000000000000599.

Hayes, A.J., Benjamin, M. and Ralphs, J.R. (2001) 'Extracellular matrix in development of the intervertebral disc', *Matrix biology : journal of the International Society for Matrix Biology*, 20(2), pp. 107–121. Available at: https://doi.org/10.1016/S0945-053X(01)00125-1.

Heathfield, S.K., Le Maitre, C.L. and Hoyland, J.A. (2008) 'Caveolin-1 expression and stress-induced premature senescence in human intervertebral disc degeneration', *Arthritis research & therapy*, 10(4). Available at: https://doi.org/10.1186/AR2468.

Heathman, T.R. *et al.* (2015) 'The translation of cell-based therapies: clinical landscape and manufacturing challenges', *Regenerative medicine*, 10(1), pp. 49–64. Available at: https://doi.org/10.2217/RME.14.73.

Hegewald, A.A. *et al.* (2011) 'Engineering of polymer-based grafts with cells derived from human nucleus pulposus tissue of the lumbar spine', *Journal of Tissue Engineering and Regenerative Medicine*, 5(4), pp. 275–282. Available at: https://doi.org/10.1002/term.312.

Helen, W. and Gough, J.E. (2008) 'Cell viability, proliferation and extracellular matrix production of human annulus fibrosus cells cultured within PDLLA/Bioglass® composite foam scaffolds in vitro', *Acta Biomaterialia*, 4(2), pp. 230–243. Available at: https://doi.org/10.1016/j.actbio.2007.09.010.

Henriksson, H.B. *et al.* (2009) 'Transplantation of human mesenchymal stems cells into intervertebral discs in a xenogeneic porcine model', *Spine*, 34(2), pp. 141–148. Available at: https://doi.org/10.1097/BRS.0b013e31818f8c20.

Henriksson, H.B. *et al.* (2012) 'Investigation of different cell types and gel carriers for cell-based intervertebral disc therapy, *in vitro* and *in vivo* studies', *Journal of Tissue Engineering and Regenerative Medicine*, 6(9), pp. 738–747. Available at: https://doi.org/10.1002/term.480.

Hiraishi, S. *et al.* (2018) 'Discogenic cell transplantation directly from a cryopreserved state in an induced intervertebral disc degeneration canine model', *JOR SPINE*, 1(2), p. e1013. Available at: https://doi.org/10.1002/jsp2.1013.

Hodgkinson, T. *et al.* (2019) 'Therapeutic potential of growth differentiation factors in the treatment of degenerative disc diseases', *JOR SPINE*, 2(1), p. e1045. Available at: https://doi.org/10.1002/jsp2.1045.

Hong, X. *et al.* (2018) 'Large Cytoplasmic Vacuoles within Notochordal Nucleus Pulposus Cells: A Possible Regulator of Intracellular Pressure That Shapes the Cytoskeleton and Controls Proliferation',

Cells, tissues, organs, 206(1–2), pp. 9–15. Available at: https://doi.org/10.1159/000493258.

Hoogendoorn, R.J. *et al.* (2007) 'Experimental intervertebral disc degeneration induced by chondroitinase ABC in the goat', *Spine*, 32(17), pp. 1816–1825. Available at: https://doi.org/10.1097/BRS.0B013E31811EBAC5.

Hoogendoorn, R.J.W. *et al.* (2008) 'Adipose stem cells for intervertebral disc regeneration: Current status and concepts for the future: Tissue Engineering Review Series', *Journal of Cellular and Molecular Medicine*, 12(6A), pp. 2205–2216. Available at: https://doi.org/10.1111/j.1582-4934.2008.00291.x.

Horner, H.A. and Urban, J.P.G. (2001) '2001 Volvo Award Winner in Basic Science Studies: Effect of nutrient supply on the viability of cells from the nucleus pulposus of the intervertebral disc', *Spine*, 26(23), pp. 2543–2549. Available at: https://doi.org/10.1097/00007632-200112010-00006.

Hoyland, J.A., Le maitre, C. and Freemont, A.J. (2008) 'Investigation of the role of IL-1 and TNF in matrix degradation in the intervertebral disc', *Rheumatology (Oxford, England)*, 47(6), pp. 809–814. Available at: https://doi.org/10.1093/RHEUMATOLOGY/KEN056.

Hu, A. *et al.* (2020) 'Thermosensitive hydrogels loaded with human-induced pluripotent stem cells overexpressing growth differentiation factor-5 ameliorate intervertebral disc degeneration in rats', *Journal of Biomedical Materials Research Part B: Applied Biomaterials*, 108(5), pp. 2005–2016. Available at: https://doi.org/10.1002/jbm.b.34541.

Hu, X. *et al.* (2014) 'Differentiation of menstrual blood-derived stem cells toward nucleus pulposus-like cells in a coculture system with nucleus pulposus cells', *Spine*, 39(9), pp. 754–760. Available at: https://doi.org/10.1097/BRS.0000000000000261.

Huang, Y.C. *et al.* (2013) 'The effects of microenvironment in mesenchymal stem cell-based regeneration of intervertebral disc', *Spine Journal*. Spine J, pp. 352–362. Available at: https://doi.org/10.1016/j.spinee.2012.12.005.

Huang, Y.C. *et al.* (2018) 'Biomaterials for intervertebral disc regeneration: Current status and looming challenges', *Journal of tissue engineering and regenerative medicine*, 12(11), pp. 2188–2202. Available at: https://doi.org/10.1002/TERM.2750.

Hubrecht, R.C. and Carter, E. (2019) 'The 3Rs and Humane Experimental Technique: Implementing Change', *Animals : an Open Access Journal from MDPI*, 9(10). Available at: https://doi.org/10.3390/ANI9100754.

Humphreys, M.D. *et al.* (2018) 'An optimized culture system for notochordal cell expansion with retention of phenotype', *JOR Spine*, 1(3), p. e1028. Available at: https://doi.org/10.1002/jsp2.1028.

Hunter, C.J. *et al.* (2007) 'Osmoregulatory function of large vacuoles found in notochordal cells of the intervertebral disc running title: An osmoregulatory vacuole', *MCB Molecular and Cellular Biomechanics*, 4(4), pp. 227–237. Available at: https://doi.org/10.3970/mcb.2007.004.227.

Hunter, C.J., Matyas, J. R. and Duncan, N.A. (2003) 'The notochordal cell in the nucleus pulposus: A review in the context of tissue engineering', *Tissue Engineering*. Tissue Eng, pp. 667–677. Available at: https://doi.org/10.1089/107632703768247368.

Hunter, C.J., Matyas, John R. and Duncan, N.A. (2003) 'The three-dimensional architecture of the notochordal nucleus pulposus: Novel observations on cell structures in the canine intervertebral disc', *Journal of Anatomy*, 202(3), pp. 279–291. Available at: https://doi.org/10.1046/j.1469-7580.2003.00162.x.

Hunter, C.J., Matyas, J.R. and Duncan, N.A. (2004a) 'Cytomorphology of notochordal and chondrocytic cells from the nucleus pulposus: A species comparison', *Journal of Anatomy*, 205(5), pp. 357–362.

Available at: https://doi.org/10.1111/j.0021-8782.2004.00352.x.

Hunter, C.J., Matyas, J.R. and Duncan, N.A. (2004b) 'The Functional Significance of Cell Clusters in the Notochordal Nucleus Pulposus: Survival and Signaling in the Canine Intervertebral Disc.', *Basic Science*, 29(10), pp. 1099–1104. Available at: https://ovidsp-dc2-ovid-com.hallam.idm.oclc.org/ovid-a/ovidweb.cgi?QS2=434f4e1a73d37e8c50b21927d035aa273ebf545a86b60c50f1f031fa05c072b329109758262744dc4d7336a6adbc24ee7a39224d654f683880c6b3c8ecef97c0fe4131d76d543717cd0c350f2fcd3838ecbdb288215ee362a2b0aaae (Accessed: 20 November 2020).

Hwang, P.Y. *et al.* (2014) 'The role of extracellular matrix elasticity and composition in regulating the nucleus pulposus cell phenotype in the intervertebral disc: a narrative review', *Journal of biomechanical engineering*, 136(2). Available at: https://doi.org/10.1115/1.4026360.

Hwang, P.Y. *et al.* (2015) 'N-Cadherin-Mediated Signaling Regulates Cell Phenotype for Nucleus Pulposus Cells of the Intervertebral Disc', *Cellular and Molecular Bioengineering,* 8(1), pp. 51–62. Available at: https://doi.org/10.1007/s12195-014-0373-4.

Hwang, P.Y. *et al.* (2016) 'N-cadherin is Key to Expression of the Nucleus Pulposus Cell Phenotype under Selective Substrate Culture Conditions', *Scientific reports*, 6. Available at: https://doi.org/10.1038/SREP28038.

Iatridis, J.C. *et al.* (1996) 'Is the nucleus pulposus a solid or a fluid? Mechanical behaviors of the nucleus pulposus of the human intervertebral disc', *Spine*, 21(10), pp. 1174–1184. Available at: https://doi.org/10.1097/00007632-199605150-00009.

Iatridis, J.C. *et al.* (1997) 'Alterations in the mechanical behavior of the human lumbar nucleus pulposus with degeneration and aging', *Journal of Orthopaedic Research*, 15(2), pp. 318–322. Available at: https://doi.org/10.1002/JOR.1100150224.

Ibrahim, A. *et al.* (2022) 'Assessment of mitotic activity in breast cancer: revisited in the digital pathology era', *Journal of Clinical Pathology*, 75(6), pp. 365–372. Available at: https://doi.org/10.1136/JCLINPATH-2021-207742.

Inaba, Y. *et al.* (2011) 'In-straw cryoprotectant dilution for bovine embryos vitrified using Cryotop', *The Journal of reproduction and development*, 57(4), pp. 437–443. Available at: https://doi.org/10.1262/JRD.10-154M.

Ishihara, H. *et al.* (1997) 'Proteoglycan synthesis in the intervertebral disk nucleus: the role of extracellular osmolality', *https://doi.org/10.1152/ajpcell.1997.272.5.C1499*, 272(5 41-5). Available at: https://doi.org/10.1152/AJPCELL.1997.272.5.C1499.

Ito, K. and Creemers, L. (2013) 'Mechanisms of intervertebral disk degeneration/injury and pain: a review', *Global spine journal*, 3(3), pp. 145–151. Available at: https://doi.org/10.1055/S-0033-1347300.

Iwashina, T. *et al.* (2006) 'Feasibility of using a human nucleus pulposus cell line as a cell source in cell transplantation therapy for intervertebral disc degeneration', *Spine*, 31(11), pp. 1177–1186. Available at: https://doi.org/10.1097/01.brs.0000217687.36874.c4.

Jager, L.D. *et al.* (2016) 'Effect of enzymatic and mechanical methods of dissociation on neural progenitor cells derived from induced pluripotent stem cells', *Advances in Medical Sciences*, 61(1), pp. 78–84. Available at: https://doi.org/10.1016/j.advms.2015.09.005.

Jaworski, L.M., Kleinhans, K.L. and Jackson, A.R. (2019) 'Effects of oxygen concentration and culture time on porcine nucleus pulposus cell metabolism: An in vitro study', *Frontiers in Bioengineering and Biotechnology*, 7(APR), p. 64. Available at: https://doi.org/10.3389/FBIOE.2019.00064/BIBTEX.

Jiang, L. *et al.* (2013) 'Apoptosis, senescence, and autophagy in rat nucleus pulposus cells: Implications for diabetic intervertebral disc degeneration', *Journal of Orthopaedic Research*, 31(5), pp. 692–702. Available at: https://doi.org/10.1002/jor.22289.

Jiang, W. *et al.* (2022) 'Single-cell atlas unveils cellular heterogeneity and novel markers in human neonatal and adult intervertebral discs', *iScience*, 25(7). Available at: https://doi.org/10.1016/J.ISCI.2022.104504.

Johnson, W.E.B., Eisenstein, S.M. and Roberts, S. (2009) 'Cell Cluster Formation in Degenerate Lumbar Intervertebral Discs is Associated with Increased Disc Cell Proliferation', *http://dx.doi.org/10.3109/03008200109005650*, 42(3), pp. 197–207. Available at: https://doi.org/10.3109/03008200109005650.

Kadow, T. *et al.* (2015) 'Molecular Basis of Intervertebral Disc Degeneration and Herniations: What Are the Important Translational Questions?', *Clinical Orthopaedics and Related Research*, 473(6), pp. 1903–1912. Available at: https://doi.org/10.1007/s11999-014-3774-8.

Kalinichenko, V. V. *et al.* (2003) 'The forkhead box F1 transcription factor is expressed in brain and head mesenchyme during mouse embryonic development', *Gene Expression Patterns*, 3(2), pp. 153–158. Available at: https://doi.org/10.1016/S1567-133X(03)00010-3.

Kalson, N.S., Richardson, S. and Hoyland, J.A. (2008) 'Strategies for regeneration of the intervertebral disc', *Regenerative Medicine*. Regen Med, pp. 715–729. Available at: https://doi.org/10.2217/17460751.3.5.717.

Kamatani, T. *et al.* (2022) 'Human iPS cell-derived cartilaginous tissue spatially and functionally replaces nucleus pulposus', *Biomaterials*, 284. Available at: https://doi.org/10.1016/J.BIOMATERIALS.2022.121491.

Kathem, S.H. *et al.* (2014) 'Ciliotherapy: A novel intervention in polycystic kidney disease', *Journal of Geriatric Cardiology*, 11(1), pp. 63–73. Available at: https://doi.org/10.3969/j.issn.1671-5411.2014.01.001.

Kauppila, L.I. (1995) 'Ingrowth of blood vessels in disc degeneration. Angiographic and histological studies of cadaveric spines', *The Journal of bone and joint surgery. American volume*, 77(1), pp. 26–31. Available at: https://doi.org/10.2106/00004623-199501000-00004.

Kelp, A. *et al.* (2017) 'Labeling Mesenchymal Stromal Cells with PKH26 or VybrantDil Significantly Diminishes their Migration, but does not affect their Viability, Attachment, Proliferation and Differentiation Capacities', *Journal of Tissue Science & Engineering*, 08(02). Available at: https://doi.org/10.4172/2157-7552.1000199.

Kim, J.H. *et al.* (2009) 'Differentiation of Intervertebral Notochordal Cells Through Live Automated Cell Imaging System In Vitro', *Spine*, 34(23), pp. 2486–2493. Available at: https://doi.org/10.1097/BRS.0b013e3181b26ed1.

Kim, P. and Yang, P. (2012) 'Bone Marrow Cell Therapy in Clinical Trials: A Review of the Literature', *Reviews on Recent Clinical Trials*, 7(3), pp. 204–213. Available at: https://doi.org/10.2174/157488712802281286.

Kimelman, D. and Griffin, K.J. (2000) 'Vertebrate mesendoderm induction and patterning', *Current opinion in genetics & development*, 10(4), pp. 350–356. Available at: https://doi.org/10.1016/S0959-437X(00)00095-2.

Kluba, T. *et al.* (2005) 'Human anulus fibrosis and nucleus pulposus cells of the intervertebral disc: Effect of degeneration and culture system on cell phenotype', *Spine*, 30(24), pp. 2743–2748. Available

at: https://doi.org/10.1097/01.brs.0000192204.89160.6d.

Korecki, C.L. *et al.* (2010) 'Notochordal cell conditioned medium stimulates mesenchymal stem cell differentiation toward a young nucleus pulposus phenotype', *Stem cell research & therapy*, 1(2). Available at: https://doi.org/10.1186/SCRT18.

Korecki, C.L., MacLean, J.J. and Iatridis, J.C. (2008) 'Dynamic compression effects on intervertebral disc mechanics and biology', *Spine*, 33(13), pp. 1403–1409. Available at: https://doi.org/10.1097/BRS.0B013E318175CAE7.

Kothari, S., Chaudry, Q. and Wang, M.D. (2009) *AUTOMATED CELL COUNTING AND CLUSTER SEGMENTATION USING CONCAVITY DETECTION AND ELLIPSE FITTING TECHNIQUES*, *Proc IEEE Int Symp Biomed Imaging*. Available at: https://ieeexplore.ieee.org/stamp/stamp.jsp?tp=&arnumber=5193169 (Accessed: 30 March 2020).

Kreuser, U. *et al.* (2020) 'Initial WNT/β-Catenin Activation Enhanced Mesoderm Commitment, Extracellular Matrix Expression, Cell Aggregation and Cartilage Tissue Yield From Induced Pluripotent Stem Cells', *Frontiers in Cell and Developmental Biology*, 8. Available at: https://doi.org/10.3389/FCELL.2020.581331/FULL.

Krouwels, A., Melchels, F.P.W., *et al.* (2018) 'Comparing Hydrogels for Human Nucleus Pulposus Regeneration: Role of Osmolarity During Expansion', *Tissue engineering. Part C, Methods*, 24(4), pp. 222–232. Available at: https://doi.org/10.1089/TEN.TEC.2017.0226.

Krouwels, A., Popov-Celeketic, J., *et al.* (2018) 'No Effects of Hyperosmolar Culture Medium on Tissue Regeneration by Human Degenerated Nucleus Pulposus Cells Despite Upregulation Extracellular Matrix Genes', *Spine*, 43(5), pp. 307–315. Available at: https://doi.org/10.1097/BRS.0000000000000920.

Kubo, A. *et al.* (2004) 'Development of definitive endoderm from embryonic stem cells in culture', *Development*, 131(7), pp. 1651–1662. Available at: https://doi.org/10.1242/DEV.01044.

Kudelko, M. *et al.* (2021) 'PRIMUS: Comprehensive proteomics of mouse intervertebral discs that inform novel biology and relevance to human disease modelling', *Matrix biology plus*, 12. Available at: https://doi.org/10.1016/J.MBPLUS.2021.100082.

Kumar, N. *et al.* (2015) 'Generation of an expandable intermediate mesoderm restricted progenitor cell line from human pluripotent stem cells', *eLife*, 4(NOVEMBER2015). Available at: https://doi.org/10.7554/ELIFE.08413.

Kurosawa, H. (2012) 'Application of Rho-associated protein kinase (ROCK) inhibitor to human pluripotent stem cells', *Journal of Bioscience and Bioengineering*, 114(6), pp. 577–581. Available at: https://doi.org/10.1016/J.JBIOSC.2012.07.013.

Kuwaki, K. *et al.* (2004) 'Heart transplantation in baboons using α1,3-galactosyltransferase gene-knockout pigs as donors: initial experience', *Nature Medicine 2004 11:1*, 11(1), pp. 29–31. Available at: https://doi.org/10.1038/NM1171.

Kwon, W.-K. *et al.* (2017) 'Influence of rabbit notochordal cells on symptomatic intervertebral disc degeneration: anti-angiogenic capacity on human endothelial cell proliferation under hypoxia', *Osteoarthritis and Cartilage*, 25, pp. 1738–1746. Available at: https://doi.org/10.1016/j.joca.2017.06.003.

Laagland, L.T. *et al.* (2022) 'Hyperosmolar expansion medium improves nucleus pulposus cell phenotype', *JOR Spine*, 5(3). Available at: https://doi.org/10.1002/JSP2.1219.

Lai, L. *et al.* (2002) 'Production of α-1,3-Galactosyltransferase Knockout Pigs by Nuclear Transfer

Cloning', *Science* [Preprint]. Available at: https://doi.org/10.1126/SCIENCE.1068228.

Lama, P. *et al.* (2019) 'Physical disruption of intervertebral disc promotes cell clustering and a degenerative phenotype', *Cell Death Discovery 2019 5:1*, 5(1), pp. 1–9. Available at: https://doi.org/10.1038/s41420-019-0233-z.

Laurent, A. *et al.* (2020) 'Bringing Safe and Standardized Cell Therapies to Industrialized Processing for Burns and Wounds', *Frontiers in Bioengineering and Biotechnology*, 8, p. 581. Available at: https://doi.org/10.3389/FBIOE.2020.00581/FULL.

Laurent, A. *et al.* (2021) 'Swiss Fetal Transplantation Program and Non-enzymatically Isolated Primary Progenitor Cell Types for Regenerative Medicine', *Methods in Molecular Biology*, 2286, pp. 1–24. Available at: https://doi.org/10.1007/7651_2020_294/FIGURES/3.

Lawson, L. and Harfe, B.D. (2015) 'Notochord to Nucleus Pulposus Transition', *Current osteoporosis reports*, 13(5), pp. 336–341. Available at: https://doi.org/10.1007/S11914-015-0284-X.

Lawson, L.Y. and Harfe, B.D. (2017) 'Developmental mechanisms of intervertebral disc and vertebral column formation', *Wiley Interdisciplinary Reviews: Developmental Biology*, 6(6), p. e283. Available at: https://doi.org/10.1002/WDEV.283.

Lee, N.N. *et al.* (2021) 'A comprehensive tool box for large animal studies of intervertebral disc degeneration', *JOR Spine*, 4(2), p. e1162. Available at: https://doi.org/10.1002/JSP2.1162.

Leung, V.Y.L. *et al.* (2009) 'Matrix Remodeling During Intervertebral Disc Growth and Degeneration Detected by Multichromatic FAST Staining', *Journal of Histochemistry and Cytochemistry*, 57(3), p. 249. Available at: https://doi.org/10.1369/JHC.2008.952184.

Li, X. *et al.* (2020) 'Ciliary IFT80 is essential for intervertebral disc development and maintenance', *The FASEB Journal*, 34(5), pp. 6741–6756. Available at: https://doi.org/10.1096/FJ.201902838R.

Li, X.C. *et al.* (2018) 'Co-culturing nucleus pulposus mesenchymal stem cells with notochordal cell-rich nucleus pulposus explants attenuates tumor necrosis factor-α-induced senescence', *Stem Cell Research and Therapy*, 9(1). Available at: https://doi.org/10.1186/s13287-018-0919-9.

Li, Y.Y. *et al.* (2014) 'Delivering mesenchymal stem cells in collagen microsphere carriers to rabbit degenerative disc: Reduced risk of osteophyte formation', *Tissue Engineering - Part A*, 20(9–10), pp. 1379–1391. Available at: https://doi.org/10.1089/ten.tea.2013.0498.

Liang, L. *et al.* (2017) 'The characteristics of stem cells in human degenerative intervertebral disc', *Medicine*, 96(25), p. e7178. Available at: https://doi.org/10.1097/MD.0000000000007178.

Liebscher, T. *et al.* (2011) 'Age-related variation in cell density of human lumbar intervertebral disc', *Spine*, 36(2), pp. 153–159. Available at: https://doi.org/10.1097/BRS.0B013E3181CD588C.

Lin, C.H. *et al.* (2013) 'Single-cell enzyme-free dissociation of neurospheres using a microfluidic chip', *Analytical Chemistry*, 85(24), pp. 11920–11928. Available at: https://doi.org/10.1021/ac402724b.

Lin, X. *et al.* (2016) 'Decellularized allogeneic intervertebral disc: Natural biomaterials for regenerating disc degeneration', *Oncotarget*, 7(11), pp. 12121–12136. Available at: https://doi.org/10.18632/oncotarget.7735.

Lindsley, R.C. *et al.* (2006) 'Canonical Wnt signaling is required for development of embryonic stem cell-derived mesoderm', *Development*, 133(19), pp. 3787–3796. Available at: https://doi.org/10.1242/DEV.02551.

Liu, K. *et al.* (2015) 'Determination of the potential of induced pluripotent stem cells to differentiate into mouse nucleus pulposus cells in vitro', *Genetics and molecular research : GMR*, 14(4), pp. 12394–

12405. Available at: https://doi.org/10.4238/2015.OCTOBER.16.6.

Liu, W. and Chen, G. (2014) 'Cryopreservation of Human Pluripotent Stem Cells in Defined Medium', *Current protocols in stem cell biology*, 31, p. 1C.17.1. Available at: https://doi.org/10.1002/9780470151808.SC01C17S31.

Liu, Y. *et al.* (2015) 'Native nucleus pulposus tissue matrix promotes notochordal differentiation of human induced pluripotent stem cells with potential for treating intervertebral disc degeneration', *Journal of biomedical materials research. Part A*, 103(3), pp. 1053–1059. Available at: https://doi.org/10.1002/JBM.A.35243.

Liu, Y., Rahaman, M.N. and Bal, B.S. (2014) 'Modulating notochordal differentiation of human induced pluripotent stem cells using natural nucleus pulposus tissue matrix', *PloS one*, 9(7). Available at: https://doi.org/10.1371/JOURNAL.PONE.0100885.

Liu, Z. *et al.* (2018) 'CD24 identifies nucleus pulposus progenitors/notochordal cells for disc regeneration', *Journal of Biological Engineering*, 12(1), p. 35. Available at: https://doi.org/10.1186/s13036-018-0129-0.

De Luca, P. *et al.* (2020) 'Intervertebral disc and endplate cell characterisation highlights annulus fibrosus cells as the most promising for tissue-specific disc degeneration therapy', *European Cells and Materials*, 39, pp. 156–170. Available at: https://doi.org/10.22203/eCM.v039a10.

Luo, T.D. *et al.* (2019) 'Evaluation of Percutaneous Intradiscal Amniotic Suspension Allograft in a Rabbit Model of Intervertebral Disc Degeneration', *Spine*, 44(6), pp. E329–E337. Available at: https://doi.org/10.1097/BRS.0000000000002851.

Luoma, K. *et al.* (2000) 'Low back pain in relation to lumbar disc degeneration', *Spine*, 25(4), pp. 487–492. Available at: https://doi.org/10.1097/00007632-200002150-00016.

Ma, W. *et al.* (2008) 'Cell-extracellular matrix interactions regulate neural differentiation of human embryonic stem cells', *BMC Developmental Biology*, 8(1), p. 90. Available at: https://doi.org/10.1186/1471-213X-8-90.

Maetzel, A. and Li, L. (2002) 'The economic burden of low back pain: A review of studies published between 1996 and 2001', *Best Practice and Research: Clinical Rheumatology*, 16(1), pp. 23–30. Available at: https://doi.org/10.1053/berh.2001.0204.

Mahmoud, K.G.M. *et al.* (2010) 'Effect of Different Combinations of Cryoprotectants on In Vitro Maturation of Immature Buffalo (Bubalus bubalis) Oocytes Vitrified by Straw and Open-Pulled Straw Methods', *Reproduction in Domestic Animals*, 45(4), pp. 565–571. Available at: https://doi.org/10.1111/J.1439-0531.2008.01293.X.

Maier, J.A., Lo, Y.T. and Harfe, B.D. (2013) 'Foxa1 and Foxa2 Are Required for Formation of the Intervertebral Discs', *PLoS ONE*, 8(1), p. 55528. Available at: https://doi.org/10.1371/JOURNAL.PONE.0055528.

Le Maitre, C.L., Pockert, A., *et al.* (2007) 'Matrix synthesis and degradation in human intervertebral disc degeneration', in *Biochemical Society Transactions*. Portland Press Ltd, pp. 652–655. Available at: https://doi.org/10.1042/BST0350652.

Le Maitre, C.L. *et al.* (2021) 'Development of a standardized histopathology scoring system for human intervertebral disc degeneration: an Orthopaedic Research Society Spine Section Initiative', *JOR Spine*, 4(2), p. e1167. Available at: https://doi.org/10.1002/JSP2.1167.

Le Maitre, C.L., Freemont, A.J. and Hoyland, J.A. (2005) 'The role of interleukin-1 in the pathogenesis of human intervertebral disc degeneration.', *Arthritis research & therapy*, 7(4), p. R732. Available at:

https://doi.org/10.1186/ar1732.

Le Maitre, C.L., Freemont, A.J. and Hoyland, J.A. (2007) 'Accelerated cellular senescence in degenerate intervertebral discs: A possible role in the pathogenesis of intervertebral disc degeneration', *Arthritis Research and Therapy*, 9(3), p. R45. Available at: https://doi.org/10.1186/ar2198.

Le Maitre, C.L., Hoyland, J.A. and Freemont, A.J. (2004) 'Studies of human intervertebral disc cell function in a constrained in vitro tissue culture system', *Spine*, 29(11), pp. 1187–1195. Available at: https://doi.org/10.1097/00007632-200406010-00006.

Maître, J.L. and Heisenberg, C.P. (2013) 'Three functions of cadherins in cell adhesion', *Current Biology*. Elsevier, p. R626. Available at: https://doi.org/10.1016/j.cub.2013.06.019.

Maldonado, M. *et al.* (2016) 'ROCK inhibitor primes human induced pluripotent stem cells to selectively differentiate towards mesendodermal lineage via epithelial-mesenchymal transition-like modulation', *Stem cell research*, 17(2), pp. 222–227. Available at: https://doi.org/10.1016/J.SCR.2016.07.009.

Malik, K.M. *et al.* (2013) 'Diagnostic criteria and treatment of discogenic pain: a systematic review of recent clinical literature', *The spine journal : official journal of the North American Spine Society*, 13(11), pp. 1675–1689. Available at: https://doi.org/10.1016/J.SPINEE.2013.06.063.

Manchikanti, L. *et al.* (2012) 'Opioid epidemic in the United States.', *Pain physician*, pp. 9–38.

Maroudas, A. *et al.* (1975) *Factors involved in the nutrition of the human lumbar intervertebral disc: cellularity and diffusion of glucose in vitro*, *J. Anat*.

Martell, B.A. *et al.* (2007) 'Systematic review: Opioid treatment for chronic back pain: Prevalence, efficacy, and association with addiction', *Annals of Internal Medicine*. American College of Physicians, pp. 116–127. Available at: https://doi.org/10.7326/0003-4819-146-2-200701160-00006.

Martin, J.R. *et al.* (2020) 'Enhanced stem cell retention and antioxidative protection with injectable, ROS-degradable PEG hydrogels', *Biomaterials*, 263. Available at: https://doi.org/10.1016/J.BIOMATERIALS.2020.120377.

Martyniak, K. *et al.* (2022) 'Biomaterial composition and stiffness as decisive properties of 3D bioprinted constructs for type II collagen stimulation', *Acta Biomaterialia*, 152, pp. 221–234. Available at: https://doi.org/10.1016/J.ACTBIO.2022.08.058.

Mason, C. and Dunnill, P. (2009) 'Assessing the value of autologous and allogeneic cells for regenerative medicine', *http://dx.doi.org/10.2217/rme.09.64*, 4(6), pp. 835–853. Available at: https://doi.org/10.2217/RME.09.64.

McCann, M.R. *et al.* (2012) 'Tracing notochord-derived cells using a Noto-cre mouse: implications for intervertebral disc development', *Disease models & mechanisms*, 5(1), pp. 73–82. Available at: https://doi.org/10.1242/DMM.008128.

McCann, M.R. and Séguin, C.A. (2016) 'Notochord cells in intervertebral disc development and degeneration', *Journal of Developmental Biology*. MDPI Multidisciplinary Digital Publishing Institute. Available at: https://doi.org/10.3390/jdb4010003.

McMahon, J.A. *et al.* (1998) 'Noggin-mediated antagonism of BMP signaling is required for growth and patterning of the neural tube and somite', *Genes & Development*, 12(10), p. 1438. Available at: https://doi.org/10.1101/GAD.12.10.1438.

McNally, D.S. and Adams, M.A. (1992) 'Internal intervertebral disc mechanics as revealed by stress profilometry', *Spine*, 17(1), pp. 66–73. Available at: https://doi.org/10.1097/00007632-199201000-

00011.

Meisel, H.J. *et al.* (2019) 'Cell Therapy for Treatment of Intervertebral Disc Degeneration: A Systematic Review', *Global Spine Journal*. SAGE Publications Ltd, pp. 39S-52S. Available at: https://doi.org/10.1177/2192568219829024.

Mellott, M.B., Searcy, K. and Pishko, M. V. (2001) 'Release of protein from highly cross-linked hydrogels of poly(ethylene glycol) diacrylate fabricated by UV polymerization', *Biomaterials*, 22(9), pp. 929–941. Available at: https://doi.org/10.1016/S0142-9612(00)00258-1.

Melvin, T. and Torre, M. (2019) 'New medical device regulations: the regulator's view', *EFORT Open Reviews*, 4(6), p. 351. Available at: https://doi.org/10.1302/2058-5241.4.180061.

Minogue, B.M. *et al.* (2010) 'Transcriptional profiling of bovine intervertebral disc cells: implications for identification of normal and degenerate human intervertebral disc cell phenotypes', *Arthritis research & therapy*, 12(1). Available at: https://doi.org/10.1186/AR2929.

Mita, M. and Hall, P.F. (1982) 'Metabolism of Round Spermatids from Rats: Lactate as the Preferred Substrate', *Biology of Reproduction*, 26(3), pp. 445–448. Available at: https://doi.org/10.1095/BIOLREPROD26.3.445.

Mitalipova, M.M. *et al.* (2005) 'Preserving the genetic integrity of human embryonic stem cells', *Nature Biotechnology 2005 23:1*, 23(1), pp. 19–20. Available at: https://doi.org/10.1038/nbt0105-19.

Miyamoto, T. *et al.* (2010) 'Intradiscal transplantation of synovial mesenchymal stem cells prevents intervertebral disc degeneration through suppression of matrix metalloproteinase-related genes in nucleus pulposus cells in rabbits', *Arthritis Research and Therapy*, 12(6), p. R206. Available at: https://doi.org/10.1186/ar3182.

Miyazaki, T. *et al.* (2009) 'A phenotypic comparison of proteoglycan production of intervertebral disc cells isolated from rats, rabbits, and bovine tails; Which animal model is most suitable to study tissue engineering and biological repair of human disc disorders?', *Tissue Engineering - Part A*, 15(12), pp. 3835–3846. Available at: https://doi.org/10.1089/ten.tea.2009.0250.

Mochida, J. *et al.* (2015) 'Intervertebral disc repair with activated nucleus pulposus cell transplantation: A three-year, prospective clinical study of its safety', *European Cells and Materials*, 29, pp. 202–212. Available at: https://doi.org/10.22203/eCM.v029a15.

Modic, M.T. *et al.* (1988) 'Degenerative disk disease: assessment of changes in vertebral body marrow with MR imaging.', *https://doi.org/10.1148/radiology.166.1.3336678*, 166(1 I), pp. 193–199. Available at: https://doi.org/10.1148/RADIOLOGY.166.1.3336678.

Mokhbi Soukane, D., Shirazi-Adl, A. and Urban, J.P.G. (2009) 'Investigation of solute concentrations in a 3D model of intervertebral disc', *European Spine Journal*, 18(2), pp. 254–262. Available at: https://doi.org/10.1007/S00586-008-0822-7/FIGURES/7.

Mount, N.M. *et al.* (2015) 'Cell-based therapy technology classifications and translational challenges', *Philosophical transactions of the Royal Society of London. Series B, Biological sciences*, 370(1680). Available at: https://doi.org/10.1098/RSTB.2015.0017.

Mueller, N.J. and Fishman, J.A. (2004) 'Herpesvirus infections in xenotransplantation: pathogenesis and approaches', *Xenotransplantation*, 11(6), pp. 486–490. Available at: https://doi.org/10.1111/J.1399-3089.2004.00180.X.

Murrell, W. *et al.* (2009) 'Olfactory stem cells can be induced to express chondrogenic phenotype in a rat intervertebral disc injury model', *Spine Journal*, 9(7), pp. 585–594. Available at: https://doi.org/10.1016/j.spinee.2009.02.011.

Mwale, F. *et al.* (2004) 'Distinction between the extracellular matrix of the nucleus pulposus and hyaline cartilage: A requisite for tissue engineering of intervertebral disc', *European Cells and Materials*, 8, pp. 58–64. Available at: https://doi.org/10.22203/eCM.v008a06.

Mwale, F. *et al.* (2011) 'Effect of oxygen levels on proteoglycan synthesis by intervertebral disc cells', *Spine*, 36(2), pp. E131–E138. Available at: https://doi.org/10.1097/BRS.0b013e3181d52b9e.

Neidlinger-Wilke, C. *et al.* (2012) 'Interactions of Environmental Conditions and Mechanical Loads Have Influence on Matrix Turnover by Nucleus Pulposus Cells', *J Orthop Res*, 30, pp. 112–121. Available at: https://doi.org/10.1002/jor.21481.

Nerlich, A.G. *et al.* (1998) 'Immunolocalization of major interstitial collagen types in human lumbar intervertebral discs of various ages', *Virchows Archiv : an international journal of pathology*, 432(1), pp. 67–76. Available at: https://doi.org/10.1007/S004280050136.

Nerlich, A.G., Schleicher, E.D. and Boos, N. (1997) '1997 Volvo Award winner in basic science studies. Immunohistologic markers for age-related changes of human lumbar intervertebral discs', *Spine*, 22(24), pp. 2781–2795. Available at: https://doi.org/10.1097/00007632-199712150-00001.

Nice (2018) *Low back pain and sciatica in over 16s*. Available at: https://doi.org/10.1016/j.febslet.2012.03.030.

NICE (2017) 'Lateral interbody fusion in the lumbar spine for low back pain Interventional procedures guidance Your responsibility'. Available at: www.nice.org.uk/guidance/ipg574 (Accessed: 1 June 2023).

Niemeyer, P. *et al.* (2022) 'Treatment of Large Cartilage Defects in the Knee by Hydrogel-Based Autologous Chondrocyte Implantation: Two-Year Results of a Prospective, Multicenter, Single-Arm Phase III Trial', *Cartilage*, 13(1). Available at: https://doi.org/10.1177/19476035221085146.

Nieuwkoop, P.D. (1997) 'Short historical survey of pattern formation in the endo-mesoderm and the neural anlage in the vertebrates: the role of vertical and planar inductive actions.', *Cellular and molecular life sciences : CMLS*, 53(4), pp. 305–18. Available at: https://doi.org/10.1007/pl00000608.

Noriega, D.C. *et al.* (2017) 'Intervertebral Disc Repair by Allogeneic Mesenchymal Bone Marrow Cells: A Randomized Controlled Trial', *Transplantation*, 101(8), pp. 1945–1951. Available at: https://doi.org/10.1097/TP.0000000000001484.

Noriega, D.C. *et al.* (2021) 'Treatment of Degenerative Disc Disease with Allogeneic Mesenchymal Stem Cells: Long-term Follow-up Results', *Transplantation*, 105(2), pp. E25–E27. Available at: https://doi.org/10.1097/TP.0000000000003471.

Nukaga, T. *et al.* (2016) 'Transplantation of activated nucleus pulposus cells after cryopreservation: Efficacy study in a canine disc degeneration model', *European Cells and Materials*, 31, pp. 95–106. Available at: https://doi.org/10.22203/eCM.v031a07.

Nukaga, T. *et al.* (2019) 'Annulus fibrosus cell sheets limit disc degeneration in a rat annulus fibrosus injury model', *JOR SPINE*, 2(2), p. e1050. Available at: https://doi.org/10.1002/jsp2.1050.

Oegema, T.R. (1993) 'Biochemistry of the intervertebral disc.', *Clinics in sports medicine*, 12(3), pp. 419–39. Available at: http://www.ncbi.nlm.nih.gov/pubmed/8364983 (Accessed: 28 April 2020).

Ohnuma, K. *et al.* (2014) 'Enzyme-free passage of human pluripotent stem cells by controlling divalent cations', *Scientific Reports*, 4. Available at: https://doi.org/10.1038/srep04646.

Ohshima, H. and Urban, J.P.G. (1992) 'The effect of lactate and pH on proteoglycan and protein synthesis rates in the intervertebral disc', *Spine*, 17(9), pp. 1079–1082. Available at:

https://doi.org/10.1097/00007632-199209000-00012.

Omlor, G.W. *et al.* (2018) 'Disc cell therapy with bone-marrow-derived autologous mesenchymal stromal cells in a large porcine disc degeneration model', *European Spine Journal*, 27(10), pp. 2639–2649. Available at: https://doi.org/10.1007/s00586-018-5728-4.

Orozco, L. *et al.* (2011) 'Intervertebral Disc Repair by Autologous Mesenchymal Bone Marrow Cells: A Pilot Study', *Transplantation*, 92(7), pp. 822–828. Available at: https://doi.org/10.1097/TP.0b013e3182298a15.

Øvrebø, Ø. *et al.* (2022) 'Design and clinical application of injectable hydrogels for musculoskeletal therapy', *Bioengineering & Translational Medicine*, 7(2). Available at: https://doi.org/10.1002/BTM2.10295.

Paavola, L.G., Wilson, D.B. and Center, E.M. (1980) 'Histochemistry of the developing notochord, perichordal sheath and vertebrae in Danforth's short-tail (Sd) and normal C57BL/6 mice', *Development*, 55(1), pp. 227–245. Available at: https://doi.org/10.1242/DEV.55.1.227.

Paillat, L. *et al.* (2023) 'Three-dimensional culture model to study the biology of vacuolated notochordal cells from mouse nucleus pulposus explants', *European cells & materials*, 45, pp. 72–87. Available at: https://doi.org/10.22203/ECM.V045A06.

Palacio-Mancheno, P.E. *et al.* (2018) 'Hyperosmolarity induces notochordal cell differentiation with aquaporin3 upregulation and reduced N-cadherin expression', *Journal of orthopaedic research : official publication of the Orthopaedic Research Society*, 36(2), pp. 788–798. Available at: https://doi.org/10.1002/JOR.23715.

Panebianco, C.J. *et al.* (2021) 'Single-cell RNA-sequencing atlas of bovine caudal intervertebral discs: Discovery of heterogeneous cell populations with distinct roles in homeostasis', *FASEB journal : official publication of the Federation of American Societies for Experimental Biology*, 35(11). Available at: https://doi.org/10.1096/FJ.202101149R.

Park, E.Y. and Park, Jong Beon (2013) 'Dose- and time-dependent effect of high glucose concentration on viability of notochordal cells and expression of matrix degrading and fibrotic enzymes', *International orthopaedics*, 37(6), pp. 1179–1186. Available at: https://doi.org/10.1007/S00264-013-1836-2.

Park, E.Y. and Park, Jong Beom (2013) 'High glucose-induced oxidative stress promotes autophagy through mitochondrial damage in rat notochordal cells', *International orthopaedics*, 37(12), pp. 2507–2514. Available at: https://doi.org/10.1007/S00264-013-2037-8.

Park, J.B., Byun, C.H. and Park, E.Y. (2015) 'Rat Notochordal Cells Undergo Premature Stress-Induced Senescence by High Glucose', *Asian spine journal*, 9(4), pp. 495–502. Available at: https://doi.org/10.4184/ASJ.2015.9.4.495.

Park, W.M., Kim, K. and Kim, Y.H. (2013) 'Effects of degenerated intervertebral discs on intersegmental rotations, intradiscal pressures, and facet joint forces of the whole lumbar spine', *Computers in Biology and Medicine*, 43(9), pp. 1234–1240. Available at: https://doi.org/10.1016/J.COMPBIOMED.2013.06.011.

Parsons, M.J. *et al.* (2002) 'Zebrafish mutants identify an essential role for laminins in notochord formation', *Development*, pp. 3137–3146.

Pattappa, G. *et al.* (2012) 'Diversity of intervertebral disc cells: Phenotype and function', *Journal of Anatomy*. J Anat, pp. 480–496. Available at: https://doi.org/10.1111/j.1469-7580.2012.01521.x.

Pazour, G.J. and Witman, G.B. (2003) 'The vertebrate primary cilium is a sensory organelle', *Current*

Opinion in Cell Biology, 15(1), pp. 105–110. Available at: https://doi.org/10.1016/S0955-0674(02)00012-1.

Peck, S.H. *et al.* (2017) 'Whole Transcriptome Analysis of Notochord-Derived Cells during Embryonic Formation of the Nucleus Pulposus', *Scientific Reports 2017 7:1*, 7(1), pp. 1–14. Available at: https://doi.org/10.1038/s41598-017-10692-5.

Périé, D. *et al.* (2006) 'Assessment of compressive modulus, hydraulic permeability and matrix content of trypsin-treated nucleus pulposus using quantitative MRI', *Journal of biomechanics*, 39(8), pp. 1392–1400. Available at: https://doi.org/10.1016/J.JBIOMECH.2005.04.015.

Peroglio, M. *et al.* (2012) 'Injectable thermoreversible hyaluronan-based hydrogels for nucleus pulposus cell encapsulation', *European Spine Journal*, 21(SUPPL. 6), p. 839. Available at: https://doi.org/10.1007/s00586-011-1976-2.

Perris, R. *et al.* (1993) 'Collagen type VI in neural crest development: distribution in situ and interaction with cells in vitro', *Developmental dynamics : an official publication of the American Association of Anatomists*, 198(2), pp. 135–149. Available at: https://doi.org/10.1002/AJA.1001980207.

Pettine, K.A. *et al.* (2017) 'Autologous bone marrow concentrate intradiscal injection for the treatment of degenerative disc disease with three-year follow-up', *International Orthopaedics*, 41(10), pp. 2097–2103. Available at: https://doi.org/10.1007/s00264-017-3560-9.

Pfirrmann, C.W.A. *et al.* (2001) 'Magnetic resonance classification of lumbar intervertebral disc degeneration', *Spine*, 26(17), pp. 1873–1878. Available at: https://doi.org/10.1097/00007632-200109010-00011.

Phillips, K. *et al.* (2003) 'Chronic low back pain management in primary care.', *The Nurse practitioner*, 28(8), pp. 26–31. Available at: https://doi.org/10.1097/00006205-200308000-00008.

Phillips, K.L.E. *et al.* (2013) 'Interleukin-1 receptor antagonist deficient mice provide insights into pathogenesis of human intervertebral disc degeneration', *Annals of the rheumatic diseases*, 72(11), pp. 1860–1867. Available at: https://doi.org/10.1136/ANNRHEUMDIS-2012-202266.

Phillips, K.L.E. *et al.* (2015) 'Potential roles of cytokines and chemokines in human intervertebral disc degeneration: Interleukin-1 is a master regulator of catabolic processes', *Osteoarthritis and Cartilage*, 23(7), pp. 1165–1177. Available at: https://doi.org/10.1016/j.joca.2015.02.017.

Platt, J.L. *et al.* (1991) 'The role of natural antibodies in the activation of xenogenic endothelial cells', *Transplantation*, 52(6), pp. 1037–1043. Available at: https://doi.org/10.1097/00007890-199112000-00019.

Poiraudeau, S. *et al.* (1999) 'Phenotypic characteristics of rabbit intervertebral disc cells comparison with cartilage cells from the same animals', *Spine*, 24(9), pp. 837–844. Available at: https://doi.org/10.1097/00007632-199905010-00002.

Pollard, S.M. *et al.* (2006) 'Essential and overlapping roles for laminin α chains in notochord and blood vessel formation', *Developmental Biology*, 289(1), pp. 64–76. Available at: https://doi.org/10.1016/j.ydbio.2005.10.006.

Potier, E. *et al.* (2014) 'POTENTIAL APPLICATION OF NOTOCHORDAL CELLS FOR INTERVERTEBRAL DISC REGENERATION: AN IN VITRO ASSESSMENT', *European Cells and Materials*, 28, pp. 68–81. Available at: https://doi.org/10.22203/eCM.v028a06.

Potier, E. and Ito, K. (2014) 'Using notochordal cells of developmental origin to stimulate nucleus pulposus cells and bone marrow stromal cells for intervertebral disc regeneration', *European Spine Journal*, 23(3), pp. 679–688. Available at: https://doi.org/10.1007/s00586-013-3107-8.

Power, K.A. *et al.* (2011) 'Identification of Cell Surface-Specific Markers to Target Human Nucleus Pulposus Cells Expression of Carbonic Anhydrase XII Varies With Age and Degeneration', *ARTHRITIS & RHEUMATISM*, 63(12), pp. 3876–3886. Available at: https://doi.org/10.1002/art.30607.

Purmessur, D. *et al.* (2013) 'A role for TNFα in intervertebral disc degeneration: a non-recoverable catabolic shift', *Biochemical and biophysical research communications*, 433(1), pp. 151–156. Available at: https://doi.org/10.1016/J.BBRC.2013.02.034.

Purmessur, Devina *et al.* (2013) *Dynamic pressurization induces transition of notochordal cells to a mature phenotype while retaining production of important patterning ligands from development*. Available at: https://doi.org/10.1186/ar4302.

Qaseem, A. *et al.* (2017) 'Noninvasive treatments for acute, subacute, and chronic low back pain: A clinical practice guideline from the American College of Physicians', *Annals of Internal Medicine*. American College of Physicians, pp. 514–530. Available at: https://doi.org/10.7326/M16-2367.

Quintin, A. *et al.* (2009) 'Isolation and in vitro chondrogenic potential of human foetal spine cells', *Journal of Cellular and Molecular Medicine*, 13(8 B), pp. 2559–2569. Available at: https://doi.org/10.1111/j.1582-4934.2008.00630.x.

Rajpurohit, R. *et al.* (2002) 'Phenotypic characteristics of the nucleus pulposus: Expression of hypoxia inducing factor-1, glucose transporter-1 and MMP-2', *Cell and Tissue Research*, 308(3), pp. 401–407. Available at: https://doi.org/10.1007/s00441-002-0563-6.

Regan, J.L. (2022) 'Protocol for isolation and functional validation of label-retaining quiescent colorectal cancer stem cells from patient-derived organoids for RNA-seq', *STAR Protocols*, 3(1). Available at: https://doi.org/10.1016/J.XPRO.2022.101225.

Reubinoff, B.E. *et al.* (2001) 'Effective cryopreservation of human embryonic stem cells by the open pulled straw vitrification method', *Human Reproduction*, 16(10), pp. 2187–2194. Available at: https://doi.org/10.1093/HUMREP/16.10.2187.

Richards, M. *et al.* (2004) 'An Efficient and Safe Xeno-Free Cryopreservation Method for the Storage of Human Embryonic Stem Cells', *Stem Cells*, 22(5), pp. 779–789. Available at: https://doi.org/10.1634/STEMCELLS.22-5-779.

Richardson, S.M. *et al.* (2008) 'Expression of glucose transporters GLUT-1, GLUT-3, GLUT-9 and HIF-1alpha in normal and degenerate human intervertebral disc', *Histochemistry and cell biology*, 129(4), pp. 503–511. Available at: https://doi.org/10.1007/S00418-007-0372-9.

Richardson, S.M. *et al.* (2017) 'Notochordal and nucleus pulposus marker expression is maintained by sub-populations of adult human nucleus pulposus cells through aging and degeneration', *Scientific reports*, 7(1). Available at: https://doi.org/10.1038/S41598-017-01567-W.

Rinkler, C. *et al.* (2010) 'Influence of low glucose supply on the regulation of gene expression by nucleus pulposus cells and their responsiveness to mechanical loading', *Journal of Neurosurgery: Spine*, 13(4), pp. 535–542. Available at: https://doi.org/10.3171/2010.4.SPINE09713.

Risbud, M. V. *et al.* (2006) 'Nucleus pulposus cells express HIF-1α under normoxic culture conditions: A metabolic adaptation to the intervertebral disc microenvironment', *Journal of Cellular Biochemistry*, 98(1), pp. 152–159. Available at: https://doi.org/10.1002/jcb.20765.

Risbud, M. V. *et al.* (2007) 'Evidence for skeletal progenitor cells in the degenerate human intervertebral disc', *Spine*, 32(23), pp. 2537–2544. Available at: https://doi.org/10.1097/BRS.0b013e318158dea6.

Risbud, M. V. *et al.* (2015) 'Defining the phenotype of young healthy nucleus pulposus cells:

Recommendations of the Spine Research Interest Group at the 2014 annual ORS meeting', *Journal of Orthopaedic Research*, 33(3), pp. 283–293. Available at: https://doi.org/10.1002/JOR.22789.

Risbud, M. V., Schaer, T.P. and Shapiro, I.M. (2010) 'Toward an understanding of the role of notochordal cells in the adult intervertebral disc: From discord to accord', *Developmental Dynamics*, 239(8), pp. 2141–2148. Available at: https://doi.org/10.1002/DVDY.22350.

Risbud, M. V. and Shapiro, I.M. (2011) 'Notochordal cells in the adult intervertebral disc: New perspective on an old question', *Critical Reviews in Eukaryotic Gene Expression*, 21(1), pp. 29–41. Available at: https://doi.org/10.1615/CritRevEukarGeneExpr.v21.i1.30.

Rivera, T. *et al.* (2020) 'Human-Induced Pluripotent Stem Cell Culture Methods Under cGMP Conditions', *Current Protocols in Stem Cell Biology*, 54(1). Available at: https://doi.org/10.1002/CPSC.117.

Roberts, S. *et al.* (1995) 'Mechanoreceptors in intervertebral discs. Morphology, distribution, and neuropeptides', *Spine*, 20(24), pp. 2645–2651. Available at: https://doi.org/10.1097/00007632-199512150-00005.

Roberts, S. *et al.* (2006) 'Senescence in human intervertebral discs', in *European Spine Journal*, pp. 312–316. Available at: https://doi.org/10.1007/s00586-006-0126-8.

Rodaway, A. and Patient, R. (2001) 'Mesendoderm: An ancient germ layer?', *Cell*, 105(2), pp. 169–172. Available at: https://doi.org/10.1016/S0092-8674(01)00307-5.

Rodin, S., Antonsson, L., Niaudet, C., *et al.* (2014) 'Clonal culturing of human embryonic stem cells on laminin-521/E-cadherin matrix in defined and xeno-free environment', *Nature Communications 2014 5:1*, 5(1), pp. 1–13. Available at: https://doi.org/10.1038/ncomms4195.

Rodin, S., Antonsson, L., Hovatta, O., *et al.* (2014) 'Monolayer culturing and cloning of human pluripotent stem cells on laminin-521-based matrices under xeno-free and chemically defined conditions', *Nature protocols*, 9(10), pp. 2354–2368. Available at: https://doi.org/10.1038/NPROT.2014.159.

Rodrigues-Pinto, R. *et al.* (2016) 'Spatiotemporal analysis of putative notochordal cell markers reveals CD24 and keratins 8, 18, and 19 as notochord-specific markers during early human intervertebral disc development', *Journal of Orthopaedic Research*, 34(8), pp. 1327–1340. Available at: https://doi.org/10.1002/JOR.23205.

Rodrigues-Pinto, R. *et al.* (2018) 'Human notochordal cell transcriptome unveils potential regulators of cell function in the developing intervertebral disc', *Scientific Reports*, 8(1), pp. 1–13. Available at: https://doi.org/10.1038/s41598-018-31172-4.

Rosenzweig, D.H. *et al.* (2017) 'COMPARATIVE ANALYSIS IN CONTINUOUS EXPANSION OF BOVINE AND HUMAN PRIMARY NUCLEUS PULPOSUS CELLS FOR TISSUE REPAIR APPLICATIOANS', 33, pp. 2240–251. Available at: https://doi.org/10.22203/eCM.v033a18.

Roughley, P. *et al.* (2006) 'The potential of chitosan-based gels containing intervertebral disc cells for nucleus pulposus supplementation', *Biomaterials*, 27(3), pp. 388–396. Available at: https://doi.org/10.1016/j.biomaterials.2005.06.037.

Roughley, P.J. (2004) 'Biology of intervertebral disc aging and degeneration: Involvement of the extracellular matrix', *Spine*, 29(23), pp. 2691–2699. Available at: https://doi.org/10.1097/01.BRS.0000146101.53784.B1.

Roughley, P.J., Geng, Y. and Mort, J.S. (2014) 'The non-aggregated aggrecan in the human intervertebral disc can arise by a non-proteolytic mechanism', *European cells & materials*, 28, pp. 129–

136. Available at: https://doi.org/10.22203/ECM.V028A10.

Rowlands, A.S., George, P.A. and Cooper-White, J.J. (2008) 'Directing osteogenic and myogenic differentiation of MSCs: interplay of stiffness and adhesive ligand presentation', *American journal of physiology. Cell physiology*, 295(4). Available at: https://doi.org/10.1152/AJPCELL.67.2008.

Sachs, D.H. (1994) 'The pig as a potential xenograft donor', *Veterinary immunology and immunopathology*, 43(1–3), pp. 185–191. Available at: https://doi.org/10.1016/0165-2427(94)90135-X.

Saggese, T. *et al.* (2020) 'Differential Response of Bovine Mature Nucleus Pulposus and Notochordal Cells to Hydrostatic Pressure and Glucose Restriction', *Cartilage*, 11(2), pp. 221–233. Available at: https://doi.org/10.1177/1947603518775795/ASSET/IMAGES/LARGE/10.1177_1947603518775795-FIG2.JPEG.

Sakai, D. (2008) 'Future perspectives of cell-based therapy for intervertebral disc disease', in *European Spine Journal*. Eur Spine J, pp. 452–458. Available at: https://doi.org/10.1007/s00586-008-0743-5.

Sakai, D. *et al.* (2012) 'Exhaustion of nucleus pulposus progenitor cells with ageing and degeneration of the intervertebral disc.', *Nature Communications*, 3, pp. 1264–1264. Available at: https://doi.org/10.1038/NCOMMS2226.

Sakai, D. *et al.* (2018) 'Successful fishing for nucleus pulposus progenitor cells of the intervertebral disc across species', *JOR spine*, 1(2). Available at: https://doi.org/10.1002/JSP2.1018.

Sakai, D. and Andersson, G.B.J. (2015) 'Stem cell therapy for intervertebral disc regeneration: Obstacles and solutions', *Nature Reviews Rheumatology*. Nature Publishing Group, pp. 243–256. Available at: https://doi.org/10.1038/nrrheum.2015.13.

Sato, M. *et al.* (2003) 'An Experimental Study of the Regeneration of the Intervertebral Disc With an Allograft of Cultured Annulus Fibrosus Cells Using a Tissue-Engineering Method', *Spine*, 28(6), pp. 548–553. Available at: https://doi.org/10.1097/01.brs.0000049909.09102.60.

Scherf, N. *et al.* (2012) 'Imaging, quantification and visualization of spatio-temporal patterning in mESC colonies under different culture conditions', *Bioinformatics*, 28(18), pp. i556–i561. Available at: https://doi.org/10.1093/BIOINFORMATICS/BTS404.

Schmitz, T.C. *et al.* (2020) 'Characterization of biomaterials intended for use in the nucleus pulposus of degenerated intervertebral discs', *Acta Biomaterialia*, 114, pp. 1–15. Available at: https://doi.org/10.1016/J.ACTBIO.2020.08.001.

Schmitz, T.C. *et al.* (2022) 'Detergent-Free Decellularization of Notochordal Cell-Derived Matrix Yields a Regenerative, Injectable, and Swellable Biomaterial', *ACS Biomaterials Science and Engineering*, 8(9), pp. 3912–3923. Available at: https://doi.org/10.1021/ACSBIOMATERIALS.2C00790/ASSET/IMAGES/LARGE/AB2C00790_0009.JPEG.

Scholl, L. *et al.* (2017) *Morbidity and Mortality Weekly Report Drug and Opioid-Involved Overdose Deaths-United States, 2013-2017*. Available at: https://surveillance.cancer.gov/joinpoint/. (Accessed: 24 April 2020).

Schubert, A.K. *et al.* (2018) 'Standardisation of basal medium for reproducible culture of human annulus fibrosus and nucleus pulposus cells', *Journal of Orthopaedic Surgery and Research*, 13(1). Available at: https://doi.org/10.1186/S13018-018-0914-Y.

Scott, N.A., Harris, P.F. and Bagnall, K.M. (1980) 'A morphological and histological study of the postnatal development of intervertebral discs in the lumbar spine of the rabbit.', *Journal of Anatomy*,

130(Pt 1), pp. 75–81. Available at: https://www.ncbi.nlm.nih.gov/pmc/articles/pmid/6154031/?tool=EBI (Accessed: 1 April 2023).

Seki, S. *et al.* (2022) 'Direct Reprogramming and Induction of Human Dermal Fibroblasts to Differentiate into iPS-Derived Nucleus Pulposus-like Cells in 3D Culture', *International journal of molecular sciences*, 23(7). Available at: https://doi.org/10.3390/IJMS23074059.

Shafa, M. *et al.* (2012) 'Expansion and long-term maintenance of induced pluripotent stem cells in stirred suspension bioreactors', *Journal of Tissue Engineering and Regenerative Medicine*, 6(6), pp. 462–472. Available at: https://doi.org/10.1002/TERM.450.

Shao-Fang, Z. *et al.* (2011) 'PKH26 as a fluorescent label for live human umbilical mesenchymal stem cells', *In Vitro Cellular and Developmental Biology - Animal*, 47(8), pp. 516–520. Available at: https://doi.org/10.1007/S11626-011-9424-5/FIGURES/2.

Shapiro, I.M. and Risbud, M. V. (2014) 'The intervertebral disc: Molecular and structural studies of the disc in health and disease', *The Intervertebral Disc: Molecular and Structural Studies of the Disc in Health and Disease*, pp. 1–446. Available at: https://doi.org/10.1007/978-3-7091-1535-0/COVER.

Sheyn, D. *et al.* (2019) 'Human iPSCs can be differentiated into notochordal cells that reduce intervertebral disc degeneration in a porcine model', *Theranostics*, 9(25), pp. 7506–7524. Available at: https://doi.org/10.7150/THNO.34898.

Shi, P. *et al.* (2019) 'Therapeutic effects of cell therapy with neonatal human dermal fibroblasts and rabbit dermal fibroblasts on disc degeneration and inflammation', *Spine Journal*, 19(1), pp. 171–181. Available at: https://doi.org/10.1016/j.spinee.2018.08.005.

Shin, J.S. *et al.* (2015) 'Long-Term Control of Diabetes in Immunosuppressed Nonhuman Primates (NHP) by the Transplantation of Adult Porcine Islets', *American Journal of Transplantation*, 15(11), pp. 2837–2850. Available at: https://doi.org/10.1111/AJT.13345.

Shu, C. *et al.* (2013) 'The ovine newborn and human foetal intervertebral disc contain perlecan and aggrecan variably substituted with native 7D4 CS sulphation motif: spatiotemporal immunolocalisation and co-distribution with Notch-1 in the human foetal disc', *Glycoconjugate journal*, 30(7), pp. 717–725. Available at: https://doi.org/10.1007/S10719-013-9475-9.

Silverman, L.I. *et al.* (2020) 'In vitro and in vivo evaluation of discogenic cells, an investigational cell therapy for disc degeneration', *Spine Journal*, 20(1), pp. 138–149. Available at: https://doi.org/10.1016/j.spinee.2019.08.006.

Sive, J.I. *et al.* (2002) 'Expression of chondrocyte markers by cells of normal and degenerate intervertebral discs', *Molecular pathology : MP*, 55(2), pp. 91–97. Available at: https://doi.org/10.1136/MP.55.2.91.

Sloan, S.R. *et al.* (2018) 'Biologic Annulus Fibrosus Repair: A Review of Preclinical in Vivo Investigations', *Tissue Engineering - Part B: Reviews*. Mary Ann Liebert Inc., pp. 179–190. Available at: https://doi.org/10.1089/ten.teb.2017.0351.

Smidsrød, O. and Skjåk-Bræk, G. (1990) 'Alginate as immobilization matrix for cells', *Trends in biotechnology*, 8(3), pp. 71–78. Available at: https://doi.org/10.1016/0167-7799(90)90139-O.

Smith, J.A. and Osborn, M. (2007) 'Pain as an assault on the self: An interpretative phenomenological analysis of the psychological impact of chronic benign low back pain', *https://doi.org/10.1080/14768320600941756*, 22(5), pp. 517–534. Available at: https://doi.org/10.1080/14768320600941756.

Smith, L.J. *et al.* (2011) 'Degeneration and regeneration of the intervertebral disc: Lessons from

development', *DMM Disease Models and Mechanisms*. The Company of Biologists Ltd, pp. 31–41. Available at: https://doi.org/10.1242/dmm.006403.

Smith, L.J. *et al.* (2018) 'Advancing cell therapies for intervertebral disc regeneration from the lab to the clinic: Recommendations of the ORS spine section', *JOR Spine*, 1(4), p. e1036. Available at: https://doi.org/10.1002/jsp2.1036.

Smits, P. and Lefebvre, V. (2003) 'Sox5 and Sox6 are required for notochord extracellular matrix sheath formation, notochord cell survival and development of the nucleus pulposus of intervertebral discs', *Development (Cambridge, England)*, 130(6), pp. 1135–1148. Available at: https://doi.org/10.1242/DEV.00331.

Smolders, L.A., Meij, B.P., *et al.* (2013) 'Gene expression profiling of early intervertebral disc degeneration reveals a down-regulation of canonical Wnt signaling and caveolin-1 expression: Implications for development of regenerative strategies', *Arthritis Research and Therapy*, 15(1), p. R23. Available at: https://doi.org/10.1186/ar4157.

Smolders, L.A., Bergknut, N., *et al.* (2013) 'Intervertebral disc degeneration in the dog. Part 2: chondrodystrophic and non-chondrodystrophic breeds', *Veterinary journal (London, England : 1997)*, 195(3), pp. 292–299. Available at: https://doi.org/10.1016/J.TVJL.2012.10.011.

Snuggs, J.W. *et al.* (2019) 'Aquaporin expression in the human and canine intervertebral disc during maturation and degeneration', *JOR SPINE*, 2(1), p. e1049. Available at: https://doi.org/10.1002/jsp2.1049.

Snuggs, J.W. *et al.* (2023) 'Injectable biomaterial induces regeneration of the intervertebral disc in a caprine loaded disc culture model', *Biomaterials Science* [Preprint]. Available at: https://doi.org/10.1039/D3BM00150D.

Snuggs, J.W., Bunning, R.A.D. and Le Maitre, C.L. (2021) 'Osmotic adaptation of nucleus pulposus cells: The role of aquaporin 1, aquaporin 4 and transient receptor potential vanilloid 4', *European Cells and Materials*, 41, pp. 121–141. Available at: https://doi.org/10.22203/ECM.V041A09.

Soukane, D., Shirazi-Adl, A. and Urban, J. (2005) 'Analysis of Nonlinear Coupled Diffusion of Oxygen and Lactic Acid in Intervertebral Discs', *Journal of Biomechanical Engineering*, 127(7), pp. 1121–1126. Available at: https://doi.org/10.1115/1.2073674.

Spasic, M. and Jacobs, C.R. (2017) 'Primary cilia: Cell and molecular mechanosensors directing whole tissue function', *Seminars in Cell and Developmental Biology*. Elsevier Ltd, pp. 42–52. Available at: https://doi.org/10.1016/j.semcdb.2017.08.036.

Spillekom, S. *et al.* (2014) 'Increased Osmolarity and Cell Clustering Preserve Canine Notochordal Cell Phenotype in Culture', *Tissue Engineering - Part C*, 20(8), pp. 652–662. Available at: https://doi.org/10.1089/ten.tec.2013.0479.

Steffens, D. *et al.* (2016) 'Prevention of lowback pain a systematic review and meta-Analysis', *JAMA Internal Medicine*. American Medical Association, pp. 199–208. Available at: https://doi.org/10.1001/jamainternmed.2015.7431.

Stergar, J. *et al.* (2019) 'Intervertebral disc tissue engineering: A brief review', *Bosnian Journal of Basic Medical Sciences*. Association of Basic Medical Sciences of FBIH, pp. 130–137. Available at: https://doi.org/10.17305/bjbms.2019.3778.

Stubbs, C. *et al.* (2020) 'Polyampholytes as Emerging Macromolecular Cryoprotectants', *Biomacromolecules*, 21(1), pp. 7–17. Available at: https://doi.org/10.1021/ACS.BIOMAC.9B01053/ASSET/IMAGES/LARGE/BM9B01053_0006.JPEG.

Suga, M. *et al.* (2015) 'Development of a Monitoring Method for Nonlabeled Human Pluripotent Stem Cell Growth by Time-Lapse Image Analysis', *Stem Cells Translational Medicine*, 4(7), pp. 720–730. Available at: https://doi.org/10.5966/SCTM.2014-0242.

Sullivan, C.B. *et al.* (2014) 'TNFα and IL-1β influence the differentiation and migration of murine MSCs independently of the NF-κB pathway', *Stem Cell Research & Therapy*, 5(4). Available at: https://doi.org/10.1186/SCRT492.

Sumi, T. *et al.* (2008) 'Defining early lineage specification of human embryonic stem cells by the orchestrated balance of canonical Wnt/β-catenin, Activin/Nodal and BMP signaling', *Development*, 135(17), pp. 2969–2979. Available at: https://doi.org/10.1242/DEV.021121.

Suyama, K. *et al.* (2018) 'Effects of interleukin-17A in nucleus pulposus cells and its small-molecule inhibitors for intervertebral disc disease', *Journal of Cellular and Molecular Medicine*, 22(11), pp. 5539–5551. Available at: https://doi.org/10.1111/jcmm.13828.

Takahashi, K. *et al.* (2007) 'Induction of Pluripotent Stem Cells from Adult Human Fibroblasts by Defined Factors', *Cell*, 131(5), pp. 861–872. Available at: https://doi.org/10.1016/j.cell.2007.11.019.

Takahashi, K. and Yamanaka, S. (2006) 'Induction of Pluripotent Stem Cells from Mouse Embryonic and Adult Fibroblast Cultures by Defined Factors', *Cell*, 126(4), pp. 663–676. Available at: https://doi.org/10.1016/j.cell.2006.07.024.

Takenaga, M., Fukumoto, M. and Hori, Y. (2007) 'Regulated Nodal signaling promotes differentiation of the definitive endoderm and mesoderm from ES cells', *Journal of cell science*, 120(Pt 12), pp. 2078–2090. Available at: https://doi.org/10.1242/JCS.004127.

Takimoto, A. *et al.* (2019) 'Differential transactivation of the upstream aggrecan enhancer regulated by PAX1/9 depends on SOX9-driven transactivation', *Scientific reports*, 9(1). Available at: https://doi.org/10.1038/S41598-019-40810-4.

Tam, V. *et al.* (2020) 'DIPPER: a spatiotemporal proteomics atlas of human intervertebral discs for exploring ageing and degeneration dynamics', *bioRxiv*, p. 2020.07.11.192948. Available at: https://doi.org/10.1101/2020.07.11.192948.

Tamagawa, S. *et al.* (2022) 'N-acetylcysteine attenuates oxidative stress-mediated cell viability loss induced by dimethyl sulfoxide in cryopreservation of human nucleus pulposus cells: A potential solution for mass production', *JOR Spine*, 5(4), p. e1223. Available at: https://doi.org/10.1002/JSP2.1223.

Tanaka, M. *et al.* (2013) 'Effect of Cryopreservation on Canine and Human Activated Nucleus Pulposus Cells: A Feasibility Study for Cell Therapy of the Intervertebral Disc', *BioResearch Open Access*, 2(4), pp. 273–282. Available at: https://doi.org/10.1089/biores.2013.0023.

Tang, R. *et al.* (2018) 'Differentiation of human induced pluripotent stem cells into nucleus pulposus-like cells', *Stem Cell Research and Therapy*, 9(1), p. 61. Available at: https://doi.org/10.1186/s13287-018-0797-1.

Tang, S., Richards, J., Khan, S., Hoyland, J., Gallego-Perez, D., *et al.* (2019) 'Nonviral Transfection With Brachyury Reprograms Human Intervertebral Disc Cells to a Pro-Anabolic Anti-Catabolic/Inflammatory Phenotype: A Proof of Concept Study', *Journal of Orthopaedic Research*, 37(11), pp. 2389–2400. Available at: https://doi.org/10.1002/jor.24408.

Tang, S., Richards, J., Khan, S., Hoyland, J., Gallego-Perez, D., *et al.* (2019) 'Nonviral Transfection With Brachyury Reprograms Human Intervertebral Disc Cells to a Pro-Anabolic Anti-Catabolic/Inflammatory Phenotype: A Proof of Concept Study', *Journal of Orthopaedic Research*, 37(11), pp. 2389–2400.

Available at: https://doi.org/10.1002/jor.24408.

Tani, S. *et al.* (2020) 'Understanding paraxial mesoderm development and sclerotome specification for skeletal repair', *Experimental and Molecular Medicine*. Springer Nature, pp. 1166–1177. Available at: https://doi.org/10.1038/s12276-020-0482-1.

Tao, Y.-Q. *et al.* (2013) 'Potential of co-culture of nucleus pulposus mesenchymal stem cells and nucleus pulposus cells in hyperosmotic microenvironment for intervertebral disc regeneration', *Cell Biology International*, 37(8), pp. 826–834. Available at: https://doi.org/10.1002/cbin.10110.

Tchieu, J. *et al.* (2017) 'A MODULAR PLATFORM FOR DIFFERENTIATION OF HUMAN PSCS INTO ALL MAJOR ECTODERMAL LINEAGES', *Cell stem cell*, 21(3), p. 399. Available at: https://doi.org/10.1016/J.STEM.2017.08.015.

Tekari, A. *et al.* (2016) 'Angiopoietin-1 receptor Tie2 distinguishes multipotent differentiation capability in bovine coccygeal nucleus pulposus cells', *Stem Cell Research and Therapy*, 7(1). Available at: https://doi.org/10.1186/s13287-016-0337-9.

Tendulkar, G. *et al.* (2019) 'Intervertebral disc nucleus repair: Hype or hope?', *International Journal of Molecular Sciences*. MDPI AG, p. 3622. Available at: https://doi.org/10.3390/ijms20153622.

Tessier, S. and Risbud, M. V. (2021) 'Understanding embryonic development for cell-based therapies of intervertebral disc degeneration: Toward an effort to treat disc degeneration subphenotypes', *Developmental Dynamics*, 250(3), pp. 302–317. Available at: https://doi.org/10.1002/DVDY.217.

THE EUROPEAN PARLIAMENT AND THE COUNCIL OF THE EUROPEAN UNION (2017) *Regulation (EU) 2017/745 of the European Parliament and of the Council of 5 April 2017 on medical devices, amending Directive 2001/83/EC, Regulation (EC) No 178/2002 and Regulation (EC) No 1223/2009 and repealing Council Directives 90/385/EEC and 93/42/EEC (Text with EEA relevance.)*, *Official Journal of the European Union*. Available at: https://eur-lex.europa.eu/legal-content/EN/TXT/?uri=CELEX:32017R0745 (Accessed: 1 June 2023).

Thompson, P. *et al.* (2011) 'Islet xenotransplantation using gal-deficient neonatal donors improves engraftment and function', *American journal of transplantation : official journal of the American Society of Transplantation and the American Society of Transplant Surgeons*, 11(12), pp. 2593–2602. Available at: https://doi.org/10.1111/J.1600-6143.2011.03720.X.

Thomson, M. *et al.* (2011) 'Pluripotency Factors in Embryonic Stem Cells Regulate Differentiation into Germ Layers', *Cell*, 145, pp. 875–889. Available at: https://doi.org/10.1016/j.cell.2011.05.017.

Thorpe, A *et al.* (2016) 'HYDROXYAPATITE NANOPARTICLE INJECTABLE HYDROGEL SCAFFOLD TO SUPPORT OSTEOGENIC DIFFERENTIATION OF HUMAN MESENCHYMAL STEM CELLS', 32, pp. 1–23. Available at: https://doi.org/10.22203/eCM.v032a01.

Thorpe, Abbey *et al.* (2016) 'Nucleus pulposus phenotypic markers to determine stem cell differentiation: Fact or fiction?', *Oncotarget*, 7(3), pp. 2189–2200. Available at: https://doi.org/10.18632/oncotarget.6782.

Thorpe, Abby *et al.* (2016) 'Thermally triggered injectable hydrogel, which induces mesenchymal stem cell differentiation to nucleus pulposus cells: Potential for regeneration of the intervertebral disc', *Acta Biomaterialia*, 36, pp. 99–111. Available at: https://doi.org/10.1016/j.actbio.2016.03.029.

Thorpe, A., Freeman, C., *et al.* (2018) 'In vivo safety and efficacy testing of a thermally triggered injectable hydrogel scaffold for bone regeneration and augmentation in a rat model', *Oncotarget*, 9(26), pp. 18277–18295. Available at: https://doi.org/10.18632/ONCOTARGET.24813.

Thorpe, A., Bach, F., *et al.* (2018) 'Leaping the hurdles in developing regenerative treatments for the

intervertebral disc from preclinical to clinical', *JOR Spine*, 1(3), p. e1027. Available at: https://doi.org/10.1002/jsp2.1027.

Tomaszewski, K.A. *et al.* (2015) 'The biology behind the human intervertebral disc and its endplates', *Folia Morphol*, 74(2), pp. 157–168. Available at: https://doi.org/10.5603/FM.2015.0026.

Tong, W. *et al.* (2017) 'Cell therapy for the degenerating intervertebral disc', *Translational Research*. Mosby Inc., pp. 49–58. Available at: https://doi.org/10.1016/j.trsl.2016.11.008.

Torre, Olivia M. *et al.* (2019) 'Annulus fibrosus cell phenotypes in homeostasis and injury: implications for regenerative strategies', *Annals of the New York Academy of Sciences*. Blackwell Publishing Inc., pp. 61–78. Available at: https://doi.org/10.1111/nyas.13964.

Torre, Olivia M *et al.* (2019) 'Annulus fibrosus cell phenotypes in homeostasis and injury: implications for regenerative strategies HHS Public Access', 1442(1), pp. 61–78. Available at: https://doi.org/10.1111/nyas.13964.

Traeger, A.C. *et al.* (2019) 'Care for low back pain: Can health systems deliver?', *Bulletin of the World Health Organization*, 97(6), pp. 423–433. Available at: https://doi.org/10.2471/BLT.18.226050.

Treffel, L. *et al.* (2016) 'Intervertebral Disc Swelling Demonstrated by 3D and Water Content Magnetic Resonance Analyses after a 3-Day Dry Immersion Simulating Microgravity', *Frontiers in Physiology*, 7(DEC), p. 605. Available at: https://doi.org/10.3389/FPHYS.2016.00605.

Trout, J.J. *et al.* (1982) 'Ultrastructure of the human intervertebral disc. I. Changes in notochordal cells with age', *Tissue & cell*, 14(2), pp. 359–369. Available at: https://doi.org/10.1016/0040-8166(82)90033-7.

Tschugg, A. *et al.* (2016) 'A prospective multicenter phase I/II clinical trial to evaluate safety and efficacy of NOVOCART Disc plus autologous disc chondrocyte transplantation in the treatment of nucleotomized and degenerative lumbar disc to avoid secondary disease: Study protocol', *Trials*, 17(1), p. 108. Available at: https://doi.org/10.1186/s13063-016-1239-y.

Tsingas, M. *et al.* (2020) 'Sox9 deletion causes severe intervertebral disc degeneration characterized by apoptosis, matrix remodeling, and compartment-specific transcriptomic changes', *Matrix biology : journal of the International Society for Matrix Biology*, 94, pp. 110–133. Available at: https://doi.org/10.1016/J.MATBIO.2020.09.003.

Uhrig, M., Ezquer, F. and Ezquer, M. (2022) 'Improving Cell Recovery: Freezing and Thawing Optimization of Induced Pluripotent Stem Cells', *Cells*, 11(5), p. 799. Available at: https://doi.org/10.3390/CELLS11050799/S1.

Ural, I.H. *et al.* (2017) 'Fibroblast Transplantation Results to the Degenerated Rabbit Lumbar Intervertebral Discs', *The Open Orthopaedics Journal*, 11(1), pp. 404–416. Available at: https://doi.org/10.2174/1874325001711010404.

Urban, J.P.G. (2002) 'The role of the physicochemical environment in determining disc cell behaviour', in *Biochemical Society Transactions*, pp. 858–864. Available at: https://doi.org/10.1042/BST0300858.

Urban, J.P.G., Holm, S. and Maroudas, A. (1978) 'Diffusion of small solutes into the intervertebral disc: An in vivo study', *Biorheology*, 15(3–4), pp. 203–223. Available at: https://doi.org/10.3233/BIR-1978-153-409.

Urban, J.P.G. and Roberts, S. (2003) 'Degeneration of the intervertebral disc', *Arthritis Research and Therapy*, pp. 120–130. Available at: https://doi.org/10.1186/ar629.

Urits, I. *et al.* (2019) 'Stem Cell Therapies for Treatment of Discogenic Low Back Pain: a Comprehensive

Review.', *Current pain and headache reports*, 23(9), p. 65. Available at: https://doi.org/10.1007/s11916-019-0804-y.

Vadalà, G. *et al.* (2008) 'In vitro interaction between muscle-derived stem cells and nucleus pulposus cells', *Spine Journal*, 8(5), pp. 804–809. Available at: https://doi.org/10.1016/j.spinee.2007.07.394.

Vadalà, G. *et al.* (2015) 'Intervertebral disc regeneration: From the degenerative cascade to molecular therapy and tissue engineering', *Journal of Tissue Engineering and Regenerative Medicine*. John Wiley and Sons Ltd, pp. 679–690. Available at: https://doi.org/10.1002/term.1719.

Vadalà, G. *et al.* (2016) 'Stem cells sources for intervertebral disc regeneration', *World J Stem Cells*, 8(5), pp. 185–201. Available at: https://doi.org/10.4252/wjsc.v8.i5.185.

Vergroesen, P.P.A. *et al.* (2015) 'Mechanics and biology in intervertebral disc degeneration: A vicious circle', *Osteoarthritis and Cartilage*. W.B. Saunders Ltd, pp. 1057–1070. Available at: https://doi.org/10.1016/j.joca.2015.03.028.

Vickers, L. *et al.* (2019) 'Mesenchymal stem cell therapies for intervertebral disc degeneration: Consideration of the degenerate niche', *JOR SPINE*, 2(2). Available at: https://doi.org/10.1002/jsp2.1055.

De Vries, S. *et al.* (2019) 'Notochordal Cell Matrix As a Therapeutic Agent for Intervertebral Disc Regeneration', *Tissue Engineering - Part A*, 25(11–12), pp. 830–841. Available at: https://doi.org/10.1089/ten.tea.2018.0026.

Wallman, L. *et al.* (2011) 'Biogrid-a microfluidic device for large-scale enzyme-free dissociation of stem cell aggregates', *Lab on a Chip*, 11(19), pp. 3241–3248. Available at: https://doi.org/10.1039/c1lc20316a.

Wang, F. *et al.* (2017) 'Formation, function, and exhaustion of notochordal cytoplasmic vacuoles within intervertebral disc: Current understanding and speculation', *Oncotarget*. Impact Journals LLC, pp. 57800–57812. Available at: https://doi.org/10.18632/oncotarget.18101.

Wang, F. *et al.* (2019) 'Injectable Hydrogel Combined with Nucleus Pulposus-Derived Mesenchymal Stem Cells for the Treatment of Degenerative Intervertebral Disc in Rats', *Stem Cells International*, 2019, p. 8496025. Available at: https://doi.org/10.1155/2019/8496025.

Wang, H. *et al.* (2019) 'The research of transgenic human nucleus pulposus cell transplantation in the treatment of lumbar disc degeneration', *The Kaohsiung Journal of Medical Sciences*, 35(8), pp. 486–492. Available at: https://doi.org/10.1002/kjm2.12084.

Wang, J.Y. *et al.* (2001) 'Intervertebral disc cells exhibit differences in gene expression in alginate and monolayer culture', *Spine*, 26(16), pp. 1747–1752. Available at: https://doi.org/10.1097/00007632-200108150-00003.

Wang, W. *et al.* (2018) 'Transplantation of allogenic nucleus pulposus cells attenuates intervertebral disc degeneration by inhibiting apoptosis and increasing migration', *International Journal of Molecular Medicine*, 41(5), pp. 2553–2564. Available at: https://doi.org/10.3892/ijmm.2018.3454.

Wang, X. *et al.* (2018) 'International Immunopharmacology Potential therapeutic role of Co-Q10 in alleviating intervertebral disc degeneration and suppressing IL-1 β -mediated in fl ammatory reaction in NP cells', *International Immunopharmacology*, 64(April), pp. 424–431. Available at: https://doi.org/10.1016/j.intimp.2018.09.029.

Wang, Y.H. *et al.* (2015) 'Effect of the mixture of bone marrow mesenchymal stromal cells and annulus fibrosus cells in repairing the degenerative discs of rabbits', *Genetics and Molecular Research*, 14(1), pp. 2365–2373. Available at: https://doi.org/10.4238/2015.March.27.22.

Wang, Y. *et al.* (2019) 'High Glucose Enhances the Odonto/Osteogenic Differentiation of Stem Cells from Apical Papilla via NF-KappaB Signaling Pathway', *BioMed Research International*, 2019. Available at: https://doi.org/10.1155/2019/5068258.

Wang, Z. *et al.* (2015) 'Efficacy of intervertebral disc regeneration with stem cells - A systematic review and meta-analysis of animal controlled trials', *Gene*, 564(1), pp. 1–8. Available at: https://doi.org/10.1016/j.gene.2015.03.022.

Ward, L. *et al.* (2018) 'The role of the notochord in amniote vertebral column segmentation', *Developmental Biology*, 439(1), pp. 3–18. Available at: https://doi.org/10.1016/j.ydbio.2018.04.005.

Watanabe, K. *et al.* (2007) 'A ROCK inhibitor permits survival of dissociated human embryonic stem cells', *Nature Biotechnology 2007 25:6*, 25(6), pp. 681–686. Available at: https://doi.org/10.1038/nbt1310.

Weiler, C. *et al.* (2010) 'Immunohistochemical identification of notochordal markers in cells in the aging human lumbar intervertebral disc', *European Spine Journal*, 19(10), p. 1761. Available at: https://doi.org/10.1007/S00586-010-1392-Z.

Wilke, H.J. *et al.* (1999) 'New in vivo measurements of pressures in the intervertebral disc in daily life', *Spine*, 24(8), pp. 755–762. Available at: https://doi.org/10.1097/00007632-199904150-00005.

Williams, D.F. (2017) '*A Paradigm for the Evaluation of Tissue-Engineering Biomaterials and Templates', *https://home.liebertpub.com/tec*, 23(12), pp. 926–937. Available at: https://doi.org/10.1089/TEN.TEC.2017.0181.

Williams, R.J. *et al.* (2021) 'Cell sources proposed for nucleus pulposus regeneration', *JOR Spine*, 4(4), p. e1175. Available at: https://doi.org/10.1002/JSP2.1175.

Williams, S., Alkhatib, B. and Serra, R. (2019) 'Development of the axial skeleton and intervertebral disc', *Current topics in developmental biology*, 133, pp. 49–90. Available at: https://doi.org/10.1016/BS.CTDB.2018.11.018.

Wilson, N. *et al.* (2020) 'Drug and Opioid-Involved Overdose Deaths — United States, 2017–2018', *MMWR. Morbidity and Mortality Weekly Report*, 69(11), pp. 290–297. Available at: https://doi.org/10.15585/mmwr.mm6911a4.

Winkler, T. *et al.* (2014) 'Wnt signaling activates Shh signaling in early postnatal intervertebral discs, and re-activates Shh signaling in old discs in the mouse', *PloS one*, 9(6). Available at: https://doi.org/10.1371/JOURNAL.PONE.0098444.

Wong, J. *et al.* (2019) 'Nutrient supply and nucleus pulposus cell function: effects of the transport properties of the cartilage endplate and potential implications for intradiscal biologic therapy', *Osteoarthritis and cartilage*, 27(6), p. 956. Available at: https://doi.org/10.1016/J.JOCA.2019.01.013.

Wopat, S. *et al.* (2018) 'Spine Patterning Is Guided by Segmentation of the Notochord Sheath', *Cell Reports*, 22(8), pp. 2026–2038. Available at: https://doi.org/10.1016/j.celrep.2018.01.084.

Wu, H. *et al.* (2018) 'Regenerative potential of human nucleus pulposus resident stem/progenitor cells declines with ageing and intervertebral disc degeneration', *International Journal of Molecular Medicine*, 42(4), pp. 1819–1826. Available at: https://doi.org/10.3892/ijmm.2018.3766.

Wu, T. *et al.* (2018) 'Cell-based therapies for lumbar discogenic low back pain systematic review and single-arm meta-analysis', *Spine*. Lippincott Williams and Wilkins, pp. 49–57. Available at: https://doi.org/10.1097/BRS.0000000000001549.

Wuertz, K. *et al.* (2008) 'Behavior of mesenchymal stem cells in the chemical microenvironment of the

intervertebral disc', *Spine*, 33(17), pp. 1843–1849. Available at: https://doi.org/10.1097/BRS.0b013e31817b8f53.

Wuertz, K., Godburn, K. and Iatridis, J.C. (2009) 'MSC response to pH levels found in degenerating intervertebral discs', *Biochemical and biophysical research communications*, 379(4), p. 824. Available at: https://doi.org/10.1016/J.BBRC.2008.12.145.

Wymeersch, F.J. *et al.* (2019) 'Transcriptionally dynamic progenitor populations organised around a stable niche drive axial patterning', *Development (Cambridge, England)*, 146(1). Available at: https://doi.org/10.1242/DEV.168161.

Xia, K., Gong, Z., *et al.* (2019) 'Differentiation of Pluripotent Stem Cells into Nucleus Pulposus Progenitor Cells for Intervertebral Disc Regeneration', *Current stem cell research & therapy*, 14(1), pp. 57–64. Available at: https://doi.org/10.2174/1574888X13666180918095121.

Xia, K., Zhu, J., *et al.* (2019) 'Intradiscal Injection of Induced Pluripotent Stem Cell-Derived Nucleus Pulposus-Like Cell-Seeded Polymeric Microspheres Promotes Rat Disc Regeneration', *Stem cells international*, 2019. Available at: https://doi.org/10.1155/2019/6806540.

Xu, G. *et al.* (2020) 'Temporal and spatial expression of Sox9, Pax1, TGF-β1 and type I and II collagen in human intervertebral disc development', *Neuro-Chirurgie*, 66(3), pp. 168–173. Available at: https://doi.org/10.1016/J.NEUCHI.2019.12.011.

Yamamizu, K., Schlessinger, D. and Ko, M.S.H. (2014) 'SOX9 accelerates ESC differentiation to three germ layer lineages by repressing SOX2 expression through P21 (WAF1/CIP1)', *Development (Cambridge)*, 141(22), pp. 4254–4266. Available at: https://doi.org/10.1242/DEV.115436/-/DC1.

Yamanaka, Y. *et al.* (2007) 'Live imaging and genetic analysis of mouse notochord formation reveals regional morphogenetic mechanisms', *Developmental cell*, 13(6), pp. 884–896. Available at: https://doi.org/10.1016/J.DEVCEL.2007.10.016.

Yang, C.H. *et al.* (2016) 'The effect of annular repair on the failure strength of the porcine lumbar disc after needle puncture and punch injury', *European Spine Journal*, 25(3), pp. 906–912. Available at: https://doi.org/10.1007/s00586-015-4316-0.

Yang, S.H. *et al.* (2017) 'The influence of oxygen concentration on the extracellular matrix production of human nucleus pulposus cells during isolation-expansion process', *Journal of Biomedical Materials Research - Part A*, 105(6), pp. 1575–1582. Available at: https://doi.org/10.1002/JBM.A.36020.

Yasunaga, M. *et al.* (2005) 'Induction and monitoring of definitive and visceral endoderm differentiation of mouse ES cells', *Nature biotechnology*, 23(12), pp. 1542–1550. Available at: https://doi.org/10.1038/NBT1167.

Yoshikawa, T. *et al.* (2010) *Disc Regeneration Therapy Using Marrow Mesenchymal Cell Transplantation A Report of Two Case Studies*, *SPINE*.

Yu, J. *et al.* (2007) 'Induced pluripotent stem cell lines derived from human somatic cells', *Science (New York, N.Y.)*, 318(5858), pp. 1917–1920. Available at: https://doi.org/10.1126/SCIENCE.1151526.

Yuan, Y. *et al.* (2016) 'Efficient long-term cryopreservation of pluripotent stem cells at −80 °C', *Scientific Reports 2016 6:1*, 6(1), pp. 1–13. Available at: https://doi.org/10.1038/srep34476.

Yung Lee, J. *et al.* (2001) 'New use of a three-dimensional pellet culture system for human intervertebral disc cells: Initial characterization and potential use for tissue engineering', *Spine*, 26(21), pp. 2316–2322. Available at: https://doi.org/10.1097/00007632-200111010-00005.

Yurube, T. *et al.* (2014) 'Notochordal cell disappearance and modes of apoptotic cell death in a rat tail

static compression-induced disc degeneration model', *Arthritis Research and Therapy*, 16(1), pp. 1–11. Available at: https://doi.org/10.1186/AR4460/FIGURES/7.

Zhang, F. *et al.* (2017) 'Optimizing mesoderm progenitor selection and three-dimensional microniche culture allows highly efficient endothelial differentiation and ischemic tissue repair from human pluripotent stem cells', *Stem Cell Research and Therapy*, 8(1), pp. 1–15. Available at: https://doi.org/10.1186/S13287-016-0455-4/FIGURES/7.

Zhang, J. *et al.* (2020) 'Mesenchymal stem cells-derived exosomes ameliorate intervertebral disc degeneration through inhibiting pyroptosis', *Journal of Cellular and Molecular Medicine*, 24(20), pp. 11742–11754. Available at: https://doi.org/10.1111/jcmm.15784.

Zhang, S. *et al.* (2022) 'Extracellular matrix in intervertebral disc: basic and translational implications', *Cell and tissue research*, 390(1), pp. 1–22. Available at: https://doi.org/10.1007/S00441-022-03662-5.

Zhang, W. *et al.* (2013) 'A Novel Core-Shell Microcapsule for Encapsulation and 3D Culture of Embryonic Stem Cells', *Journal of materials chemistry. B, Materials for biology and medicine*, 2013(7), p. 1002. Available at: https://doi.org/10.1039/C2TB00058J.

Zhang, X. *et al.* (2020) 'Spheroid-like cultures for expanding angiopoietin receptor-1 (aka. Tie2) positive cells from the human intervertebral disc', *International Journal of Molecular Sciences*, 21(24), pp. 1–17. Available at: https://doi.org/10.3390/ijms21249423.

Zhang, Y. *et al.* (2015) 'The effects of human Wharton's jelly cell transplantation on the intervertebral disc in a canine disc degeneration model', *Stem Cell Research and Therapy*, 6(1), p. 154. Available at: https://doi.org/10.1186/s13287-015-0132-z.

Zhang, Y. *et al.* (2020) 'Directed Differentiation of Notochord-like and Nucleus Pulposus-like Cells Using Human Pluripotent Stem Cells', *Cell Reports*, 30(8), pp. 2791-2806.e5. Available at: https://doi.org/10.1016/j.celrep.2020.01.100.

Zhao, X. *et al.* (2022) 'Precision medicine strategies for spinal degenerative diseases: Injectable biomaterials with in situ repair and regeneration', *Materials Today Bio*, 16, p. 100336. Available at: https://doi.org/10.1016/J.MTBIO.2022.100336.

Zheng, C.J. and Chen, J. (2015) 'Disc degeneration implies low back pain', *Theoretical Biology and Medical Modelling*, 12(1), p. 24. Available at: https://doi.org/10.1186/s12976-015-0020-3.

Zhu, Y. *et al.* (2017) 'The generation and functional characterization of induced pluripotent stem cells from human intervertebral disc nucleus pulposus cells', *Oncotarget*, 8(26), pp. 42700–42711. Available at: https://doi.org/10.18632/oncotarget.17446.

Ziello, J.E., Jovin, I.S. and Huang, Y. (2007) 'Hypoxia-Inducible Factor (HIF)-1 regulatory pathway and its potential for therapeutic intervention in malignancy and ischemia', *Yale Journal of Biology and Medicine*. Yale Journal of Biology and Medicine, pp. 51–60. Available at: /pmc/articles/PMC2140184/?report=abstract (Accessed: 5 January 2021).